IFM-GEOMAR REPORT

IFM-GEOMAR

Leibniz-Institut für Meereswissenschaften
an der Universität Kiel

FS SONNE
Fahrtbericht / Cruise Report
SO-214 NEMESYS

09.03. - 05.04.2011
Wellington - Wellington

06. - 22.04.2011
Wellington - Auckland

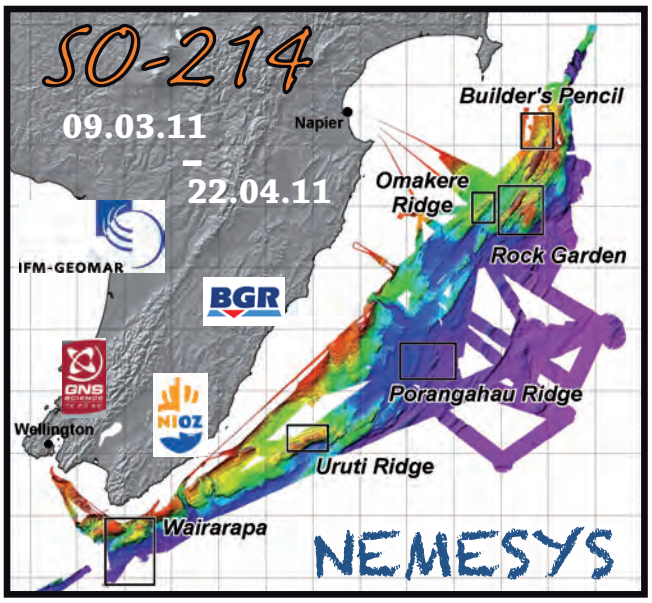

Berichte aus dem Leibniz-Institut
für Meereswissenschaften an der
Christian-Albrechts-Universität zu Kiel

Nr. 47

August 2011

IFM-GEOMAR
Leibniz-Institut für Meereswissenschaften
an der Universität Kiel

FS SONNE
Fahrtbericht / Cruise Report
SO-214 NEMESYS

09.03. - 05.04.2011
Wellington - Wellington
06. - 22.04.2011
Wellington - Auckland

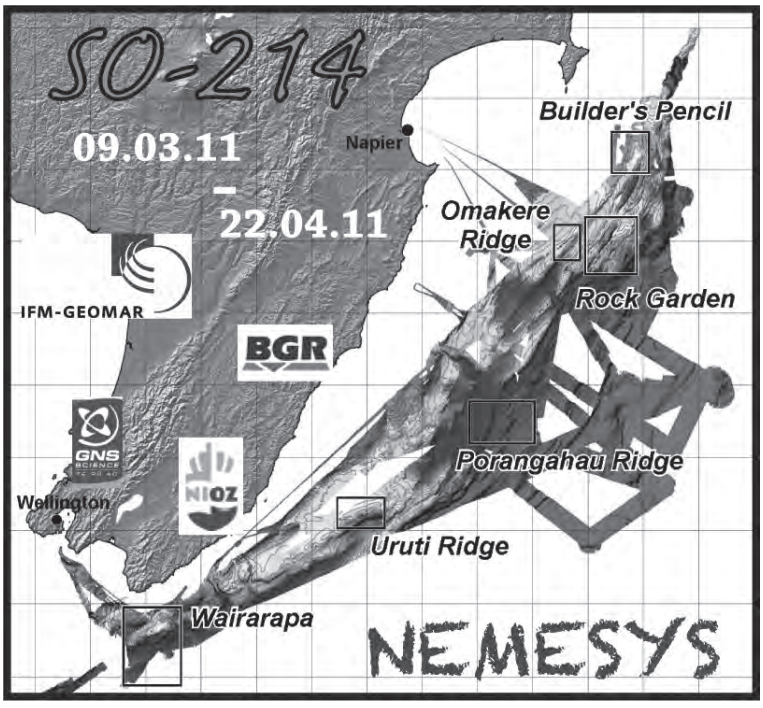

Berichte aus dem Leibniz-Institut
für Meereswissenschaften an der
Christian-Albrechts-Universität zu Kiel

Nr. 47
August 2011

ISSN Nr.: 1614-6298

IFM-GEOMAR
Leibniz-Institut für Meereswissenschaften
an der Universität Kiel

Das Leibniz-Institut für Meereswissenschaften ist ein Institut der Wissenschaftsgemeinschaft Gottfried Wilhelm Leibniz (WGL)

The Leibniz-Institute of Marine Sciences is a member of the Leibniz Association (Wissenschaftsgemeinschaft Gottfried Wilhelm Leibniz).

Herausgeber / Editor:
J. Bialas

IFM-GEOMAR Report
ISSN Nr.: 1614-6298

Leibniz-Institut für Meereswissenschaften / Leibniz Institute of Marine Sciences
IFM-GEOMAR
Dienstgebäude Westufer / West Shore Building
Düsternbrooker Weg 20
D-24105 Kiel
Germany

Leibniz-Institut für Meereswissenschaften / Leibniz Institute of Marine Sciences
IFM-GEOMAR
Dienstgebäude Ostufer / East Shore Building
Wischhofstr. 1-3
D-24148 Kiel
Germany

Tel.: ++49 431 600-0
Fax: ++49 431 600-2805
www.ifm-geomar.de

Content

1. Summary 5
2. Introduction 6
2.1. The objectives of the cruise SO-214 6
2.2. Regional geologic-tectonic setting 7
2.3. Previous investigations 8
3. Participants 8
3.1 Scientists 8
3.1.1 Scientists of SO214 Leg 1 8
3.1.2 Scientists Leg 2 9
3.2 Crew 10
3.2.1 Crew of Leg 1 10
3.2.2 Crew of Leg 2 11
4. Agenda of the cruise 11
4.1 Agenda of the cruise SO-214/1 11
4.2 Agenda of the cruise SO-214/2 13
5. Scientific Equipment 14
5.1 Shipboard Equipment 14
5.1.1 Navigation 14
5.1.2 Simrad EM120 Multibeam 16
5.1.3 L3-ELAC Nautik SBE 3050 Multibeam 17
5.1.4 Parasound 18
5.1.5 CTD (Conductivity-Temperature-Depth) operations 22
5.1.6 OFOS 23
5.2 Geophysical instrumentation 25
5.2.1 GI-gun 25
5.2.2 P-Cable streamer 25
5.2.3 The Ocean Bottom Seismometer (OBS) 28
5.2.4 DTMCS – Deep Towed Multichannel Streamer 31
5.3 Sidescan sonar 32
5.4 Controlled Source Electromagnetics (CSEM) for gas hydrate assessment 34
5.4.1 CSEM-BGR Instrument description 36
5.4.2 OBEM stations and transmitter frame of the IFM-GEOMAR 38
5.5 Geological instrumentation 40
5.5.1 Gravity corer 40

5.5.2 Multicorer 40
5.5.3 Sediment temperature measurements 42
5.6 Methane analyses 43
5.6.1 System 44
5.6.2 Sample preparation 44
5.6.3 Conversion from peak area to CH4 ppm in the head space 45
5.6.4 Calculating the original methane concentration of the water 45
5.6.5 Equilibration/shaking time experiments 47
5.6.6 Triplicate measurements 47
5.7 Geochemistry 48
5.8 Thermistor mooring 50
5.9 Atmospheric Methane Measurements 52
6. Work completed and first results 53
6.1 Parasound Acquisition and Processing 57
6.1.1 Omakere Parasound 57
6.1.2 Porangahau Ridge Parasound 59
6.1.3 Wairarapa Parasound 60
6.2 Seimics 64
6.2.1 Omakere 64
6.2.1.1 P-Cable Omakere 64
6.2.1.2 OBS Omakere 68
6.2.2 Porangahau 71
6.2.2.1 2D Seismic Porangahau Ridge 71
6.2.2.2 OBS Porangahau Ridge 79
6.2.3 Wairarapa 85
6.2.3.1 2-D Seismic 85
6.2.3.2 3-D Seismic 85
6.2.3.3 OBS Wairarapa 86
6.3. Deep-towed sidescan sonar and streamer deployments 95
6.3.1 Omakere Ridge 95
6.3.2 Rock Garden 99
6.3.3 Wairarapa (Opouawe Bank) 99
6.4. Marine CSEM 101
6.4.1 Marine CSEM-BGR at Opouawe Bank 101
6.4.2 Marine CSEM- IFM-GEOMAR 110

6.5 CTD and CH4 measurements 113
6.5.1 Opouawa Bank 114
6.5.2 Omakere Ridge 117
6.5.2 Rock Garden 117
6.6 Ofos 118
6.6.1 Wairarapa 118
6.7 Biology 123
6.7.1 Wairarapa 126
6.7.2 Omakere Ridge 127
6.8 Geochemistry of the Takahe site (Wairarapa) 127
6.9 Gravity cores 131
6.10 Results of sediment temperature measurements 139
7. Acknowledgments 141
8. References 142
9. Appendices 144
9.1. List of Porewater Sampling Sites and Collected Sub-samples. 144
9.2 On board description of GCs 145
9.3. OBS Station lists 158
9.3.1 P1 Omakere 158
9.3.2 P2 Porangahau 159
9.3.3 P3 Wairarapa 160
9.4 CSEM Deployment Details 161
9.5 CTD Locations 163

All meta data of the cruise are available through the IFM-GEOMAR Data Management Portal (https://portal.ifm-geomar.de/web/guest/home)

1. Summary

Cruise SO-214 of R/V SONNE headed by IFM-GEOMAR served two legs of project NEMESYS, funded through the German Ministry of Education and Research (BMBF). Major partners of the project are Leibniz Institute of Marine Science (IFM-GEOMAR) and the Federal Institute of Geosciences and Natural Resources (BGR) Germany, as well as the Institute of Geological and Nuclear Sciences (GNS) and the Royal Netherlands Institute for Sea Research (NIOZ). NEMESYS aims to extend understanding and modelling of cold vents along the Hikurangi Margin (HM) off the east coast of the North Island of New Zealand. Since the first findings in the late 80´s several cruises have been dedicated to map and investigate the active seepage of Methane in this area. Results of these cruises headed by New Zealand and international scientists provided the database for the first joint German – New Zealand expedition SO-191 in 2007. During this cruise with R/V SONNE the HM was investigated within three legs comprising all marine geo-scientific disciplines. The major findings in geophysical, geological, geo-chemical, and biological research were published in a special issue by Marine Geology (Vol. 272, 2010).

Nevertheless a lot of questions remained or were raised by the upcoming results. Still the lateral continuation of feeder channels and a possible relation between internal structure, activity and tectonic regime of a seep site were not understood. The geological, geo-chemical and biological analysis has been related to the overall description and study of the seep sites along the margin. Detailed studies across a seep site and high-resolution sampling to study the internal variation of Methane production and the influences to chemistry and habitat have not been complete with the required intensity. These exemplary listed investigations together with an additional list of questions to seepage led to the follow-up project SO-214 NEMESYS, which was funded through the German Ministry of Education and Research (BMBF). Aim of the project NEMESYS is to confirm derived models of seep structures and to extend the existing database and knowledge by high-resolution sampling in all disciplines.

Based on the findings of the SO-191 New Vents project Opouawe Bank and Omakere Ridge were identified as the areas with the highest interest for our additional studies. Opouawe Bank provides a high density of active seep sites with various expressions of feeder channels in seismic images. Omakere did provide the only seep sites that were found without feeder channels underneath. In between the Porangahau Ridge was selected as third target due to the indications of either gas or hydrate formation without active gas expulsion.

Cruise SO-214 with R/V SONNE was split into two legs. The seismic part started on 09th March 2011 in the port of Wellington. Two 3D seismic cubes were acquired above active seep sites at Omakere and Opouawe Bank. A third cube at Porangahau Ridge could not be completed due to technical problems with the equipment and rough weather conditions. Intensive Parasound Profiling and extended 2D seismic with high resolution (up to 1.2 m migration grid) were undertaken. Many more feeder channels were identified than previously known from the SO-191 data, although not all of them terminate in a seafloor expression.

The second leg left the port of Wellington on 6th April 2011 dedicated to intensive geological, geo-chemical and biological investigations. The major work was completed at Opouawe Bank. Based on images of the seismic data compilation North and South Tower seeps and seep site Takahe were chosen for the intensive sampling program. CTD and gravity cores were taken in dense spacing to investigate the local interaction of seepage and surrounding seafloor and water column. The water column showed limited stratification but seemed to be influenced from stormy weather. Biologic investigations showed limited variations compared with the SO-191 expedition, mainly in the distribution of fauna. The

variety of amphipods seems to be a unique feature of the NZ seeps. The second leg suffered from bad weather conditions, which anticipated work during 100 hrs. out of scheduled 330 hrs.

All meta data of the cruise are available through the IFM-GEOMAR Data Management Portal (https://portal.ifm-geomar.de/web/guest/home)

2. Introduction

Jörg Bialas

2.1. The objectives of the cruise SO-214

Gas hydrates are a worldwide-observed occurrence of mainly Methane gas bound in solid phase within the sediment column. Speculations about the available Carbon from these sources have changed by numbers of orders but still are expected to be larger than the actual known and available resources from oil and gas (ca. 3500 Gt [Marquardt et al., 2010]) and hence investigations about the potential usage as energy reservoirs are continuing. To enable an environmentally save production from those reservoirs a detailed understanding of the stability field, dynamics and chemical processes of the hydrates are crucial. This holds especially for the unusual but often observed migration of free gas within the stability field of gas hydrates.

Sites with active gas expulsion above gas hydrate containing areas are known from various places in the oceans. Wide spread and large amounts of such "Cold Vents" (Seeps) in connection with a BSR have been mapped and documented from the Hikurangi Margin off the North Island of New Zealand (e.g. [*Faure et al.*, 2006; *Jens Greinert et al.*, 2010; *Henrys et al.*, 2003; *Lewis and Marshall*, 1996]). Several expeditions with R/V TANGAROA (TAN0411, TAN0607, TAN0616) and R/V SONNE SO-191 [*Bialas et al.*, 2007b] contributed to the actual knowledge of the active and passive seep sites along this accretionary margin (Fig. 2.1.1)

2-D seismic images of the feeder channels underneath the seep sites indicate that there are different systems of migration pathways supporting free gas transport through the gas hydrate stability field [*Netzeband et al.*, 2010]. Ruptured and distributed strong reflections at BSR level underneath or at the root of a chimney, chimneys with internal reflections, and possibly connected feeder systems are suggested from the 2-D seismic data. It is clear that these are three-dimensional structures and major parts of the described features are not imaged by the 2-D lines as they are out of plane. The recently developed IFM-GEOMAR 3-D P-Cable multichannel seismic acquisition system was applied to provide 3-D images of the feeder channels and the gas hydrate reservoirs. Parasound and deep towed sub-bottom profiler data were acquired along dense spaced grids to link the high resolution seismic with the seafloor images from the deep towed sidescan sonar. Comparison with the elder maps from SO-191 might indicate if significant changes in seafloor composition occurred during the last four years.

Analysis of gas samples from the previous expeditions confirmed that the majority of the gas is of biological origin. But there are sites were deeper sources and other than pure Methane compositions were indicated ([*Faure et al.*, 2006], Kipfer, EAWAG, priv. comm.). Revisiting of the sites with intensive water sampling and seafloor sampling should enlarge the available database. Distinct profiles crossing or networks of sample points above selected seep sites will help to reveal the lateral extend of seep activity and the related isotopic composition.

∂13C isotopic compositions analysed by [*Campbell et al.*, 2010] implied significant temperature variations or episodes of gas hydrate formation. [*Thurber et al.*, 2010] discovered two unique biota assemblages fuelled by Methane. The high use of Methane by the fauna offers ideal conditions for on-going studies on seeps and related interactions of fauna and seep cycles. OFOS and TV guided MUC will support the continuation of this work.

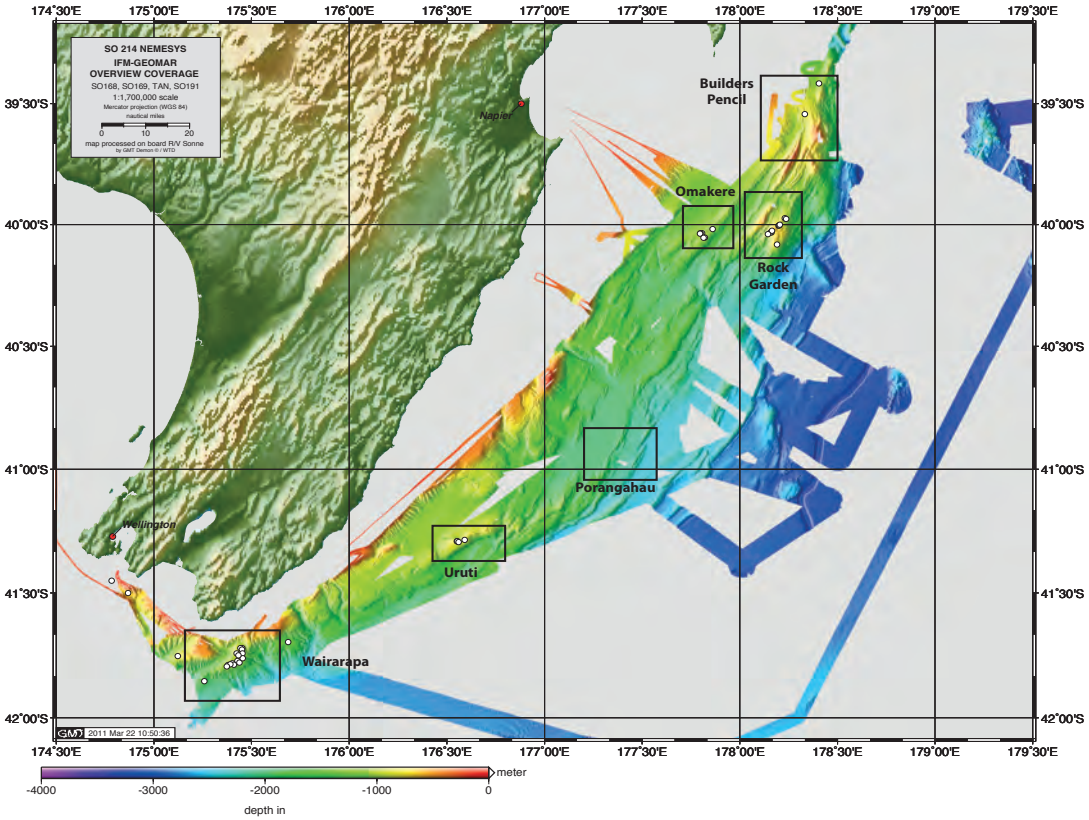

Figure 2.1.1: Bathymetric map of the Hikurangi Margin. White dots indicate known seep sites

2.2. Regional geologic-tectonic setting

The Hikurangi Margin (HM) is dominated by the East-West oriented subduction of the Pacific plate underneath the Australian plate. It is located east of the North Island of New Zealand. To the North the trench continues along the Tonga-Kermadec subduction. The HM is formed by the accretion of the 500 – 2000 m thick marine sediments of Pliocene to Quaternary age. They are topped on the 10 – 15 km thick crust of the Hikurangi Plateau (HP) formed by MORB of Pre-Tertiary age [*Davy and Wood*, 1994]. A general slope of less than 4° of the margin indicates low friction at the plate interface, which most probably is the result of high water content in the accreting sediments. The New Zealand Geologists call it a "saturated sponge" [*Lewis and Marshall*, 1996]. The fast growing accretionary wedge forms the ridges where the past and present seep sites are located. Prior to the SO-191 cruise in 2007 geophysical investigations were used to map a 40.000 km^2 area where BSR reflections of various strength were observed [*Collot et al.*, 1996; *Henrys et al.*, 2003]. A stratigraphic analysis of the Wairarapa area [*Bialas et al.*, 2007a] discussed the distribution of palaeo-channels and erosional interfaces together with BSR distribution and feeder channels. Due to their 3-D continuation parts of the feeder channels could not be tracked until the seafloor. They may continue out of the plane of the acquired 2-D seismic data or terminate below the seafloor. Interference between the termination of feeder channels and slope failures cannot be ruled out. Although most of the sampled gas hydrates from Wairarapa and Omakere do not show contents of higher carbons [*Faure et al.*, 2010] mixed gas compositions as known from

the subduction related volcanism and fluid flow on land were found at Rock Garden ([*Giggenbach et al.*, 1993], Kipfer, EAWAG, priv. comm.).

2.3. Previous investigations

Since the identification of seep sites by [Lewis and Marshall, 1996] several campaigns were dedicated to the investigation of the phenomena. In 2004 R/V Tangaroa was used to sample the water column during TAN0411. Methane expulsion could be verified at Rock Garden and a new flare was identified at Faure-Site [Faure et al., 2006]. A more detailed investigation of the gas hydrate occurrences was completed during TAN0607 in 2006. Multichannel seismic profiles were shot across the Porangahau Ridge, and imaged a clear BSR, which is interrupted by fractures. Nevertheless heat flow, pore water samples from gravity cores, and methane analysis in the water column did not show any signs for active seepage in this area. Later in the year during TAN0616 active seepage could be confirmed for all seeps of Lewis and Marshall (1996), while additional five new seep sites were identified. During cruise SO-191 in 2007 (e.g. [J. Greinert et al., 2010]) intensive multidisciplinary investigations were undertaken in the working areas of Wairarapa, Uruti Ridge, Porangahau, Omakere Ridge, Rock Garden and Builders Pencil. During this cruise additional seep sites were located summing up to a total of 21.

2-D seismic investigations imaged the feeder channels of various seep sites (e.g. [*Netzeband et al.*, 2010]). Besides Omakere all seep sites were characterised by a discontinuous BSR. Strong amplitudes were identified at BSR level clustering at the root of the feeder channel. Feeder channels were observed with or without internal reflections. Due to the rapid lateral change of these structural features a complete image and description of the clustering amplitudes could not be given. More over the continuity towards the seafloor of feeder channels could not be documented at all sites. They may either terminate at shallow depth underneath the seafloor or penetrate the seafloor out of the 2-D plane of the multichannel seismic section.

Controlled Source Electromagnetic (CSEM) investigations at seep sites in Wairarapa nicely documented gas hydrate accumulations at the seep site South Tower by increased resistivity [*Schwalenberg et al.*, 2010a]. At Porangahau Ridge [*Schwalenberg et al.*, 2010b] used CSEM data, heat flow and geochemical investigation to test a prominent seismic reflection underneath the Western extend of the Ridge for its gas hydrate content. It was suggested that due to rising fluids the base of the hydrate stability field is uplifted.

Repeated observations of gas flares in the water column proved that some seep sites have been active over more than 10 years [*Faure et al.*, 2010; *Lewis and Marshall*, 1996]. Foraminifera taken from on-shore ancient seep sites [*Campbell et al.*, 2008] indicated the fluid activity of the Hikurangi Margin since the late Miocene. Isotope analysis from seafloor samples did show values typical for cold seeps found on other places worldwide [*Campbell et al.*, 2010]. Grab and corer samples showed clear AOM origin in their isotopic signal with a biogenic Methane source.

3. Participants

3.1 Scientists

3.1.1 Scientists of SO214 Leg 1

Name	Given Name	Institute	Discipline
Bialas	Joerg	IFM-GEOMAR	Chief Scientist
Bruce	Callum	OTAGO	MCS/OBS seismic

Crutchley	Gareth	IFM-GEOMAR	MCS processing
Dumke	Ines	IFM-GEOMAR	DTS-1
Golding	Thomas	GNS	MCS / OBS seismic
Greinert	Jens	NIOZ	Co-Chief scientist
Haffert	Laura	IFM-GEOMAR	CTD
Kampmeier	Mareike	IGM	OBS seismic
Klaeschen	Dirk	IFM-GEOMAR	3-D seismic processing
Klaucke	Ingo	IFM-GEOMAR	DTS-1
Koch	Stephanie	IFM-GEOMAR	3-D seismic / bathymetry
Matthiessen	Torge	IFM-GEOMAR	Technician
Moeller	Stefan	IFM-GEOMAR	OBS
Moscoso	Eduardo	IFM-GEOMAR	OBS
Papenberg	Cord	IFM-GEOMAR	3-D navigation / WCI
Pecher	Ingo	GNS	MCS seismic
Plaza-Vaverola	Andreia	GNS	MCS seismic
Urban	Peter	NIOZ	Parasound / bathymetry
Veloso	Mario	NIOZ	Parasound / bathymetry
Wetzel	Gero	IFM-GEOMAR	Electronics
Wollatz-Vogt	Martin	IFM-GEOMAR	Electronics

3.1.2 Scientists Leg 2

Name	Given Name	Institute	Discipline
Bialas	Joerg	IFM-GEOMAR	Chief Scientist
Bowden	David	NIWA	Video / Biology
Crutchley	Gareth	IFM-GEOMAR	P-Cable
Dale	Andy	IFM-GEOMAR	Pore Water
de Haas	Henk	NIOZ	Coring / Pore Water
de Stigter	Henko	NIOZ	Sediment
Deppe	Joachim	BGR	Electronics
Engels	Martin	BGR	CSEM
Gebhardt	Wolf	DW-World	DW-TV
Greinert	Jens	NIOZ	Co-Chief Scientist
Haffert	Laura	IFM-GEOMAR	CTD
Henry-Edwards	Aneurin	NIOZ	Oceanography
Hoelz	Sebastian	IFM-GEOMAR	CSEM / MT
Huetten	Edna	RCMG	Coring / Pore Water
Sztybor	Kamila	UiT	Sediment
Matthiessen	Torge	IFM-GEOMAR	Technician
Mir	Reza	BGR	CSEM
Nestler	Stefan	DW-World	DW-TV
Schwalenberg	Katrin	BGR	CSEM
Thurber	Andrew	FIU	Biology
Toulmin	Suzannah	GNS	CSEM / MT
van Gaever	Piet	NIOZ	Methane Analysis
Wollatz-Vogt	Martin	IFM-GEOMAR	Electronics

BGR: Bundesanstalt für Geowissenschaften und Rohstoffe, Hannover, Germany

DW-World: Deutsche Welle Radio, Kurt-Schuhmacher-Str. 3, 53115 Bonn, Germany
Deutsche Welle TV, Voltastr. 6, 13355 Berlin, Germany

GNS: Institute of Geology and Nuclear Sciences LTD, P.O. Box 30-368, Lower Hutt, New Zealand

IFM-GEOMAR: Leibniz Institute of Marine Sciences Wischhofstr. 1-3. 24148 Kiel, Germany

IGM: Institut für Geologie und Mineralogie Köln, Zülpicherstr. 49a, 50674 Köln

NIOZ: Nederlands Instituut voor Onderzoek der Zee, Landsdiep 4, 1797 Texel 't Hoerntje, Netherlands

NIWA: National Institute for Water and Atmosphere LTD, 301 Evans Bay Parade, Greta. Point PO Box 14901, Kilbirnie, Wellington, New Zealand

OTAGO: The University of Otago, Otago, New Zealand

RCMG: Renard Centre of Marine Geology, Department of Geology and Soil Science Ghent University, Krijgslaan 281 s.8, B-9000 Gent

FIU: Florida International University, MSB-353, 3000 NE 151 Street, North Miami, FL 33181

UiT: University of Tromsoe, 9037 Tromsoe, Norway

3.2 Crew

3.2.1 Crew of Leg 1

Name	Given Name	Rank
Meyer	Oliver	Master
Korte	Detlef	Chief Mate
Büchele	Ulrich	2nd Mate
Hoffsommer	Lars	2nd Mate
Walther	Anke	Surgeon
Rex	Andreas	Chief Engineer
Klinder	Klaus-Dieter	2nd Engineer
Hermesmeyer	Dieter	2nd Engineer
Rieper	Uwe	Electrician
Grossmann	Matthias	Chief Electrician
Wolfgang	Borchert	System Manager
Ehmer	Andreas	System Manager
Krawczak	Ryszard	Motorman
Bolik	Torsten	Motorman
Wieden	Wilhelm	Chief Cook
Ganagaraj	Antony	2nd Cook
Schmandtke	Harald	Chief Steward
Royo	Luis	2nd Steward
Schrapel	Andreas	Boatswain
Dolief	Joachim	A. B.
Bierstedt	Torsten	A. B.
Ross	Reno	A. B.
Weinhold	Rolf	A. B.
Mohrdiek	Finn	A. B.
Schröder	Christopher	A. B.
Kallenbach	Christian	Apprentice
Grawe	Manuel	Apprentice

3.2.2 Crew of Leg 2

Name	Given Name	Rank
Meyer	Oliver	Master
Korte	Detlef	Chief Mate
Büchele	Ulrich	2nd Mate
Hoffsommer	Lars	2nd Mate
Walther	Anke	Surgeon
Rex	Andreas	Chief Engineer
Klinder	Klaus-Dieter	2nd Engineer
Hermesmeyer	Dieter	2nd Engineer
Rieper	Uwe	Electrician
Grossmann	Matthias	Chief Electrician
Wolfgang	Borchert	System Manager
Ehmer	Andreas	System Manager
Krawczak	Ryszard	Motorman
Bolik	Torsten	Motorman
Dehne	Dirk	Motorman
Wieden	Wilhelm	Chief Cook
Schmandtke	Harald	Chief Steward
Royo	Luis	2nd Steward
Schrapel	Andreas	Boatswain
Dolief	Joachim	A. B.
Stängl	Günther	A. B.
Ross	Reno	A. B.
Mohrdiek	Finn	A. B.
Schröder	Christopher	A. B.
Kallenbach	Christian	Apprentice
Grawe	Manuel	Apprentice

4. Agenda of the cruise

Joerg Bialas

4.1 Agenda of the cruise SO-214/1

On March 09th 2011 21 scientists from six different institutions joined in the port of Wellington, New Zealand, R/V SONNE to prepare for the first leg of cruise SO-214 NEMESYS. Five containers were shipped from Germany, South Africa and Thailand to provide vessel and scientists with the required equipment. Two days were used in port to equip the laboratories and to set up streamers, trawl doors and airguns at the working deck. In addition divers installed an ELAC Nautik SBE3050 multibeam for water column imaging underneath the front moon pool of R/V SONNE.

On 11th March R/V SONNE left the port of Wellington. After the usual security training and advice the trawl doors were set into position outside the aft of the vessel. This could only be done after departure as the mooring winches serve as trawl winches at sea. After a CTD cast with test of the acoustic releases course was set to the northern most working area Omakere.

At 13:40 on 12th March preparations for the first seismic acquisition began with the deployment of 10 Ocean-Bottom seismometers. While crossing the foreseen survey area the bridge carefully searched the sea for mammals. As no sightings were reported the trawl doors

and 3-D seismic streamer system was deployed. Shooting with a 210 cinch GI airgun started on 22:30 hours. Due to cable problems along the cross cable parts of the survey were completed with half of the streamers only. The survey continued until 15th March 19:20 hrs. when a broken cross cable required recovery of the whole system. During the night bathymetry and Parasound profiles were completed. In the morning of the 16th one member of the science crew needed medical treatment from shore. Therefore the cruise was interrupted and R/V SONNE headed for the port of Napier. While waiting for the crewmembers the rescue boats were tested. At 16:00 hrs. the crewmembers returned on board, R/V SONNE returned to the survey area at 22:00 hrs. CTD stations and OBS recovery last until early morning of the 17th. After calibration of the POSIDONIA USBL system the deep towed sidescan was deployed. Until the 19th 14:45 hrs. two sidescan surveys were completed. The first one over the Omakere seep site, while the second one covered the nearby Faure site, which has not been mapped during the SO-191 cruise. During the evening hours the sea state calmed down too less than 2 m height again and the 3-D acquisition system was deployed again. Until the morning of the 20th March a good coverage of the Omakere site was achieved. Due to intensive repair times the survey required more time than scheduled and it was decided to head for Porangahau.

At 15:30 in the afternoon 4 OBS were deployed prior to the preparation of the 3-D P-Cable system. As usual careful expectation of the sea for mammals was done prior to the start of the single airgun. Weather condition decreased during the night. Wind speed of up to 12 m/s and rising wave height of more than 2.5 m called for an interruption of the survey. With further decreasing weather conditions the night could be used for bathymetry and Parasound profiles, which were interrupted in the morning of the 22nd when wind speeds of more than 13 m/s and wave heights of up to 5 m did not allow any useful data collection any more. Slightly decreasing wind speed allowed continuing acoustic profiling courses until 22:30 hrs. With again rising sea state the trawl doors at the stern started to move in the wave splash. Again all work needed to be stopped. During the 23rd sea conditions did not allow to deploy the 3-D system again. Hence Parasound profiles over the Porangahau Ridge were continued and a CTD was collected at Uruti seep site. Despite a still high sea state of 3 m an attempt to deploy the 3-D seismic system again was undertaken in the morning of the 24th. Unfortunately the sea conditions forced the last deployed starboard trawl door to move in the wrong direction. During ships manoeuvre to overcome the situation the port site trawl door came to stop and was washed across the trawl wire. All equipment had to be recovered again. During this operation the port site trawl wire was cut by the trawl door and could no longer be used. The only alternative available was a spare wire of the vessel. As preparation and replacement would require some time it was decided to change the program from 3-D to 2-D profiling. Additional 9 OBS were deployed to enlarge the existing coverage. In the evening the 3-D system was switched into 2-D mode and a 200 m active length streamer could be deployed. 20 hours of multichannel profiling were used to sail across the Porangahau ridge and to add some tie-in lines for the existing multichannel profiles of our New Zealand colleagues. Recovery of the OBS on 25th March lost one instrument. The release system confirms release and lift from the anchor weight, but the unit stuck at deployment depth. It is assumed that the anchor has caught a cable or rope holding the system at depth. We left Porangahau Ridge at 23:30 and headed for Wairarapa.

On our way south we investigated Pahaua seep site but could not locate any flare.

At 15:20 on 26th March we deployed the deep towed sidescan and newly build streamer at Wairarapa area. Unfortunately the streamer failed after one hour and the profiles were sailed with sidescan and sub-bottom profiler only. In the morning of the 27th we recovered the sidescan and deployed the 2-D streamer again. Seismic profiles were shot across most of the

seep sites until we need to interrupt the measurements at 20:30 hrs. due to bad weather conditions (> 17 m/s wind). Announcement of 40 kn to 50 kn wind speed for the night caused us to move away from the Cook Straight during the night. At 11:00 on 28th weather conditions improved and allowed to run three CTDs at Tui, Takahe and North Tower. The evening hours were used to deploy 3 OBS for a 3-D experiment on Opouawe Bank. Parasound and multibeam mapping at night was used to investigate a diapir structure seen on NZ seismic profiles some nautical miles northeast of Wairarapa. In the morning of the 29th weather had improved and allowed deployment of the P-Cable system. The survey was continued until the 2nd April. Varying weather conditions during this time proved that the 3-D system is capable to operate even at wind speeds of up to 30 kn and wave state of up to 3 m. During times of higher swell we stopped profiling and sailed straight away avoiding the danger of having the trawl doors washed across the trawl wire at low speed during the turns. During the morning of the 2nd April the deep towed streamer was deployed again. After an interruption for repair of two broken hydrophones the system worked fine. We completed the profile across Takahe all the way until crossing Piwakawaka seep site. During the night 12 OBS were recovered. OBS-05 did not show up although we received clear distant ranging. The night was finished with courses used to calculate the calibration angles for the ELAC Multibeam. Due to northerly winds the sea conditions were still favourable in the morning of the 3rd and the deep towed streamer was deployed again. Until 16:00 we completed the reverse direction of the profile shot the day before. Two CTD casts were completed before we headed towards OBS05 waiting for the time release at 01:00 on the 04th April. The system did show up in time and will be inspected for the reason of not replying to the acoustic release command. With again rising wind speeds we sailed closer to shore to enable the scientific crew to pack the equipment. Due to urgently required medical treatment for a crewmember we docked in the port of Wellington in the evening hours of the 3rd April already. Leg one terminated on the 4th when the science crew of leg two arrived. Unloading and container packing for the seismic equipment lasted the whole day, while new equipment for leg two was already moved on board.

4.2 Agenda of the cruise SO-214/2

Departure on the 6th April was postponed to 16:30 in the afternoon, as the weather forecast did not announce favourable sea conditions. Therefore most of the laboratory set up could be completed in port. The scientific work was continued when Parasound profiles were completed over Miromiro and Ruru seep sites. The OFOS program at night could only be completed in parts. Heavy sea state caused the instrument to touch ground very often. Due to strong wind and seas conditions it was decided to get the OFOS back on board before the ship modes to another position. This operation became very tough in the morning and therefore the work was stopped at 04:30 at the 7th April. Rough sea state with sometimes more than 5 m high waves did not allow any safe system operation. Moreover the waves washed over the working deck time by time and access was forbidden.

The weather conditions did not improve until the 9th April, when SONNE returned to the working area. The scientific work program was continued with CTD and TV-MUC work. Successful gravity cores were recovered from Takahe seep site. On the 10th 12 Ocean-Bottom stations for magneto-telluric and electromagnetic observations were deployed over South Tower. A mooring with a 60 m thermistor string was deployed at Tui seep site. The night hours were used to collect the first CSEM line with the bottom towed BGR array. In the course of the 11th April the IFM-GEOMAR CSEM source was set up and the first time connected to the 8 km long deep-sea cable. Unfortunately the data connection failed and the night hours were used for additional CTD and coring work around Takahe. After reinstallation of the original slip ring for the fibre optic winch cable the IFM-GEOMAR

CSEM source completed a deck test next day. Unfortunately one of the pressure cylinders was not completely sealed and the deployment needs to be postponed again. The night hours of the 13th were dedicated to TV-MUC and OFOS tracks instead. In the afternoon the first deployment of the CSEM-GEOMAR source could be completed with one transmitting station before the cable adapter of the deep-sea cable connection failed. In the night all bottom station were retrieved to give room on South Tower for the scheduled towed experiment with the CSEM-BGR equipment. Two profiles were almost completed when the front weight of the BGR array got stuck at South Tower. Only when the vessel was direct above of the instrument it could be freed from ground. Unfortunately the strength member of the towed receiver array was broken and could not be recovered. The afternoon and night hours were dedicated to coring and CTD work. In the morning hours of the 16th the large TV-grab was prepared to search for the missing receiver array. Although the cable was spotted after short time it could not be grabbed. Repair time of the modems in TV grab was used to continue recovery trials with a ship build search anchor and the OFOS TV sledge. A last trial with the TV grab failed on 23:40 hrs. on the 16th. Video observation of the search anchor and tension display of the TV grab showed that the cable has been grabbed during the search but was lost while the equipment was carefully lifted to the surface. Obviously the head still stuck at some seafloor obstacle at South Tower. After a last core R/V SONNE set course towards the 100 nm distant Porangahau area.

On the 17th at 15:00 SONNE returned to the Porangahau area where one OBS could not be retrieved during leg 1. Distant measurements showed that the instrument is still at the ground, some 180 South of the surface deployment position. Four hours search with the TV grab were undertaken with no sighting of the instrument. At 20:15 the area was left in order to continue the scientific work on Omakere ridge.

During the five-hour transit to Omakere southerly winds increased up to 8 Bft. with increasing wave state. No secure working was possible under this conditions and the vessel set course to Hawks Bay for shelter. The weather forecast did announce strong winds up to 9 Bft. – 10 Bft for Monday 18th. The calm water conditions in Hawkes Bay were used for further equipment tests of the CSEM source.

On 19th April decreasing wind conditions and a promising forecast for the afternoon supported the transit to the last working area on Omakere Ridge. After arrival on site we need to wait for another 4 hrs. until sea state conditions improved enough to risk the deployment of the OFOS frame. After a two hours dive across Bears Paw seep site the MUC was deployed for a last sampling. At 19:00 hrs. local time research activities of cruise SO-214 were terminated and R/V SONNE set course to the port of Auckland.

All meta data of the cruise are available through the IFM-GEOMAR Data Management Portal (https://portal.ifm-geomar.de/web/guest/home)

5. Scientific Equipment

5.1 Shipboard Equipment

5.1.1 Navigation

Joerg Bialas

Several Ashtec AC12 GPS receivers were set up to provide position information of the various systems. On-board a GPS antenna was mounted on the port side airgun rail next to the stern of the ship (Fig. 5.1.1.1). Additional GPS receivers were mounted on the two trawl doors for the 3-D P-Cable system. NMEA strings from the remote GPS were transmitted via radio link on-board R/V SONNE. RS232 links submitted the position information to the

OFOP PC. OFOP was used to display the ships and trawl doors positions on top of a bathymetric map. Track keeping accuracy could be controlled by the display of the waypoints. In addition offsets between trawl doors and trawl door – ship were displayed. A connecting line between the trawl doors is drawn in user-selected intervals. Its width can be adjusted to the expected CDP coverage. Storage of the coverage lines enables to redraw the achieved coverage any time. Additional backup for the online data processing was done through HyperTerminal capturing (Fig 5.1.1.2).

Although the GPS receivers were setup with the same parameters one of them showed unstable position delivery. For unknown reasons the system could track only two satellites over shorter or wider time spans, sometimes the tracking was lost for several hours. At the same time a third receiver on the second trawl door and the shipboard receiver behaved well. The GPS was replaced by the spare unit, which was dedicated to be mounted on the airgun.

With the P-Cable system the streamer sections are not distributed along a straight line. Due to drag forces in the water the cross cable can best be described forming a shape somewhere between a triangular and a half circle. Navigation processing sets out to calculate the exact shape by using the GPS positions of the trawl doors and the first arrival time of the direct wave from the airgun signal. During the course of profiling the trawl doors were affected by water currents and sea state. Therefore offsets between starboard and port side door and the airgun in the centre are varying depending on the heading of the sail line (Fig. 5.1.1.3). Based on GPS positions of the trawl doors and the first arrival of the airgun shots at the streamer hydrophones the position of each streamer segment is calculated. Triangulation is applied and provides coordinates for the streamer groups within a range of less than 5 m. The assumption of a catenary shaped outline for the cross cable provides best results (Fig. 5.1.1.3). Based on the resulting shot table interpolation, stacking and migration of the entire data cube can be done. For the raw processing on-board R/V SONNE a migration grid of 6.25 m * 6.25 m could be achieved.

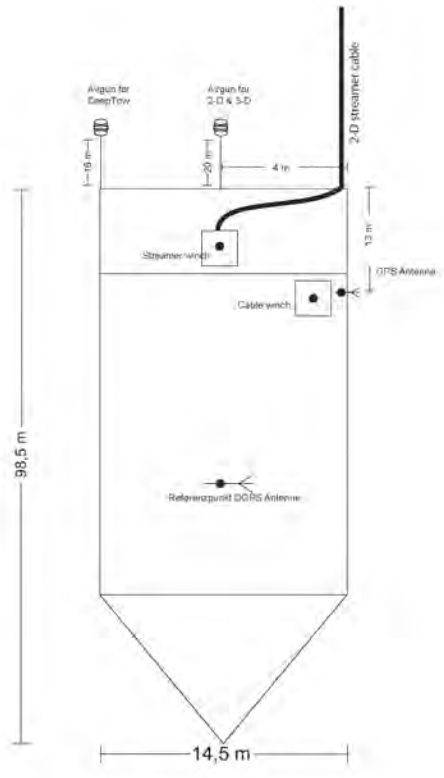

Figure 5.1.1.1: Measures used for the positioning of gun and streamers during the seismic surveys

For 2-D multichannel acquisition the streamer was deployed through the rear A-frame. The streamer composes of 200 m active length, 25 m stretch section and 40 m tow cable. Once the full length was paid out a large diameter block was used to move the streamer to the port side of the ships stern. The GI-Airgun was then deployed and towed as usual from the centre of the stern (Fig. 5.1.1.1).

With the deep towed multichannel streamer application the deep-sea cable need to be guided through the main A-frame sheave in the centre. Therefore the airgun needed to be moved to the starboard side. In order to avoid collisions between the deep-sea cable and the gun the gun tow wire was shortened to 16 m length (Fig. 5.1.1.1).

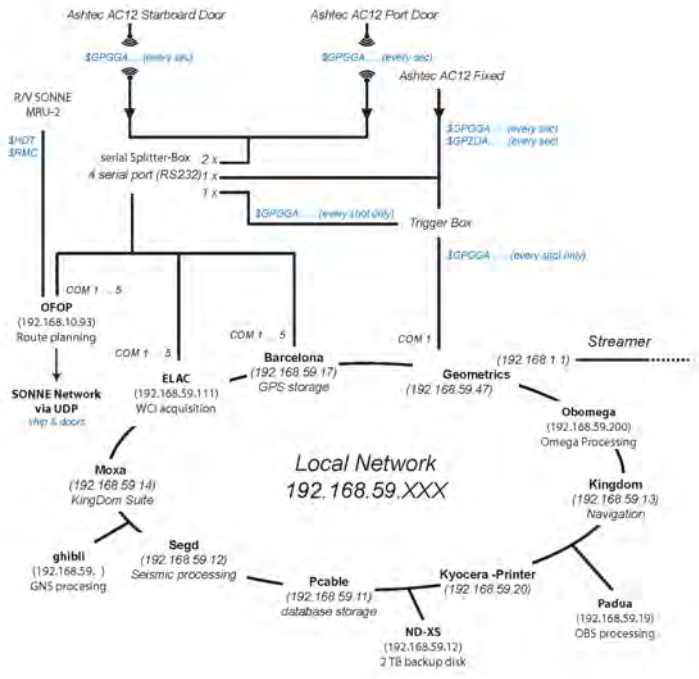

Figure 5.1.1.2: Local Area Network set up for the seismic data handling

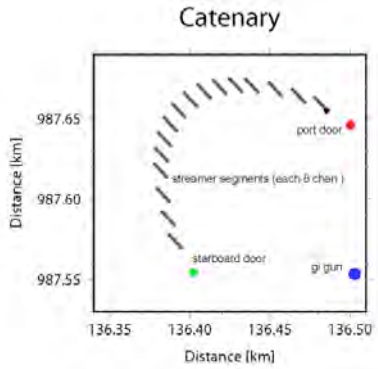

Figure 5.1.1.3: Triangulation of the P-Cable streamers and the airgun

5.1.2 Simrad EM120 Multibeam

J. Greinert

Knowing the depth and morphology of the seafloor is essential for cold seep research. It is important for deploying and towing gear at/over the seafloor and of course gives a detailed insight into tectonic and sedimentary developments.

System

The EM120 system is a multibeam echo sounder (with 191 beams) providing accurate bathymetric mapping up to depths higher than 11000 m. This system is composed of two transducer arrays fixed on the hull of the ship, which send successive frequency coded acoustic signals (11.25 to 12.6 kHz). Data acquisition is based on successive emission-reception cycles of this signal. The emission beam is 150° wide across track, and 2° along track direction. The reception is obtained from 191 overlapping beams, with widths of 2° across track and 20° along it. The beam spacing can be defined as equidistant or equiangular, and the maximum seafloor coverage fixed or not. The echoes from the intersection area (2°x 2°) between transmission and reception pattern, produce a signal from which depth and reflectivity are extracted.

For depth measurements, 191 isolated depth values are obtained perpendicular to the track for each signal. Using the 2-way-travel-time and the beam angle known for each beam, and taking into account the ray bending due to refraction in the water column by sound speed variations, depth is estimated for each beam. A combination of phase (for the central beams) and amplitude (lateral beams) is used to provide measurement accuracy practically independent of the beam pointing angle. The raw depth data need then to be processed to obtain depth-contour maps. In the first step, the data are merged with navigation files to compute their geographic position, and the depth values are plotted on a regular grid to obtain a digital terrain model (*DTM)*. In the last stage, the grid is interpolated, and finally smoothed to obtain a better graphic representation.

Together with depth measurements, the acoustic signal is sampled each 3.2 ms and processed to obtain a cartographic representation, commonly named mosaic, where grey levels are representative of backscatter amplitudes. These data provide thus information on the sea-floor nature and texture; it can be simply said that a smooth and soft seabed will backscatter little energy, whereas a rough and hard relief will return a stronger echo.

Method

During SO214 a swath width of 120 or 100° was usually used for mapping. The system kept running during the entire time and only occasionally the recoding was turned off when the ship was on station (e.g. recovery of OBS stations). New raw data files were started about every hour. During the cruise no additional data processing was performed except data editing in Fledermaus and export of xyz data. Those xyz data where integrated in the existing data set from previous cruise in 2006 and 2007 namely TAN0607, TAN0616 and SO191.

Later processing will also deal with a more sophisticated backscatter analyses (MB Systems, Fledermaus) and merging of multibeam data with sidescan and sub seafloor information.

5.1.3 L3-ELAC Nautik SBE 3050 Multibeam

Cord Papenberg

The SeaBeam 3050 is the latest generation of mid and shallow water multibeam bathymetric sonar systems from L-3 Communications ELAC Nautik GmbH. The new multi-ping technology of the SeaBeam 3050 allows a higher maximum survey speed without losing 100% bottom coverage by creating two swaths per ping cycle. The system operates in the 50 kHz frequency band in water depths ranging from 3 m below the transducers to approx. 3,000 m. The system can be utilized at survey speeds of up to 14 knots. It has an across-ship swath wide of up to 140 degrees. A maximum of 386 reception beams is provided for each multi-ping. The SeaBeam 3050 uses a transmit technique, which compensates fully for vessel pitch

and yaw motion. The compensation is achieved by splitting the transmit fan in several sectors which can be steered individually. This technique achieves full motion compensation and guarantees a stable straight coverage under the vessel. The SeaBeam 3050 generates sonar data for wide-swath contour charts, backscatter data for seabed sediment classification, raw data for water column imaging (WCI) and sidescan data for side-scan images.

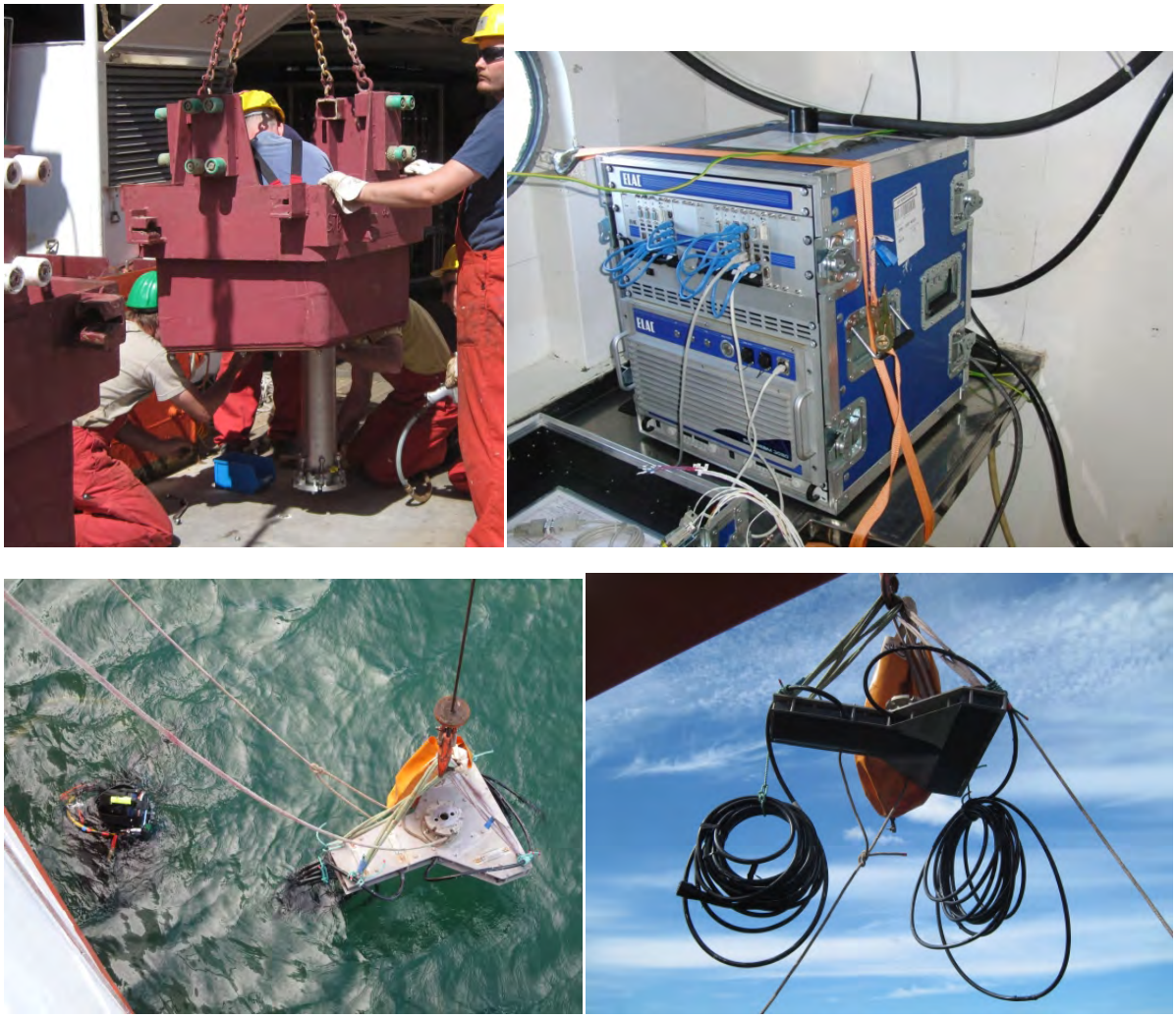

Figure 5.1.3.1: Mobile ELAC-Multibeam. Top:

5.1.4 Parasound

J. Greinert

The PARASOUND system works both as a low-frequency sediment echo sounder and as a high-frequency narrow beam sounder to determine the water depth. It utilizes the parametric effect, which produces additional frequencies through nonlinear acoustic interaction of finite amplitude waves. If two sound waves of similar frequencies (here 18 kHz and e.g. 22 kHz) are emitted simultaneously, a signal of the difference frequency (e.g. 4 kHz) is generated for sufficiently high primary amplitudes. The new component travels within the emission cone of the original high frequency waves, which are limited to an angle of only 4° for the equipment used. Therefore, the footprint size of 7% of the water depth is much smaller than for conventional systems and both vertical and lateral resolutions are significantly improved.

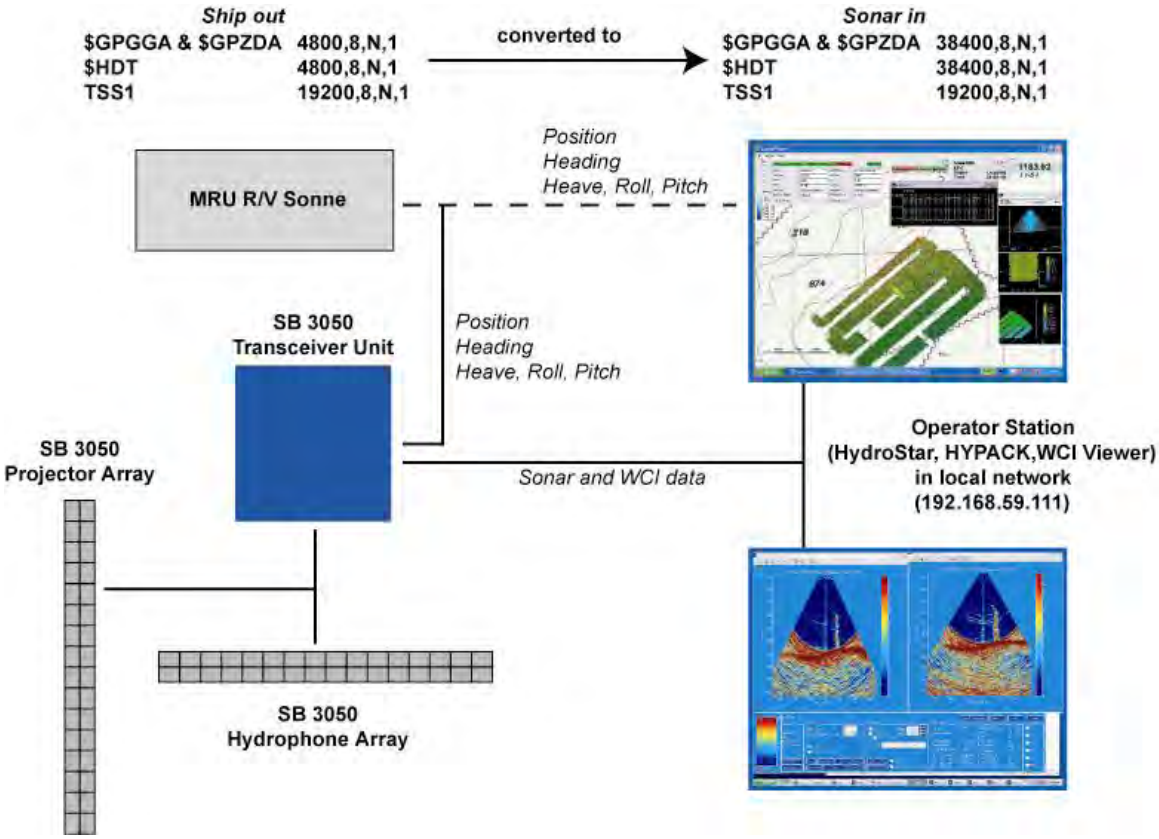

Figure 5.1.3.2: Mobile ELAC-Multibeam. Top:

The PARASOUND system is permanently installed on the ship. The hull-mounted transducer array has 128 elements within an area of 1 m by 2 m. It requires up to 70 kW of electric power due to the low degree of efficiency of the parametric effect. In 2 electronic cabinets, beam formation, signal generation and the separation of the primary (18, 22 kHz) and secondary frequencies (4 kHz) is carried out.

The source signal was a band limited, 2-6 kHz sinusoidal wavelet with a dominant frequency of 4 kHz and duration of 1 period (250 µs total length).

We used the following settings for the primary high frequency (PHF -> 18 kHz water column signal) and the secondary low frequency (SLF -> parametric wave for sub-bottom signal). We changed the Transmission beam width to a broader signal by manually selecting 8 x 8 elements to be used in the transducer. The settings in the control window of PARASOUND were as shown in Figure 5.1.4.1.

The Hydromap sounder environment settings were as shown in Figure 5.1.4.2. During Leg 2 we adjusted the sound velocity at the keel to the real value and also entered the correct average value of the mean sound velocity of the water column.

The online display settings were adjusted as shown in Figures 5.1.4.3, 5.1.4.4, 5.1.4.5, and 5.1.4.6, giving very good online results for sub bottom information and the water column at the same time. It is important to note that the 18 kHz (PHF) recording window was set to 600 m and the seafloor was kept at the bottom of the screen. The sub-bottom (SLF) window was 200 m wide and was kept at the top screen.

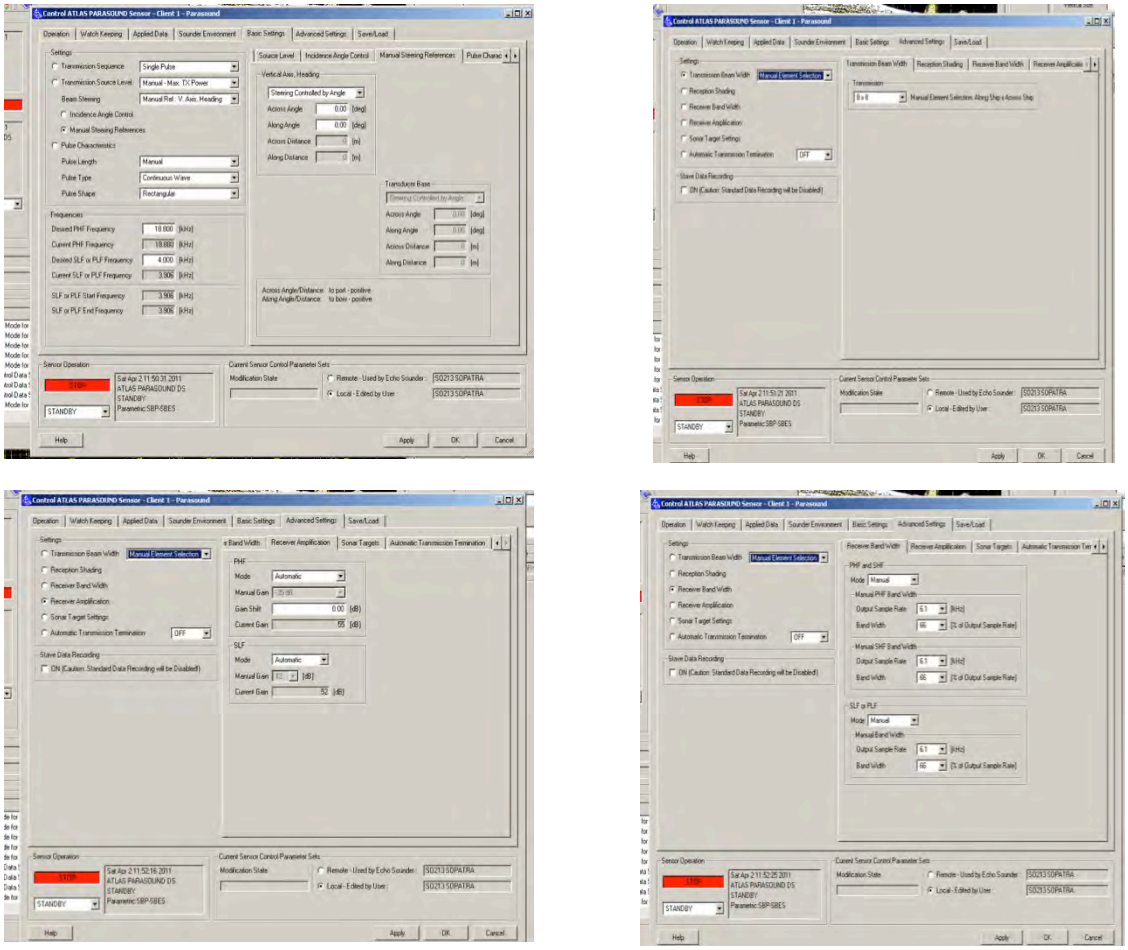

Figure 5.1.4.1 Basic and advanced PARASOUND settings used during SO214. Of note is that a manual element selection for the transmission beam width was selected (8 by 8 elements) in order to generate a broader signal.

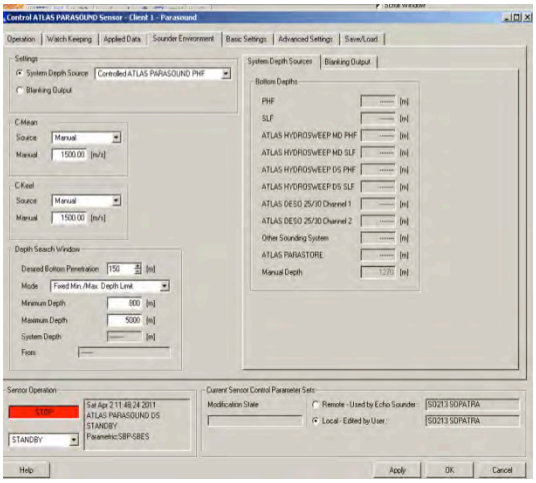

Figure 5.1.4.2 The Hydromap sounder environment settings. The sound velocity at the keel and the average water column velocity are used together with the PHF signal to predict the water depth.

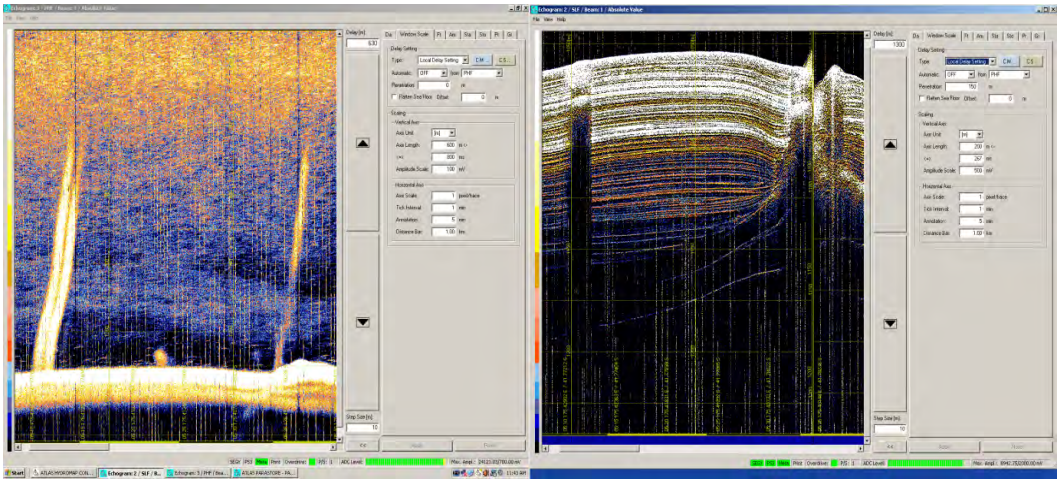

Figure 5.1.4.3 Examples of PHF (left) and SLF (right) acquisition over gas seeps. The window scale settings used are shown to the right of each data display. The seafloor in the PHF acquisition was kept close to the bottom of the screen so that entire flares in the water column could be imaged. In contrast, the seafloor in the SLF acquisition was kept as close to the top of the screen as possible to record as much sub-seafloor data as possible.

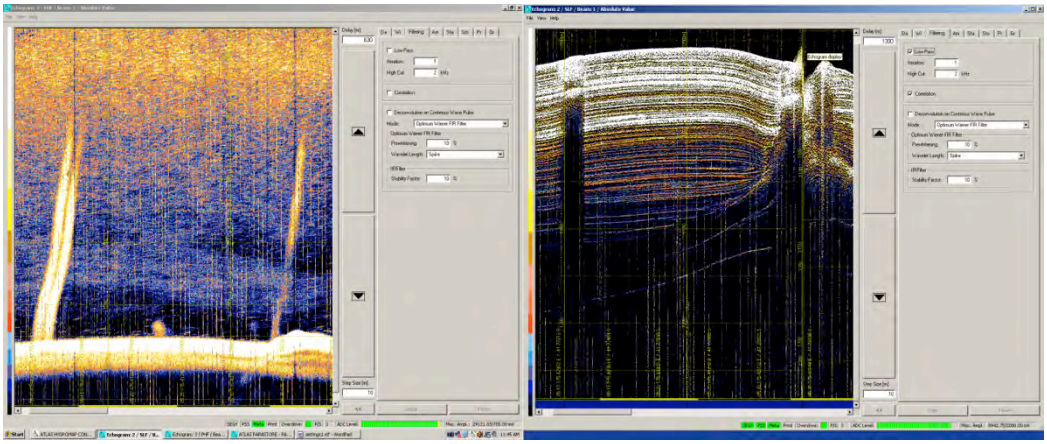

Figure 5.1.4.4. Same PHF and SLF data displays as those given in Figure 5.1.4.3. Here the filtering parameters for the online display are shown. Note: data are filtered on screen, but it is the raw data that are saved.

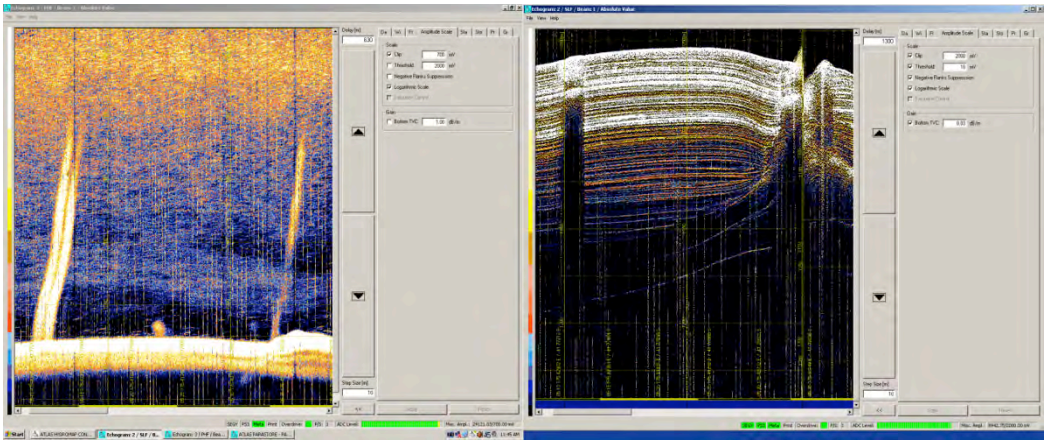

Figure 5.1.4.5. Same PHF and SLF data displays as those given in Figure 5.1.4.3. Here the amplitude scale parameters for the online display are shown. Negative flank suppression in SLF mode was used to produce a clearer image.

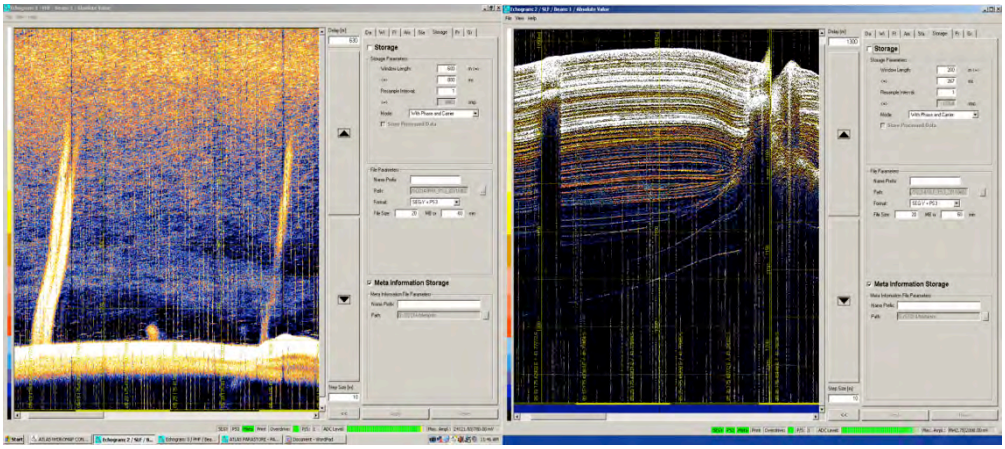

Figure 5.1.4.6. Same PHF and SLF data displays as those given in Figure 5.1.4.3. Here the storage parameters are shown. Note: data were saved both as SEG-Y format, and as PS3 format.

5.1.5 CTD (Conductivity-Temperature-Depth) operations

Jens Greinert, Laura Haffert, Mario Veloso, Peter Urban, Aneurin Henry-Edwards, Piet van Gaever, Kamila Sztybor

The goals of the CTD program were to; (1) provide a sampling platform for the collection of water samples, and (2) map the distribution of (methane) signals within a previously identified survey area (information from side scan sonar, historical, etc.), and (3) attempt to determine the input mechanism of subsurface methane (diffusive, bubble or plume) and (4) to study the possible changes of seepage activity by comparing the analyses from 2011 with those from 2007 and 2006. 23 CTD casts have been performed in total during SO214. Submarine methane seepage is a major source of methane to the ocean. Methane is also one of the most commonly used chemical tracers for shipboard detection of seeps due to its relative ease of shipboard measurement, low CH_4 background concentrations in deep sea water, and its relatively short residence time (ca. 10 days) in plumes rising above seeps. A total of 544 samples were collected and analysed for CH_4 during SO214.

System

All casts used a high-precision *SeaBird 911plus* CTD that samples at 24 Hz with a temperature accuracy was better than 0.001°C; accuracy of the conductivity cell is nominally 0.0003 S/m. Water samples were collected and CH_4 analyses determined by GC on-board using mainly a head-space equilibration extraction method and also to a lesser extent a vacuum extraction system. The bottom contact alarm allowed us to safely lower the CTD to within 3-5 m of the bottom. The rosette holds twenty-four 10l Niskin Bottles.

Method

Data were recorded using the Seabird Seasave7 program. Post processing for data conversion, binning and ASCII export were performed with the SBE-Data-Processing software also from Seabird. One meter binned data were converted to ODV (Ocean Data View from AWI-Bremerhaven) readable files and merged with the already existing data set of CTD measurements from 2006 and 2007 (TAN0607, TAN0616, SO191). Bottle data information was also incorporated into the ODV database and methane concentrations were entered for the complete data set.

Navigation

To accurately position the CTD in flares we run most of the CTD casts with USBL navigation, which was displayed online on an OFOP computer next to the Seabird recording computer. In addition we had the 18 kHz signal of the Parasound displayed as well and could

check online the progress of the CTD going down and manoeuvre the ship in the correct position to sample the flares.

5.1.6 OFOS

David Bowden

Specifications

The Ocean Floor Observation System (OFOS) is a towed camera system owned and operated by RF GmbH aboard RV SONNE. For voyage SO214-2, the platform was deployed with three video cameras and one still image camera, all orientated vertically downwards.

Two standard definition (SD) video cameras (one colour and one monochrome) were viewed and recorded in real time at the surface via the ship's conducting cable. A Sony HDR XR520VE video camera fitted with a wide-angle lens adapter recorded high definition (HD 1080 50i format) digital colour video to an integral hard disc drive, which was downloaded on return to the surface. A Panasonic DMC-LX2 digital compact still image camera with focal length 6.3 mm (equivalent to 28 mm in full-frame 35 mm format) took images at 15 s intervals. Still images were saved in the camera and downloaded at the surface.

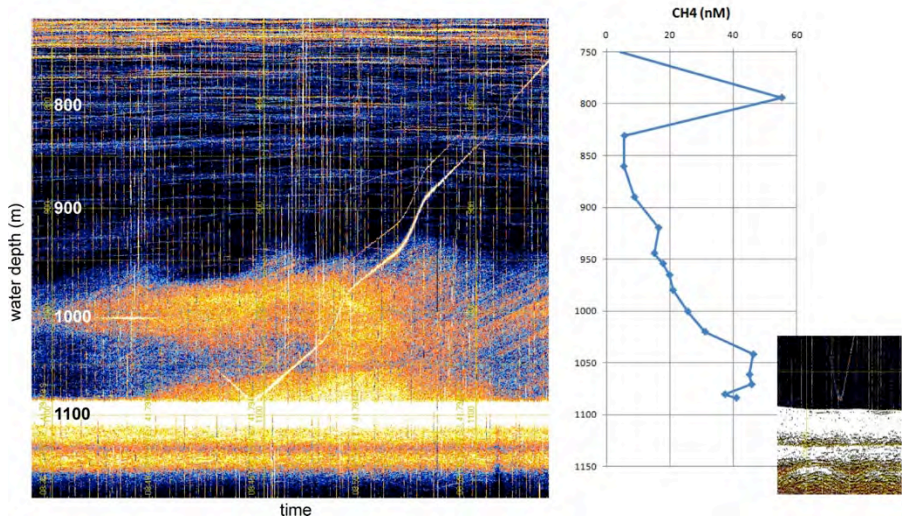

Figure 5.1.5.1: Screenshots of the low (right) and high (left) frequency of Parasound during CTD 10 at Piwakawaka at Opouawe Bank. On the right image the CTD is about 5m above the seafloor. During the operation, the CTD was slowly towed into the flare and the ship was kept on station while the CTD samples the water column on its way up. The methane concentrations show a "normal" increased towards the seafloor with a CH_4-enriched layer at 800m water depth

Lighting for video was from four halogen flood lamps and, for still images, from two strobe heads. A pair of parallel red laser pointers set 20 cm apart and projected on to the seabed provided a scaling reference, while a third laser set at an angle to the plane of the scaling lasers indicated when the platform was at its target operating altitude: the three laser points were in line when the platform was 3 m above the seabed. A weight suspended by rope from the camera platform provided an additional aid to judging altitude. At 3 m altitude, individual OFOS still images covered 3.5 m^2 of seabed, and the HD video frame width was 2.0 m. The seabed position of OFOS was monitored using the Posidonia ultra-short baseline (USBL) acoustic tracking system.

OFOS was deployed from the starboard side gantry on the fibre-optic cable, and its position was plotted in real time against high-resolution side-scan sonar (SSS) images of the

seabed (5.3 and 6.3) using the application Ocean Floor Observation Protocol (OFOP, [*Huetten and Greinert*, 2008]. Target tow speed was 0.5 to 1.0 knots and transect duration was determined by the size of the SSS target being investigated. Transects were planned to cross high backscatter targets associated with acoustic flares detected in earlier voyages.

Seabed observations

The aim of real-time logging during OFOS video transects was to generate immediate maps of the seabed which could be used to assess the spatial extent of seep-related substrates and fauna at each of the putative seeps sites.

Observations of substrate type, benthic invertebrate fauna, sediment bioturbation marks, and fishes, were recorded throughout each transect. Observers selected from a set of pre-determined labels by clicking lists in the OFOP interface, which recorded each observation referenced by UTC time, seabed coordinates, depth, and full navigation data. Substrate observations were recorded every few seconds through the transect to provide a near-continuous record of seabed type.

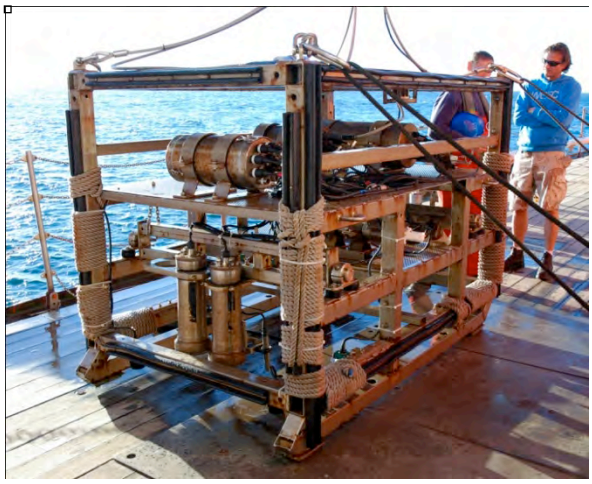

Figure 5.1.6.1: Ocean Floor Observation System (OFOS): a towed camera platform carrying video (SD colour, SD monochrome, and HD colour) and still image (12 megapixel digital compact) cameras. Ready for deployment procedure

Substrate types were recorded on a simplified categorical scale: bedrock (continuous rock substrata); boulders (rocks >25 cm); cobbles (rocks <25 cm); muddy sediments (no discernible grain structure in video images), sulphidic sediments (black muddy sediments). All rock seen was assumed to be authigenic carbonate and thus the first three categories indicate differing amounts of seep-derived carbonate rock. An additional substrate category; 'Clam shell', was used to indicate areas covered by dead shells of vesicomyid clams (*Calyptogena* sp.) which can be locally abundant at New Zealand seeps sites[*Baco et al.*, 2010]. Because it was not possible to differentiate between live and dead clams from the real-time video images, all clams were recorded as 'Clam shell'

Seep-associated mega-fauna (i.e. those identifiable from real-time video) were recorded under four categories: *Lamellibrachia* sp. tube worms; *Calyptogena* sp. clams and clam shells; bacterial mats, and the encrusting white sponge *Pseudosuberites* sp.. Non seep-associated fauna on background sediments were recorded at a range of higher taxonomic levels (e.g. Class, Order) or by common names (e.g. orange roughly). All fauna were recorded as individual observations until their abundances became too high to capture in real time (e.g. with *Lamellibrachia* sp. tube worms at some seeps), when observations were clicked continuously to indicate high abundances.

5.2 Geophysical instrumentation

5.2.1 GI-gun

Joerg Bialas

For the high-resolution seismic a GI-gun manufactured by *Sercel Marine Sources Division* with a volume of 3.8l (105 cinch generator chamber, 105 cinch injector chamber) was used. It was operated in harmonic mode. The compressed air was supplied by the super charger of R/V SONNE with a pressure of 210 bar. The profiles were acquired with a shot interval of 6 s or 7 s. The GI-gun was attached with chains to a steel frame and towed either from the centre at 20 m or at the starboard side 16 m behind the stern in a depth of 2 m (Fig. 5.1.1). The setup with the floatation is shown in Figure 5.2.1.1.

Figure 5.2.1.1: GI-gun mounted below the carrier to which a Polyform floatation is attached.

External trigger during SO214-1

With the development of the 3-D P-Cable system IFM-GEOMAR has build its own GPS based trigger system. The shipboard GPS receiver delivers ZDA and PPS to timing box. The timing box allows selecting the shot interval by a wheel switch in full second intervals. The TTL trigger pulse is delivered to a distribution box, from which the LongShot gun controller the Geometrics streamer system receive the signal. Together with the trigger generation a time stamp is written to an internal SD memory card with shot coordinates.

To ensure all systems trigger with the same reference all trigger circuits were adjusted to work on the uprising flank (TTL+). The LongShot gun controller was set to a 50 ms aim point. Later the aim point was shifted to 63 ms. It is the time delay after the trigger to which the gun fire is aligned. The automatic adjustment based on the received shot signal from the gun hydrophone usually was within +/- 5 ms.

5.2.2 P-Cable streamer

Joerg Bialas

Compared to standard reflection seismic applications in 2-D and 3-D the basic difference is that the P-Cable is build by a cross cable towed perpendicular to the ships heading (Fig. 6.2.3.1.1.a & b). Instead of a few single streamers the P-Cable uses a large number of short streamer sections towed parallel from the cross cable. Drawback is the limited depth penetration due to the short offsets, which do not allow the removal of the multiple energy. This is well compensated by the reduced costs of the system and the ability to operate it even from small multipurpose vessels, the usual academic platform for marine research.

Figure 5.2.2.1 shows the basic principle of the P-Cable design. The advantages of the IFM-GEOMAR development are twofold. The cross cable is based on a strength member, a Dyneema rope, which takes the stretch forces of the trawl doors (Fig. 5.2.2.2). Attached to this rope is the data cable with the streamer connections (Fig. 5.2.2.3). IFM-GEOMAR developed a modular cross cable, which allows exchanging each single streamer connector (node) in case of a malfunction. This allows easy service and reduced service costs. Other systems were built by a data cable moulded in one piece, which need to be replaced as whole part if one node fails. As well the modular design enables to insert connecting cables of different length between the nodes. Hence an adoption to different resolutions of P-Cable and SwathSeis application is possible. The current grade of the system provides 16 active nodes connected by 15 m and 10 m long data cables. On both sides the first node is located 12 m off the triple point. The 190 m long cross cable is stretched by two trawl doors, floating at the sea surface. Floats attached to each break out help to keep the streamers at 2 m depth (Fig. 5.2.2.4). Each one of the trawl doors provides a lifting force of 2 tons. Although the doors are designed to provide maximum lift at 4 kn sailing speed the cross cable was stretched to 125 m width at 3 kn already.

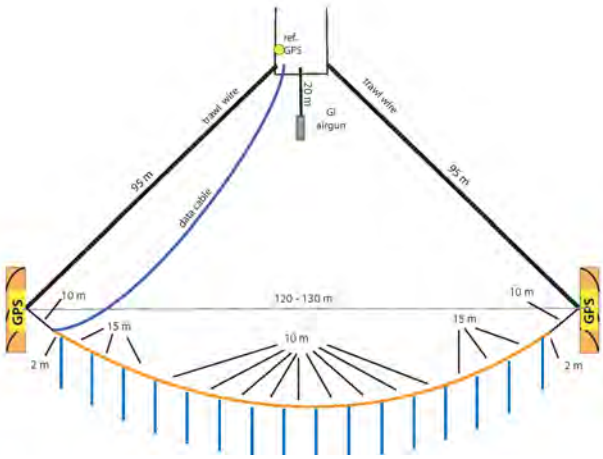

Figure 5.2.2.1: Sketch of the P-Cable design applied during the SO-214 cruise

Upon deployment the door next to the umbilical is released from its rest position (Fig. 5.2.2.5) while the ship sails at 0.5 kn through water against wind and waves. The door is lowered into the water while a 10 m long lead cable between door and connection point of cross cable is kept on board. Next the data cable from the recording device to the door is hooked to the connection between lead wire and cross cable. Now trawl wire, data cable and cross cable are paid out simultaneously (Fig. 5.2.2.5). At the same time streamer sections are connected to the nodes of the cross cable. Floats are fixed to each node in order to keep the cross cable at even depth (Fig. 5.2.2.4). When the entire cross cable is paid out a 50 m support rope on the support winch is used for secure transmit of the cross cable from the support winch to the lead wire of the second trawl door (Fig. 5.2.2.5). Now both trawl wires are given out until the final length with sufficient stretch of the trawl doors is reached (Fig. 5.2.2.5).

Positions of the trawl doors with real coordinates and relative distance to the vessel are provided within an online navigation package. Autonomous GPS receivers were mounted on each trawl door together with a serial radio link to the vessel (Fig. 5.2.2.6). GPS positions from the vessel and trawl doors are recorded via a serial multiport on a laptop. Splitters provide the NMEA strings for a second laptop. The OFOP program is used to display ship and trawl door positions online on top of bathymetric map. Scheduled track lines can be displayed as well. Moreover the offsets between trawl doors and between doors and vessel are calculated. A connection line between the two trawl doors can be drawn in selectable time

intervals. The length of the line can be adjusted to the expected CDP coverage. Hence a coverage map is build up on the screen and allows identifying possible gaps in the 3-D coverage immediately.

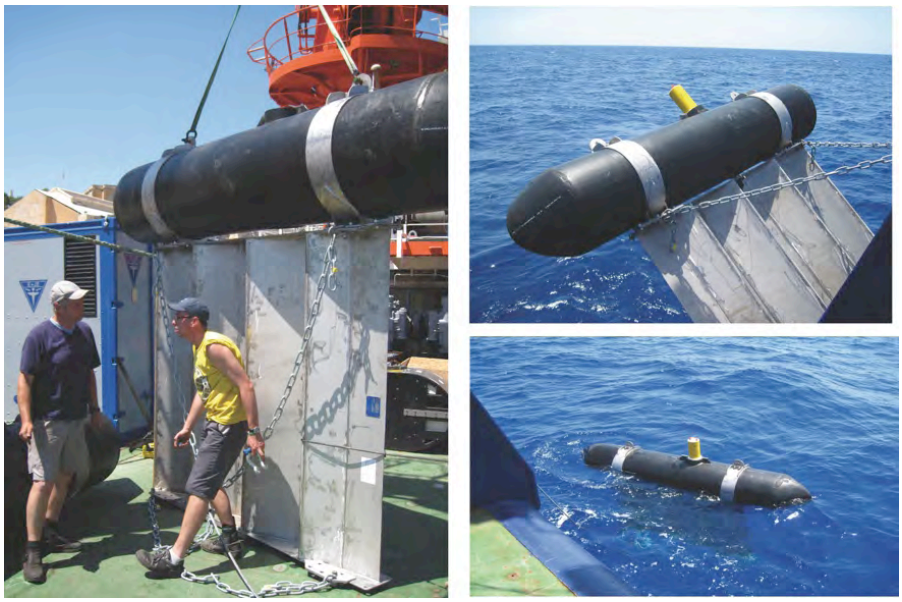

Figure 5.2.2.2: Photographs of the trawl doors.
Left: floats are mounted on the paravanes, Top right: halfway lowered, ready for deployment. The yellow cylinder houses the GPS receiver and the radio modem. Bottom right: floating away from the vessel

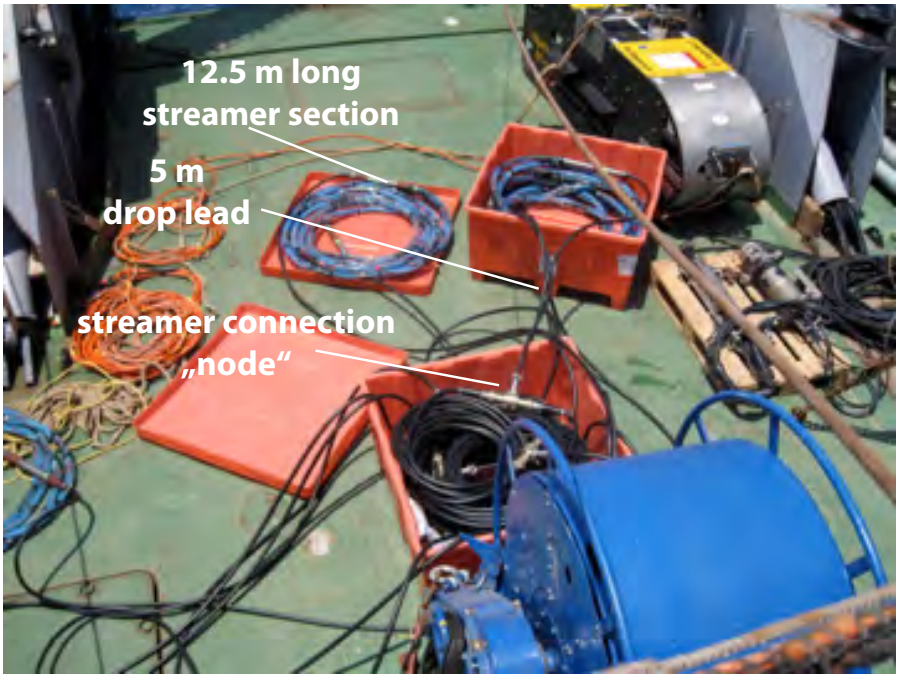

Figure 5.2.2.3: Photograph of cross cable, drop leads and streamer section during dry test on board

Figure 5.2.2.4: Floats are fixed on the cross cable in order to keep it at about 2 m depth during profiling

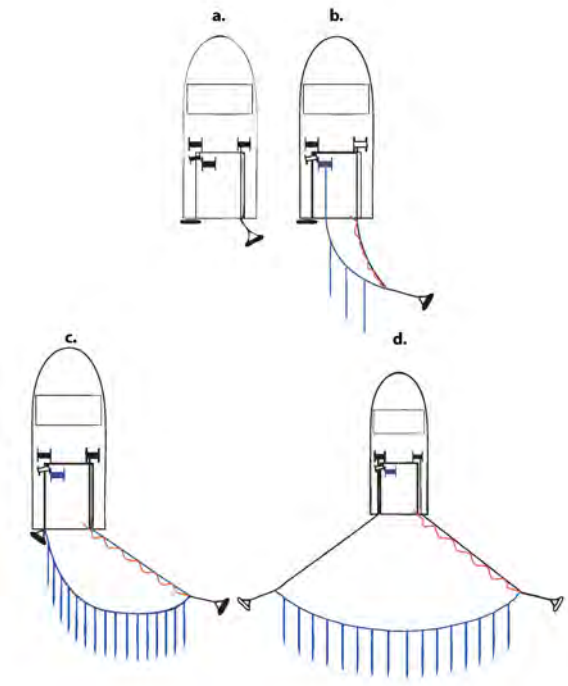

Figure 5.2.2.5: Sketch illustrating the steps during deployment

5.2.3 The Ocean Bottom Seismometer (OBS)

Joerg Bialas

Technical Description

The first GEOMAR Ocean Bottom Hydrophone (OBH) was built in 1991 and tested at sea in January 1992. This type of instrument has proved to have a high reliability; more than 4000 successful deployments were conducted since 1991.

Figure 5.2.2.6: Layout of the entire configuration scheme.

Top: photograph of the towed equipment with indication of system parts

Bottom: schematic drawing of the control and processing PCs, radio, data and network connections are indicated

The IFM-GEOMAR Ocean Bottom Seismometer 2002 (OBS-2002, Fig. 5.2.3.1) is a new design based on experiences gained with the IFM-GEOMAR Ocean Bottom Hydrophone (OBH)[*Flüh and Bialas*, 1996] and the IFM-GEOMAR Ocean Bottom Seismometer (OBS)[*Bialas and Flüh*, 1999]. For system compatibility the acoustic release, pressure tubes, and the hydrophones are identical to those used for the OBH. Syntactic foam is used as floatation body again but compared to the IFM-GEOMAR OBH/S in a less expensive cylinder shape. The entire frame can be dismounted for transportation, which allows storage of more than 50 instruments in one 20" container. A total of 20 OBS instruments were available on RV SONNE for the NEMESYS project. Altogether 28 sites were deployed for recording seismic data during SO-214.

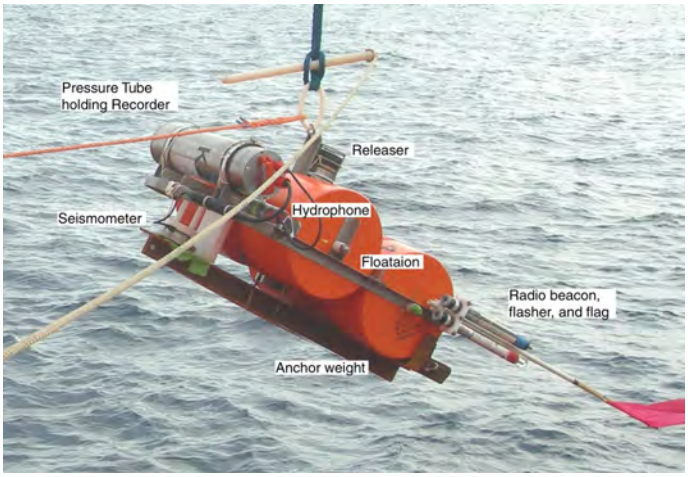

Fig. 5.2.3.1 The IFM-GEOMAR Ocean Bottom Seismometer design 2002

Four main floatation cylinders are fixed within the system frame, while additional disks can be added to the sides without changes. The basic system is designed to carry a hydrophone and a small seismometer for higher frequency active seismic profiling. The sensitive seismometer is deployed between the anchor and the OBS frame, which allows good coupling with the sea floor. The three-component seismometer (*KUM*) is housed in a titanium case, modified from a package built by Tim Owen (Cambridge) earlier. Geophones of 4.5 Hz natural frequency were used.

While deployed to the seafloor the entire system rests horizontally on the anchor frame. After releasing its anchor weight the instrument turns 90° into the vertical and ascends to the surface with the floatation on top. This ensures a maximally reduced system height and water current sensibility at the ground (during measurement). On the other hand the sensors are well protected against damage during recovery and the transponder is kept under water, allowing permanent ranging, while the instrument floats at the surface.

At the beginning of the cruise a releaser tests were carried out. For this we attached all instruments to the CTD-frame and lowered it to a water depth of 2000 m. The acoustic signal unit was used to operate all of them. Twenty releasers passed the test successfully and could be fixed to the OBS-frames for further use. In case one should fail to react to the acoustic signal, they all had a time release programmed for April 04.

The Marine Broadband/ Long-term Seismic Recorder (MBS & MLS)

The signals of the sensors are recorded by use of the *Marine Broadband Seismic Recorder* ***(MBS)*** and the *Marine Long-term Seismic Recorder* ***(MLS)*** that are manufactured by *SEND GmbH.* The MBS-Recorders are specially designed for short-time high-resolution recordings due to their high precision internal clock. Depending on the sampling rate, data

output could be in 15 to 18 bit signed data. Based on digital decimation filtering, the recorder systems were developed to serve a variety of seismic recording requirements. Therefore, the bandwidth reaches from 0.1 Hz for seismological observations up to the 50 Hz range for refraction seismic experiments and up to 10 kHz for high resolution seismic surveys. For our purpose we run the MBS-Recorder with 1000 Hz sampling frequency and MLS-Recorder with 200 Hz.

Before deployment, setting and synchronizing the time as well as monitoring the drift was carried out automatically by synchronization signals (DCF77 format) from a GPS-based coded time signal generator. Clock synchronization and drift are checked after recovery and compared with the original GPS unit. The samples are saved on PCMCIA storage cards together with timing information. After recovery the flashcards need to be copied to a PC workstation. During this transcription the data are decompressed and data files from a maximum of four flash memories are combined into one data set and formatted according to the PASSCAL data scheme used by the *Methusalem* system.

5.2.4 DTMCS – Deep Towed Multichannel Streamer

Jörg Bialas, Ingo Klaucke

With standard surface streamers the lateral resolution is reduced with increasing water depth. Using a deep-towed streamer could provide a constant improved resolution as the receiver array is towed about 100 to 200 meters above the seafloor (Fig. 5.2.4.1). Due to the drag of the deep sea cable in the water the towfish is expected to be 2 to 2.5 times the water depth offset behind the vessel. Operating a standard GI airgun as sound source this allows undershooting of high reflective seafloor elements (e.g. carbonate crusts). Therefore the DeepTow provides the opportunity to resolve reflection interfaces in regions where standard surface streamers can image blanking areas only. With the source still at the sea surface and the receiver deployed at depth the ray path for the sound emission is no longer symmetric and hence the concept of CDP stacking does not hold any more. Therefore full waveform migration need to be applied to integrate all streamer channels into one seismic section.

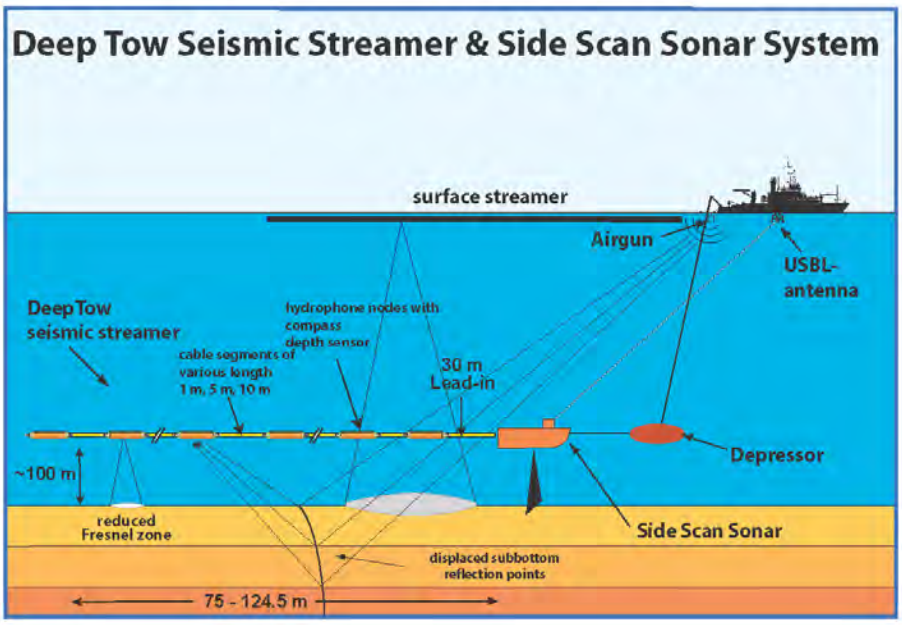

Figure 5.2.4.1: Sketch of the Deep Tow system with multichannel streamer and Sidescan

The deep towed multichannel streamer is a custom made new development designed by companies SEND Off-shore, Hamburg, and KUM, Kiel. It comprises of single hydrophone modules and modular cable connections (Fig. 5.2.4.2). A 20m-long lead-in cable and up to 40 individual hydrophones are connected by 1m, 5m or 10m cable segments. Each hydrophone is attached to a titanium pressure tube containing the node electronics, a pressure sensor and a gyro. The pressure tubes are surrounded by syntactic foam that makes the nodes neutrally buoyant and transmits the towing forces.

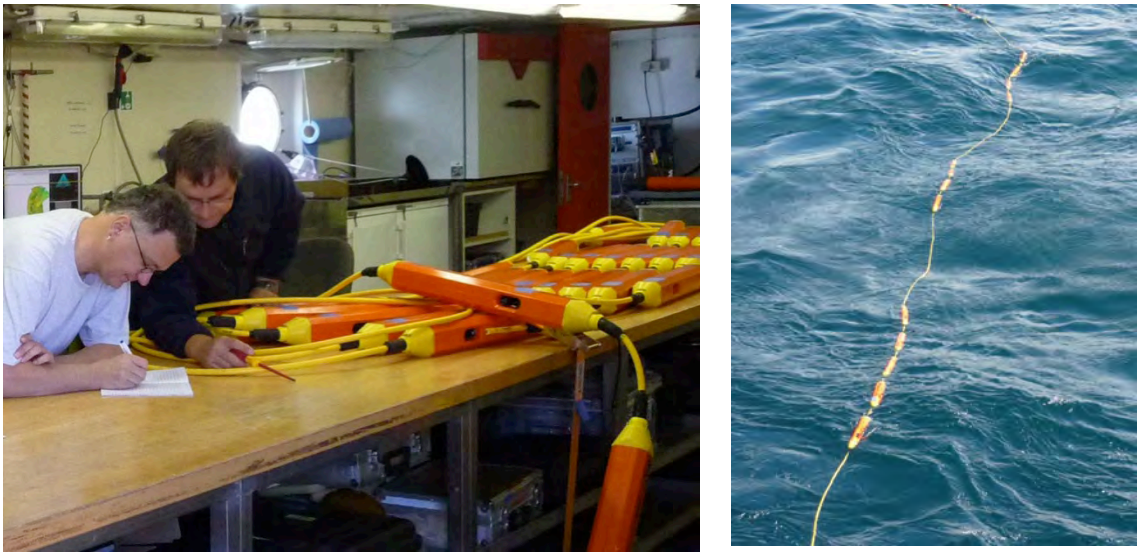

Figure 5.2.4.2: Photograph of the streamer hydrophones and cable segments
left: during setup of the multichannel chain in the laboratory
right: during deployment from board of R/V SONNE

From a so-called Top-PC (TPC, Linux OS) Ethernet connections to the Bottom-PC (BPC) in the towfish and the GeoEel seismic QC recording system from Geometrics (GPC) are provided. In addition the sidescan sonar PCs in the towfish and on board the vessel are connected via the TPC, BPC and the modems of the telemetry system (Fig. 5.2.4.3). The TPC runs a control program for the deep towed streamer. Here all parameters (shot interval, record length, etc.) are specified and submitted to the streamer and the recording system. Moreover the control program displays heading and depth distribution of the hydrophones and other statistical system information. During profiling a GPS based time code is interpreted to generate the wanted shot interval and to distribute the trigger signal to all external systems and the streamer at depth. All data (hydrophone, compass, depth) of the single nodes are stored in raw format within the BPC. Depending on the bandwidth of the towing cable a certain number of hydrophone data can be transmitted real-time via the cable on board. Here the GPS is used to display the data and to store the selected seismic data in SEG-Y format. During operation the USBL system POSIDONIA is used to track the position of the towfish. From this data base exact positions for each hydrophone at each shot time can be calculated.

5.3 Sidescan sonar

Ingo Klaucke

High-resolution backscatter information of cold seeps offshore New Zealand was to be obtained using the DTS-1 sidescan sonar system (Fig. 5.3.1) operated by IFM-GEOMAR. The DTS-1 sidescan sonar is a dual-frequency, chirp sidescan sonar (*EdgeTech Full-Spectrum*) working with 75 and 410 kHz centre frequencies. The 410 kHz sidescan sonar emits a pulse of 40 kHz bandwidth and 2.4 ms duration (giving a range resolution of 1.8 cm), and the 75 kHz sidescan sonar provides a choice between two pulses of 7.5 and 2 kHz

bandwidth and 14 and 50 ms pulse length, respectively. They provide a maximum across-track resolution of 10 cm. With typical towing speeds of 2.5 to 3.0 kn and a range of 750 m for the 75 kHz sidescan sonar, maximum along-track resolution is on the order of 1.3 metres. In addition to the sidescan sonar sensors, the DTS-1 contains a 2-16 kHz chirp sub bottom profiler providing a choice of three different pulses of 20 ms pulse length each. The 2-10 kHz, 2-12 kHz or 2-15 kHz pulse gives a nominal vertical resolution between 6 and 10 cm. The sidescan sonar and the sub bottom profiler can be run with different trigger modes, internal, external, coupled and gated triggers. Coupled and gated trigger modes also allow specifying trigger delays. The sonar electronics provide four serial ports (RS232) to attach up to four additional sensors. One of these ports is used for a *Honeywell* attitude sensor providing information on heading, roll and pitch and a second port is used for a *Sea&Sun* pressure sensor. Finally, there is the possibility of recording data directly in the underwater unit through a mass-storage option with a total storage capacity of 30 GByte (plus 30 Gbyte emergency backup).

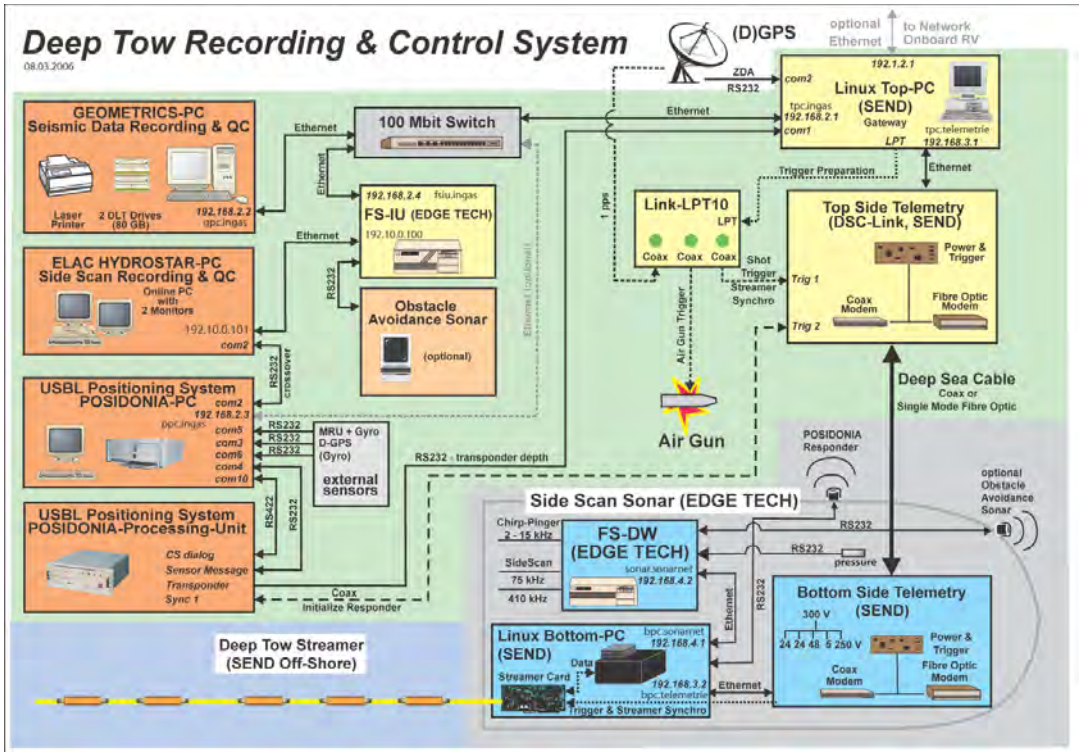

Figure 5.2.4.3: Overview of the data connections within the DeepTow control system

The sonar electronic is housed in a titanium pressure vessel mounted on a towfish of 2.8 m x 0.8 m x 0.9 m in dimension (Fig. 5.3.1). The towfish houses a second titanium pressure vessel containing the underwater part of the telemetry system (*SEND DSC-Link*). In addition, a releaser capable to work with the USBL positioning system *POSIDONIA* (*IXSEA-OCEANO)* with separate receiver head, and an emergency flash and radio beacon (*NOVATECH)* are included in the towfish. The towfish is also equipped with a deflector at the rear in order to reduce negative pitch of the towfish due to the weight of the depressor and buoyancy of the towfish.

The towfish is connected to the sea cable via the depressor through a 45-m long umbilical cable (Fig. 5.3.2). The umbilical cable is tied to a buoyant rope that takes up the actual towing forces. An additional rope has been taped to the buoyant rope and serves to pull in the instrument during recovery.

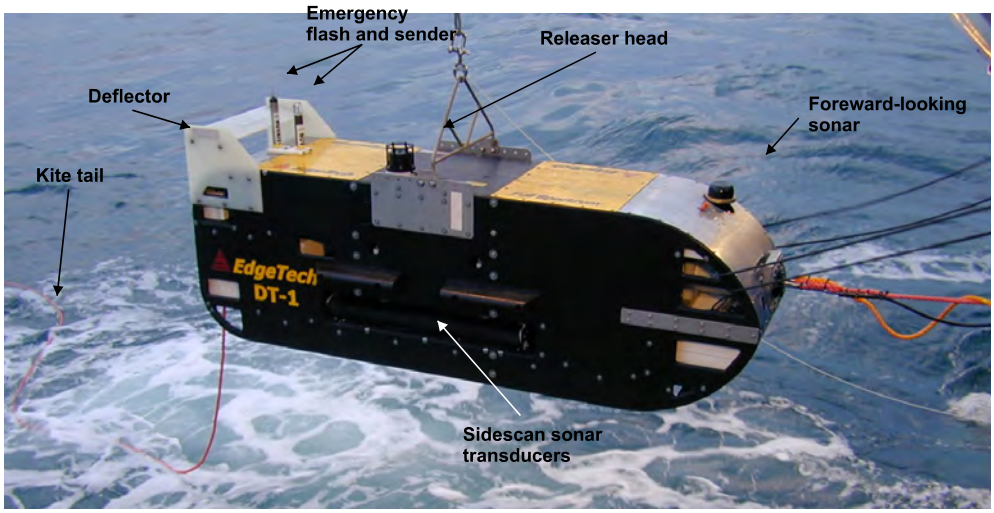

Figure 5.3.1: A picture of the DTS-1 sidescan sonar towfish. The forward-looking sonar is no longer mounted.

The main operations of the DTS-1 sidescan sonar are run using *HydroStar Online*, the multibeam bathymetry software developed by *ELAC Nautik GmbH* and adapted to the acquisition of *EdgeTech* sidescan sonar data. This software package allows onscreen presentation of the data, of the towfish's attitude, and the towfish's navigation when connected to the *POSIDONIA* USBL positioning system. It also allows setting the main parameters of the sonar electronics, such as selected pulse, range, power output, gain, ping rate, and range of registered data. *HydroStar Online* also allows activating data storage either in XSE-format on the *HydroStar Online* PC or in JSF-format underwater on the full-spectrum deep-water unit *FS-DW*. Simultaneous storage in both XSE and JSF-formats is also possible. Accessing the underwater electronics directly via the surface full-spectrum interface-unit FS-IU and modifying the sonar.ini file of the *FS-DW* allows changing additional settings such as trigger mode. The *FS-IU* also runs *JStar*, a diagnostic software tool that also allows running some basic data acquisition and data display functions. *HydroStar Online* creates a new XSE-file when a file size of 25 MB is reached, while a new JSF-file is created every 40 MB. How fast this file size is reached depends on the amount of data generated, which depends on the use or not use of the high-frequency (410 kHz) sidescan sonar. The amount of data generated is also a function of the sidescan sonar and sub bottom pulses and of the data window that is specified in the initialisation file (sonar.ini) on the *FS-DW*. The data window specifies the range over which data are sampled.

The sub bottom profiler data have to be corrected for varying water depths in which the towfish is flying. These corrections are based on depth information provided by the pressure sensor mounted on the towfish and have been carried out with in-house processing scripts based on *GMT* and *Seismic Unix* software packages.

The sidescan sonar serves as attachment point for a deep-towed seismic streamer (see Chapter 5.2.4) that can be used simultaneously with the sidescan sonar (Fig. 5.2.4.1).

5.4 Controlled Source Electromagnetics (CSEM) for gas hydrate assessment

Katrin Schwalenberg, Martin Engels, BGR Hannover

Marine electromagnetic methods are used to derive bulk resistivity of the sub-seafloor sediment sections, which can be helpful to determine the presence of gas and gas hydrate. Natural hydrocarbons like oil, gas and gas hydrate are electrically resistive in contrast to the conductive seawater filling pore space under normal conditions. Active or controlled source

electromagnetic (CSEM) methods are used when the shallow seafloor down to some hundred meter depths is investigated. Together with seismic profiling CSEM is the only remote method covering the entire gas hydrate stability zone. The two methods provide complementary information: structure from seismic data, bulk properties from CSEM data.

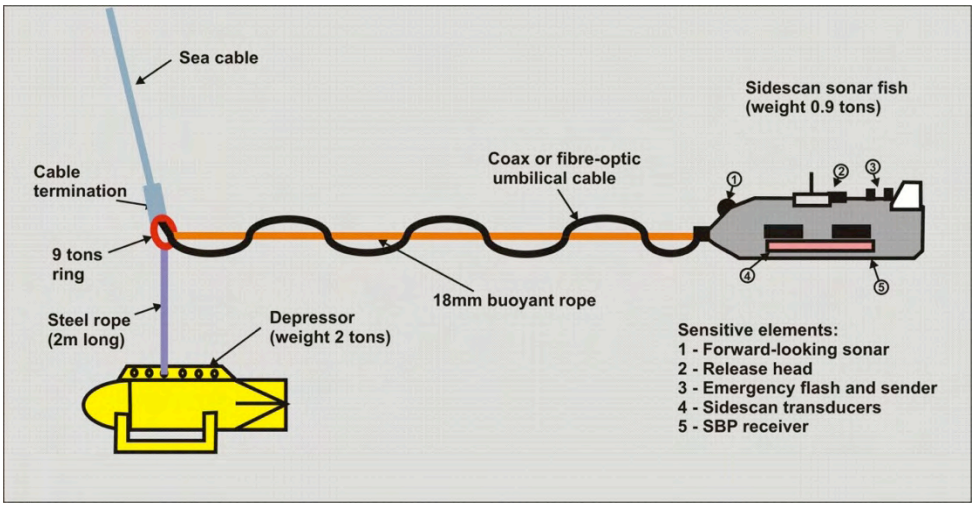

Figure 5.3.2: The DTS-1 towing configuration.

Electrical Resistivity

The electrical resistivity of marine sediments is mainly controlled by the amount of conductive seawater in the available pore space, and thus depends on the porosity. It is in the order of 1-2 Ohm*m within the first few hundred of meters below seafloor. The conductivity of seawater on the seafloor varies between 3 and 3.5 S/m and is mainly a function of temperature and salinity. Both gas hydrate and free gas are electrically resistive and replace conductive pore fluid. Thus, the resistivity derived from CSEM data is elevated where hydrate and/or gas is present in sufficient quantities.

The electrical resistivity can be related to the gas and gas hydrate concentration using Archie's law. The general form is $\rho_f = a\rho_\omega \phi^{-m} S_\omega^{-n}$, with ρ_f: formation resistivity, ρ_ω: seawater resistivity, ϕ:sediment porosity, S_ω: pore water saturation, S_h=(1- S_ω): gas hydrate fraction, *a, m, n*: coefficient, cementation factor, saturation factor. Table CSEM-1 lists the expected formation resistivities for various gas hydrate fractions for two sets of Archie coefficients. While it is not possible to distinguish between gas and gas hydrate from CSEM data alone, we believe that the presence of gas within the gas hydrate stability zone will result in gas hydrate formation and the resistivity anomalies observed are mainly attributed to gas hydrate.

CSEM principle

The basic principle of CSEM field propagation can be described as follows: Electromagnetic (EM) signals (typically a continuous square wave) are emitted from a horizontal electric dipole on or close to the seafloor. The signals propagate by diffusion away from the source dipole (TX) through the conductive seawater and the more resistive seafloor, and are recorded by electric dipole receivers (RX) on the seafloor at some distance from the transmitter dipole. Delay times and amplitudes of the electric field data recorded at each receiver depend on the seafloor resistivity and can be interpreted using forward modeling and inversion techniques. The more gas hydrates and gas, the faster arrives the signal and the higher are the electrical field amplitudes. The depth of investigation is less than half the TX-RX offset. It also depends on the recorded time interval or frequency range.

Gas (Hydrate) Fraction [%]	Formation Resistivity A [Ωm] ϕ=50%, a=1, m=n=2,	Formation Resistivity B [Ωm] ϕ=60%, a=1, m=2.8, n=1.94
0 %	1.2 Ωm	1.25 Ωm
5 %	1.33 Ωm	1.39 Ωm
10 %	1.48 Ωm	1.54 Ωm
20 %	1.88 Ωm	1.93 Ωm
40 %	3.33 Ωm	3.38 Ωm
80 %	30 Ωm	28.50 Ωm

Table 5.4.1: Relation between gas and/or gas hydrate fraction and formation resistivity for two sets of Archie parameters. The formation resistivity derived from CSEM data is a robust parameter to evaluate highly concentrated gas and gas hydrate deposits. Small amounts of gas and gas hydrate are more difficult to resolve from CSEM data alone.

The experimental set-up can be adjusted to cover the entire gas hydrate stability zone from the seafloor to some hundred meters below, thus covers similar depth ranges than seismic methods. The results of the CSEM data analysis are resistivity profiles or resistivity models which may indicate zones and areas of increased gas and gas hydrate concentration.

Marine CSEM in NEMESYS

Within the NEMESYS project marine CSEM is used to complement the seismic and hydro-acoustic experiments, which provide detailed images of vent structures, gas and fluid chimneys, gas and gas hydrate pockets, but are often ambiguous regarding the nature and concentration of the pore fluid.

During SO214-2 two different CSEM experimental setups were applied: a) BGR deployed a newly developed seafloor-towed electric dipole-dipole system to collect electrical resistivity information along profiles (Table. 5.4.1), and b) IFM-GEOMAR deployed a 3D array of stationary seafloor electromagnetic receiver stations (OBEMs) over a seep site to record the ambient electric field of a newly developed two-component current transmitter moved from site to site on the seafloor (Fig. 5.4.2).

5.4.1 CSEM-BGR Instrument description

Katrin Schwalenberg, Martin Engels, BGR Hannover

BGR has developed a new seafloor-towed marine CSEM system as part of the SUGAR project (Fig. 5.4.1.1). The general set-up is based on a previous system designed at the University of Toronto, which was deployed on SO191 in 2007 but is no longer in use.

HYDRA is a modular system that consists of a transmitting dipole and four electrical receiving dipoles at increasing offsets. Transmitter and receivers are linked with Kevlar-enforced data cable segments with a total length of up to 1000 m. The whole system is towed in-line along profiles in contact with the seafloor behind a plough called ‘pig’.

The pig hosts the control unit, which sends a timing, pulse along the data cable to synch the four receiving units and records the current signal. It also hosts an acoustic transponder to locate the seafloor position of the system and a CTD sensor to measure seawater conductivities and velocities. The source signal is generated by a current transmitter on board and is sent down to the source dipole on the seafloor via the coaxial deep-tow cable. The source or transmitter dipole (TX) is 100 m long and attached in parallel to the first data cable segment behind the pig (see Fig 5.4.1.1). 70 cm long copper pipes are used as current electrodes. The signal form is typically a square wave with a period between 2 and 6 seconds, but any signal i.e. sine, ramp can be applied. Each receiver unit is battery powered and stores

data locally at a continuous sampling rate of 10 kHz. The ambient electric fields are measured with a pair of Ag Ag/Cl electrodes on 10 m to20 m long dipoles attached to the data cable segment behind each receiver unit. The transmitter-receiver offsets applied on SO214 are given in tables 6.4.1.1 and 6.4.1.2.

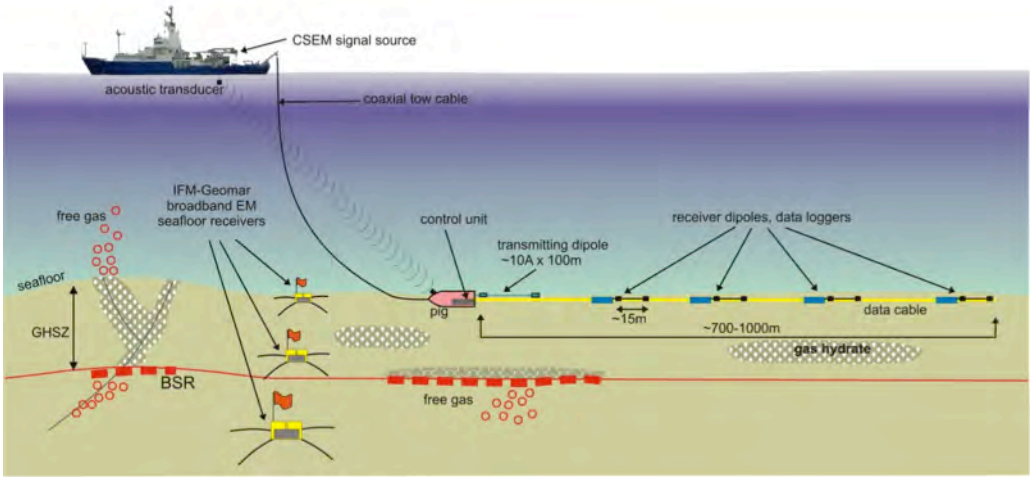

Figure 5.4.1.1: Setup of the towed BGR marine CSEM System. Also shown are IFM-GEOMAR ocean bottom EM receivers.

The system is deployed over the aft deck starting with the last receiver unit. Finally the pig is picked up with the A-frame and deployed. Then the system is slowly lowered to the seafloor paying out the deep tow cable. No online communication with the seafloor array is possible during deployment. However, the acoustic transponder is used to monitor the movements of the pig during the deployment.

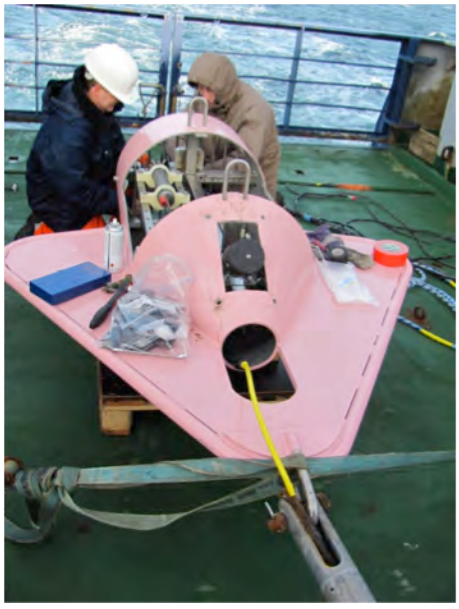

Figure 5.4.1.2: The plough-shaped 'pig' is towed in front of the seafloor array. It hosts the control unit, a CTD sensor and an acoustic transponder system to monitor movements during the deployment.

HYDRA was tested during two cruises in the St. Lawrence River, Quebec, in September 2010, and in the Black Sea in the Danube Delta in December 2010. All units recorded data and all system parts were safely deployed and recovered. The preliminary analysis of the data from these test cruises showed that a high noise level is generated by the transmitter. The noise is passed on via the shield and the digital ground line of the first data cable segment to the following receivers. Therefore, the original design was changed on SO214-2, and the first data cable segment between CU and R1 was replaced with a 200 m long rope (Dyneema) to

interrupt the propagation path of noise along the data cable. This modification afforded a second real time clock module with a high-precision clock in the first receiver (R1). This has now the function of a receiver control unit to synchronize the following receivers. The time difference to GPS time of both CU clock module and R1 clock module was measured prior and after deployments.

CSEM Current Transmitter and Shipboard Connections

The current transmitter is located on board. On RV SONNE it was located in the 'Geolabor' and powered from a three phase 440 V transformer with its own electric generator located in the next door 'Luftpulserraum'. On other vessels we experienced repeatedly occurring shutdowns due to current peaks in the ships power supply, which could be prevented on SO214. The maximum output of the current transmitter is 13 A, 1000 V for deep-water applications. However, the maximum current which could be transmitted on R/V SONNE for the CSEM experiment was limited by the tow cable and the specifications of the slip ring and the splice box attached to the tow cable. On Leg SO214-2 winch W1 was used for the CSEM experiments. The deep tow cable has a coaxial and a fibre-optical conductor and a length of 7600 m in 21 layers on the reel. Sending current through the conductors of the cable produces heat, which cannot circulate for the inner layers. Thus the maximum current is limited by the number of layers remaining on the reel. The original slip ring of the W1 which can handle the coaxial and the optical conductor was replaced with the slip ring of the W6 which handles only coaxial conductor, but is designed to send a current of up to 8 A through the slip ring. The original slip ring was reinstalled for OFOS, which requires the fibre optical connection for video and data transfer. Two flying RG 213 coaxial cable were wired from the Geolabor to the W1 to connect the current transmitter with the slip ring of W1. Coaxial cable was used to provide extra shielding through the hull.

Figure 5.4.1.3: Shipboard Current Transmitter for the seafloor towed CSEM System. Input: 3-Phase 380-440V, 50Hz,60Hz. Output: 13A, 1000V, and 40A, 200V

5.4.2 OBEM stations and transmitter frame of the IFM-GEOMAR

Sebastian Hoelz

The controlled source electromagnetic (CSEM) method uses an active source to generate a primary electromagnetic signal and receivers, which record the earth / water response of this primary signal. Generally, an exact knowledge about distances and orientations of transmitter and receivers is of paramount importance for the interpretation of CSEM data.

In the past years, the EM group at the IFM-GEOMAR has developed a new CSEM system, which is especially designed for the investigation of small-scale targets. In this

system, transmitter and receiver(s) are autonomous units. Thus, distances, unlike for the BGR-system, are neither fixed nor known a priori. The system was successfully used for a first experiment during a cruise to the westerly Nile-Delta in November 2008. During this experiment, the CSEM transmitter was moved around using a ROV (U of Ghent) and for ranging and positioning of transmitter and receivers, an external USBL (ultra short base line) system (GAPS, iXSea) was used. Since both systems (ROV, USBL) are not standard equipment on-board vessels, we have started to investigate options to become independent of such systems and reconfigure our system to only rely on standard equipment available on regular research vessels.

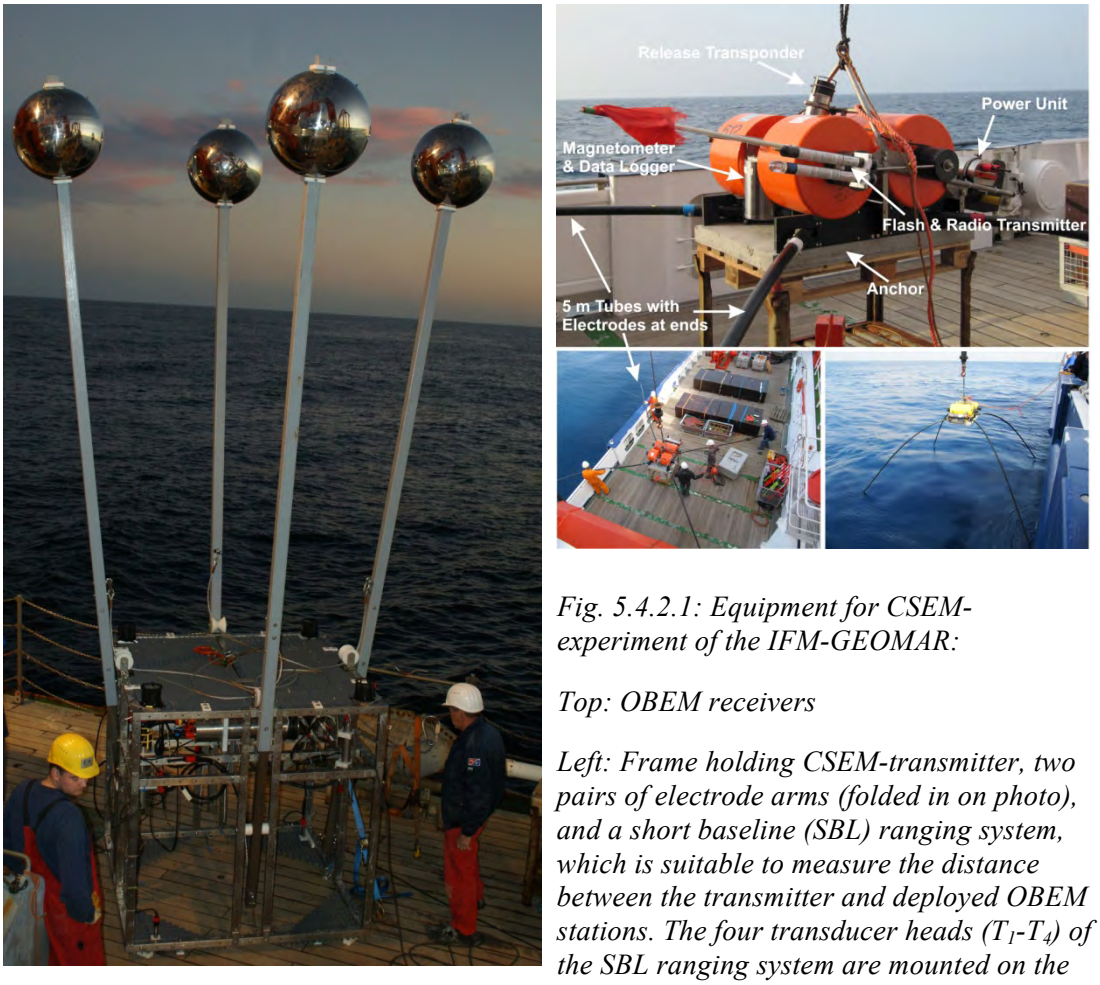

Fig. 5.4.2.1: Equipment for CSEM-experiment of the IFM-GEOMAR:

Top: OBEM receivers

Left: Frame holding CSEM-transmitter, two pairs of electrode arms (folded in on photo), and a short baseline (SBL) ranging system, which is suitable to measure the distance between the transmitter and deployed OBEM stations. The four transducer heads (T_1-T_4) of the SBL ranging system are mounted on the upper corners of the frame.

Based on experiences gained during testing of a basic prototype (MSM 14/3, 2010), the refitted transmitter system now consists of a frame (Fig. 5.4.2.1, left), which holds the CSEM-transmitter, two pairs of perpendicular electrode arms and a short baseline (SBL) ranging system. The transmitter system is operated similar to a temperature lance, i.e. it is lowered to the seafloor using a regular winch cable, remains stationary during measurements before being moved to the next location. The winch cable is used for both, power-supply of the transmitter and communication to the electronics of the transmitter system via a DSL-modem. The SBL ranging system, which is made up of standard components available at the IFM-GEOMAR, interrogates transducer heads, which are part of the releaser units mounted to each OBEM receiver stations. Thus, the SBL system allows for a direct ranging between the transmitter and OBEM receivers directly on the sea floor.

5.5 Geological instrumentation

5.5.1 Gravity corer

Henk de Haas

Description of the coring system

Gravity coring was performed using a corer consisting of a 5.73 m long steel barrel attached to a lead filled weight (bomb), which has fins for stabilisation (Figures 5.5.1.1.a & .b). A core liner with an internal diameter of 104 mm is inserted in the barrel. The top of the liner is supplied with a one-way valve letting water out during the coring, but avoids sinking out of the sediments after retrieval. A stainless steel core catcher is placed at the lower end of the liner. The net length of the liner available for sediments is 5.23 m. The liner is kept at its place by means of a steel cutting nose attached to the barrel. The bomb to barrel and barrel to nose connections are made by means of nails inserted into coinciding grooves onto the respective parts. The complete system weighs about 1500 kg. A Posidonia USBL (Ultra Short Base Line) underwater navigation transponder was attached to the hoisting cable at a height of 100 m above the corer. The corer penetrated the seabed with a velocity of 1 m/s (maximum available speed for the winch in use).

After retrieval the cores were cut in sections of 110 cm or less. They were split lengthwise, opened, described and subsampled for gas analysis on board.

Attached to the core barrel were 5 temperature sensors, accompanied by a tilt meter mounted on the fin of the bomb. The temperature at different depths in the seabed sediment was determined by letting the corer into the seabed for a period of 15 minutes after penetration. This allowed the sensors to reach equilibrium with the local sediment temperature. The temperature data in combination with the angle of core penetration, as determined by the tilt meter will be used to calculate the local heat flow. The temperature sensors were mounted at 59, 109, 159.5, 259.5 and 360.5 cm above the base of the core.

5.5.2 Multicorer

Andrew R. Thurber

Direct biological sampling was undertaken to identify NZ's seep biodiversity and to quantify the functional link between the metazoan (multicellular) and microbial fauna within seep sediments. A total of 7 video-guided multicore deployments were made, 5 recovering samples with a newly adapted video guidance system provided by NIOZ. The multiple corer used was an Ocean Instruments model leant by NIWA Wellington, which use an 9.8cm internal diameter liners (Fig. 5.5.2.1). Three of the samples were of microbial mats at Takahe seep area with one in located in the sulfidic sediment patches (ampharetid beds) at Bear's Paw. Deployments and analysis are described in chapter 6.7.

Figure 5.5.1.1.a Photograph of the lead filled weight with fins

Figure 5.5.1.1: Views of the gravity corer.

Figure 5.5.1.2. One of the 5 temperature sensors, attached to the core barrel.

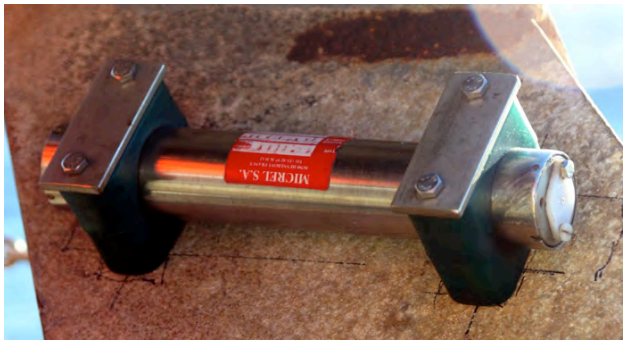

Figure 5.5.1.3. The tilt meter mounted to the fin of the bomb.

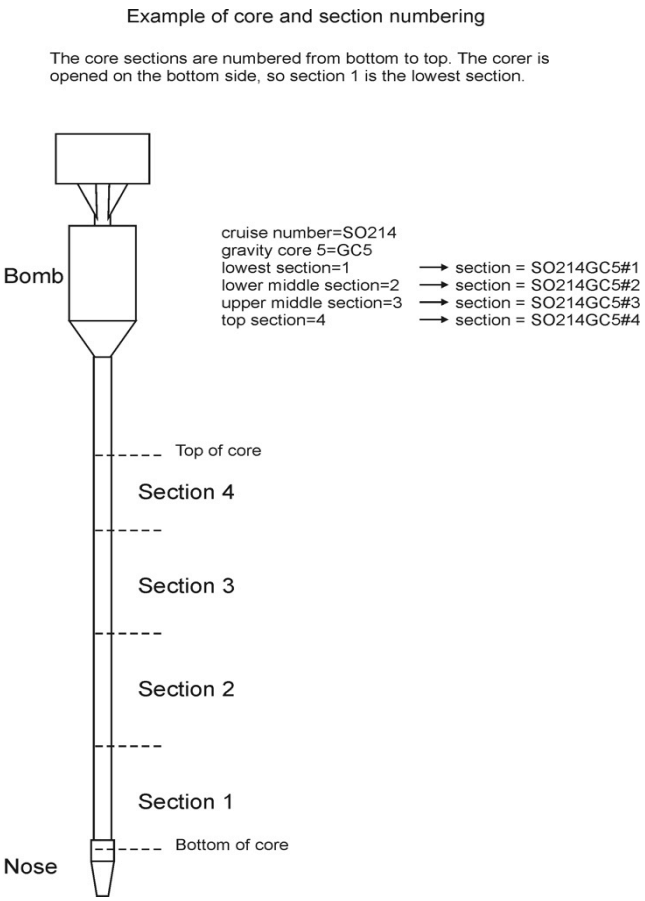

5.5.1.5. Fig. Numbering of the sections

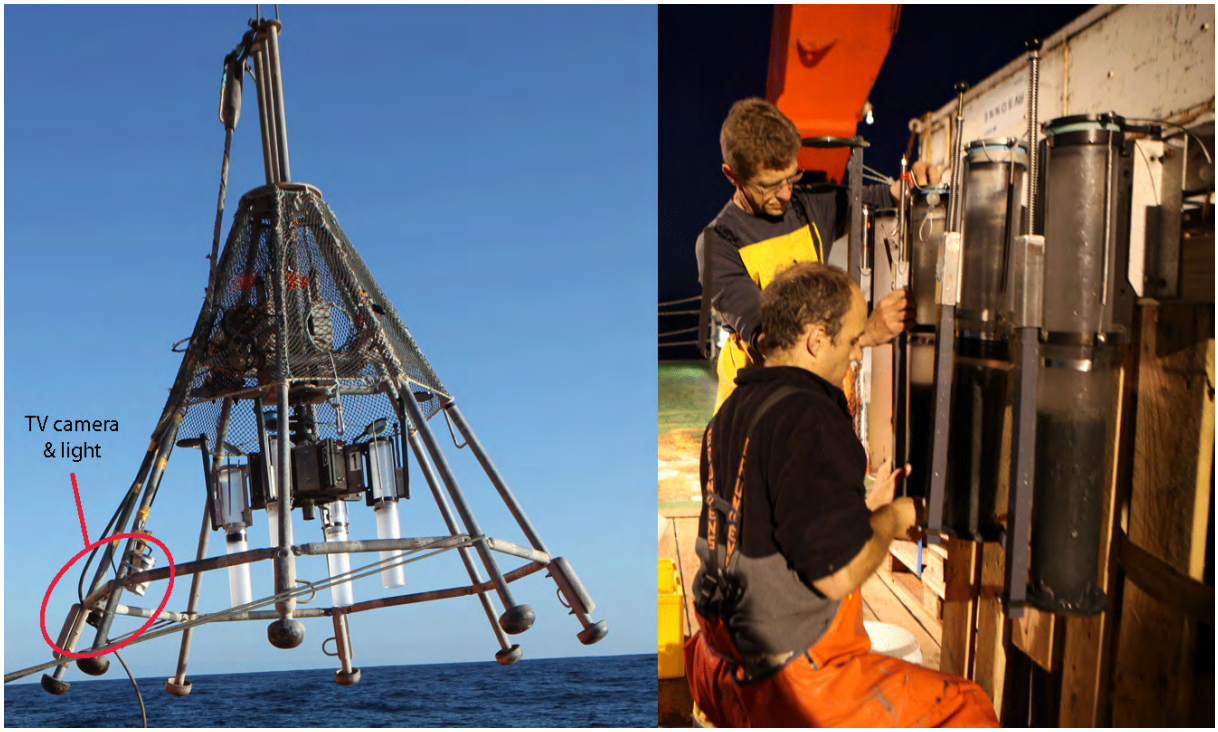

Figure 5.5.2.1. left: Photograph of the Multicorer during deployment
right: Photograph of the filled liners already moved to the working bench

5.5.3 Sediment temperature measurements

Jens Greinert & Henk de Haas

Heat flow and thermal gradient data provide first-order constraints for the thermal modelling of geodynamical processes such as subduction or rifting processes. On a local scale geothermal data may also identify active faults and seepage areas. The near-surface thermal regime can be strongly disturbed at faults and seeps due to upflowing warm fluids and formation and dissociation of gas hydrates. During SO214 Leg 2 it was aimed to characterize the geothermal setting of the seep environments during gravity coring at the Opouawe Bank (Takahe Seep site) and Omakere Ridge; due to bad weather we could not use the gravity corer at Omakere Ridge. We used THP temperature sensors that were attached to the NIOZ gravity corer (Figure 5.5.3.1). The THP temperature sensors (NKE product) are autonomous temperature data loggers. Arbitrarily attached at different depth intervals of a coring device, they provided temperature and thermal gradients along the sediment core down to the depth to which the corer penetrated.

System

Five sensors were connected to a gravity corer of 6 m length and over an active length of 3 meters. The first sensor was placed at 59 cm distance from the rim of core catcher, the interval distance of the sensors was set at 0.5 m between sensor 1 to 2, and 2 to 3. One-meter intervals were between sensor 3 to 4 and 4 to 5. The THP sensors have been calibrated prior the cruise at NIOZ and will be re-calibrated after the cruise for comparison reasons. The order of the sensors was as follows: Serial number 27002 (bottom), 24005, 24004, 24001, 24002 (top).

The lateral distance from the core barrel to the sensors is 6 cm. The recording interval was set to either 5 or 2 sec. The angle of tilting of the corer was registered with a tilt meter

with accuracy of 1°. The tilt meter had serial number 24003 and was fixed next to the weight of the corer. Data were downloaded upon arrival of the corer on-board. The THP thermistors have an accuracy of 0.007 °C and a resolution of 0.0007 °C at 20 °C.

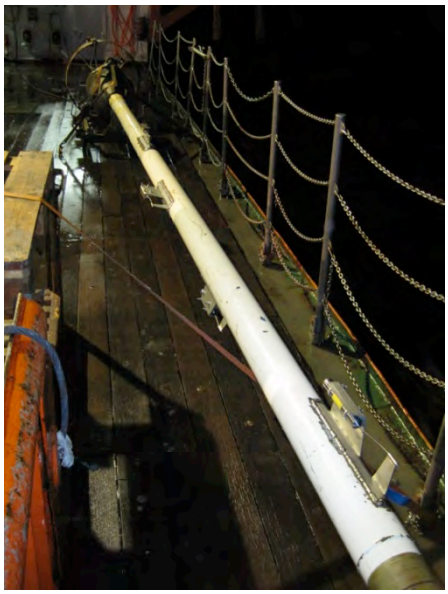

Figure 5.5.3.1: The gravity corer with its THP sensors welded to it. Some of the sensors got bend during deployment but worked until the very end.

Method

The corer was kept in the sediment for a period of min. 15 min at each station. Prior to this the corer was kept about 50m above the ground for 3 to 5 minutes to give time for the sensors to equilibrate. During SO214 only preliminary processing has been done. More accurate processing will be performed onshore where the accurate calibration of the sensors will occur and the equilibrium temperatures can be obtained by extrapolation from the transient temperature curves. Thermal conductivity of the sediments will be estimated from the heat friction decay curves that results from the penetration of the data-loggers. The product of the thermal gradient with the thermal conductivity in each interval will give us heat flow values.

5.6 Methane analyses

Jens Greinert, Laura Haffert, Piet van Gaever

Analyzing methane concentrations in the water is routinely done by two different methods, one is vacuum extraction (e.g.[*Schmale et al.*, 2010]) the other one head space analysis. During SO191 both methods have been employed and showed up as very comparable. During SO214 we choose the headspace method, as it is easier and less work intensive as the vacuum extraction. However, although the general idea of head space is always the same, the methane concentration in a gas volume that is in contact with a known volume water is brought into equilibrium, the ration between water and head space volume as well as the head space gas (e.g. Ar, N2, methane free air) and the equilibration time (plus the way of shaking) are crucial for a accurate determination of the gas concentration in the water.

During Leg 1 we performed several test to determine the best way of preparing the headspace before it is measured by a gas chromatograph. Results of these experiments are described below.

5.6.1 System

The GC we used was a Thermo Scientific FOCUS GC run with direct injection. We sued H2 as carrier gas as well as zero air and zero N2 to run the FID (N2 was the mask-gas which helps to keep the flame stable). The injector temperature was set to 150 °C and the septum was constantly purged to avoid bleeding of septum into the column flow. FID temperature was set to 170 °C and the oven temperature was ramped from 40 °C to 120 °C with the following ramping intervals: 40 °C for 4min, ramping to 70 °C (15 °C/min), 70 °C for 3 min, ramping to 100 °C (15 °C/min), 100 °C for 3 min, ramping to 120 °C (20 °C/min), 120 °C for 5 min.

The flow through the column (RESTECK Packed Column HS-Q 80/100, 2 m length 2 mm inner diameter) was set to constant pressure of 40 kP and the entire injection was run in a split-less mode. The software used for recording the data and integration was Chrome Card 6.01.

5.6.2 Sample preparation

Glass bottles (118.4 mL volume) were completely filled with sample fluid carefully avoiding any air inclusion and bubbling of the water (put the tubing at the very bottom of the bottle and fill it slowly from bottom to top, let sufficient water run through and pull out the tube slowly). The water was poisoned with 50 µl of super saturated HgCl solution immediately after the sample was taken and closed with a butyl rubber stopper crimp seal. The bottles were stored at 4 °C before emplacement of a 5 mL Argon headspace (Figure 5.6.1). For this a silicon tube with needle was attached to the Ar gas bottle pressure regulator and adjusted to a little bit of overpressure relative to the ambient pressure (just enough to create slow bubbling in a water filled beaker). This needle is pierced into the headspace vial and 5 ml of water are taken out from the headspace vial with a syringe finally introducing the gas headspace. The headspace volume of 5 ml has been chosen as it gives quite high absolute ppm concentrations which increase the detection limit; it allows for repeated measurements of the same sample if an error occurred during the GC analyses; it allows easy handling with extracting the gas volume for the GC analyses and it extracts about 65% of the methane from the water already.

Before analysis the samples were warmed to ambient laboratory temperature (~28 °C) and shaken for two hours. Analyses of 0.5 mL headspace (or 1 mL in the lowest concentration range) were undertaken with the GC.

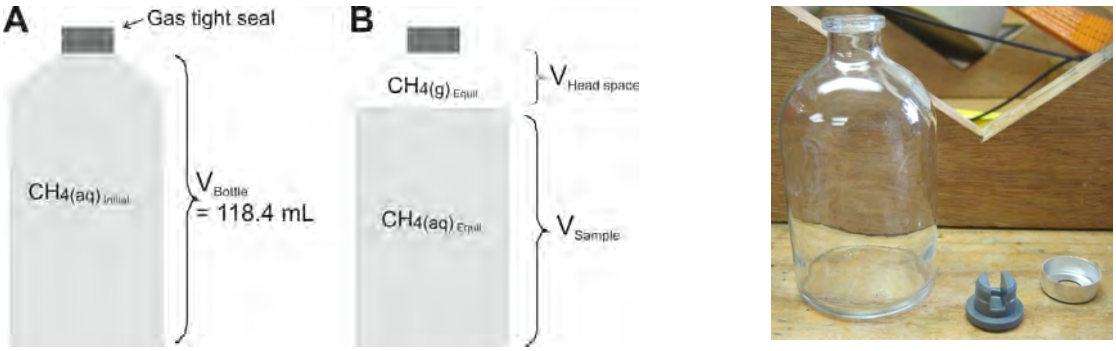

Figure 5.6.1 Head space insertion and symbology. On the right hand side the real bottle and the used rubber stoppers (those with a central slit to allow excess water to be squeezed out when the bottle is closed).

5.6.3 Conversion from peak area to CH4 ppm in the headspace

To calibrate the recorded area of the methane peak we used in a first attempt the ambient air which was measured by a PICARRO system CRDS system at the beginning of the cruise to have $CH_{4\ Air}$= 1.71 ppm. We simply assumed that the concentration area changes with a slope of 1 and is linear.

Average (n=3) A_{Peak} of air = 38198 area unit
One area unit is equivalent to 4.71232 E-5 ppm (= $area_{factor}$).
The ppm concentration of the gas is then calculated after:

$$CH4(gas)[ppm] = area_{factor}\left[{}^{ppm}/_{area-unite}\right] * A_{peak}[area-unit]$$

However, the above-described method is only an approximation and a proper calibration curve derived from different standard concentration should be preferred.

5.6.4 Calculating the original methane concentration of the water

During SO214 we evaluated two methods, one based on the assumption that after a while an equilibrium between the water and head space established and that the equilibrium concentration equation published by [*Wiesenburg and Guinasso*, 1979](W&G) can be used to calculate the CH_4 concentration of the water in the sample bottle based on the measured ppm concentrations in the head space, the ambient pressure, the temperature of the water in the lab and the salinity from the CTD measurements. We performed a series of equilibration experiments with different headspace volumes for high and low concentration water and different head space gas. The results show that the ppm concentration in the bottles with different headspaces in sample batch fits very well with the trend calculated after W&G. As expected larger errors occur at small headspace volumes due to the fact that small absolute errors in headspace volume will have a large effect. The increasing error at larger headspaces is linked to the quickly decreasing ppm concentrations in the headspace and in-accurate GC analyses. Based on the results a headspace of 10ml should give the most accurate results as small absolute errors during introducing the headspace are relatively small and ppm concentrations in the headspace are still quite high.

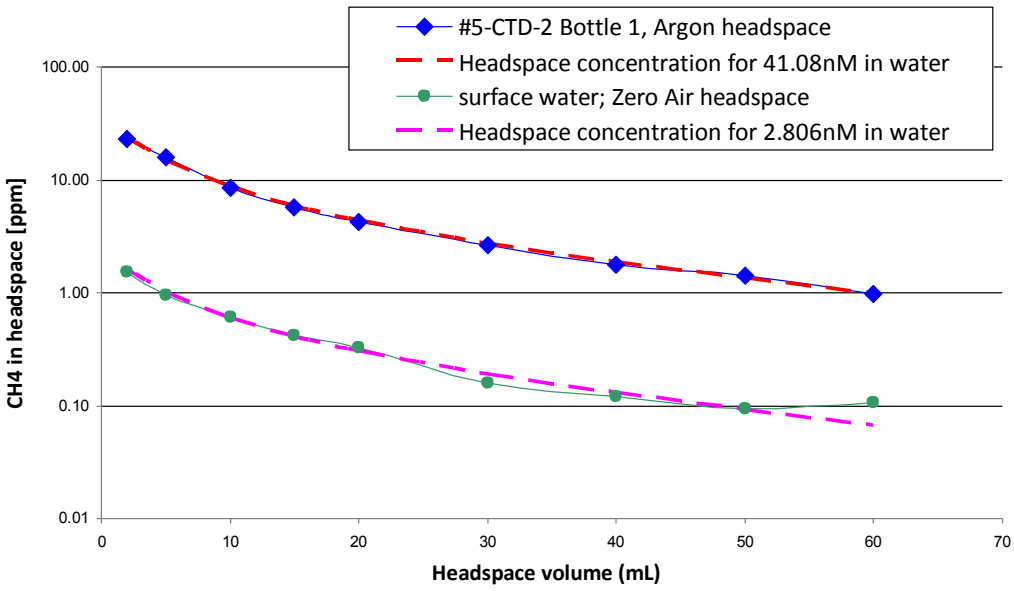

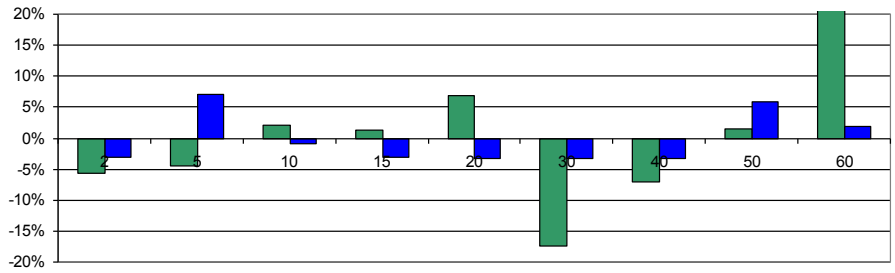

Figure 5.6.2: Top: Headspace methane concentrations of different headspace volumes for one high and one low concentration sample. Dashed lines are the calculated headspace concentrations using the formula of W&G. Bottom: Difference between the calculated headspace concentration and the measured one. Optimising the absolute water concentration of #5-CTD-2 samples (a slightly lower concentration in the W&G calculation) might have given even less differences to the actual measured concentrations.

Wiesenburg and Guinasso (1979) have developed an equation that provides methane concentrations of a solution in equilibrium with a gas phase (here head space) for various salinities (S in ‰) and temperatures (T in Kelvin).

$$\ln(CH4_{aq})\left[\frac{nmol}{L}\right] = \ln(fG) + A1 + A2\left(\frac{100}{T}\right) + A3\ln\left(\frac{T}{100}\right) + A4\left(\frac{T}{100}\right) + S\left[B1 + B2\left(\frac{T}{100}\right) + B3\left(\frac{T}{100}\right)^2\right]$$

With $fG = CH4_{equlibrated-gas}[ppm]\cdot 10^{-6}$

The constants to get nmol/L (or nM) are:

A1 (nmol/L)	-415.2807
A2 (nmol/L)	596.8104
A3 (nmol/L)	379.2599
A4 (nmol/L)	-62.0757
B1 (nmol/L)	-0.059160
B2 (nmol/L)	0.032174
B3 (nmol/L)	-0.0048198

Analysing the concentration of CH_4 in the equilibrated headspace enables to calculate the concentration of methane in the water within the headspace vial (in nM). IMPORTANT, as a headspace gas was introduced with no methane (Ar, He, N2) the total number of mol methane in the headspace vial, headspace and water, needs to be calculated. The volume of the water and the headspace needs to be determined very accurately.

As the number of moles in a gas phase depends on the pressure and temperature $(PV = nRT)$ the volume of 1 mol gas is calculated as:

$$V_{mol-gas}\left[\frac{L}{mol}\right] = \frac{n[=1]*R[bar\cdot cm^3 mol^{-1}K^{-1}]*T[K]}{P[atm]} = \frac{n[=1]*0.0821[barLmol^{-1}K^{-1}]*T[K]}{P[bar]}$$

where n is the number of moles, R is the universal gas constant (83.1441 cm^3 bar mol^{-1} K^{-1}), P_{atm} is pressure in atm (1 atm = 1.01325 bar), P_{bar} is the pressure in bar and T is the temperature in Kelvin. The total number of moles in the headspace ($n_{headspace}$) is calculated as:

$$n_{headspace}[mol] = \frac{V_{headspace}[L]}{V_{mol-gas}\left[\frac{L}{mol}\right]}$$

The total number of mol in the water are calculated as:

$$n_{water}[mol] = \exp(\ln(CH4_{aq}))\left[\frac{nmol}{L}\right] * V_{water}[L] * 10^{-9}$$

The sum of $n_{headspace}$ and n_{water} gives the total amount of CH4 molecules in the sampled water of the headspace bottle. To get the total amount of CH4 in the water as nano-mol per litre (nM) the final step is needed.

$$CH4[nM] = n_{headspace}[mol] + n_{water}[mol] * \frac{1}{V_{water}[L]} * 10^{9}$$

List of parameters:

$V_{Headspace}$	Volume of headspace
V_{Sample}	Volume of sample after headspace insertion
V_{Bottle}	Volume of sample bottle
$V_{analysis}$	Volume of headspace analysed by chromatograph
V_{mol}	Volume of 1 mole gas
$n_{headspace}$	Number of all moles in headspace
n_{tCH4}	Number of total number of moles present in bottle
$CH_4(aq)_{Initial}$	Initial methane concentration in water sample
$CH_4(aq)_{Equil}$	Methane concentration of sample after equilibration with the headspace
$CH_4(g)_{Equil}$	Methane concentration in the headspace after equilibration with sample
$CH_4(g)_{100\%}$	Methane concentration in headspace if 100 % of CH_4 was stripped from sample
$CH_4(g)_{Air}$	Methane concentration in atmospheric air
A_{Peak}	Area of the methane peak in the chromatographic spectrum
$t_{Shaking}$	Duration of sample shaking

5.6.5 Equilibration/shaking time experiments

Calculating the equilibrium concentration after W&G as described above only works if the water is properly equilibrated with the overlaying headspace. We performed a few equilibration experiments (Table 5.6.5.1) by taking several samples from one water depth and analysed them after they have been shaken in an overhead shaking device for different times. The shaker was set to almost the highest rotation possible.

5.6.6 Triplicate measurements

We also performed a series of triplicate measurements from CTD 4 bottle 1 and 16. All bottles were shaken for 2 hrs. and had 5 ml or Ar headspace. In addition we shook one sample of CTD bottle 1 and 16 vigorously by hand for about 1 minute. The results show that the reproducibility is very good for this very simple procedure of introducing the headspace, equilibration and headspace measurement.

Table 5.6.5.1: Equilibration experiments with CTD 1 bottles

	CH4 peak area for different head space gases		
Shake time	**N2**	**Ar**	**air**
2 hrs. (CTD1 bottle 20)	63317	63284	48602
CTD 1 bottle 21			
6 min		34780	
15 min		50171	
1 hr. 30 min		60610	
2 hrs. 30min	51114		
3 hrs. 30min	52973		
Not shaken for 3 hrs. 30 min	51295		

Table 5.6.6.1: Triplicate measurements

Sample	Peak area
CTD-4 bottle 1 vigorously shaken	186210
CTD-4 bottle 1 A	190752
CTD-4 bottle 1 B	189825
CTD-4 bottle 1 C	189451
CTD-4 bottle 16 vigorously shaken	25272
CTD-4 bottle 16 A	25696
CTD-4 bottle 16 B	25890
CTD-4 bottle 16 C	26220

5.7 Geochemistry

A. Dale, L. Haffert, E. Hütten

The initial results presented in this report address the pore water geochemistry at selected sites along the Hikurangi Margin offshore New Zealand's northern island. The main objectives of performing a detailed pore water analysis are (i) to quantify the rates of abiotic and biotic geochemical processes in the upper meters of sediment, (ii) to quantify the exchange fluxes between the sediments and the ocean, and (ii) to investigate the major geochemical processes occurring in the deep-seated upper plate sediments.

In total, the pore water was analysed at 14 sites at two locations along the continental margin off New Zealand. The sampling locations were chosen based on seismic and hydroacoustic studies on Leg 1 as well as video observations during video sled (OFOS) surveys on Leg 2 that suggested potential fluid and gas seepage. The on-board focus was on the chemical analyses of the composition of the pore fluids.

Methods

Sediment and pore water sampling

Samples were taken with a TV-guided multi-corer (TV-MUC; see chapter 5.5.2 & 6.9) and a gravity corer (GC; see chapter 5.5.1 & 6.7) at the locations listed in Table 9.1 (Appendix 9.1). After sampling with the GC, the core liner was immediately sectioned on deck into lengths of ≤ 1 m and samples for methane (CH_4) were taken using cut-off 3 ml polypropylene syringes from the ends of each core section. The sediment plugs were immediately injected into 30 ml glass vials filled with 9 ml of saturated NaCl solution to

poison the bacteria. The vials were sealed and vigorously shaken to disaggregate the mud and to stop all bacterial activity. The samples were stored upside-down to minimize the potential gas exchange with the atmosphere and transported to the onshore IFM-GEOMAR laboratory to quantify CH_4 and its homologues as well as stable isotopes (^{13}C, ^{18}O). Additional sediment samples for on-board analysis of methane and higher hydrocarbons (see chapter 5.1.5 & 6.5). Each section of the gravity core was then sealed, labelled and split open lengthways inside the on-board cold room at 4 ^{o}C. One (archive) half was described for sedimentological characteristics and the other (work) half was processed for geochemical analysis. Thereafter, the two halves were packaged for transport and storage at NIOZ. Short sediment cores retrieved with the TV-MUC were transferred into the cold room immediately after retrieval and the supernatant was filtered for subsequent analysis.

The sediments were mainly sampled for pore water by squeezing in a press under Argon gas (1-5 bar). This procedure was performed rapidly to minimize the effect of exposure to air on the pore water geochemistry. While squeezing, the pore water was filtered through 0.2 µm cellulose acetate Nuclepore filters and collected in recipient vessels. In selected cores, the pore water was sampled using rhizone® filters which were inserted through pre-drilled holes in the MUC liners or pushed into the work-half of the gravity core sediments. With this technique, the pore water is extracted anaerobically by suction using 20 ml plastic syringes and required 1-2 hours for the more consolidated sediments. The first 0.5 ml of pore water filtered from the sediment through the rhizones was discarded. Additional sediment sub-samples were taken in pre-weighed plastic vials for the determination of physical sediment properties such as porosity in addition to inorganic and organic particulate carbon, and total particulate nitrogen and sulphur. All sediment samples (squeeze cakes, wet sediment and unused pore water) were stored refrigerated for analyses at the onshore laboratory.

Pore water geochemical analyses

Water samples were analysed on-board for dissolved silicate (H_4SiO_4), ammonium (NH_4^+), total dissolved hydrogen sulphide (TH_2S) and total alkalinity (TA). H_4SiO_4, NH_4^+ and TH_2S were determined using standard photometric procedures following [*Grasshoff et al.*, 1997] on a Thermo Scientific Sprectronic 200 photometer. TA was measured by titrating pore water aliquots with 0.02 M HCl [*Ivanenkov and Lyakhin*, 1978] which was standardized using an IAPSO seawater solution. Since high sulphide contents (> 1 mmol/L) interfere with the reactions of NH_4^+ and H_4SiO_4, these sub-samples were acidified with 20 µl of HCl and left to degas overnight or bubbled with argon for 1 hour to strip any sulphide prior to the analysis.

The total alkalinity of the pore water was determined by titration with 0.02 N HCl using the Tashiro indicator; a mixture of methyl red and methylene blue. The titration vessel was bubbled with nitrogen to strip any CO_2 and H_2S produced during the titration. The IAPSO seawater standard was used for the calibration of the method.

Pore water and bottom water aliquots were also taken for shore-based chemical analysis. 2 ml of water were transferred to acid-cleaned plastic vials and acidified with 70% HNO_3 for determination of seawater ions by ICP-AES analysis (e.g. Mg^{2+}, Ca^{2+}, Mn^{2+}, Fe^{2+}, Li^+, Na^+). An additional 1.7 ml of pore water was added to plastic vials for ion-chromatography for the determination of SO_4^{2-}, Br^- and Cl^-. 1 ml pore water was separated and stored in glass vials for $\delta^{18}O$ isotope analysis. Pore water samples collected by rhizones in 6 cores were fixed with ZnAc and refrigerated for onshore analysis of stable sulphur isotopes ($^{32,34}S$) of SO_4^{2-} and H_2S. A detailed description of the analytical methods can be found on the website of IFM-GEOMAR (http://www.ifm-geomar.de/index.php?id=mg_analytik&L=O).

5.8 Thermistor mooring

Jens Greinert, Hans van Haren

Rising bubbles create turbulences in the water column disturbing the temperature structure of the water column. Depending on the strength of the bubble release such turbulences are getting more or less and their occurrence in general gives indications about the active periods of the bubble release. During SO214 we used a 60m long thermistor string from NIOZ (Hans van Haren) for deployment at the Tete seep at Opouawe Bank. The original plan was to have 2 long deployments, one at North Tower and the other one at LM-9 at Omakere Ridge, but this did not happen due to bad weather and at the end time constrains. The reason why we pick the Tete site was due to the planned CSEM work, which aimed for pulling through North Tower.

System

The mooring was composed of a release unite of two iXSea releasers, a metal anchor weight of 350 kg, one flotation body of syntactic foam (smarty), a benthos glass sphere as top buoy and the thermistor string itself (Figure 5.8.1). In addition an Iridium beacon was attached to the flotation device. The sensors are developed at NIOZ and have been calibrated prior to the cruise and shipped by airfreight. Accuracy of the sensors is 1 mK and logging was set to one second. Data will be only read out and analysed when the thermistor string has been send back to NIOZ.

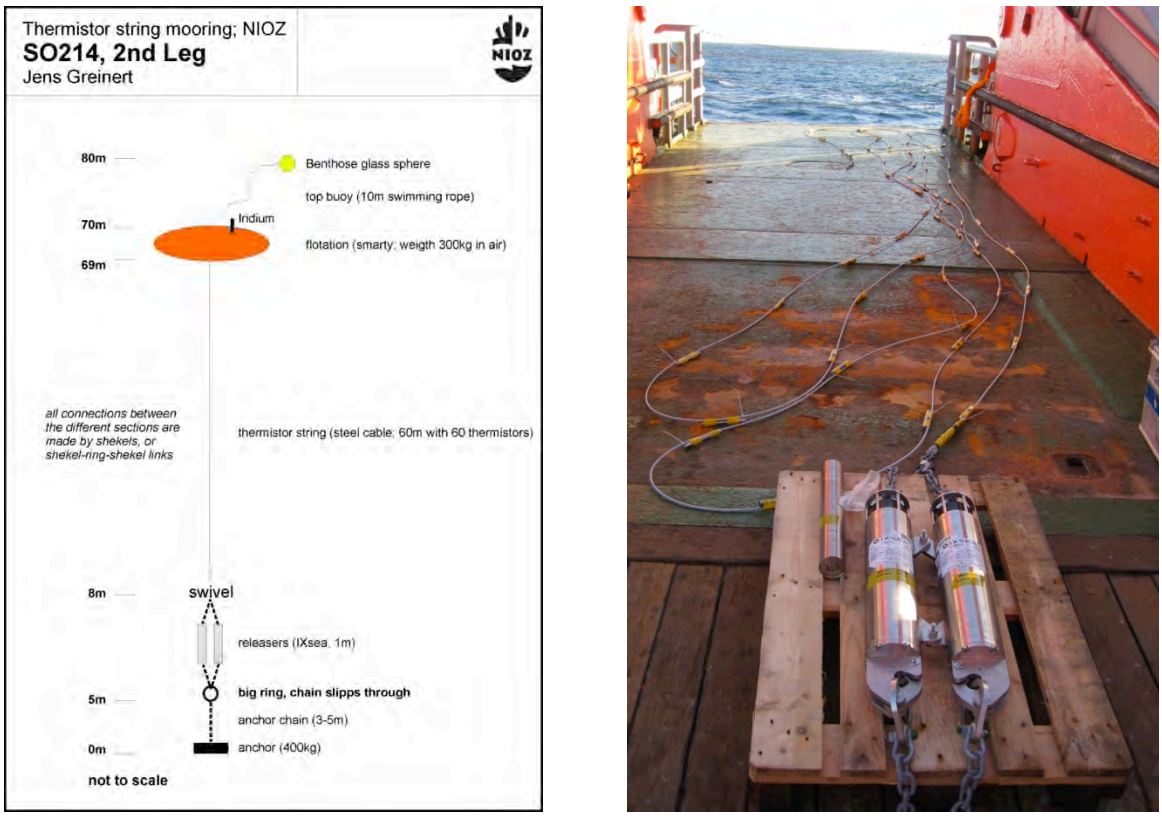

Figure 5.8.1: Sketch of the mooring layout (left) and parts of the mooring (releasers and thermistor string) laying on the back deck of SONNE during assembling.

Deployments

The details of the mooring deployed at the Tete site at Opouawe Bank are listed in Table 5.8.1. A screenshot of the 18 kHz hydroacoustic signal shows the two floatation bodies in the water column directly over the bubble releasing Tete site.

Table 5.8.1: Details of the mooring deployment.

SO214 #53 Mooring-1 (Tete Seep at Opouawe Bank)			
Deployment (UTC)	Position	Water depth	Recovery (UTC)
10 April 2011 7:12	175:27.177 -41:44.544	959	15 April 2011 02:42

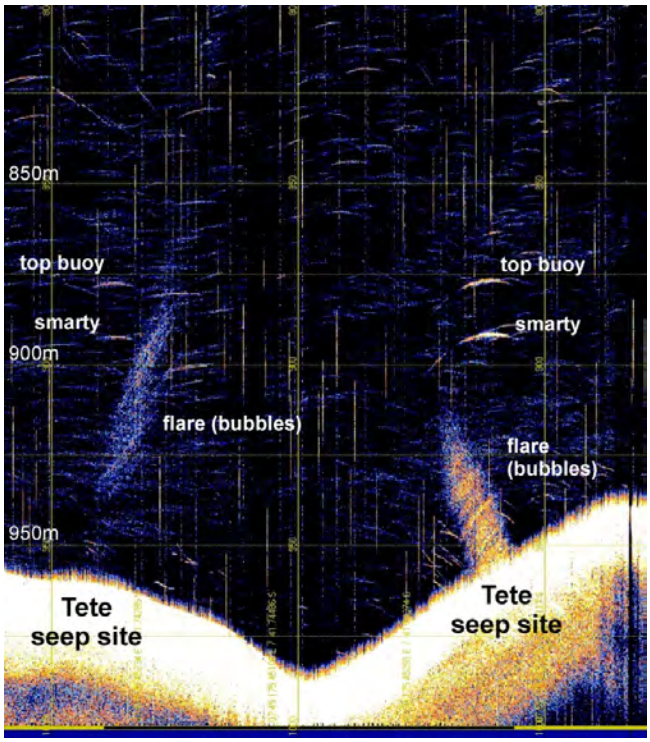

Figure 5.8.2: Echogram showing the top buoy and the main flotation (smarty) as clear reflections in the water column.

Figure 5.8.3: Mooring drifting by the vessel and being recovered.

5.9 Atmospheric Methane Measurements

Jens Greinert

Seeps emit methane into the water column and there is a small chance that some of this methane might reach the atmosphere. During SO191 we used an equilibrator system to determine if the activity of the seeps is strong enough to transport methane into the sea surface water layers and into the atmosphere, they were not. During SO214 we used a state-of-the-art cavity-ringdown-spectrometer from PICARRO (G1301) to measure continuously the atmospheric methane concentration during leg 1 and leg 2. We did this to increase the global data set of long-term methane measurements, which is vital to fine tune climate models.

System and Method

A detailed description of the PICARRO system itself can be found on the PICARRO website www.picarro.com. We put the PICARRO on the 'Wissenschaftsbrücke' and installed an air tube through the telephone room to the top deck and attached the end of the tube next to the compass on this deck. Unfortunately the CO2 laser of the system stopped working at the very beginning of the first leg, so we do not have CO2 from this cruise. Due to these problems we arranged that PICARRO checks the system remotely while in harbour between the first and second leg and they managed to change the settings of the system to only measure CH4 and H2O every 5 seconds. A calibration gas from the Royal Holloway University London (Rebecca Fisher) was used to check if the systems drifts over time; it did not and the calibration gas value of 2.0000 ± 0.0002 was twice confirmed during the cruise.

Figure 5.9.1: The PICARRO system installed on the Wissenschaftsbrücke on RV SONNE

Data have been logged as ASCII files and will be merged later with position and weather information data extracted from data base system on RV SONNE. In general the variations of the methane concentrations where quite low and the concentrations varied between 1.71 ppm to 1.75 ppm showing a clear relation to changing weather conditions and wind directions. When entering the Auckland area values significantly rose up to 1.78 ppm. Once the data have been finally processed and merged with the position data, the data can be requested from Jens Greinert at Royal NIOZ.

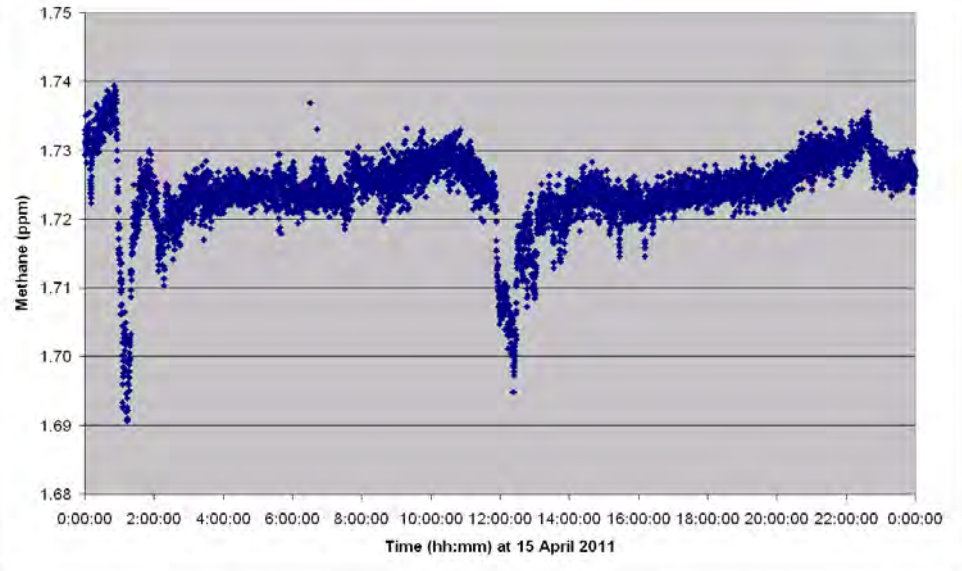

Figure 5.9.2: Example of the unfiltered data as produced by the PICARRO system.

6. Work completed and first results

Leg 1 of cruise SO-214 was dedicated to geo-acoustic imaging of the seep sites along the Hikurangi Margin. Most of our working time was dedicated to the acquisition of 3-D multichannel seismic data (chapter 6.2). 2-D multichannel profiles complement the database (chapter 6.2). The Parasound system was operated on all courses in order to provide detailed sediment images and check the water column for gas flares (chapter 6.1). Deep towed Sidescan sonar mapping was done in order to identify changes in the seafloor expression of the seep sites since cruise SO-191 in 2007 (chapter 6.3). Wide-angle observations by Ocean Bottom Seismometers should provide velocity depth information and may be used for reflectivity and amplitude analysis (chapter 6.2).

Maps of the areas and deployment positions of Leg 1 are shown in Figures 6.1 to 6.3.

Leg 2 was dedicated to geologic and biologic sampling, ground truthing with video observations and sampling of the water column. Structural images and mapping information obtained during the first leg was used to pinpoint the exact sampling locations and to compare repetitive measurements with results from the previous SO-191 and earlier expeditions. Instead of covering all working areas along the Hikurangi Margin we concentrated the work on dense sampling networks and profiles to provide a high-resolution study of the lateral gradation of selected seep sites. Opouawe Bank with the Tower seeps and seep Takahe became the core area of the work. Due to difficult weather conditions (work need to be terminated during 100 hrs. out of 330 appointed hrs.) only a very short MUC and video program remained for Omakere.

All meta data of the cruise are available through the IFM-GEOMAR Data Management Portal (https://portal.ifm-geomar.de/web/guest/home)

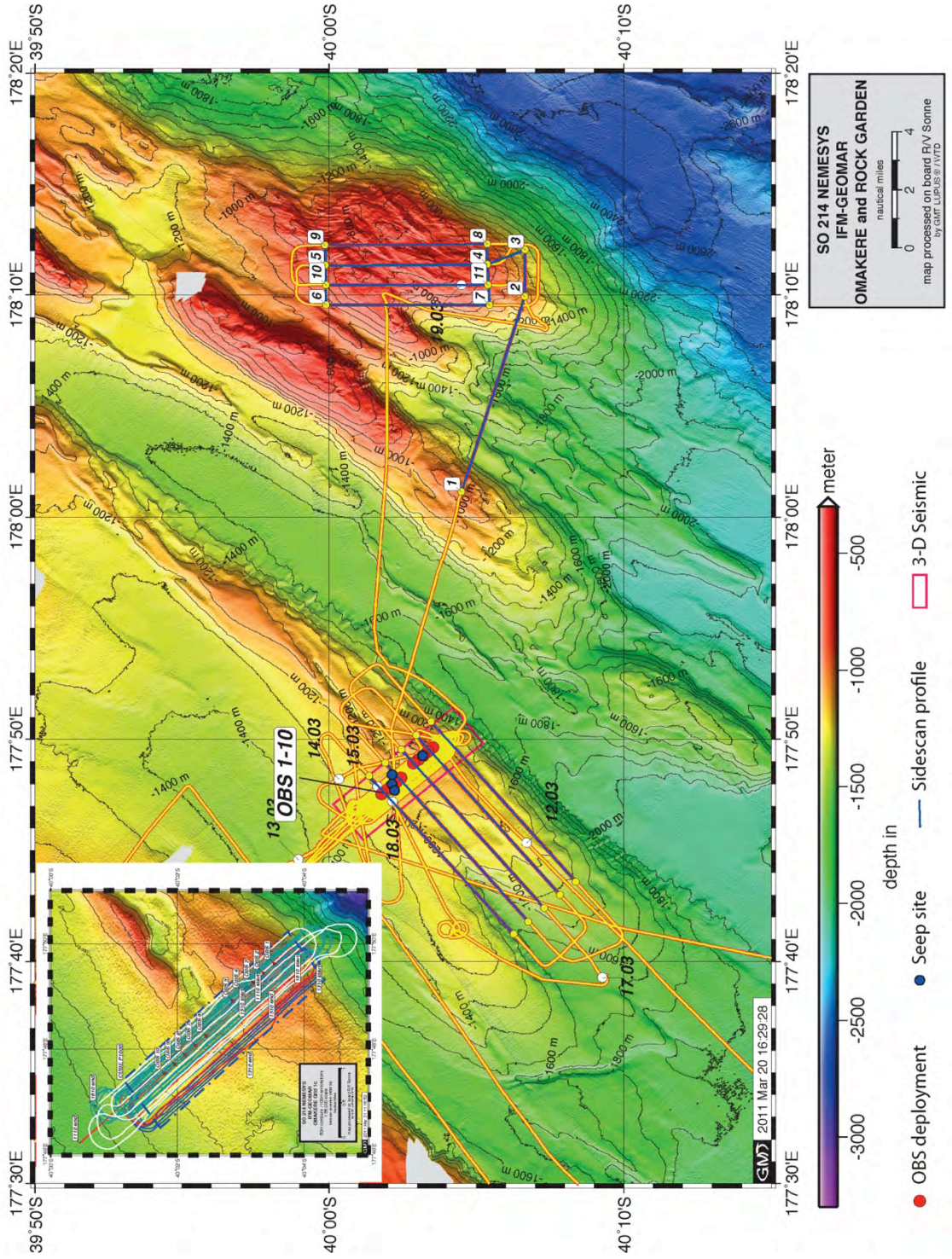

Figure 6.1: Map of the Omakere area with the geo-acoustic profiles shown. The inset shows the track lines of the 3-D seismic survey

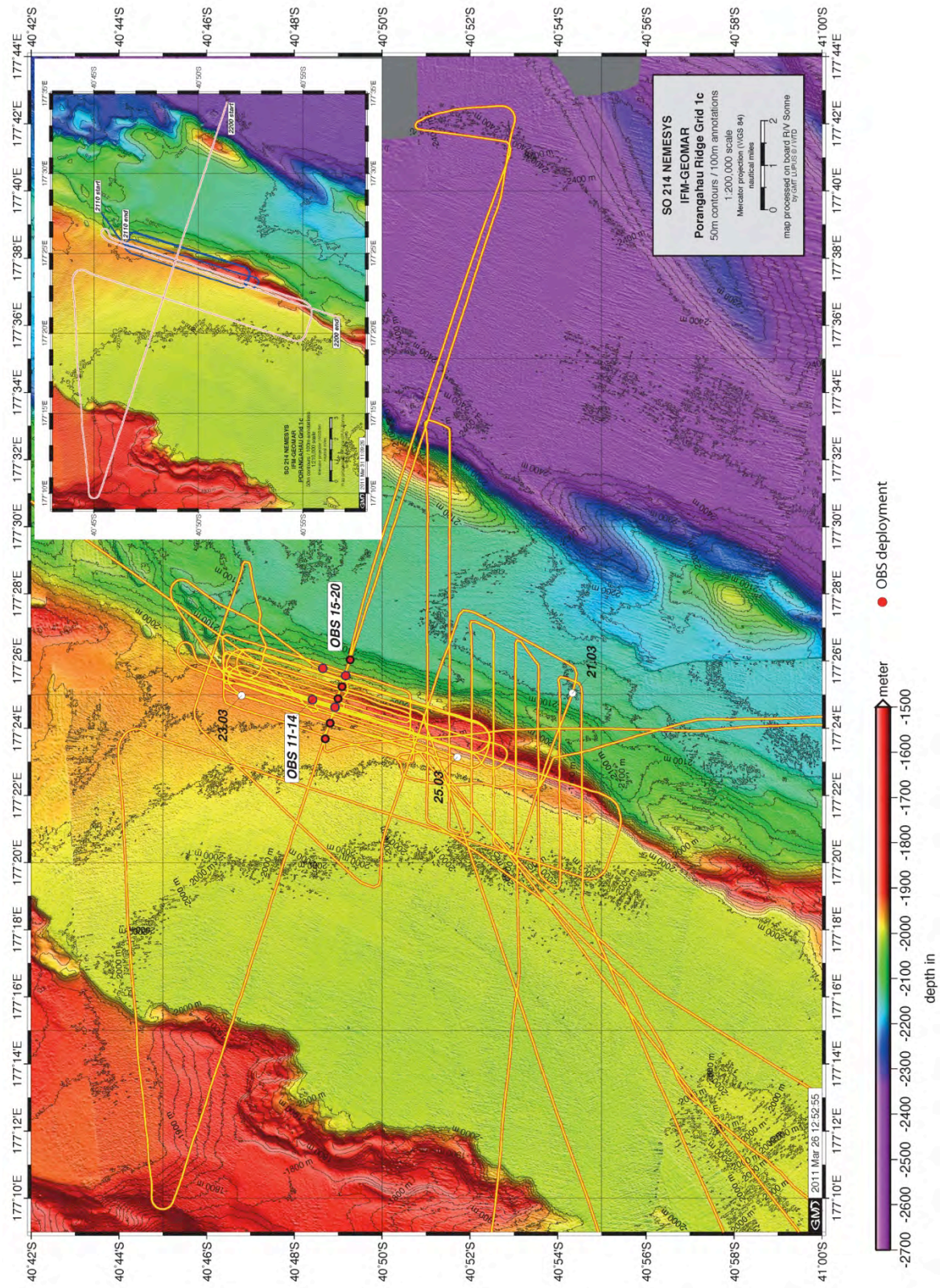

Figure 6.2: Map of the Porangahau area with the geo-acoustic profiles. The inset shows the track lines of the 2-D seismic survey (red) and the few lines completed with the 3-D system (blue)

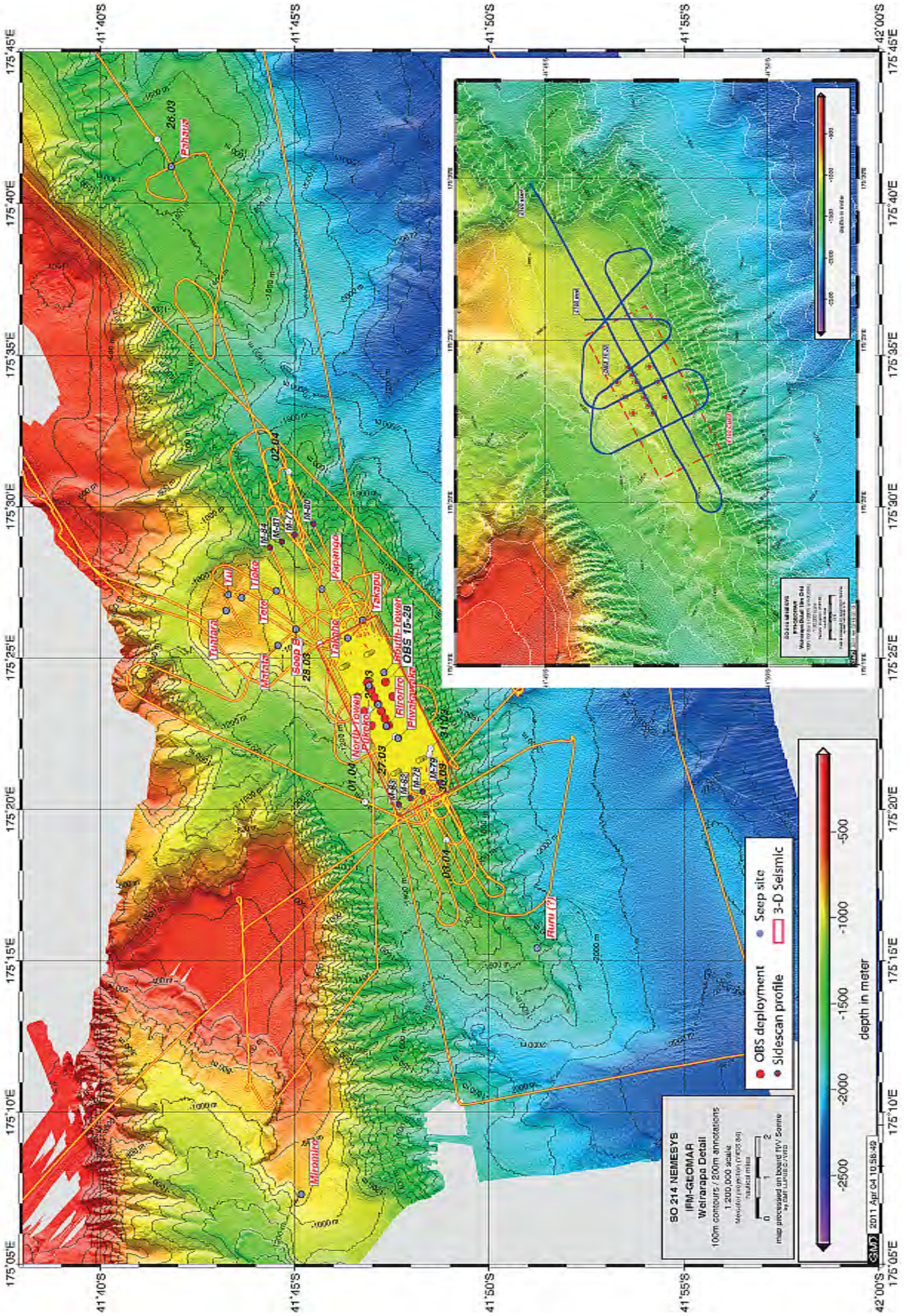

Figure 6.3: Map of the Wairarapa area with the geo-acoustic profiles shown. The inset shows the track lines of the 2-D seismic survey (blue) and the outline of the 3-D acquisition area (red)

6.1 Parasound Acquisition and Processing

Gareth Crutchley, Jens Greinert

The Atlas Parasound System P70 on-board R/V SONNE was used to acquire data at both 4 kHz and 18 kHz. The lower frequency beams were used for sub-bottom profiling, while the higher frequency component was used to image the water column. Raw SEG-Y format 4 kHz data, written out approximately every 40 minutes, were processed with the following flow in order to achieve good sub-bottom imaging:

1. Merge all data files for each day into a single SEG-Y file
2. Navigation in arc milliseconds stored in the headers converted to UTM zone 60S
3. Apply static shifts to correct for the window delay applied as part of the acquisition
4. Bandpass filter applied (kHz): Low cut: 1.5, Low pass: 2.0, High pass: 10.0, High cut: 12.0
5. Resample to half the sampling rate (rate reduced from 0.040 ms to 0.08 ms)
6. Static shifts and trace truncations were applied to sections of the data to reduce the length of the output trace to that which was useful (the water column and sections deeper than observed reflections were removed)
7. Amplitude correction for spherical divergence applied
8. Burst noise removal
9. Hilbert transform applied to convert the seismic traces to reflection strength traces (the envelope of the seismic trace)
10. Envelopes differentiated (gradient extracted) to generate smoother wiggle traces than the raw seismic wiggles
11. Stolt Migration of differentiated wiggle traces assuming Vp=1500 m/s and a constant trace spacing of 7 m
12. Integration of post-migration traces to restore them to the reflection strength (envelope) traces

Stages 10 – 12 were carried out to test the effectiveness of migration on the data. Wiggle traces were generated from the envelope traces by calculating the derivative along the envelope traces. These resulting wiggle traces were much more spatially coherent than the raw seismic data, and therefore, served as a better input to a 2D migration routine than the data output after Stage 8. After the data were migrated, the traces were integrated in order to restore them to envelope traces (i.e. the trace type that existed prior to differentiation). Figure 6.1.1 compares envelope data prior to (A) and after (B) migration. The migration does quite a good job, and in some places the data appear more coherent. However, any improvement in imaging after migration seems to be negligible.

The higher frequency (18 kHz) data were processed more simply, with a flow consisting of Steps 1-3, Step 6 and finally Step 9. An example of water column imaging plotted above sub-bottom profiling is given in Figure 6.1.1 for gas flares observed on Opouawe Bank (Section 6.1.5).

6.1.1 Omakere Parasound

The Parasound data at the Omakere Site was acquired in tandem with the 3D P-Cable survey (Fig. 6.1). As a result, a dense network of Parasound profiles has been collected that deliver excellent quality imaging of the shallow subsurface (4 kHz data) and the water column (18 kHz) around several known seep sites (Kea, Kaka, Kakapo, Moa and Bear's Paw) that were discovered during R/V SONNE Cruise SO191 in 2007. 4 kHz data provide very good quality imaging beneath Omakere Ridge. The subsurface beneath known seep sites is

characterized by anomalous reflectivity. Examples from the seeps sites are shown in figures 6.1.1.1 to 6.1.1.4.

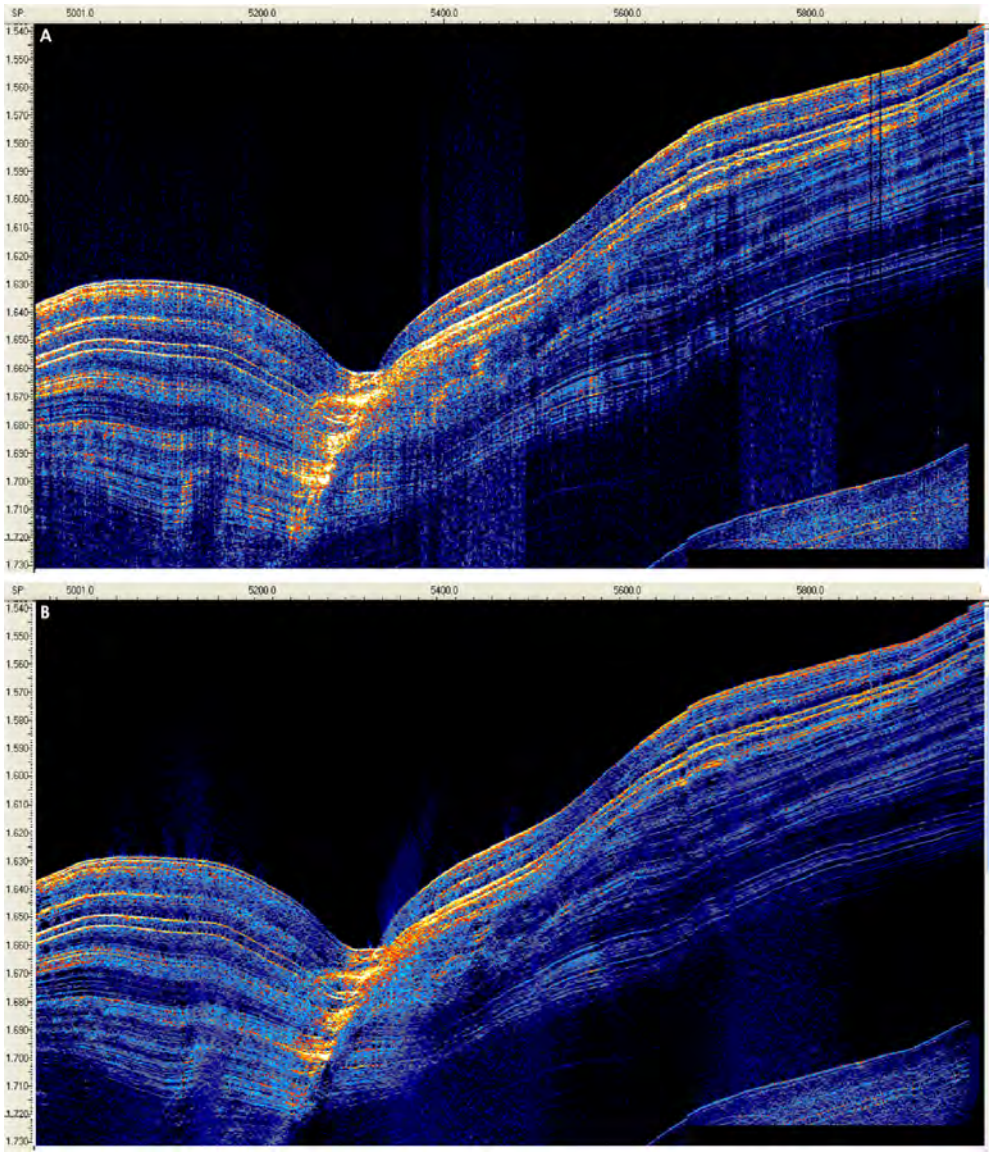

Figure 6.1.1: A) Example section of envelope traces (i.e. after processing stages 1-9). B) The same section as (A) but after 2D Stolt migration (extra stages 10-12 applied to the data given in (A)).

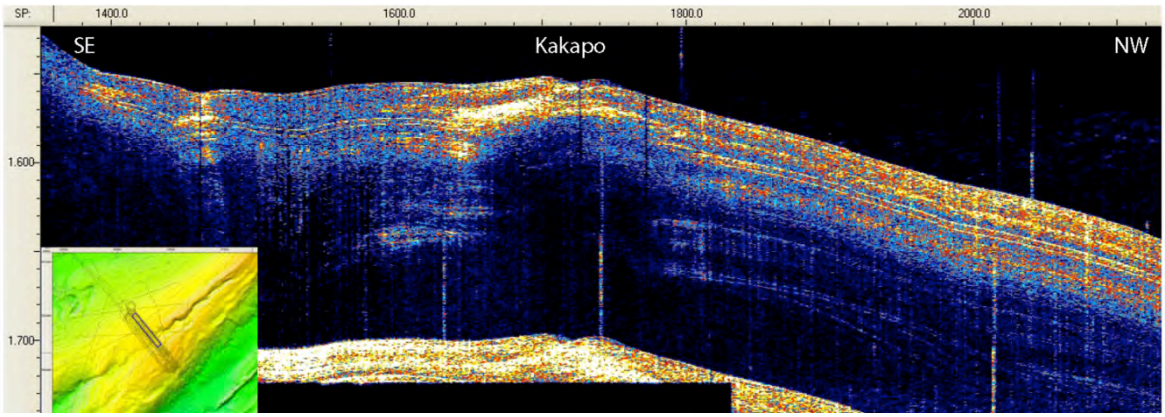

Figure 6.1.1.1 Parasound profile crossing seep site Kakapo

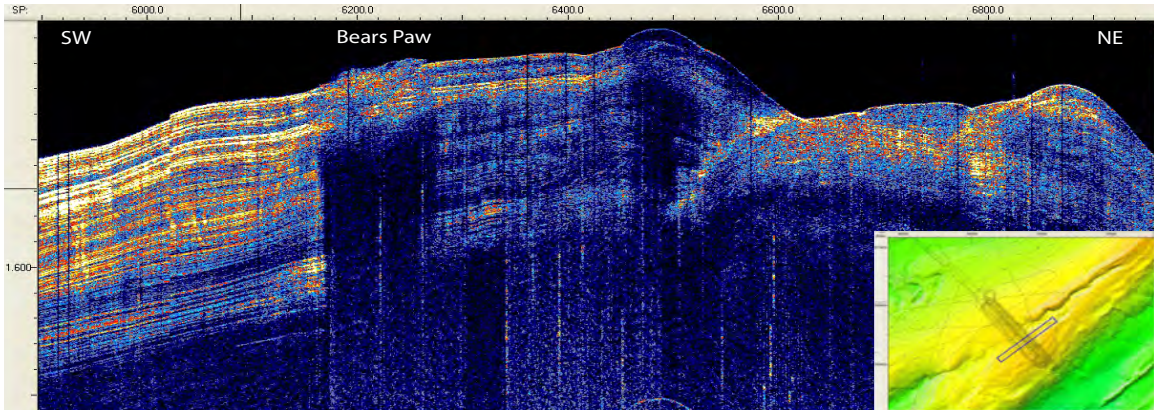

Figure 6.1.1.2 Parasound profile crossing seep site Bears Paw

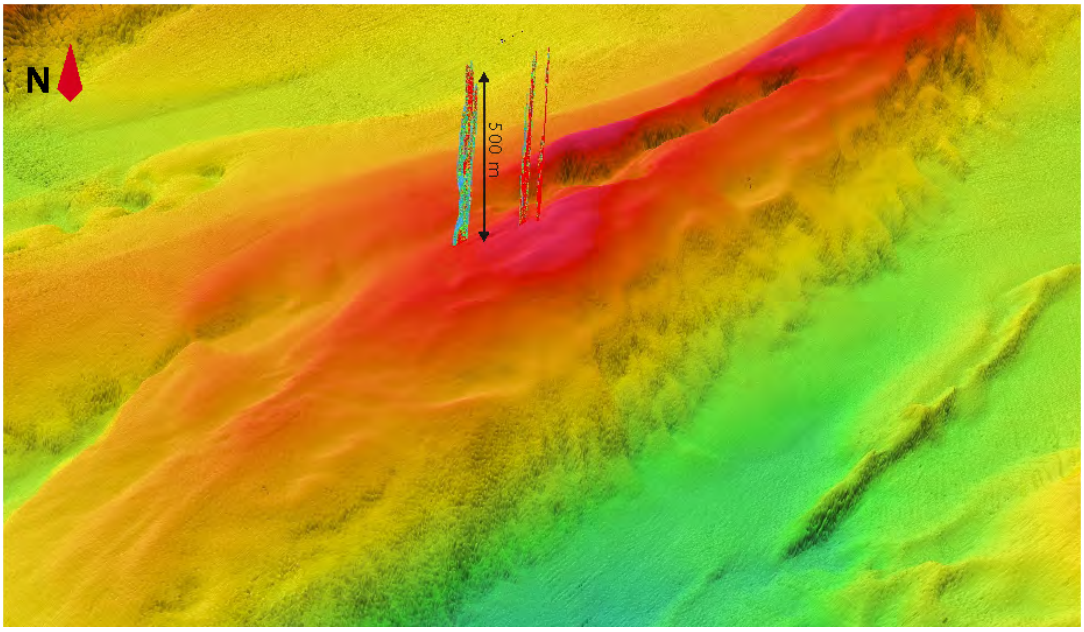

Figure 6.1.1.3 Bathymetry at Omakere with Bears paw flares

6.1.2 Porangahau Ridge Parasound

Callum Bruce

Parasound data were collected in the Porangahau Ridge survey area to characterise shallow subsurface geology (using the 4 kHz channel) and to attempt to image gas flares within the water column (18 kHz channel). As with Omakere Ridge, the parasound data at Porangahau Ridge were acquired in tandem with the 3D survey.

Unfortunately, due to adverse weather conditions, not many of the planned ship tracks could be completed. The distribution of Parasound profiles is coincident with the track lines sailed in the Porangahau area (Fig. 6.2). All data underwent shipboard processing in accordance with the sequence outlined in Section 6.1 (Parasound Processing).

Penetration of up to approximately 80 m was achieved using the 4 kHz signal in areas with relatively subdued bathymetry throughout the Porangahau Ridge survey area. Several zones of strong acoustic blanking were observed, some of which show associated seafloor relief. Several sedimentary structures were observed including sediment waves and erosive sedimentation boundaries. Relatively flat-lying sediments were imaged on the crest of

Porangahau Ridge along with a possible fault causing localised folding of these strata. Examples of the data are given in Figures 6.1.2 to 6.1.2.4.

The 18 KHz data revealed four acoustic flares on the crest of Porangahau Ridge (Figure 6.1.2.4). These flares give the first evidence for active methane seepage from the seafloor at this site. A fifth location, where a less-conspicuous acoustic disturbance exists in the water column, is at this stage considered a possible flare and requires follow-up work to determine its origin. The sub-seafloor character beneath two adjacent flares shown in Figure 6.1.2.4 (the two on the right) is shown by the 4 KHz data in Figure 6.1.2.5. Regions of suppressed amplitude are observed in numerous places, where they disrupt otherwise well-defined stratigraphic reflections.

6.1.3 Wairarapa Parasound

Gareth Crutchley

As with Omakere Ridge, Parasound data at the Wairarapa Site were acquired in tandem with the 3D P-Cable survey. A dense network of Parasound profiles has been collected (Figure 6.3), delivering excellent quality imaging of the shallow subsurface and the water column around numerous known seep sites (Piwakawaka, Riroriro, Pukeko, North Tower, South Tower, Takapu and Takahe) discovered during SONNE Cruise SO191 in 2007 [*Bialas et al.*, 2007b]. Adjacent profiles are approximately 60 m from each other, meaning that strata, unconformities and gas fronts can be traced in pseudo 3D.

Over much of the grid, 4 kHz signal penetration beneath the seafloor exceeds 100 m. Data examples are given in Figures 6.1.3.1 and 6.1.3.2. Pronounced, sub-vertical, low-amplitude zones are observed throughout the dataset beneath the known seep sites (e.g. Figure 6.1.3.3). Additionally, however, numerous sub-vertical zones of suppressed reflectivity are observed in other areas. Many of the zones do not reach the seafloor, terminating at various stratigraphic levels. Strong reflection fronts are often observed within the low-amplitude zones close to the seafloor, which are likely, in many cases, to be caused by the presence of gas.

The 18 kHz data revealed acoustic flares at each of the main seep sites. Examples are given in Figure 6.1.3.3, where the water column imaging is overlain on a sub-bottom profile image. The acoustic flares emanate from the seafloor directly above zones of acoustic blanking. Over the survey period of eight days, acoustic flares were imaged approximately 80 times as the vessel passed over the seep sites time and again (e.g. Figure 6.1.3.4).

Both the water column imaging and the sub-bottom profiling were used to guide electro-magnetic and geochemical studies in the second leg of SO214. Extents of blanking zones, as well as flare locations and a prominent unconformity were mapped in 3D in Fledermaus.

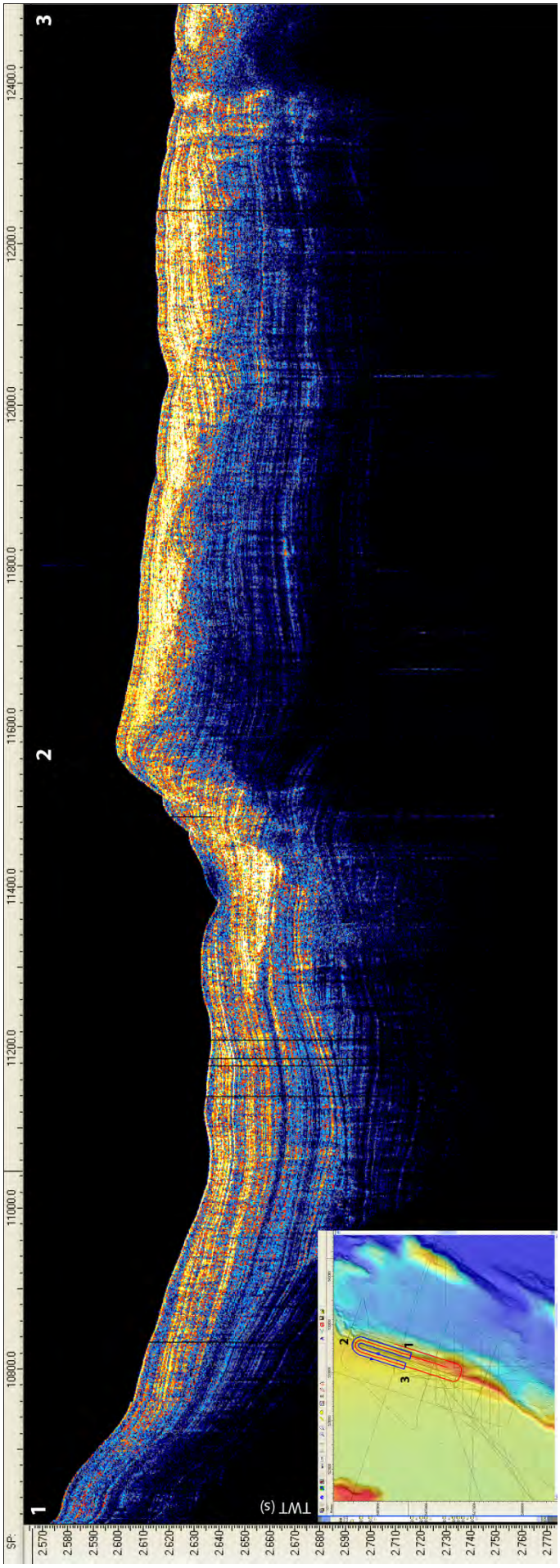

Figure 6.1.2.1 – Example of 4 kHz Parasound Data from the Porangahau Ridge site. Vertical scale is in second two-way time. Trace spacing approximately 7 m.

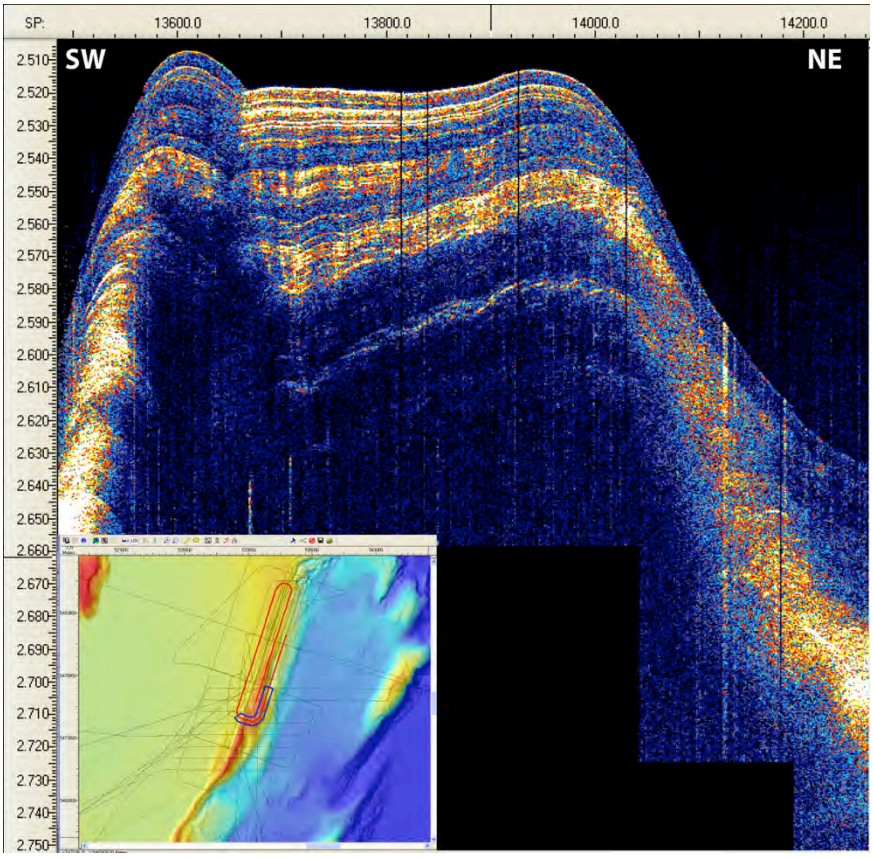

Figure 6.1.2.2 – Example of 4 kHz data crossing the crest of Porangahau Ridge. Note the presence of relatively undisturbed sediment on the ridge crest. Vertical scale in seconds two-way time. Trace spacing approximately 7 m.

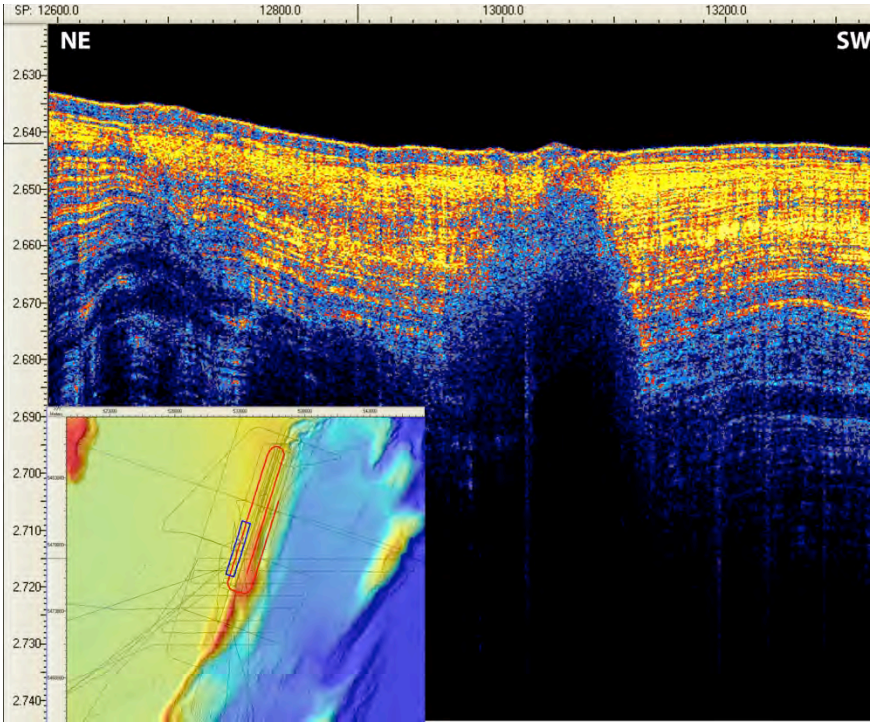

Figure 6.1.2.3 – 4 kHz data showing a zone of strong amplitude blanking. Note that presence of localised seafloor relief above the blanked zone. Vertical scale in seconds two-way time. Trace spacing approximately 7 m.

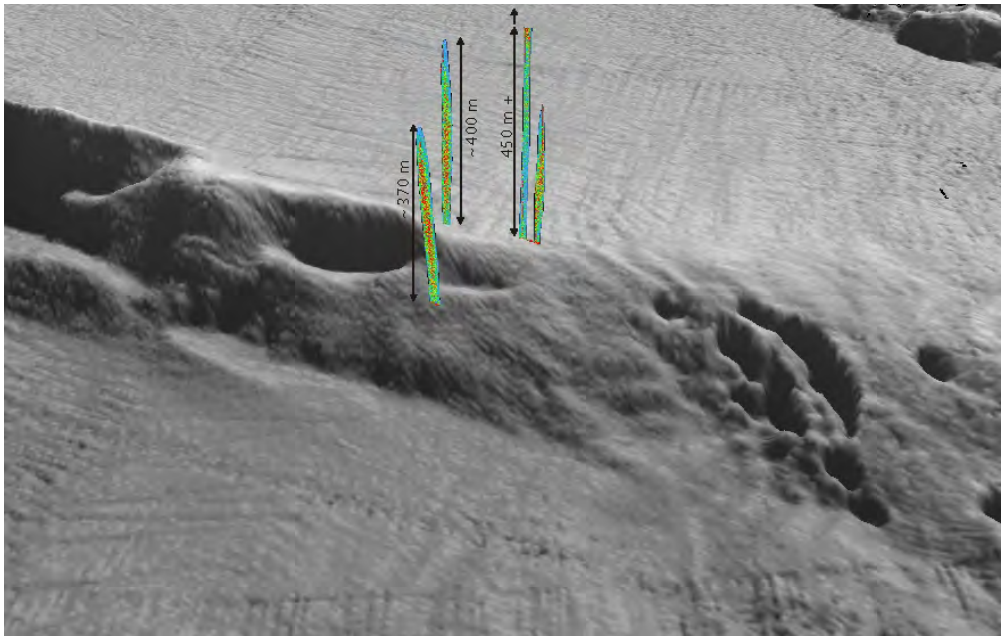

Figure 6.1.2.4 – 3D image of the northern reaches of Porangahau Ridge, close to the prominent arcuate scarps that were at the northern limit of the survey area (see Figure 1). The view is looking towards the West, with a 10x vertical exaggeration. The approximate heights of the flares above the seafloor are indicated. The largest flare exceeds a height of 450 m (the top of the flare was not imaged due to truncation from the recording window).

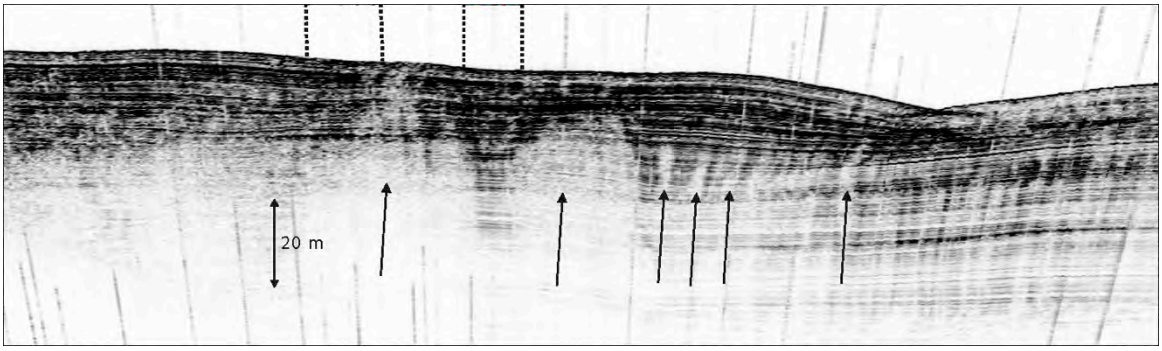

Figure 6.1.2.5 – An example section of 4 kHz Parasound data from beneath two adjacent flares of Porangahau Ridge (the two on farthest to the right in Figure 5). The dotted black lines above the seafloor shown the locations of the flare routes as taken from 18 kHz data.

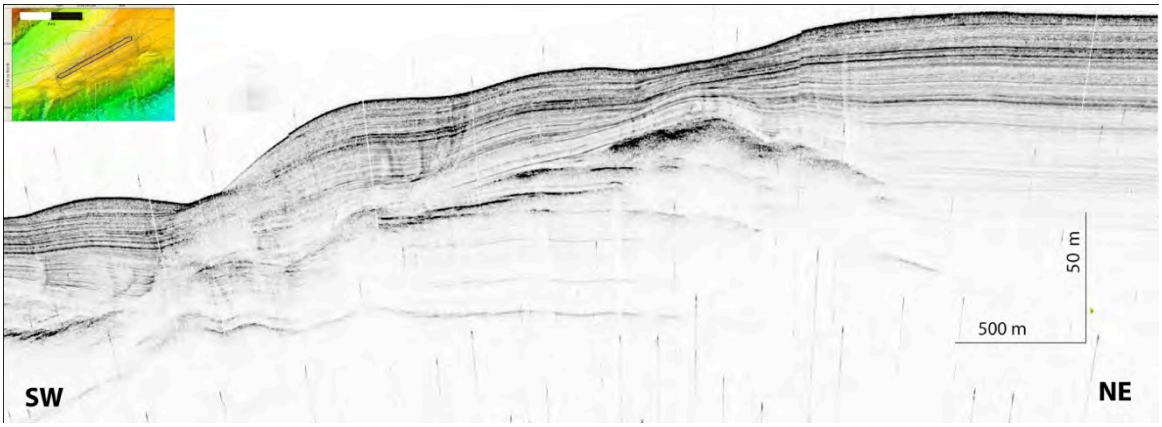

Figure 6.1.3.1: An example of 4 KHz Parasound data beneath Opouawe Bank, looking towards the NNW. Data are plotted at a 10x vertical exaggeration. Vertical streaks in this image (as well as in Figure 4) are noise bursts that have not been removed for this particular image.

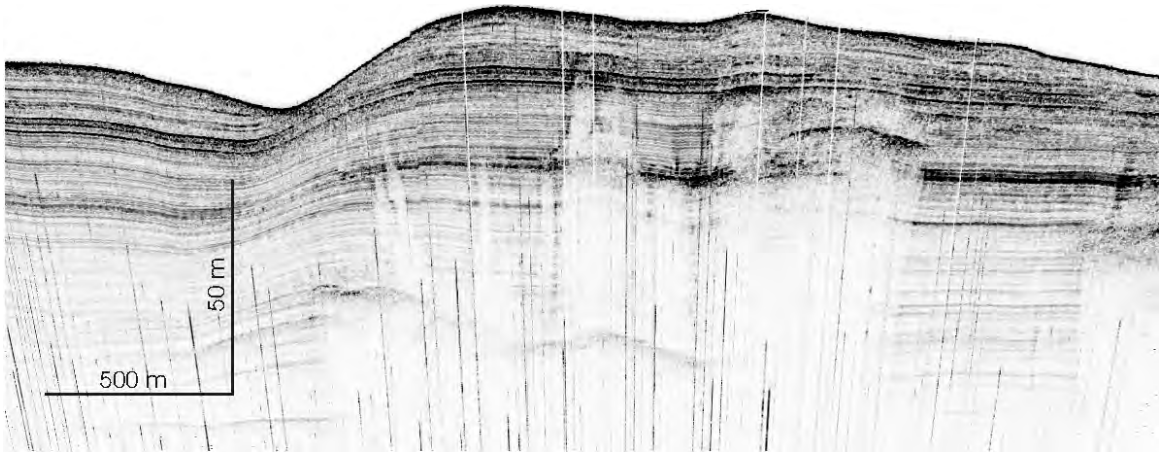

Figure 6.1.3.2: An example of 4 KHz Parasound data beneath Opouawe Bank, looking towards the SSE. Data are plotted at a 10x vertical exaggeration.

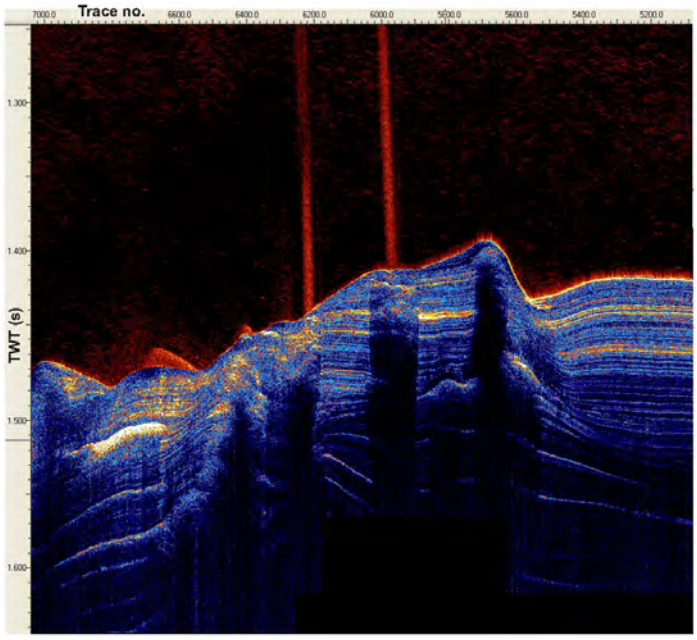

Figure 6.1.3.3. A compilation image of 4 kHz (beneath the seafloor) and 18 kHz (above the seafloor) constructed from data acquired along the profile outlined by the blue box in Figure 1. Acoustic flares in the water column emanate from the seafloor above sub-vertical zones of suppressed reflectivity.

6.2 Seismic

6.2.1 Omakere

6.2.1.1 P-Cable Omakere

Gareth Crutchley, Dirk Klaeschen, Cord Papenberg, Stephanie Koch

The 3D survey at Omakere Ridge was designed to image fluid migration pathways beneath seep sites (Kea, Kaka, Kakapo, Moa and Bear's Paw) discovered during R/V SONNE cruise SO191 (Figure 6.1 & 6.2.1.1.1).

Data acquisition

The 3D seismic survey was acquired over a period of ~7 days, in which time a surface area of 10 km^2 was covered, with 6.25 km long in-lines by 1.625 km long cross-lines. The source consisted of one 4.2 l airgun towed at a depth of 2 m directly behind the vessel, which

was fired at 6 s intervals, based on GPS time. Data were sampled at 0.25 ms and revealed a dominant frequency of ~60 Hz.

Processing

The geometrics CNT-2 software was used for data acquisition. GPS antennae were installed on each of the trawl doors, and radio transmitted on board. For the most part of the survey the GPS positions functioned reliably. At times, however, the GPS signal for one, or even both of the trawl doors was lost. In these cases, predictive navigation curves were calculated to interpolate the positions of the doors.

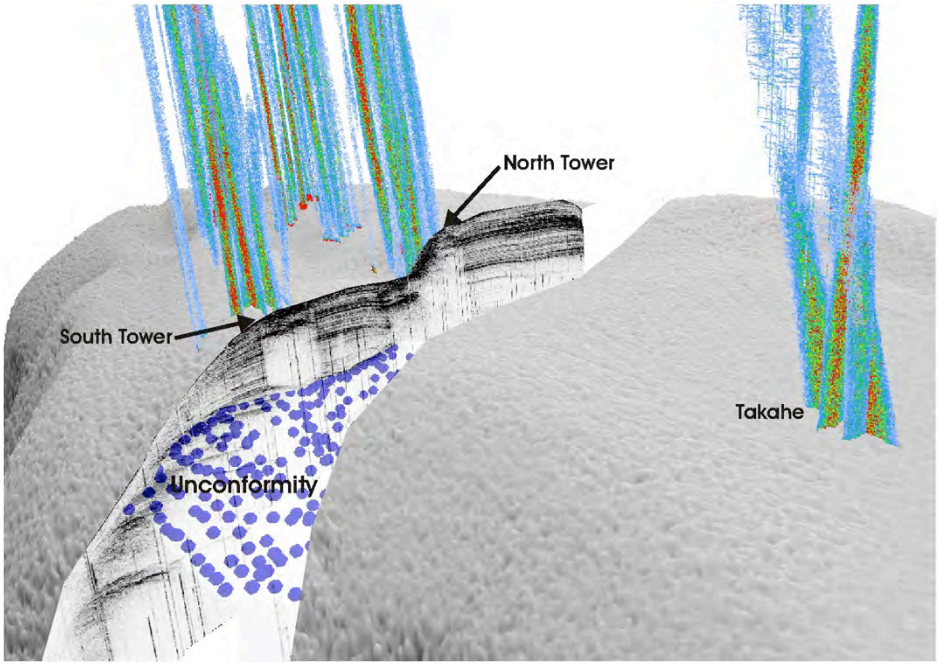

Figure 6.1.3.4: A 3D image showing numerous flares plotted on top of each other from seep sites on Opouawe Bank. The view is looking west, and the vertical exaggeration is 10x. The blue dots were picked in numerous lines at an unconformity beneath the seafloor that was a target of one of the gravity cores acquired during the second leg.

The gun position was calculated using the arrival time (converted to distance assuming a velocity of 1500 m/s) of the direct wave on the outermost channels. A predictive geometry of the streamer configuration was then calculated assuming that the cross cable adopts a catenary form as it is towed through the water. The orientation of the catenary (i.e. its apex) was assumed to be perpendicular to the imaginary line between the doors. The predicted streamer positions were then fine-tuned by examining the direct arrival on the first channel of each streamer. The entire process of geometry calculation is summarized in Figure 6.2.1.1.2.

Reasonably good trace coverage enabled an initial CMP grid spacing of 6.25 m. The resulting fold map for this grid spacing is given in Figure 6.2.1.1.3. Data were then corrected for normal move-out and stacked, both with a constant velocity of 1500 m/s. An initial 2D TK migration was applied to the in-lines and cross-lines to check the imaging. A final 3D true-amplitude Kirchhoff time migration was then carried out to deliver the data displayed in Figure 6.2.1.1.4.

Imaging

The data in the final Omakere Ridge cube are of very good quality, exhibiting excellent signal/noise ratios in both in-line and cross-line directions. An example of 3D details are given in Figure 6.2.1.1.4, where in-lines, cross-lines and time-slices are extracted to reveal

geological relationships beneath the seafloor. Well-stratified sediments are imaged, as well as disturbed reflections and faults, which may act as fluid migration pathways. The time slice of the cube in Figure 6.2.1.1.4A reveals the seismic character of seep site Bears Paw on the seafloor (towards the top of the figure).

Post-stack trace interpolation and migration

As can be seen in the fold map in Figure 6.2.1.1.3, reasonably large data gaps exist in the coverage – principally in the southwestern half of the cube. In order to fill these gaps, which are problematic for migration, a post-stack trace interpolation processing sequence was carried out. The first stage involved interpolating traces in the cross-line direction. Beginning with the cross-line direction (as opposed to the inline direction) was crucial as entire in-lines were missing. The routine employed, part of Western Geco's Omega2 processing software, interpolates missing traces by summing existing adjacent traces (either side of gaps) that have been time-shifted by various amounts such that they line up at the angles of maximum coherency. Correlation widths and stacking widths can be set such that the routine considers sufficient data in its search for coherent dips in the processing direction.

After completing an interpolation in the cross-line direction, traces were interpolated in the in-line direction as well. Figure 6.2.1.1.5A shows the distribution of live traces in the Omakere grid prior to any trace interpolation and Figure 6.2.1.1.5B shows the distribution after trace interpolation in both the cross-line and in-line directions. An example of the quality of the generated traces is shown in the comparison between Figures 6.2.1.1.6A and B.

In addition to the interpolation on the 6.25 m grid, a further flow was constructed to decrease the trace spacing in both dimensions to 3.125 m. Previous experience has shown that such an exercise can significantly increase both the spatial and temporal resolution by providing a cube to the subsequent migration algorithm that has increased trace to trace coherency. In particular, the increase in resolution can decrease any spatial aliasing in steeply dipping sections of diffraction tails. Figure 6.2.1.1.6A shows an example region of the grid where traces from the 6.25 m grid have been interpolated in both directions to result in a 3.125 m grid spacing. 3D post-stack Kirchhoff and Stolt migrations were then tested on both the 6.25 m and 3.125 m resolution cubes, using a constant velocity of 1500 m/s.

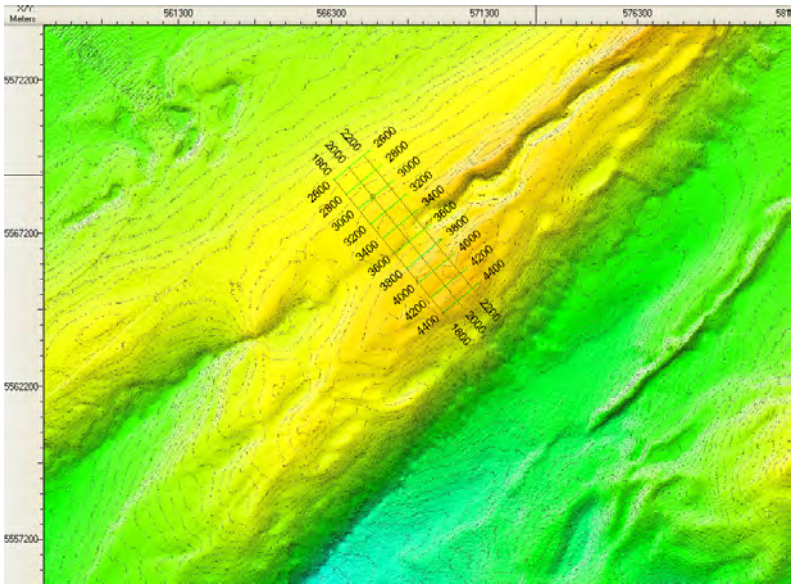

Figure 6.2.1.1.1: Location map of the Omakere study area showing the extent of the final 3D cube that was acquired.

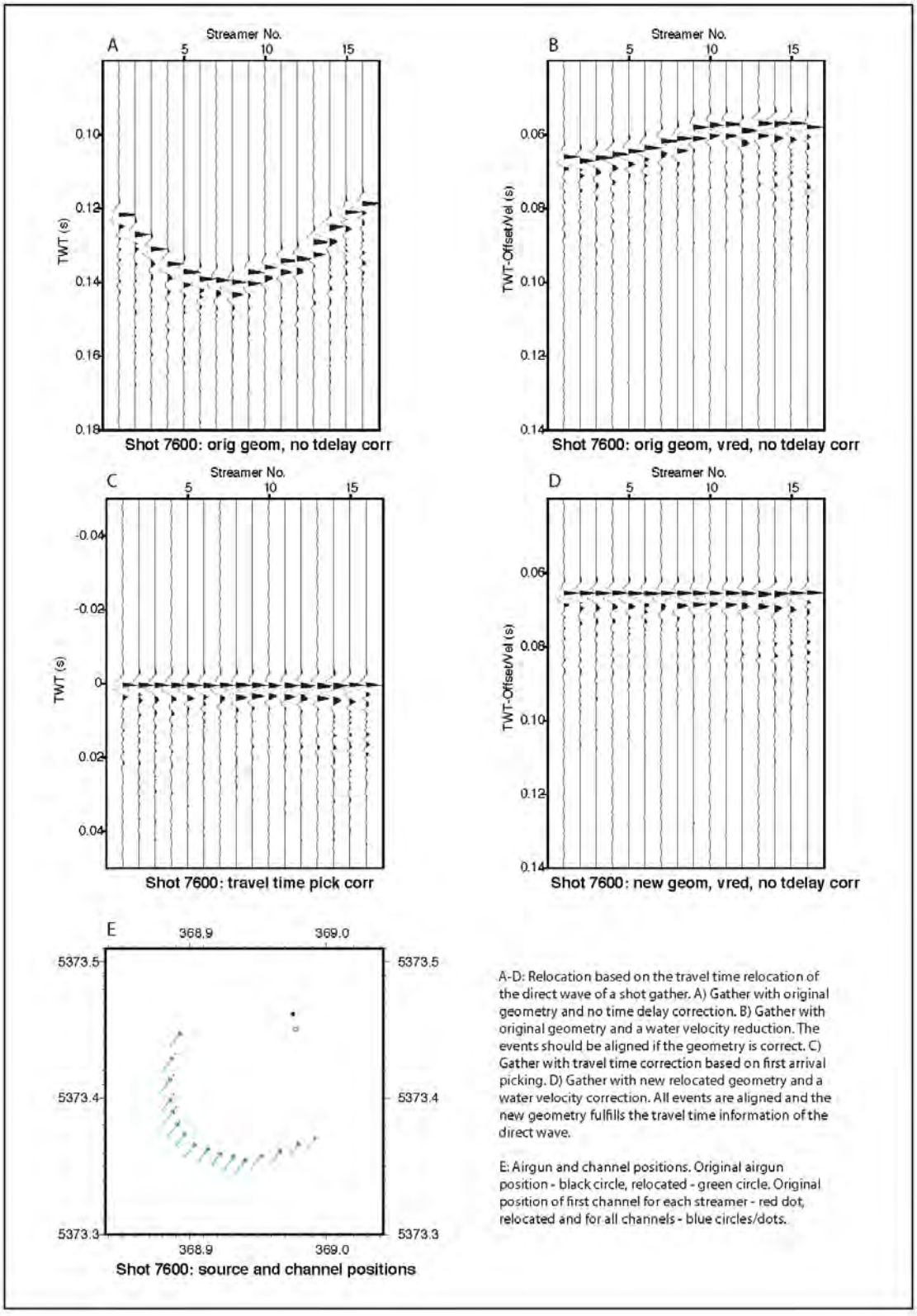

Figure 6.2.1.1.2: Summary figure showing the process of geometry prediction and adjustment.

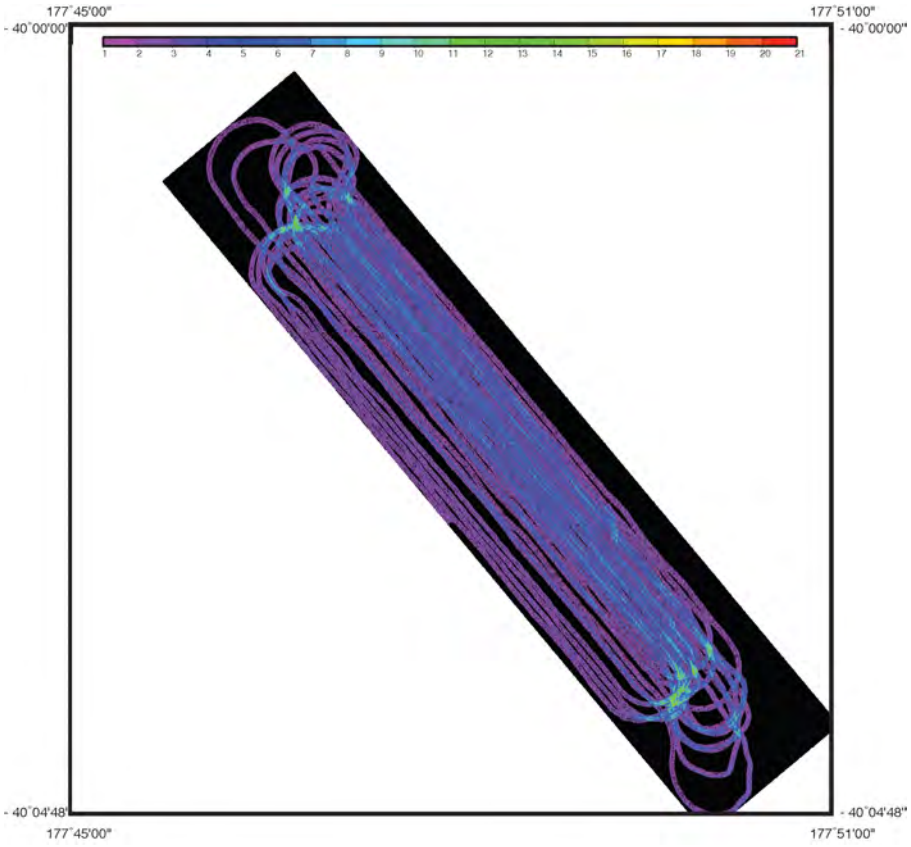

Figure 6.2.1.1.3: Colour-coded fold map of the 3D cube at Omakere Ridge.

6.2.1.2 OBS Omakere

Stefan Moeller, Mareike Kampmeier, Eduardo Moscoso

In the area of Omakere (-40°00’ S/178°00’ E to -40°06’ S/177°36’ E, (Figure 6.2.1.2.1) 10 OBSs were deployed. They recorded the shots for the 3D data to get velocity information in this area. The ridge lies in a water depth of around 1100 m and has a bathymetric relief about 500 m. All OBSs were deployed in a water depth between 1100 and 1200 m. They were arranged in two lines of 5 OBSs each (Figure 6.2.1.2.1); close to the seep sites Moa and Bear’s Paw (OBS_01 – OBS_05) as well as Kea, Kaka and Kakapo (OBS_06 - BS_10).

Seven of the OBSs were supplied with MLS-recorders, sampling with 200 Hz and three with MBS recorder, sampling with 1000 Hz. Additionally Methane sensors were attached to OBS02 and OBS03. For the first processing we used the sail-line crossing directly the OBS profile (profile A). On the seismic record sections the direct wave, several reflections and refracted phases can be identified (see examples Fig 6.2.1.2.2 - 5).

Unfortunately, three of them did not record useful data (OBS02, OBS07, OBS09).

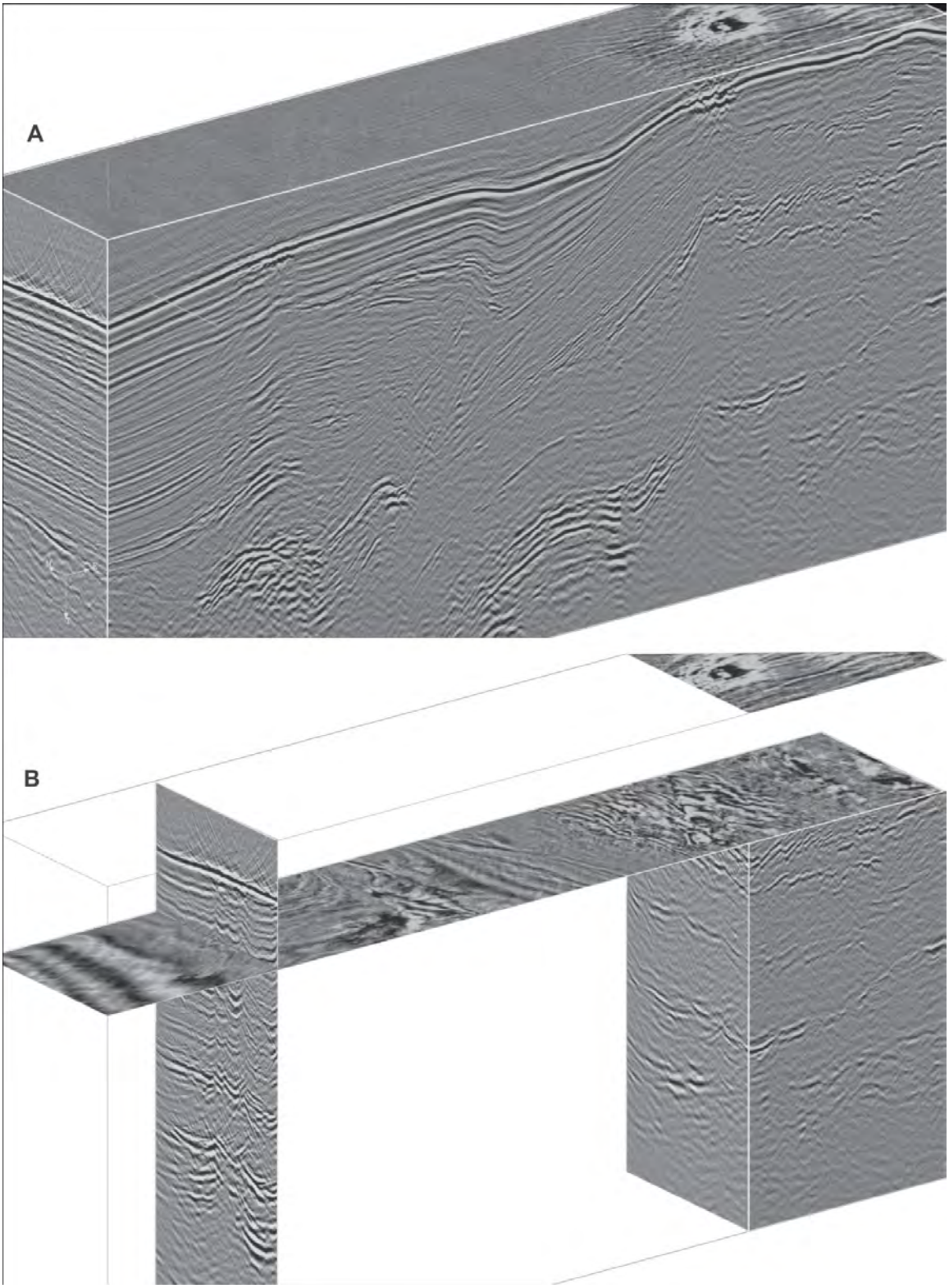

Figure 6.2.1.1.4: A 3D plot of representative inlines, crosslines and timeslices extracted from the 6.25 m resolution cube.

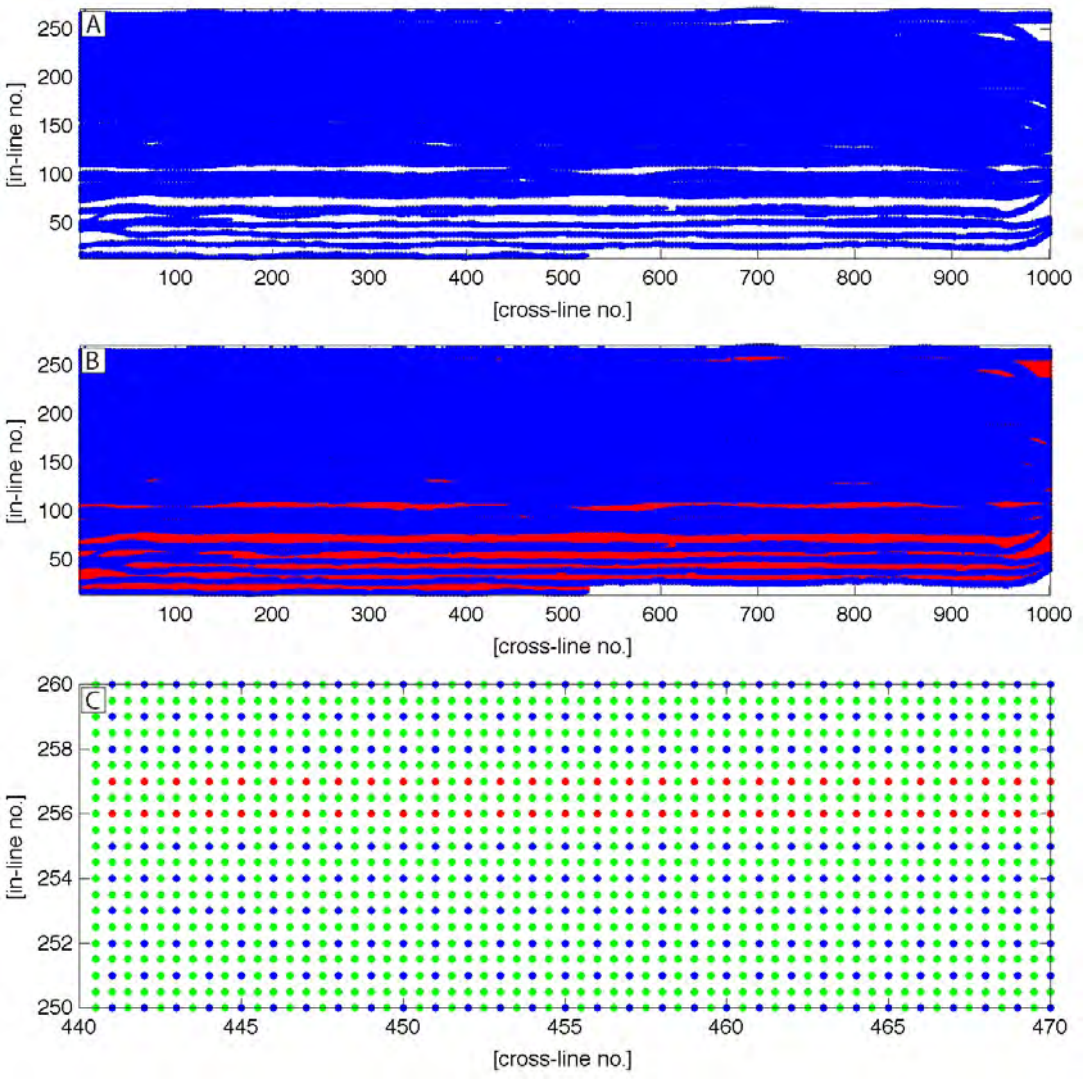

Figure 6.2.1.1.5: Coverage map of the 3D area before (A) and after (B) cross-line and in-line interpolation

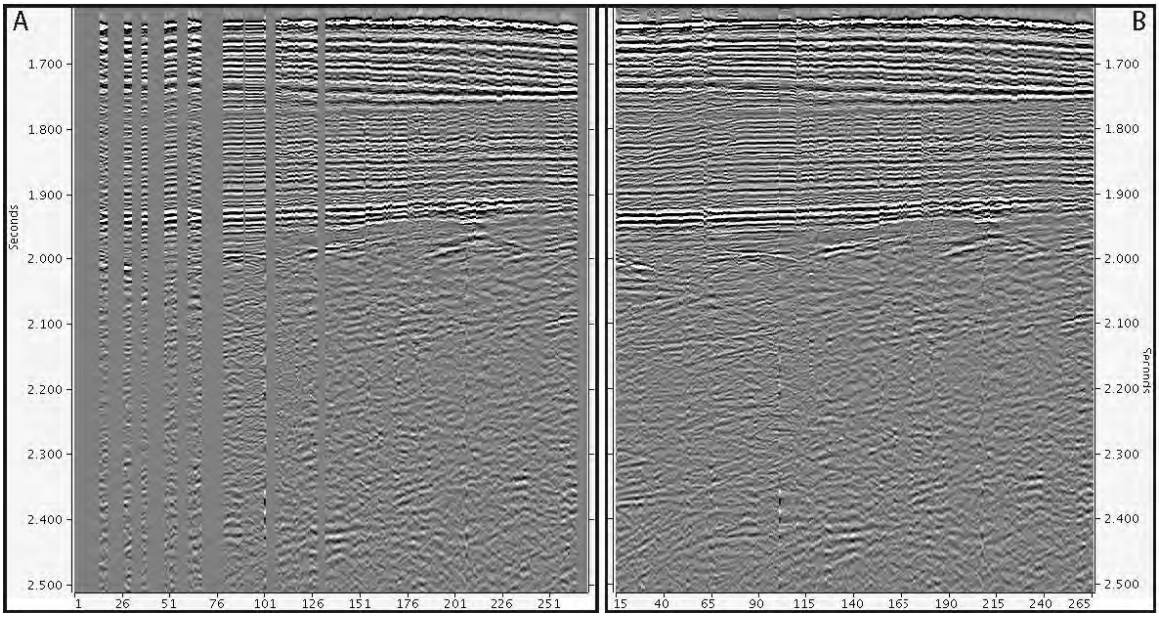

Figure 6.2.1.1.6: Data comparison between 6.25 m grid (A) and interpolated 3.125 m grid (B)

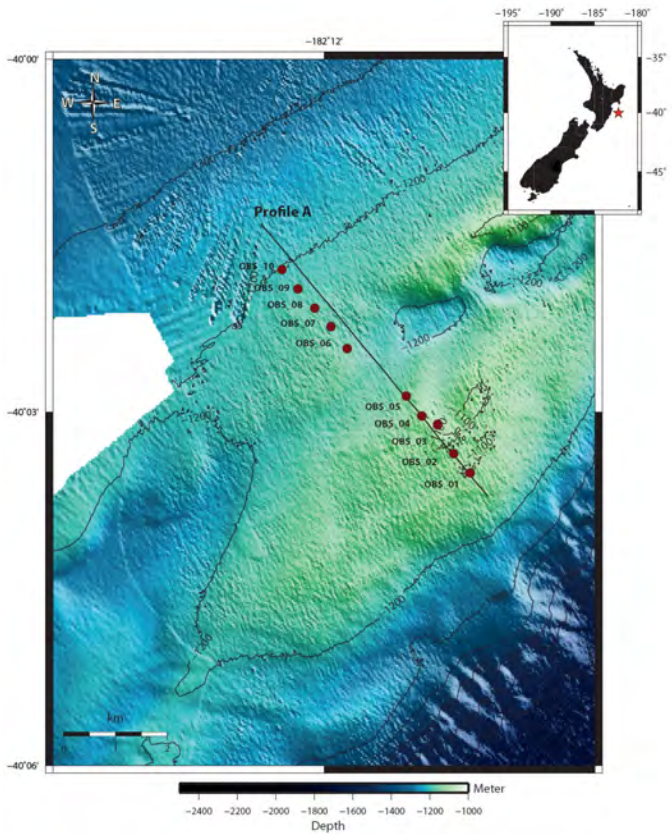

Fig. 6.2.1.2.1: Location map of deployed OBSs on the Omakere Ridge.

6.2.2 Porangahau

6.2.2.1 2D Seismic Porangahau Ridge

Ingo Pecher, Andreia Plaza-Vaverola, Thomas Golding, Callum Bruce

Scientific Motivation

Porangahau Ridge was a study area of both SO-191 and the R/V *Tangaroa's* voyage TAN-0607 in 2006. Echo sounder data and methane concentrations in the water column did not indicate any active gas escape. Seismic data however, show a pronounced amplitude anomaly reaching up to >300 m above the regional level of bottom simulating reflections (BSRs) beneath the ridge. This has been interpreted as gas based on its polarity [*I A Pecher et al.*, 2010] and its fine velocity structure from full-waveform inversion [*Crutchley et al.*].

The presence of thick (i.e., seismically resolvable) layers that contain gas well above the regional base of gas hydrate stability (BGHS) has been explained by a heat flow anomaly caused by advection: Warm fluids are thought to migrate upwards from the decollement along a thrust fault into the ridge leading to local upwarping of the BGHS [*I A Pecher et al.*, 2010].

Seafloor thermometry during TAN-0607 however, does not show any thermal anomaly across the ridge. This apparent contradiction is still being investigated. One possibility would be transient heat flow [*Wood et al.*, 2008], i.e., fluid flow is in the process of being initiated or shutting down. A significant contradiction between seafloor thermal gradients of ~0.055 °C/m and gradients derived from the depth of regional BSRs of ~0.025 °C/m [*I Pecher et al.*, 2010] would suggest the latter, as proposed for a similar anomaly offshore Chile [*Grevemeyer et al.*, 2006]. This would lead to a downward moving BGHS with respect to the sediment column and gas to "freeze" to hydrate.

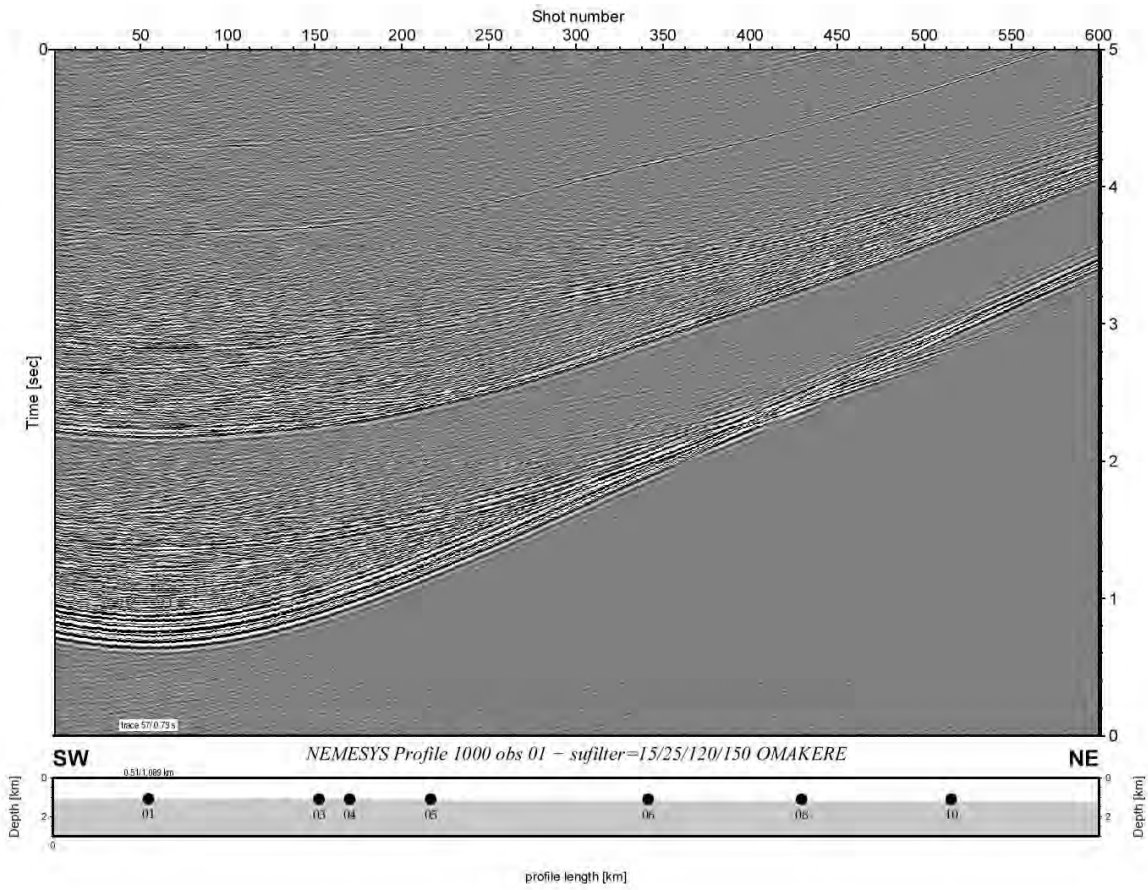

Fig 6.2.1.2.2 : Record section of OBS01 , hydrophone channel.

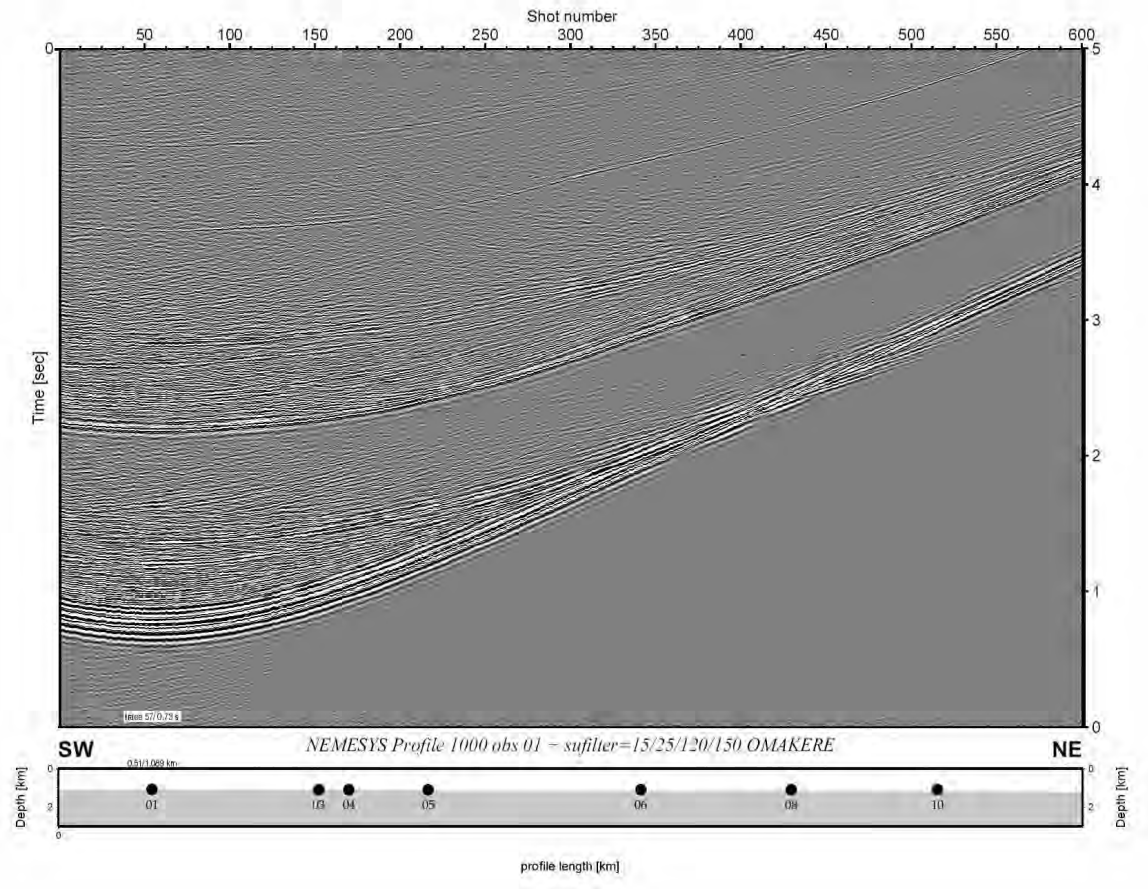

Fig 6.2.1.2.3 : Record section of OBS01, vertical component.

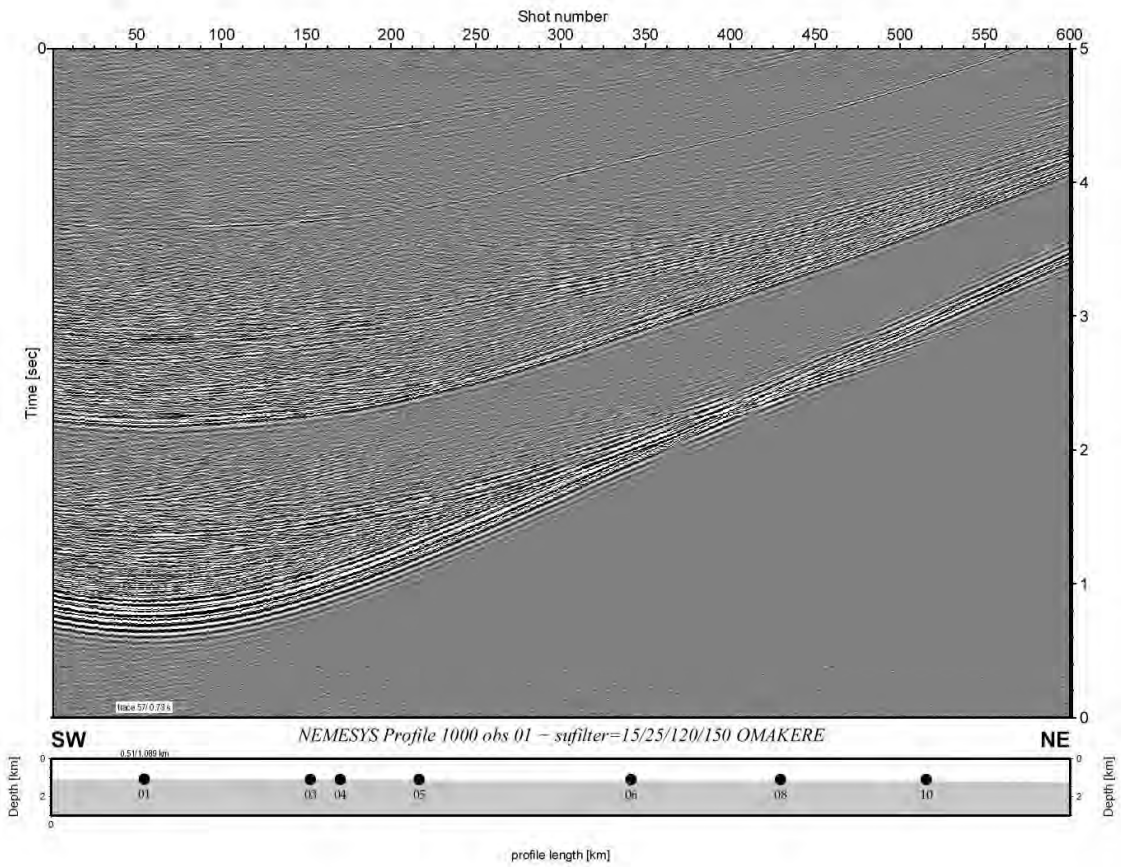

Fig 6.2.1.2.4 : Record section of OBS01 , horizontal component.

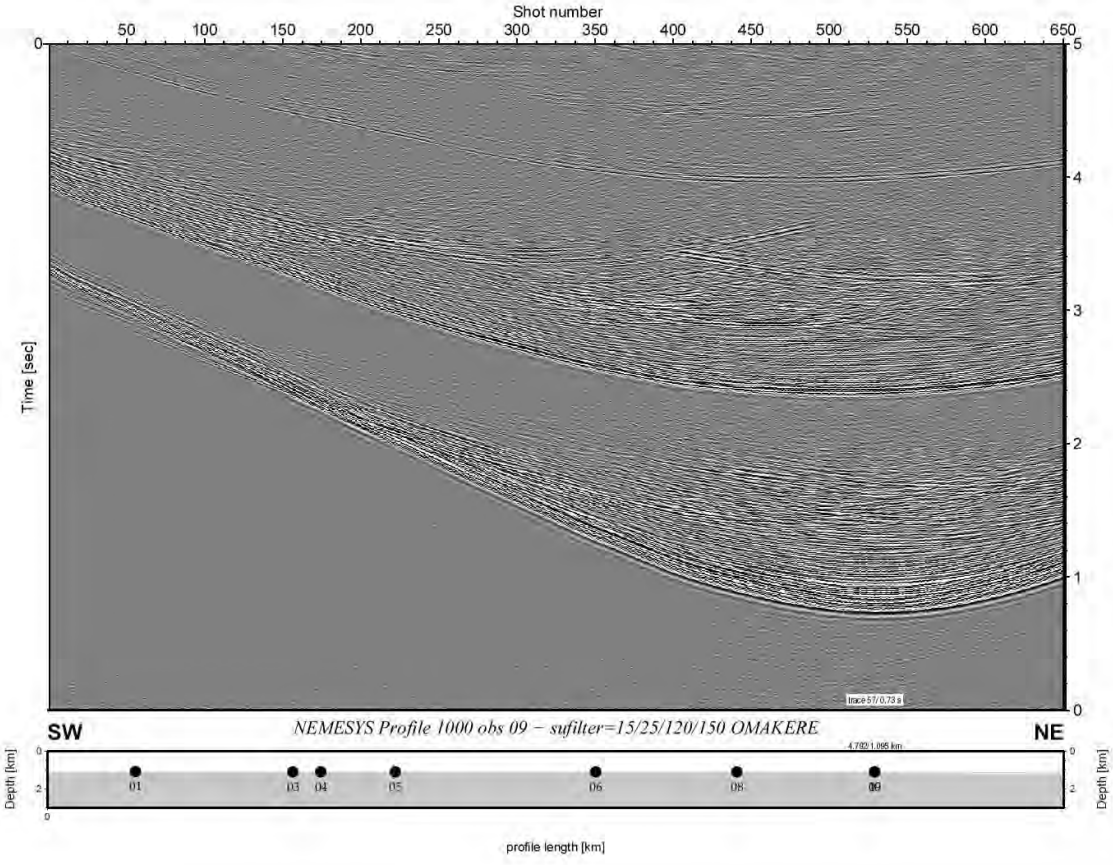

Fig 6.2.1.2.5 : Record section of OBS10, hydrophone channel.

Alternatively, gas may be injected in the gas phase into the hydrate stability zone either along highly permeable layers or along fractures. This process would not be predicted to cause any significant advective heat flow. Gas would then be transformed to hydrates, a process that may take significant time [*Liu and Flemings*, 2007]

In both cases, gas hydrates would currently be in the process of formation. The key objective of our survey on the Porangahau Ridge is to investigate the mechanisms for gas hydrate emplacement proposed above. Gas injection requires significant amounts of gas to accumulate beneath the BGHS in order to build a gas column that leads to sufficient buoyancy-driven gas pressure. It will be investigated if amplitudes along the anomaly decrease from north to south, which would indicate depletion of gas and thus, relatively low amounts of available gas, speaking against gas injection. A search for vent sites and near-seafloor gas pockets will be conducted, features that would indicate availability of significant amounts of gas supporting the model of gas injection.

A survey combining 2-D seismic, OBSs and Parasound profiles was conducted to address these questions (Figure 6.2.2.1.1)

Crooked-line acquisition: A 3-D cube was originally planned to cover an area of near-vertical faults seen in 2-D data from TAN0607. These faults appear to be linked to the deeper anomaly. In particular, it was planned to find evidence for shallow gas pockets in these faults. Due to weather-related problems, only a few tracks of this cube could be acquired (Figure 6.2.2.1.2). While not being suitable for 3-D imaging, crooked-line 2-D images of several in-lines will still provide constraints on sizes and dips of anomalies (Figure 6.2.2.1.3).

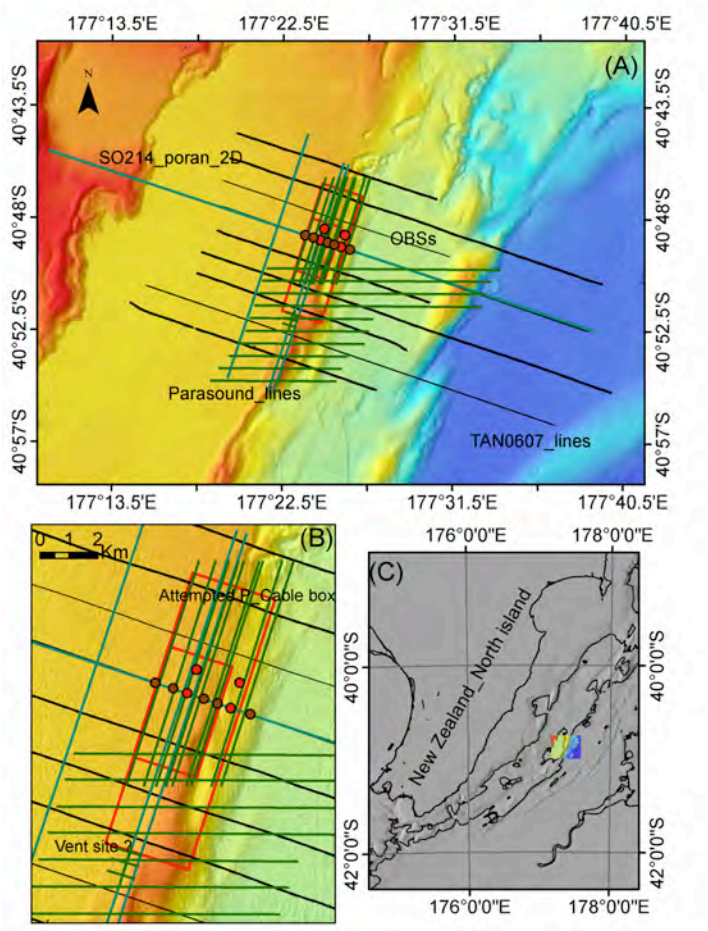

Figure 6.2.2.1.1. Overview on seismic and Parasound surveys on Porangahau Ridge.

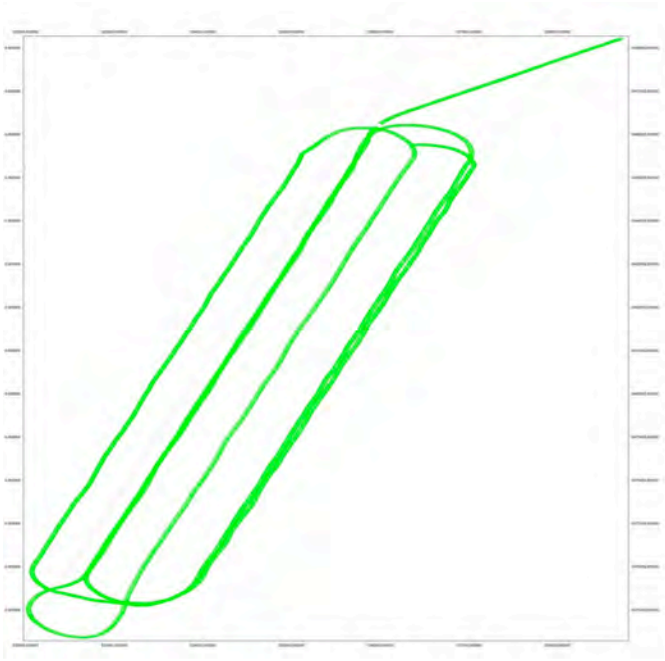

Figure 6.2.2.1.2: CDP coverage for crooked-line acquisition across the Porangahau Ridge. CDP binning: 3.125 m

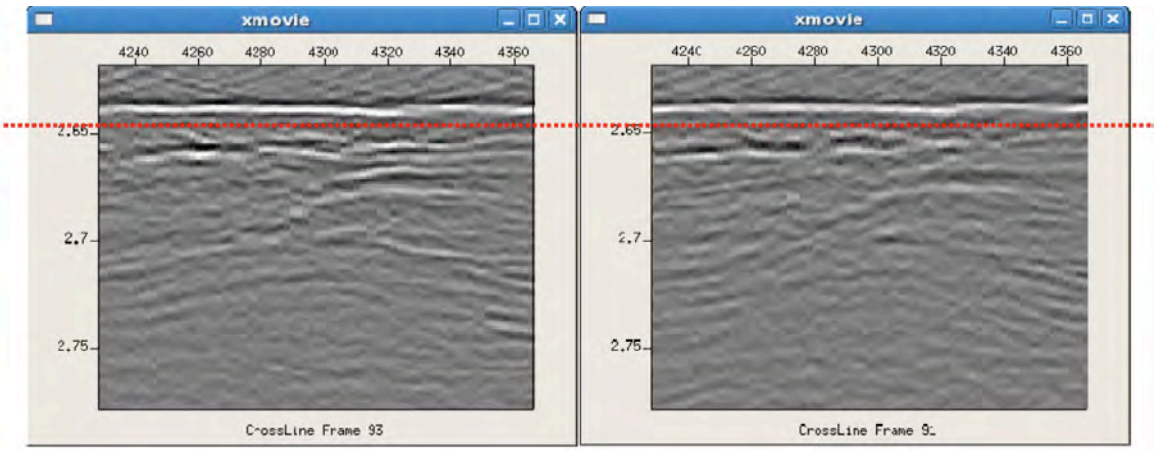

Figure 6.2.2.1.3: Screenshots of two in-lines, 6.25 m apart (two cross-line CDPS), across near-seafloor faults. In the right panel, the bright reflection is slightly closer to that line in the right panel.

2-D lines: It was decided to re-configure the streamer for 2-D acquisition and acquire several 2-D lines (Figure 6.2.2.1.4) because of sea-state related problems with deployment of the trawl doors. For exact streamer configuration and geometry refer to chapter 5.2.

The objectives of the lines included:

- Shoot to OBSs (see section 6.2.2.2)
- Provide a stratigraphic tie-in for profiles across the ridge acquired during TAN-0607
- Track the seismic anomaly along the ridge further to the south

The data were binned at 1.25 m and migrated in the T-K domain (sumigtk) using a velocity of 1500 m/s.

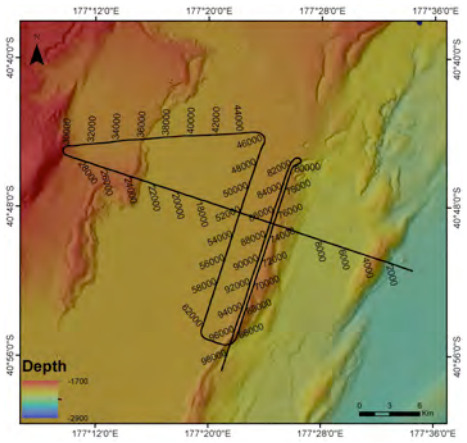

Figure 6.2.2.1.4: Track chart of 2-D lines with CDP numbering as in shipboard migration (see below).

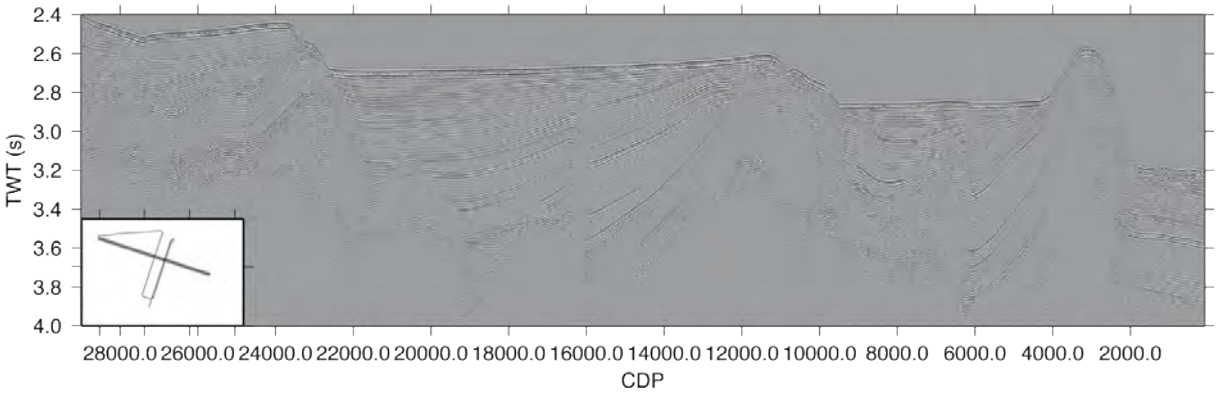

Figure 6.2.2.1.5: Segment 1 of 2-D seismic lines across Porangahau Ridge, CDP 100-29000. Refer to Figure 6.2.2.1.4 for locations

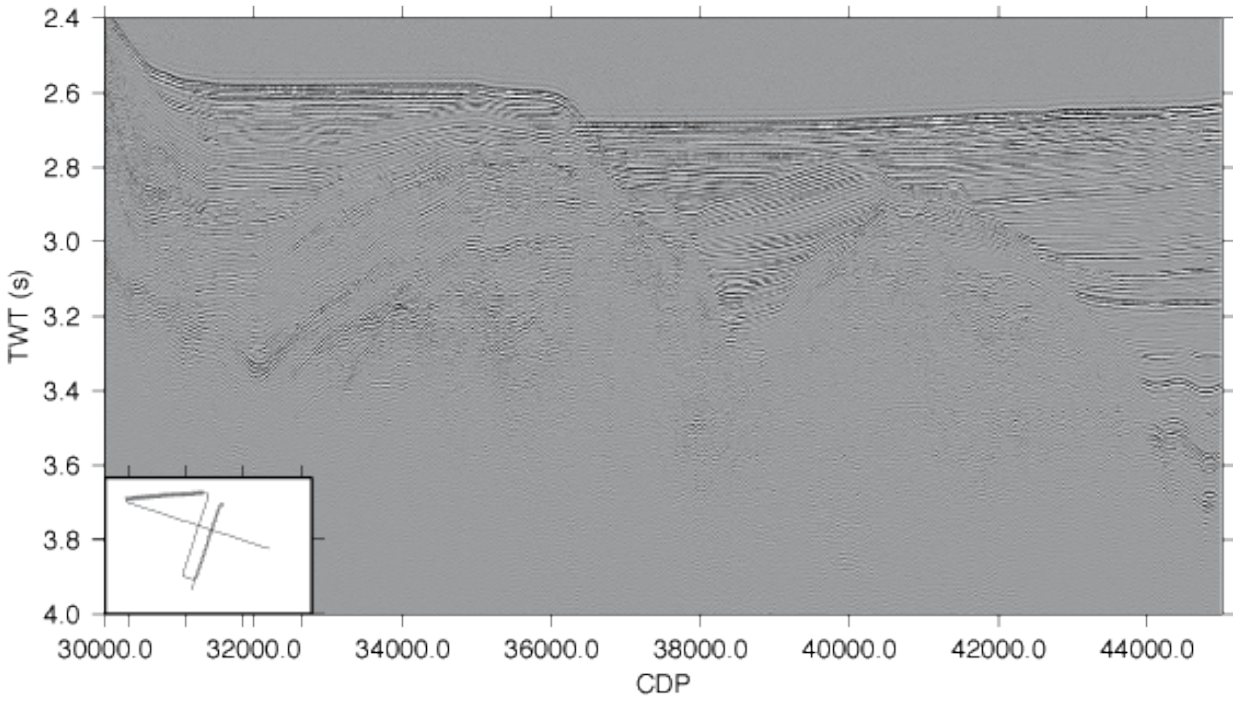

Figure 6.2.2.1.6: Segment 2 of 2-D seismic lines across Porangahau Ridge, CDP 30000-45000. Refer to Figure 6.2.2.1.4 for locations.

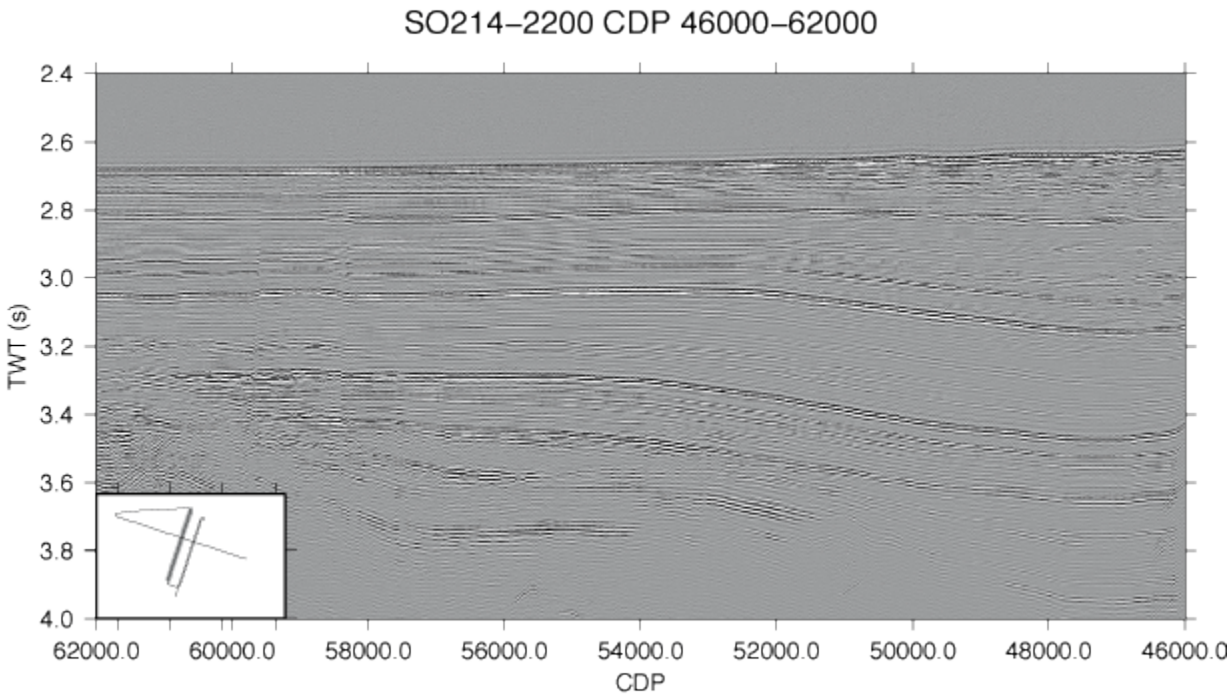

Figure 6.2.2.1.7: Segment 3 of 2-D seismic lines across Porangahau Ridge, CDP 46000-62000. Refer to Figure 6.2.2.1.4 for locations.

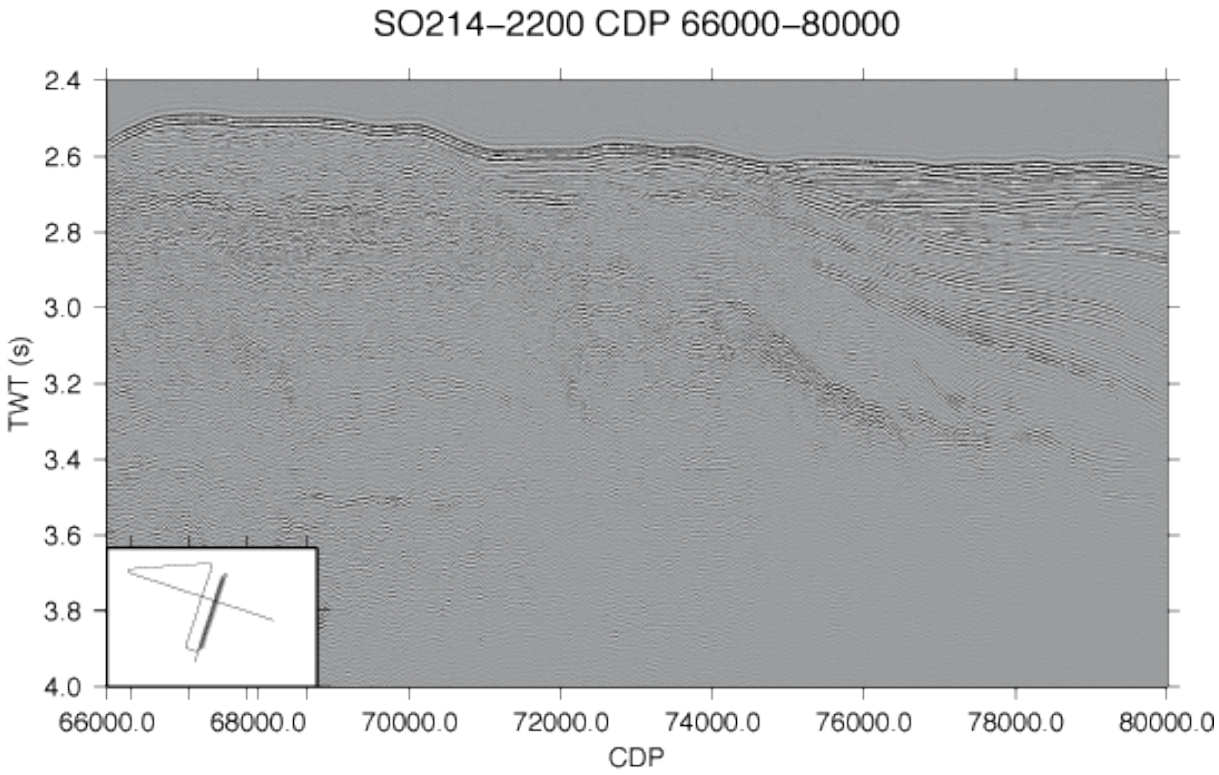

Figure 6.2.2.1.8: Segment 4 of 2-D seismic lines across Porangahau Ridge, CDP 66000-80000. Refer to Figure 6.2.2.1.4 for locations.

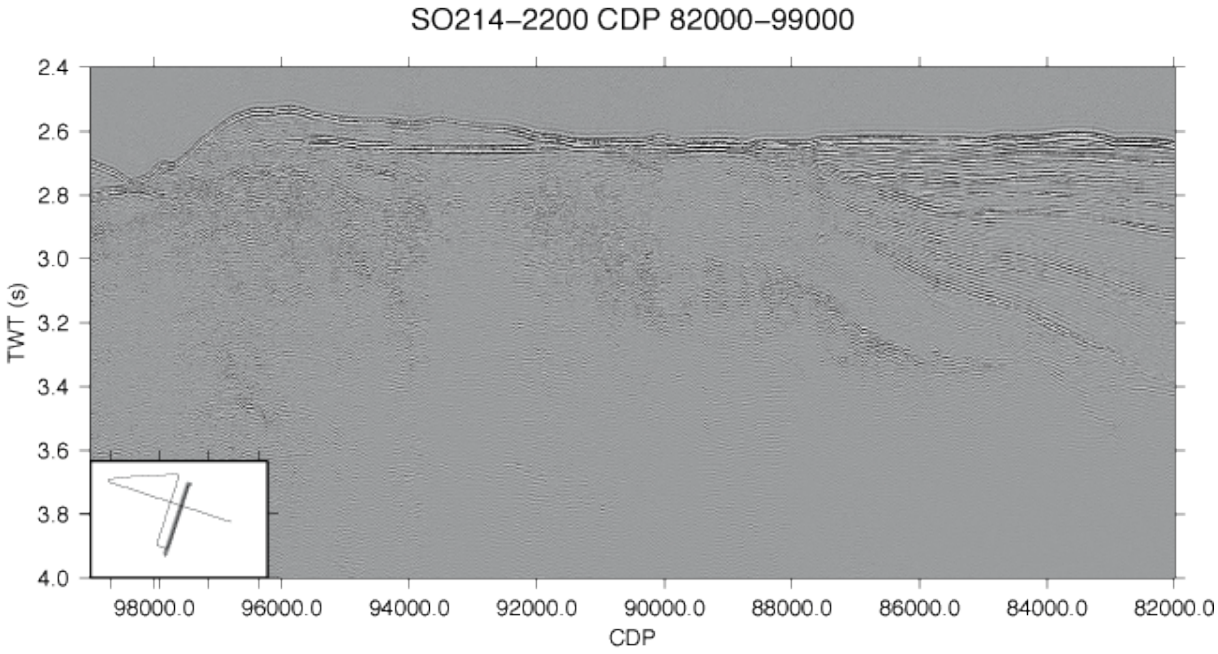

Figure 6.2.2.1.9: Segment 5 of 2-D seismic lines across Porangahau Ridge, CDP 82000-92000. Refer to Figure 6.2.2.1.4 for locations.

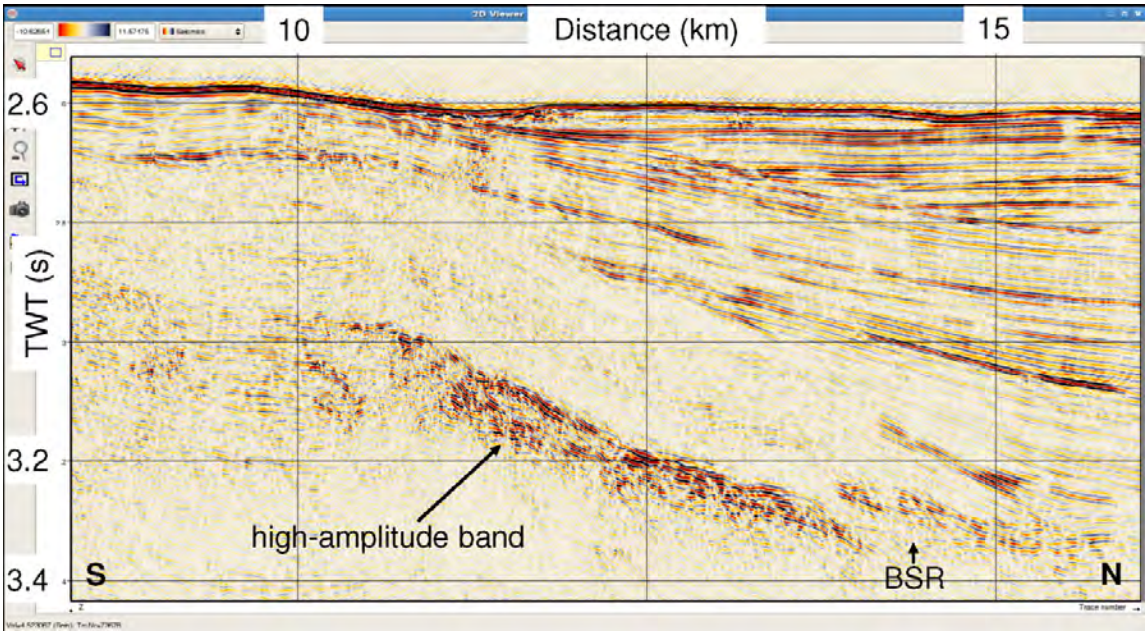

Figure 6.2.2.1.10: The high-amplitude band and its possible relation to near-seafloor anomalies, (Segment 5, Figure 6.2.2.1.9). Similar observations have been made in a lines acquired perpendicularly to this line during TAN-0607 [Pecher et al., 2007].

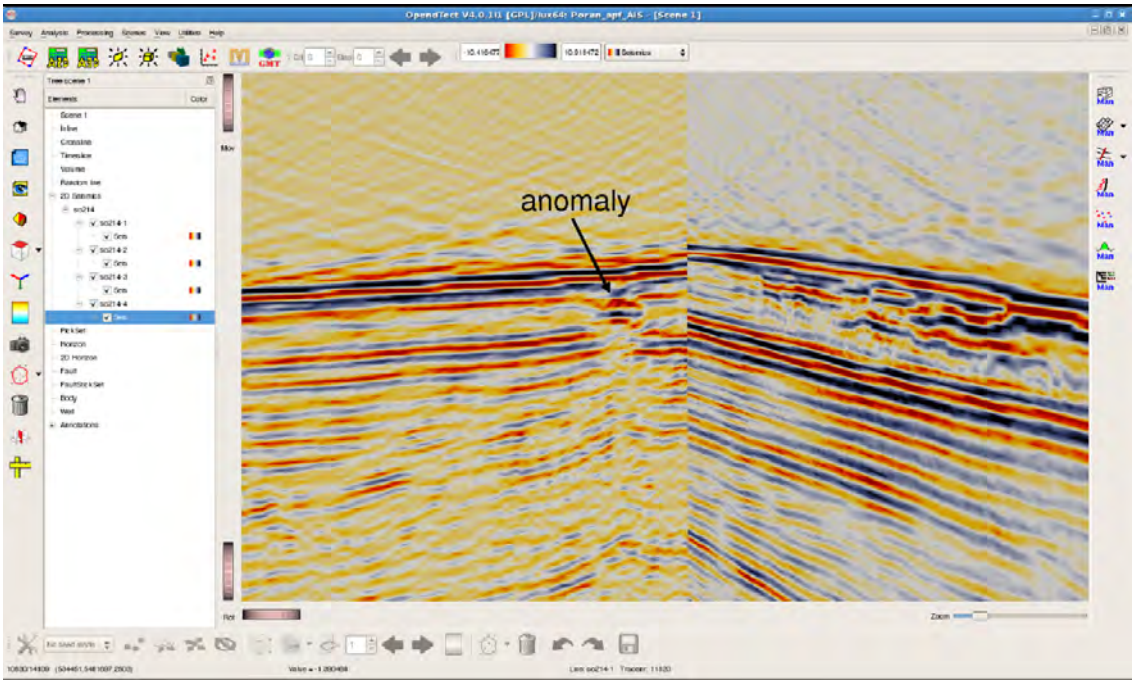

Figure 6.2.2.1.11: Tie-in between two segments, from NW to Segments 1 and 5 and in figures above. Note the anomaly near the seafloor.

6.2.2.2 OBS Porangahau Ridge

Thomas Golding, Ingo Pecher, Stefan Moeller, Mareike Kampmeier

Operations

Day 1

Deployed OBS 01-04
Shot lines 1-6

Day 2

Deployed OBS 10-14
Shot lines 7-11

Recovery of OBS and data

OBS 03 did not resurface.
OBS 10 did not record any data.
OBS 11 did not record on any geophone channels.

Table 6.2.2.2.1. OBS number and channel. Y=recorded, N=did not record.

	Channel Number			
OBS	**1**	**2**	**3**	**4**
01	Y	Y	Y	Y
02	Y	Y	Y	Y
04	Y	Y	Y	Y
11	Y	N	N	N
12	Y	Y	Y	Y
13	Y	Y	Y	Y
14	Y	Y	Y	Y

From the raw OBS data, one SEGY file was written for each channel for each OBS, containing the full set of shots.

Lines

The shot tracks were split into discrete lines based on shot numbers. SEGY files for each OBS, for each channel, for each line were then created. Figures 6.2.2.2.3 and 6.2.2.2.4 show OBS and line locations.

Relocation

Relocation of the OBSs was done manually, by first finding the optimal inline location, and then the optimal crossline location. Line 7 was used as the inline for all OBSs, line 10 was used as the crossline for all OBSs except OBS04, for which line 6 was the crossline used. The optimal inline and crossline locations were determined by visual comparison of receiver gathers with flattened direct wave. The flattest direct wave corresponds to the best location. Visual differences in the direct wave flatness were observed for 10 metre inline and crossline shift increments. This suggests the relocated coordinates should be accurate to within 10 or 20 metres. The .uko file containing the relocated coordinates is in the 6.2.2.2 folder. Unrelocated and relocated OBS locations are best seen in Figure 6.2.2.2.4.

Data discussion

In general the data look good. The dynamic range may have been exceeded for OBS01. We succeeded in recording refracted waves for the long-offset lines as well as P-to-S converted waves.

Table 6.2.2.2.2. Line definitions based on shot numbers for Porangahau Ridge OBS data.

line	shot_min	shot_max	day
1	300	1250	1
2	1600	2500	1
3	2650	3650	1
4	3900	4900	1
5	5050	6050	1
6	6200	7200	1
7	7350	9950	2
9	11450	12750	2
10	13100	14500	2
11	14750	16050	2

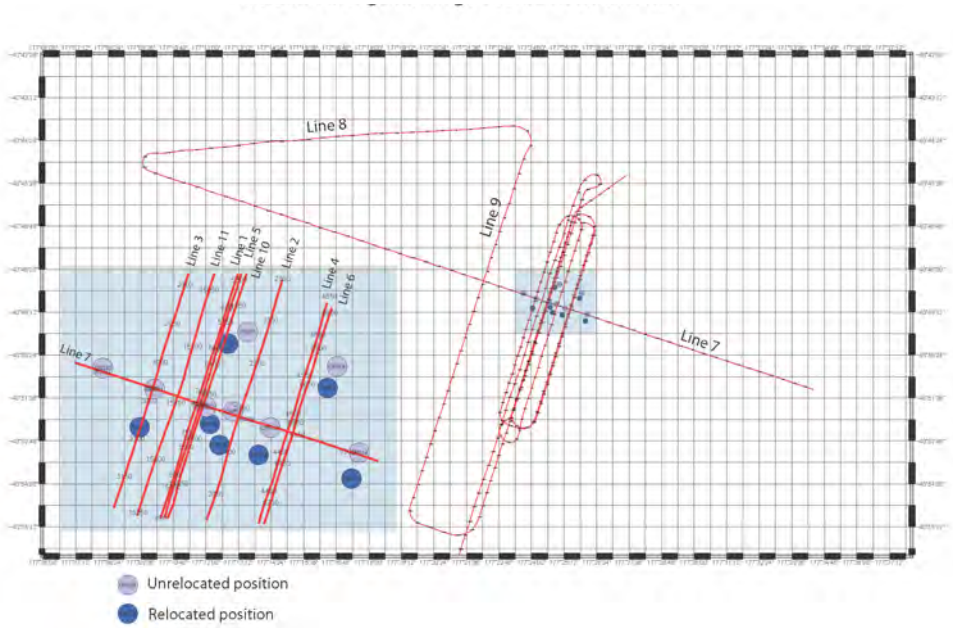

Figure 6.2.2.2.3: Large-scale shot tracks, inset with OBS deployment locs.

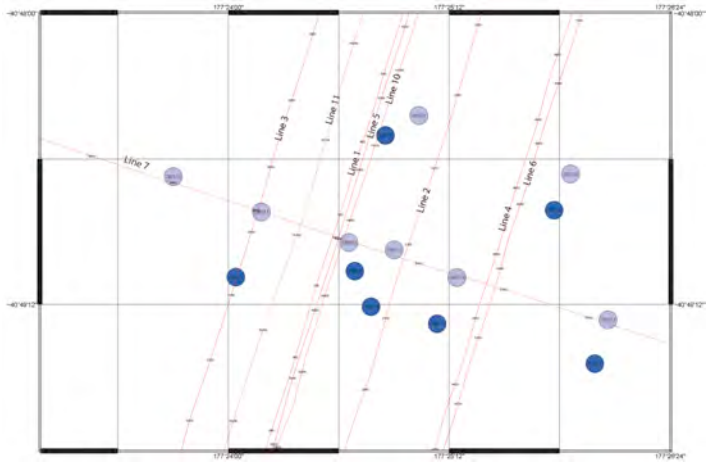

Figure 6.2.2.2.4: OBS deployment and re-located positions

The following are receiver gathers for the Hydrophone. Each plot has a reduction velocity of 2.5 km/s:

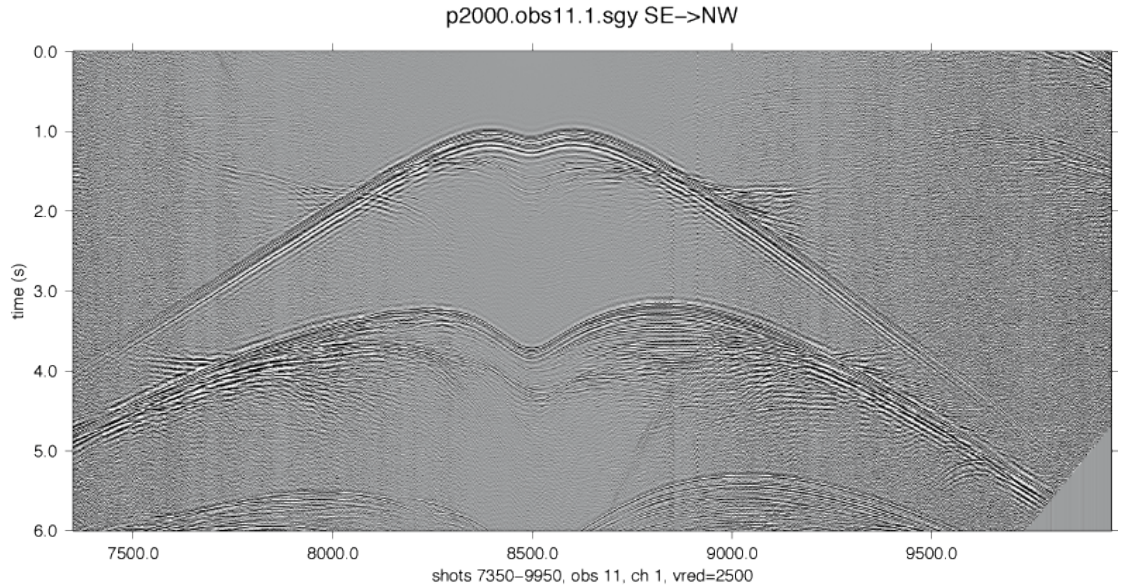

Figure 6.2.2.2.3: Line 7, OBS 11

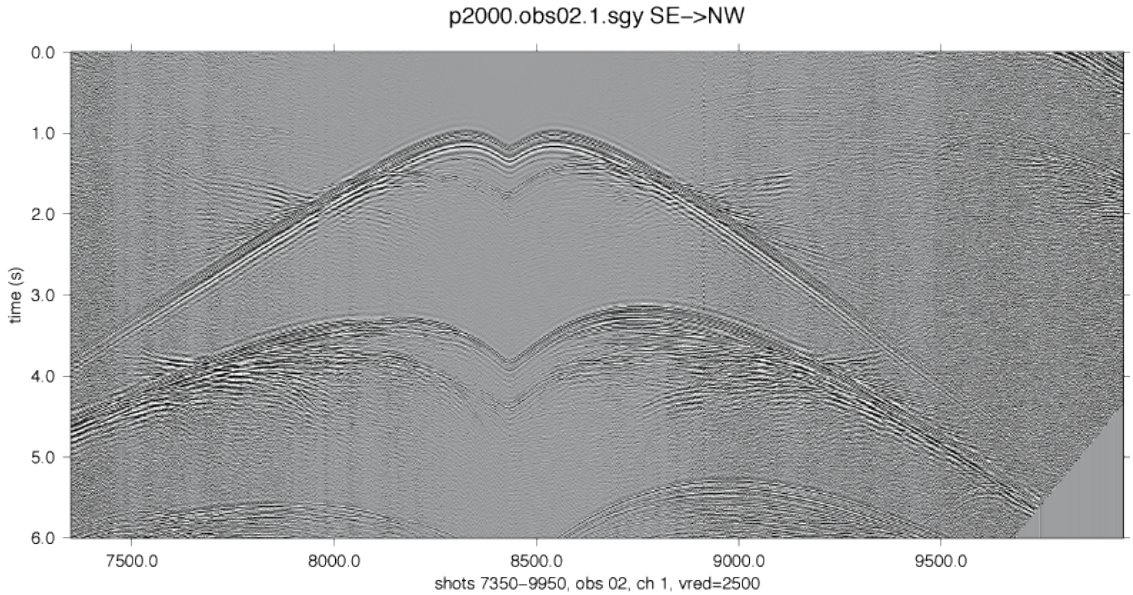

Figure 6.2.2.2.4: Line 7, OBS 02

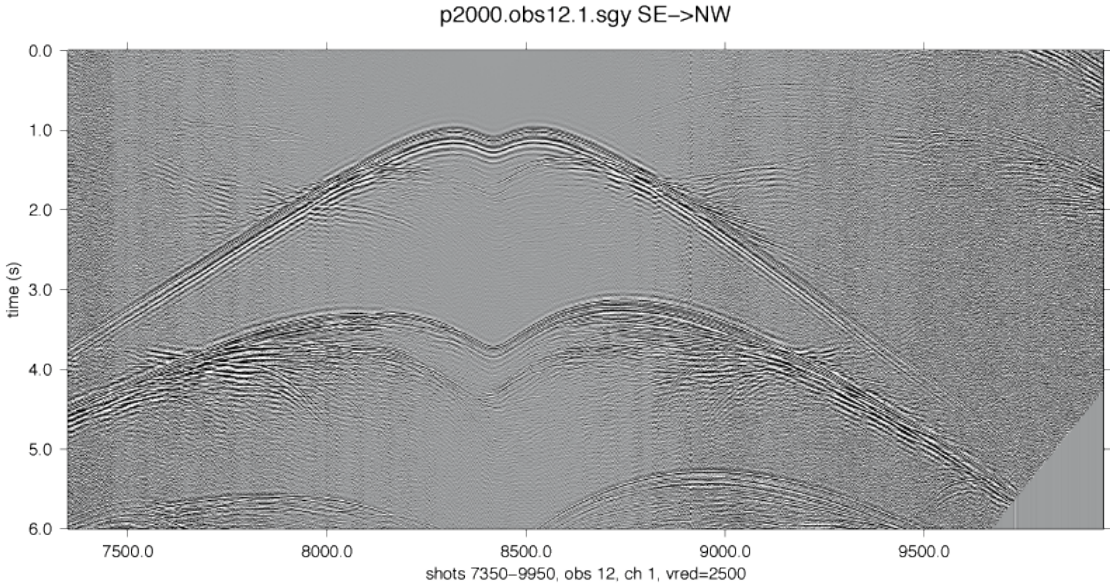

Figure 6.2.2.2.5: Line 7, OBS 12

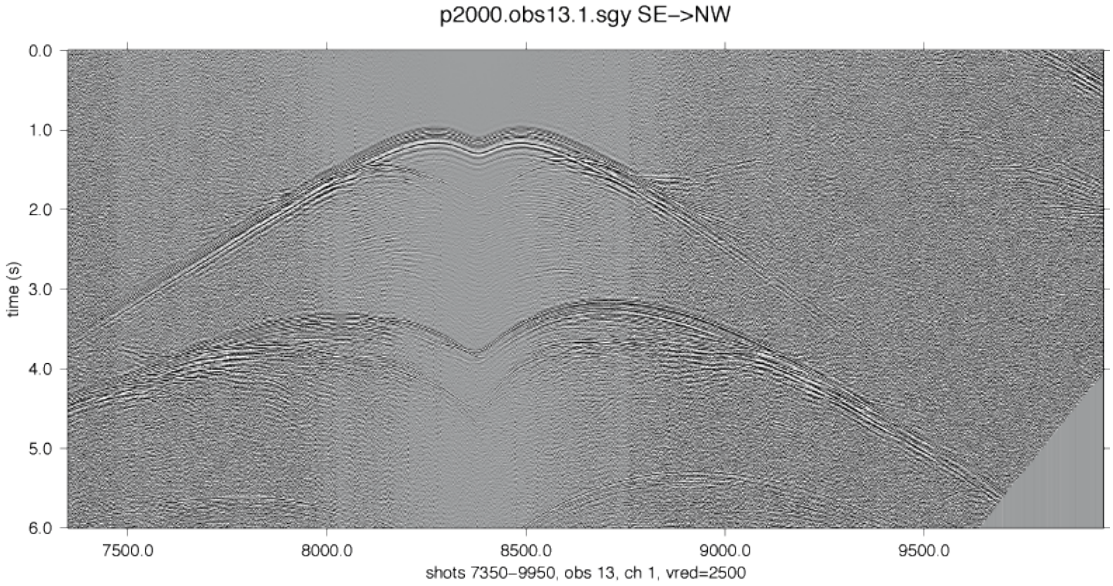

Figure 6.2.2.2.6: Line 7, OBS 13

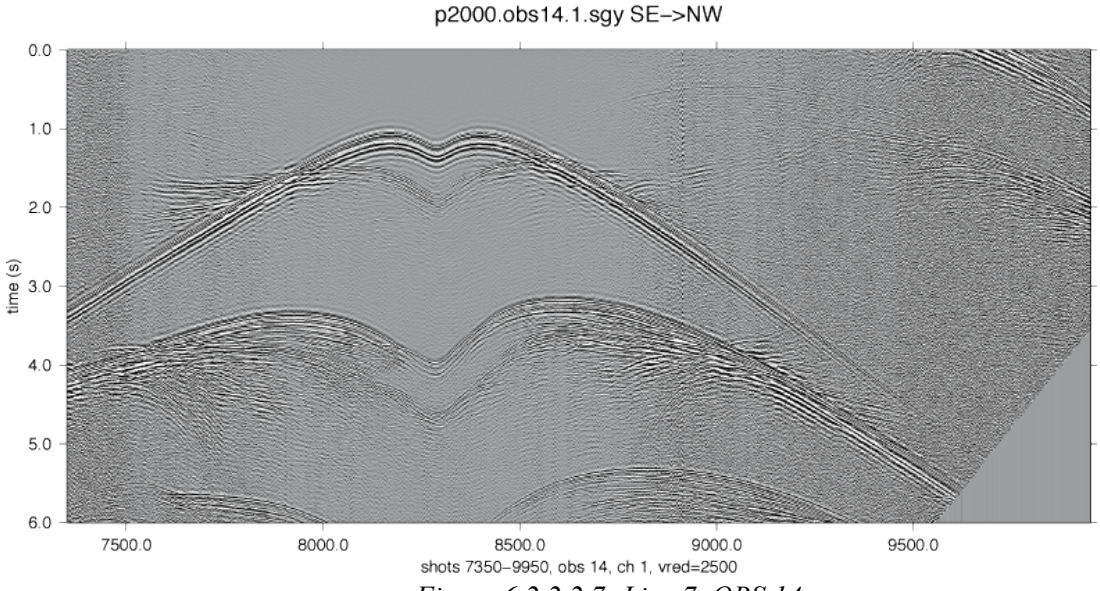

Figure 6.2.2.2.7: Line 7, OBS 14

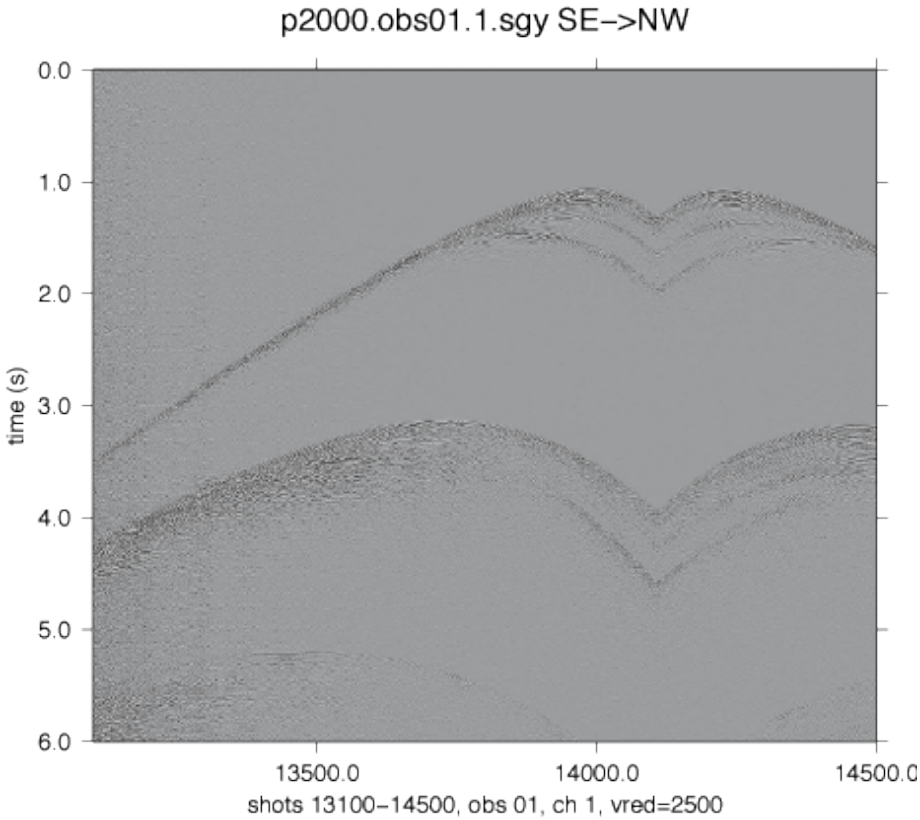

Figure 6.2.2.2.8: Line 10, OBS 01

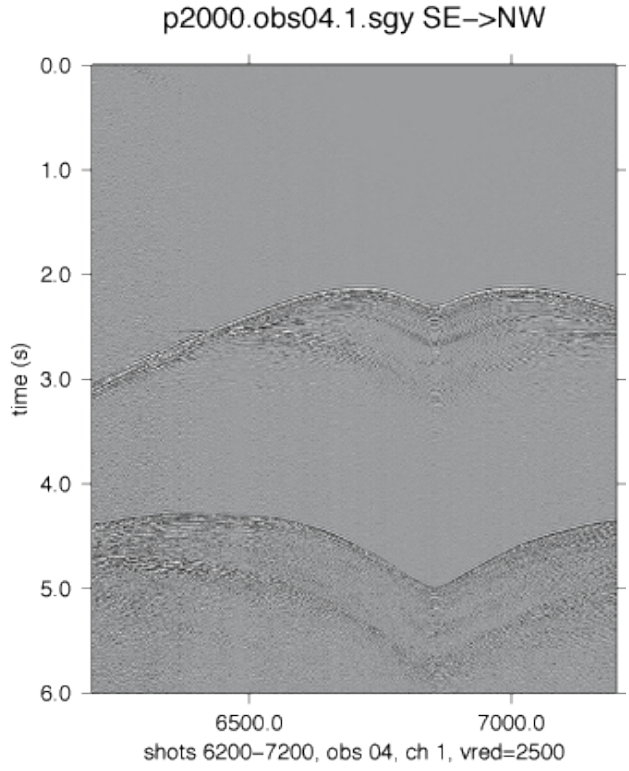

Figure 6.2.2.2.9: Line 6, OBS 04

The following plots show each of the 4 components, with fixed-level NMO (depth of 1.9 km, velocity of 1.5 km/s) for Line 10, OBS 02:

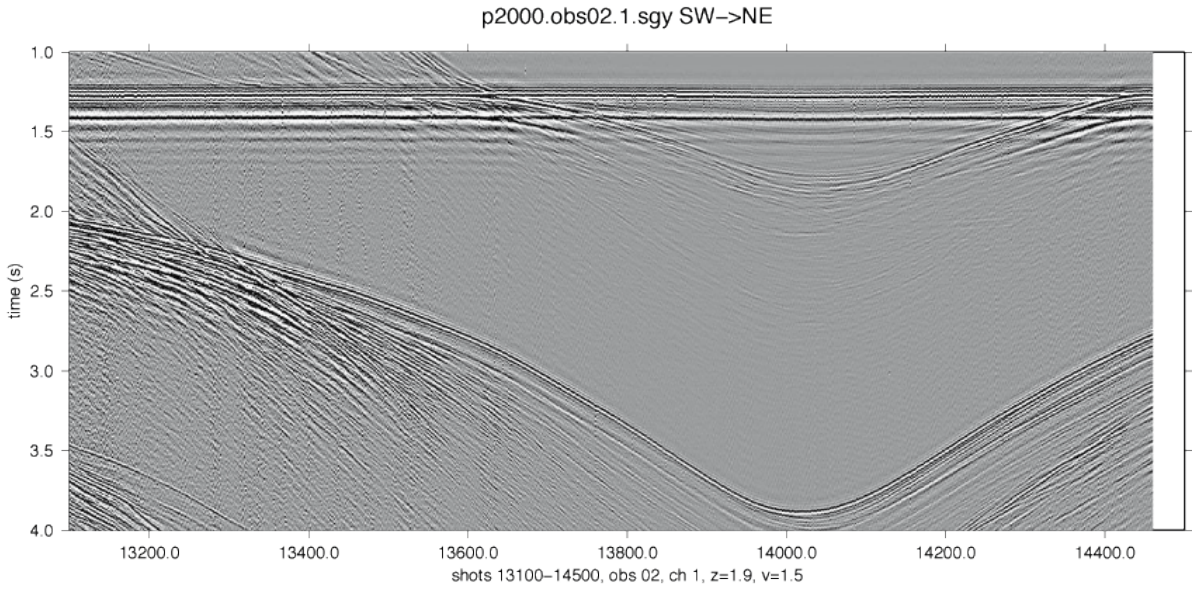

Figure 6.2.2.2.10: CH 1 (hydrophone)

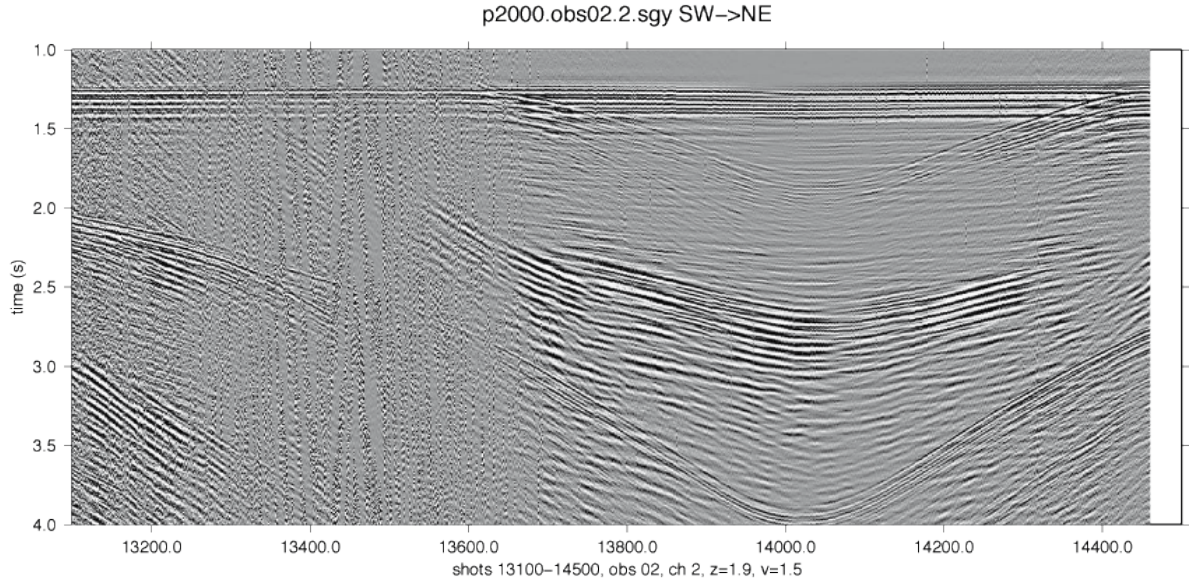

Figure 6.2.2.2.11: CH 2 (hor. 1)

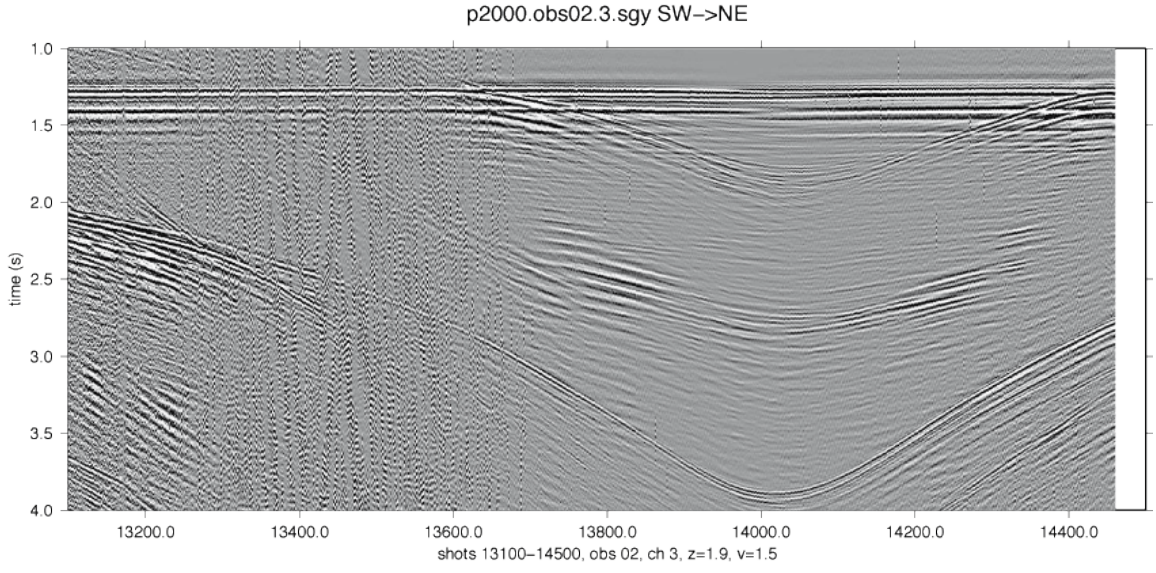

Figure 6.2.2.2.12: CH 3 (hor. 2)

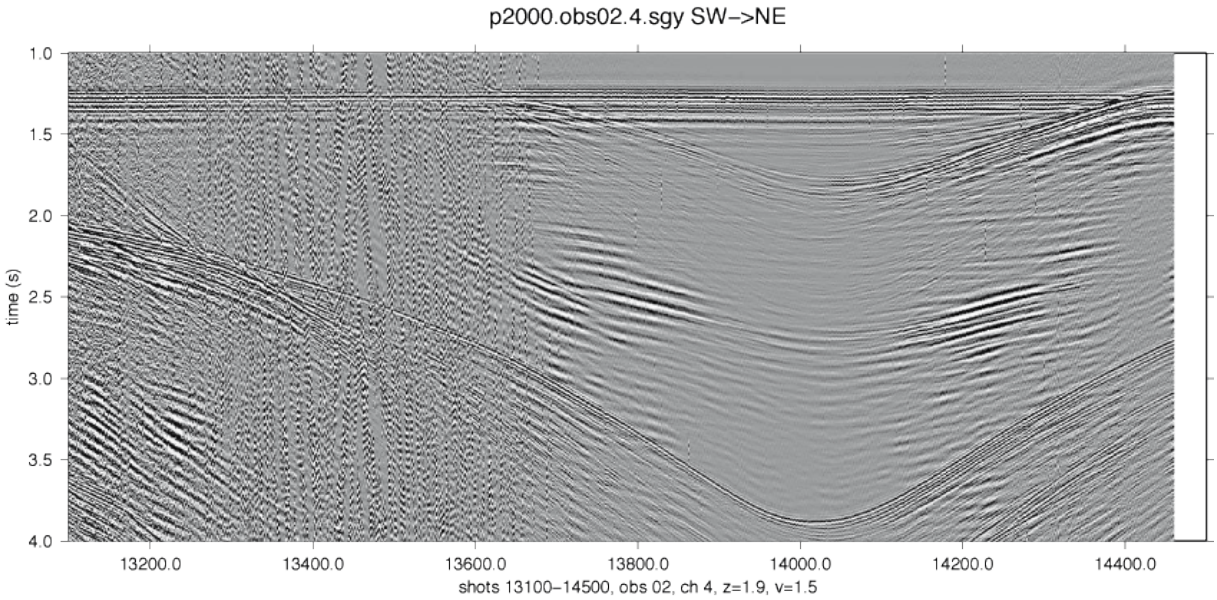

Figure 6.2.2.2.13: CH 4 (vertical)

6.2.3 Wairarapa

Gareth Crutchley, Dirk Klaeschen, Cord Papenberg, Ingo Pecher

Wairarapa is the area of the smallest extension of the accretionary wedge along the Hikurangi Margin. To the South the subduction changes into a strike slip movement, while to the North the wedge widens remarkably. It is the area with the densest population of known active seep sites. Therefore it became one of the two major focus areas during cruise SO-214.

6.2.3.1 2-D Seismic

Upon arrival at the Wairarapa site the repair of the 3-D system and replacement of the trawl wire was not completed and did not allow a deployment of the 3-D system. Therefore it was decided to first acquire a grid of 2-D seismic lines with the re-configured the streamer for 2-D acquisition and acquire several 2-D lines (Figure 6.2.3.1.1). The key objective was to ensure tie-ins with lines acquired in 2007 and to identify the best dimensions for a 3-D cube. Simultaneous Parasound and ELAC WCI recording provided a first overview of the seep activity and comparison with the situation from 2007 during cruise SO-191, New Vents.

The data were binned at 1.25 m and migrated in the T-K domain (sumigtk) using a velocity of 1500 m/s. A comparison of the 2-D data with the identical track of the 3-D cube shows the tremendous advantage of this highest resolution image (Fig. 6.2.3.1.8). Nevertheless it should not be forgotten that a full coverage of the 3-D volume with the single streamer would taken as long as 16 times the 3-D cube.

6.2.3.2 3-D Seismic

For the acquisition of the 3-D seismic cube the southeastern part of the Wairarapa area was chosen. A box of 4 km * 7.5 km was selected including the seep sites of Piwakawaka, Pukeko, North-Tower, and South-Tower. Takahe could only be touch at the northeastern border during turns from one track to another. This decision needs to be made as a compromise between expected time for profiling and required offset between the limits of the box and the included seep sites. Several tracks were sailed across and next to Takahe, which

enable to study the seep site with parallel 2-D lines at 10 m offset. The entire cube was completed after 50300 shots, which were done during 3 days of profiling.

A first Kirchhoff Time Migration at 6.25 m * 6.25 m grid spacing using water sound velocity could be completed on board. The value of the 3-D imaginary of the seep sites and the surrounding sediment matrix becomes already visible from the first chair-cutting display of the data cube (Fig. 6.2.3.2.1). Surprisingly the feeder channels of the seeps seem to be elongated in NW-SE orientation, which is perpendicular to the subduction. Therefore it seems they are not related to extensional fracturing caused by subduction parallel uplift of the accretionary ridges. This first impression is supported by a similarity image of the cube as well (Fig. 6.2.3.2.2).

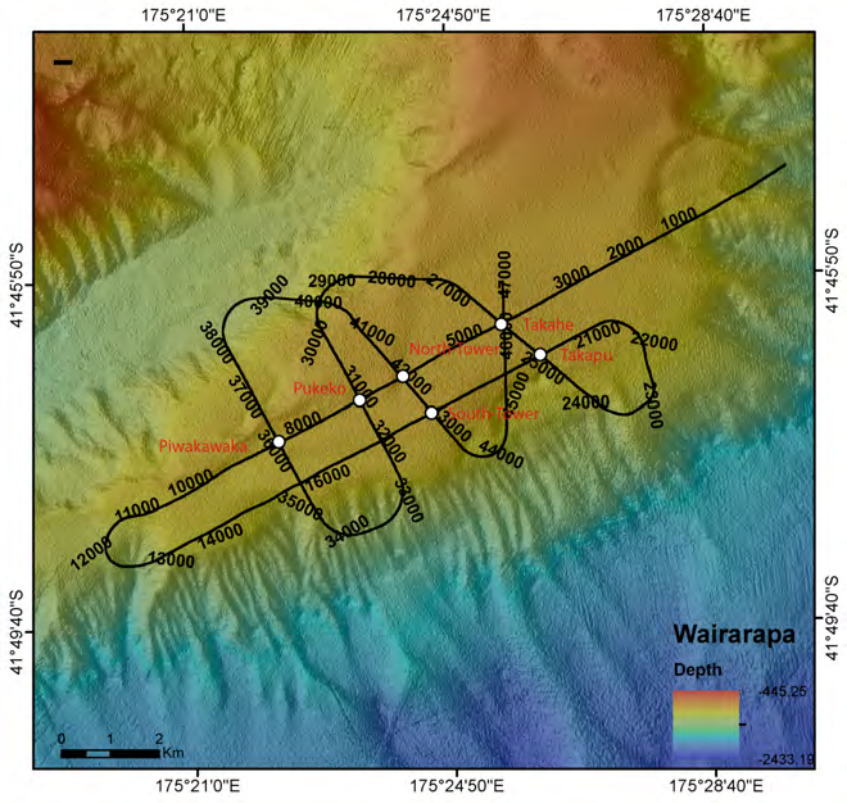

Figure 6.2.3.1.1: Track chart of 2-D lines with CDP numbering as in shipboard migration (see below).

6.2.3.3 OBS Wairarapa

Cord Papenberg, Stefan Moeller, Mareike Kampmeier, Eduardo Moscoso

During the seismic fieldwork along Opouawe Bank 13 OBS (see Fig. 6.3) were deployed. Two of them could be equipped with MBS data loggers, while the others used MLS. One system carrier was extended with an additional Methane sensor. The distribution of the OBS was chosen to provide a dense coverage over the main line of seeps Rironiro to North Tower. Ten instruments were deployed along one profile in the centre of the 3-D coverage area. 2D seismic data were acquired along this line with the surface streamer (see inset of Fig. 6.3) and during the operation of the deep towed streamer (see chapter 6.3.3). Four instruments were deployed to both sides of the profile in order to widen the image area during the 3D seismic acquisition.

Due to the recovery of the instruments short before termination of the cruise selected plots as QC example are available only.

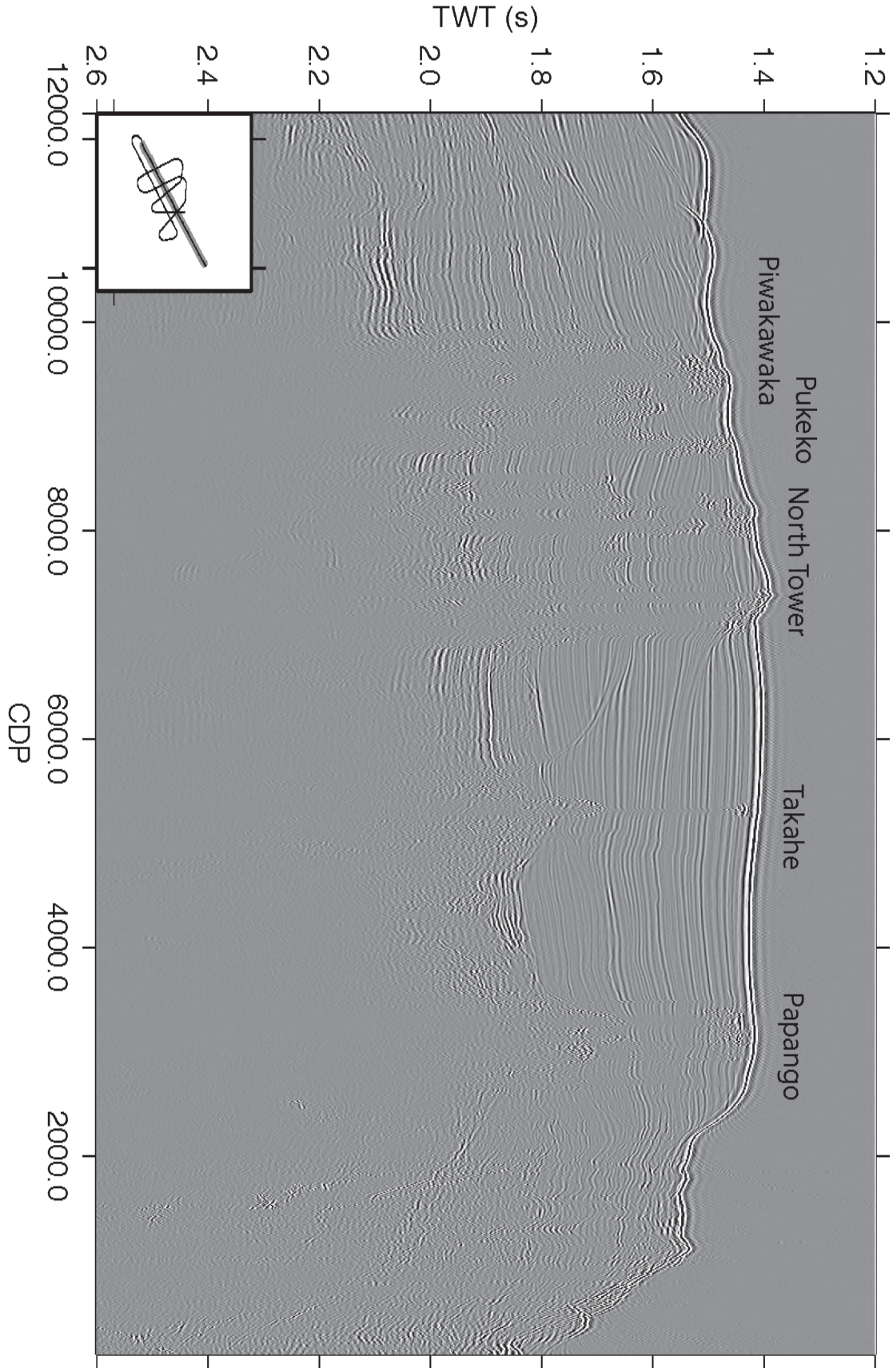

Figure 6.2.3.1.2: Segment 1 of 2-D seismic lines across the Wairarapa Site, CDP 100-12000. Refer to Figure 6.2.3.1.1 for locations.

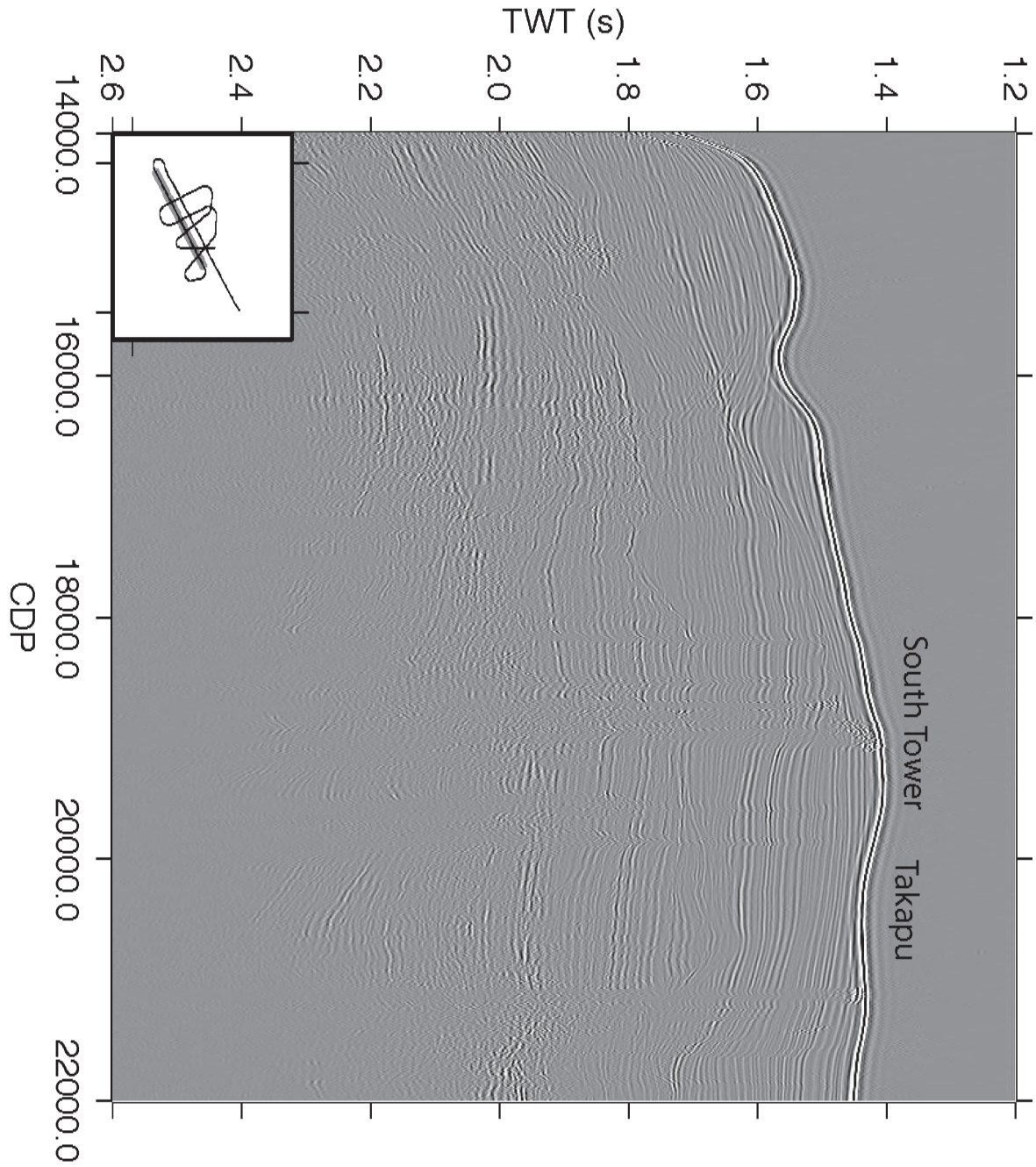

Figure 6.2.3.1.3: Segment 2 of 2-D seismic lines across the Wairarapa Site, CDP 14000-22000. Refer to Figure 6.2.3.1.1 for locations.

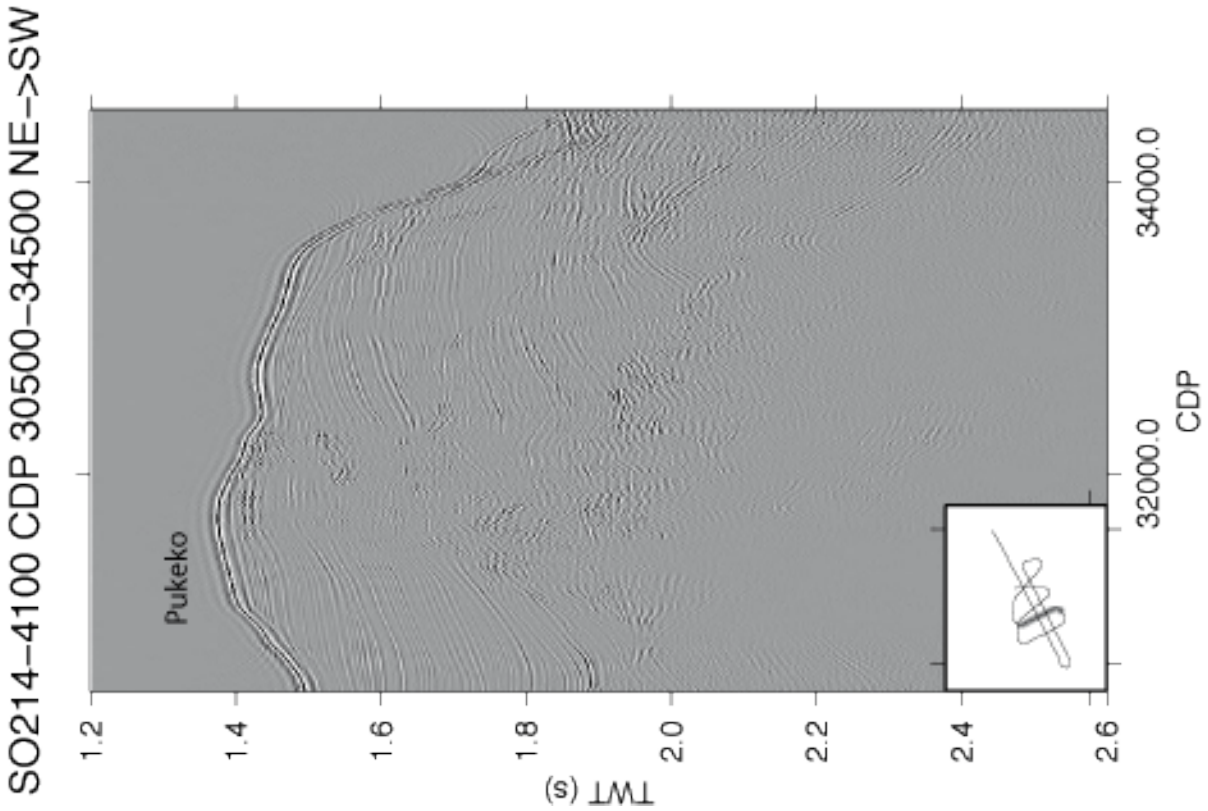

Figure 6.2.3.1.4: Segment 4 of 2-D seismic lines the Wairarapa Site, CDP 30500-34500. Refer to Figure 6.2.3.1.1 for locations.

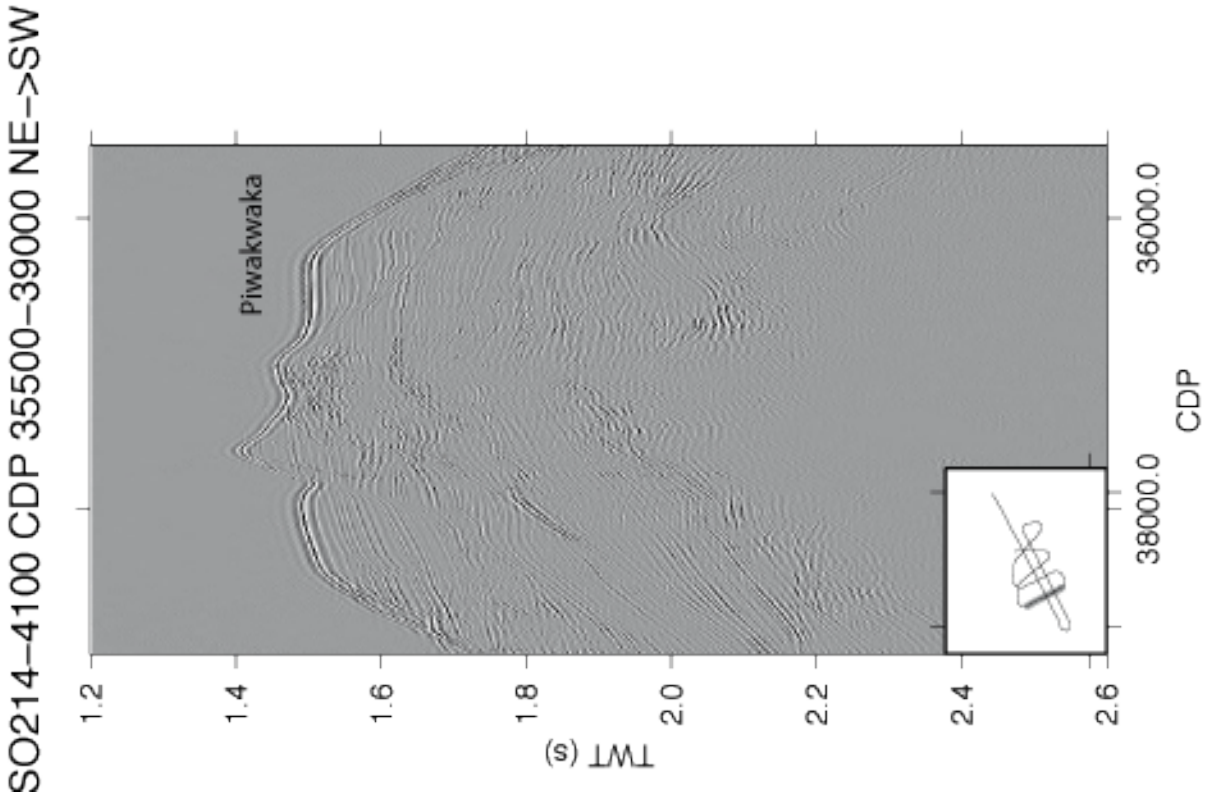

Figure 6.2.3.1.5: Segment 5 of 2-D seismic lines the Wairarapa Site, CDP 35500-39000. Refer to Figure 6.2.3.1.1 for locations.

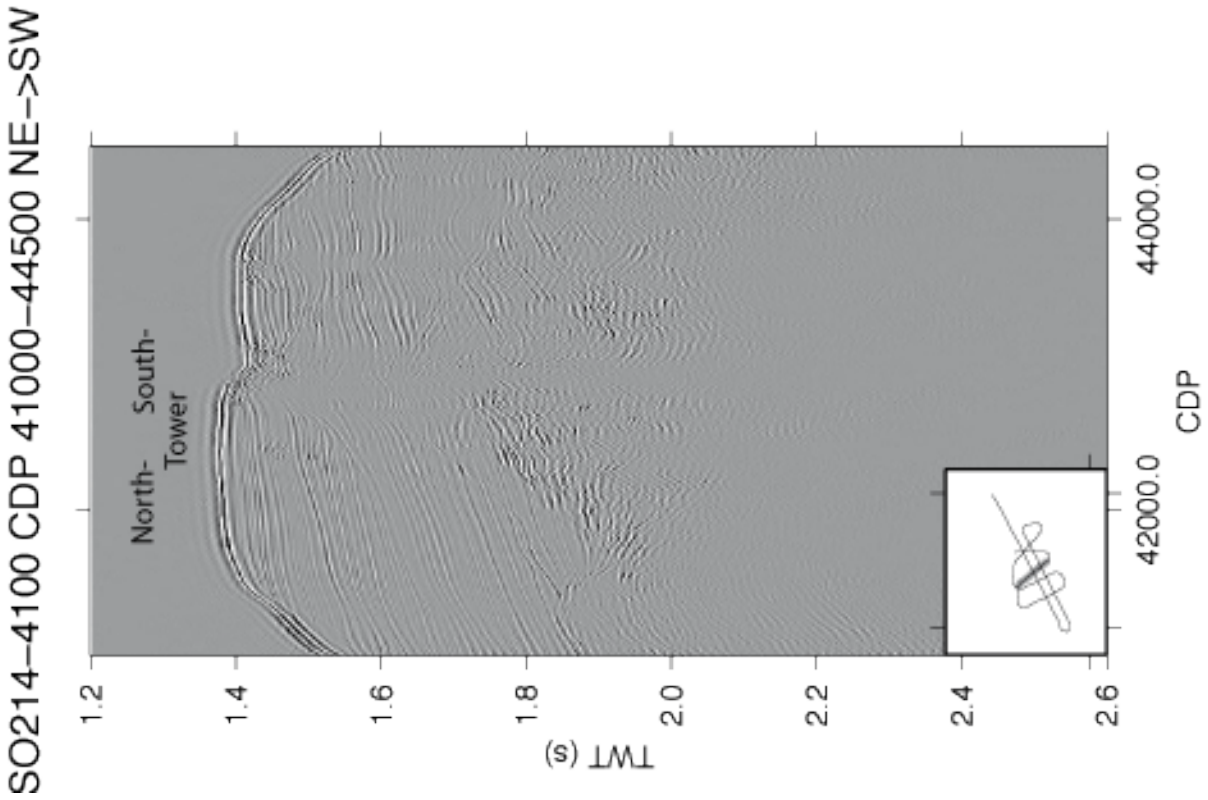

Figure 6.2.3.1.6: Segment 6 of 2-D seismic lines the Wairarapa Site, CDP 41000-44500. Refer to Figure 6.2.3.1.1 for locations.

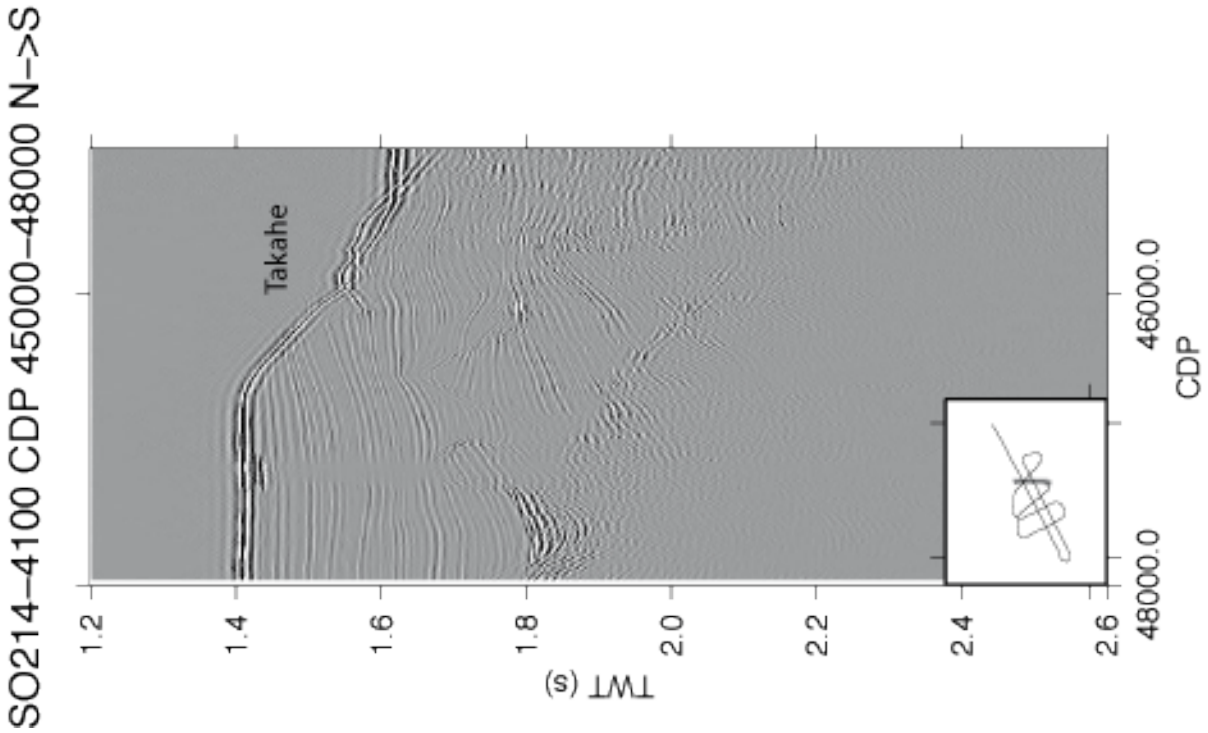

Figure 6.2.3.1.7: Segment 7 of 2-D seismic lines the Wairarapa Site, CDP 45000-48000. Refer to Figure 6.2.3.1.1 for locations.

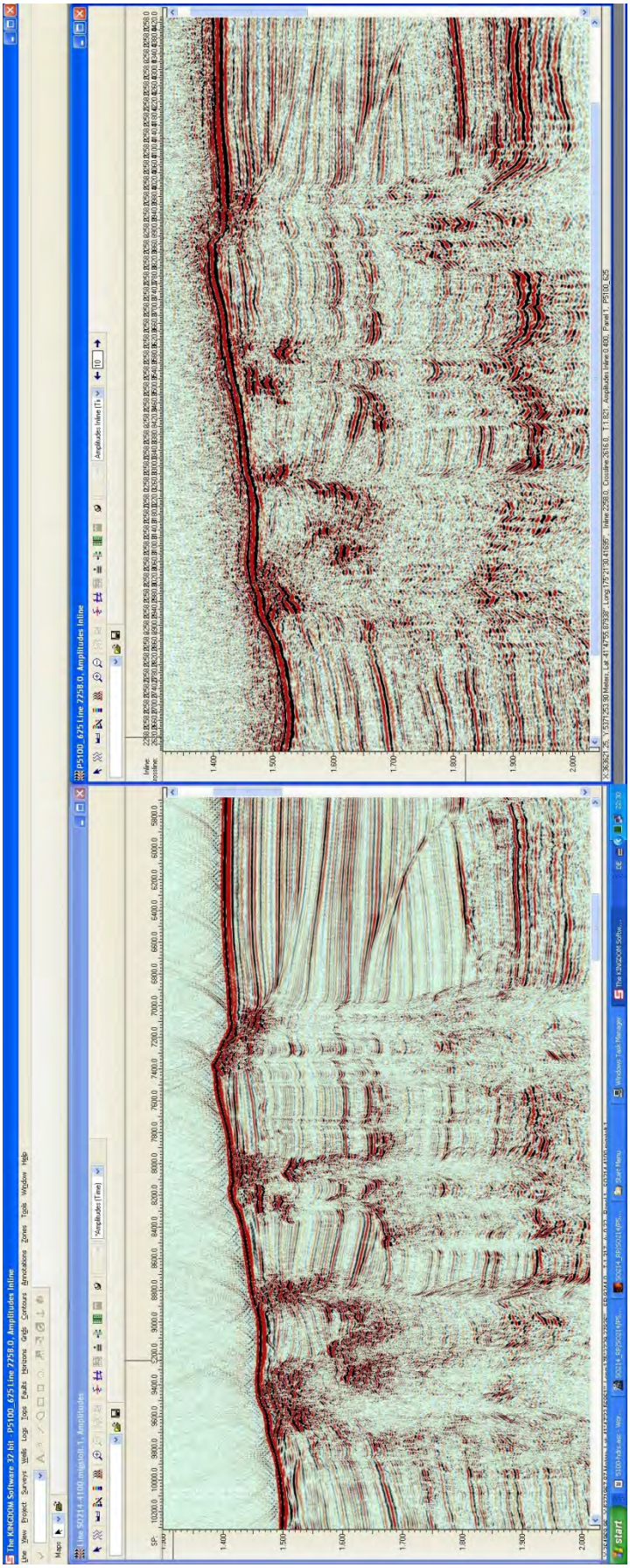

Figure 6.2.3.1.8: Comparison of the highest resolution 2-D line (left) with the coincident section of the 3-D data cube (right). It is remarkably how detailed the 2-D image is.

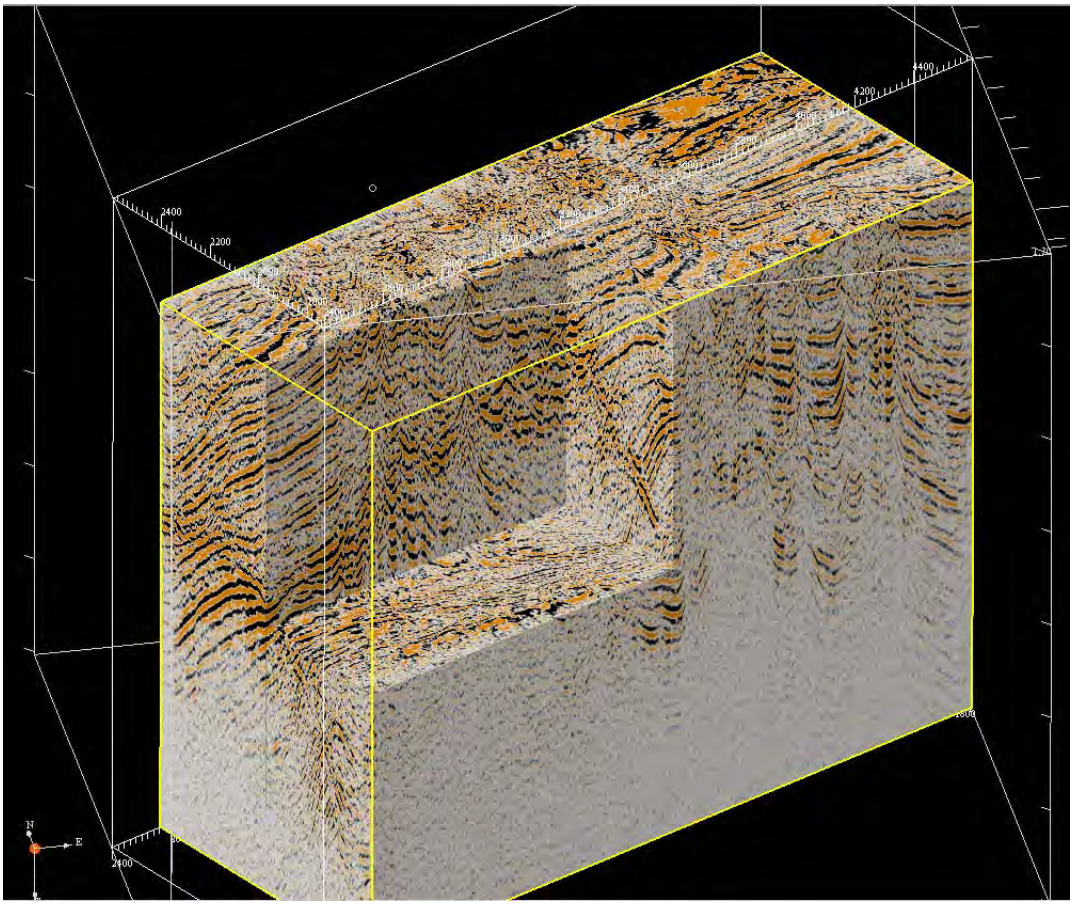

Figure 6.2.3.2.1: Chair-cutting image of the 3-D cube at Wairarapa

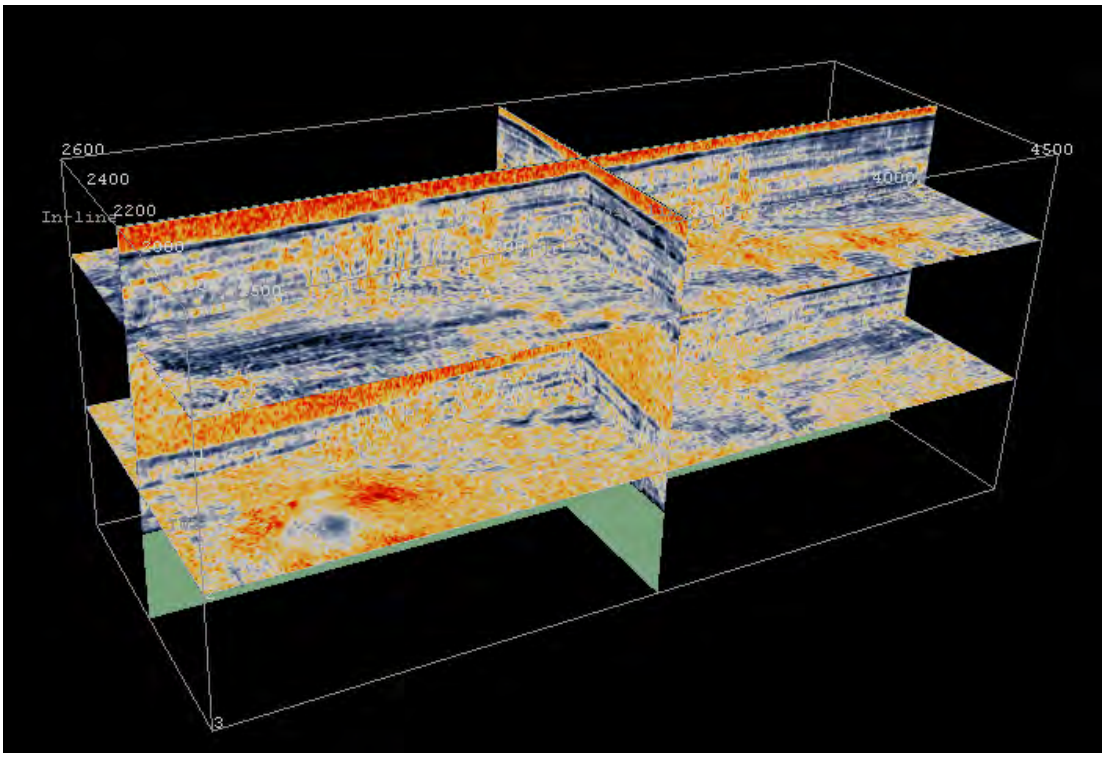

Figure 6.2.3.2.2: Fence diagram showing major events of the similarity cube calculated from the Wairarapa 3-D volume

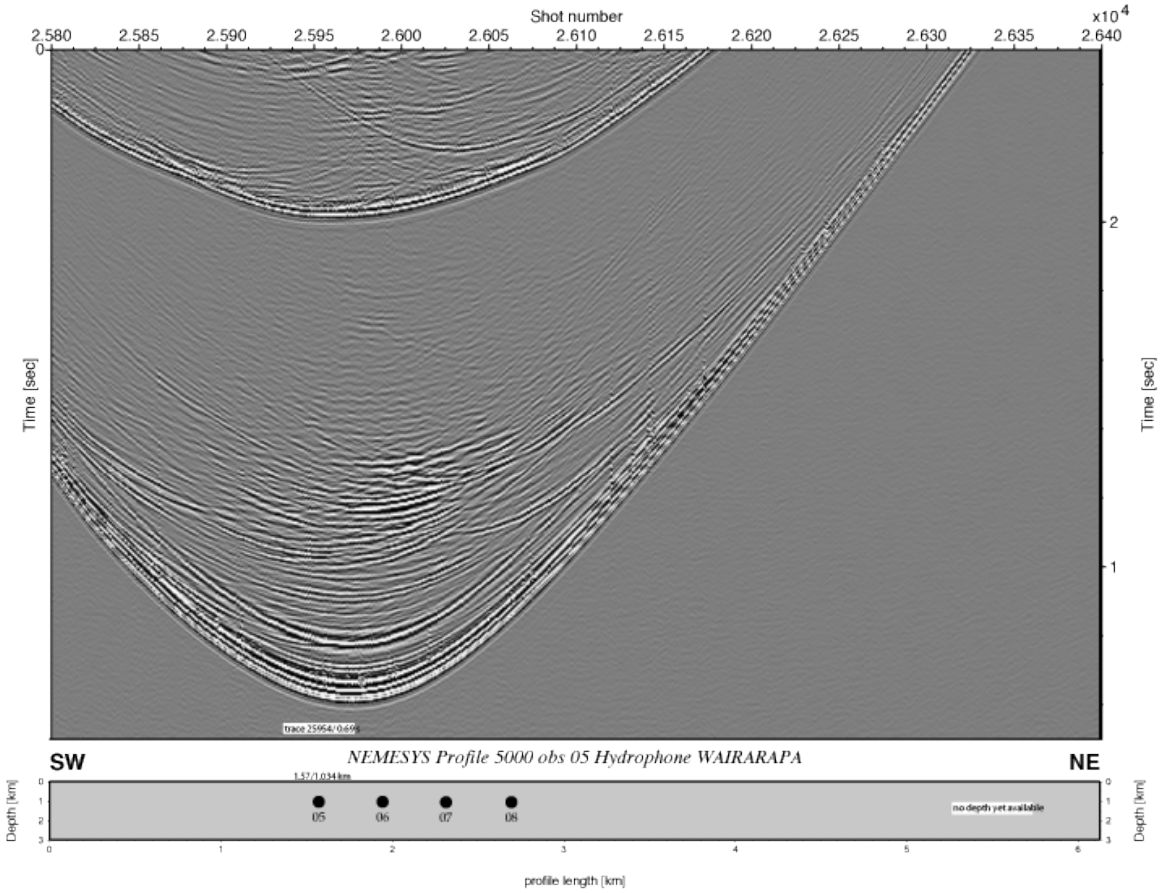

Figure 6.2.3.3.1 : Record section from obs 05 WAIRARAPA, Profile 5000.

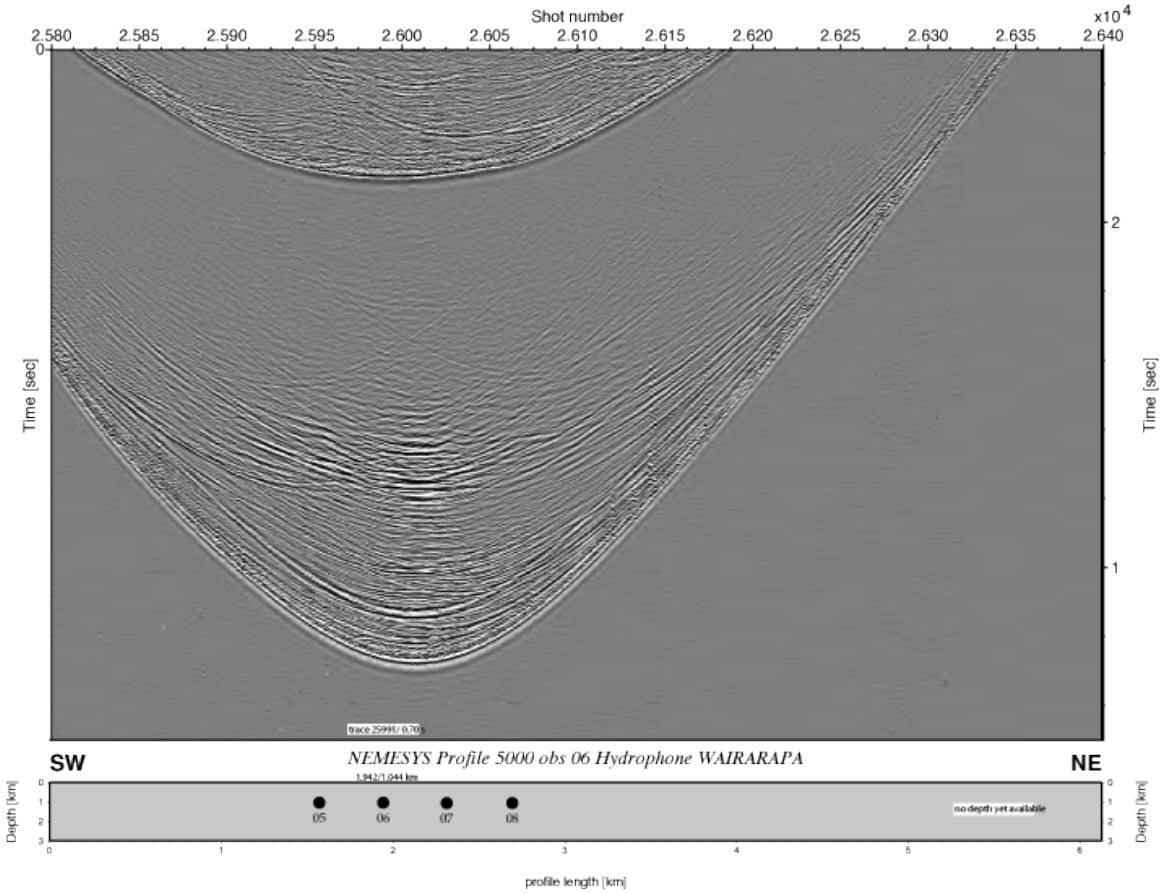

Figure 6.2.3.3.2 : Record section from obs 06 WAIRARAPA, Profile 5000.

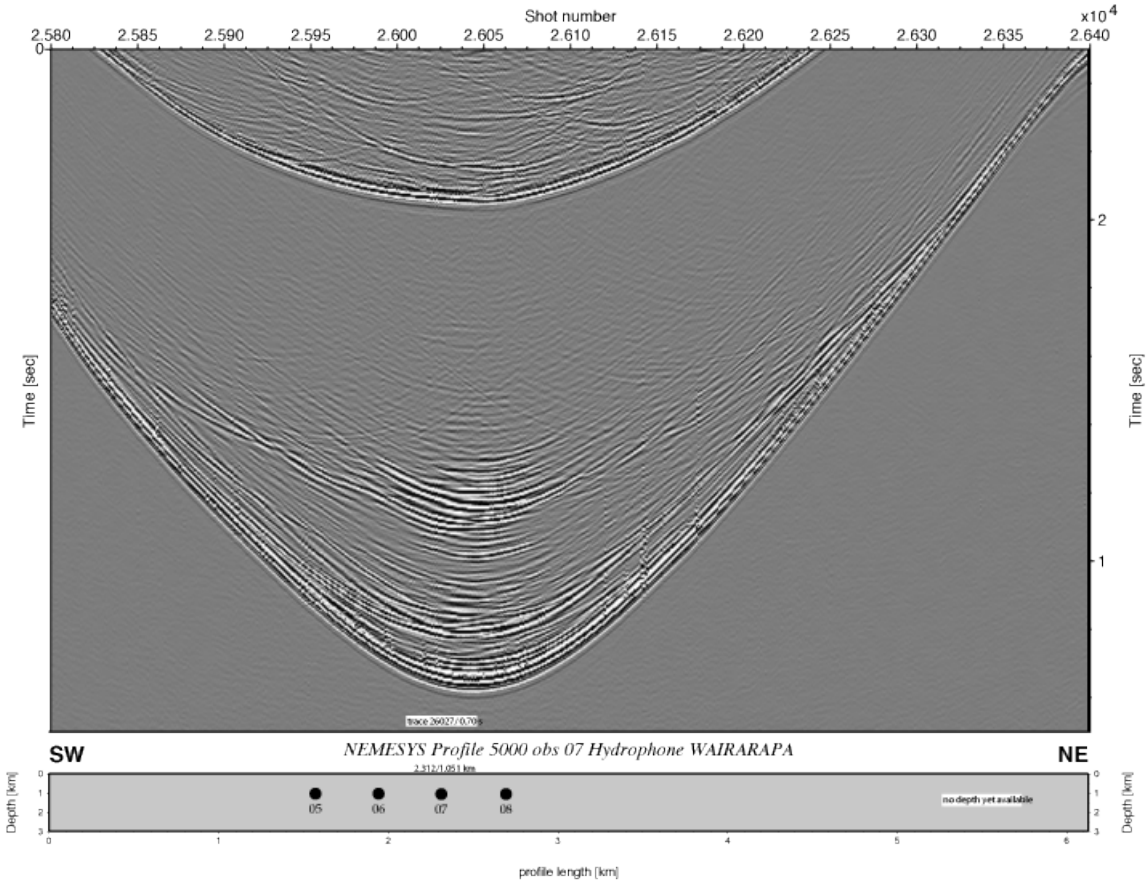

Figure 6.2.3.3.1 : Record section from obs 07 WAIRARAPA, Profile 5000.

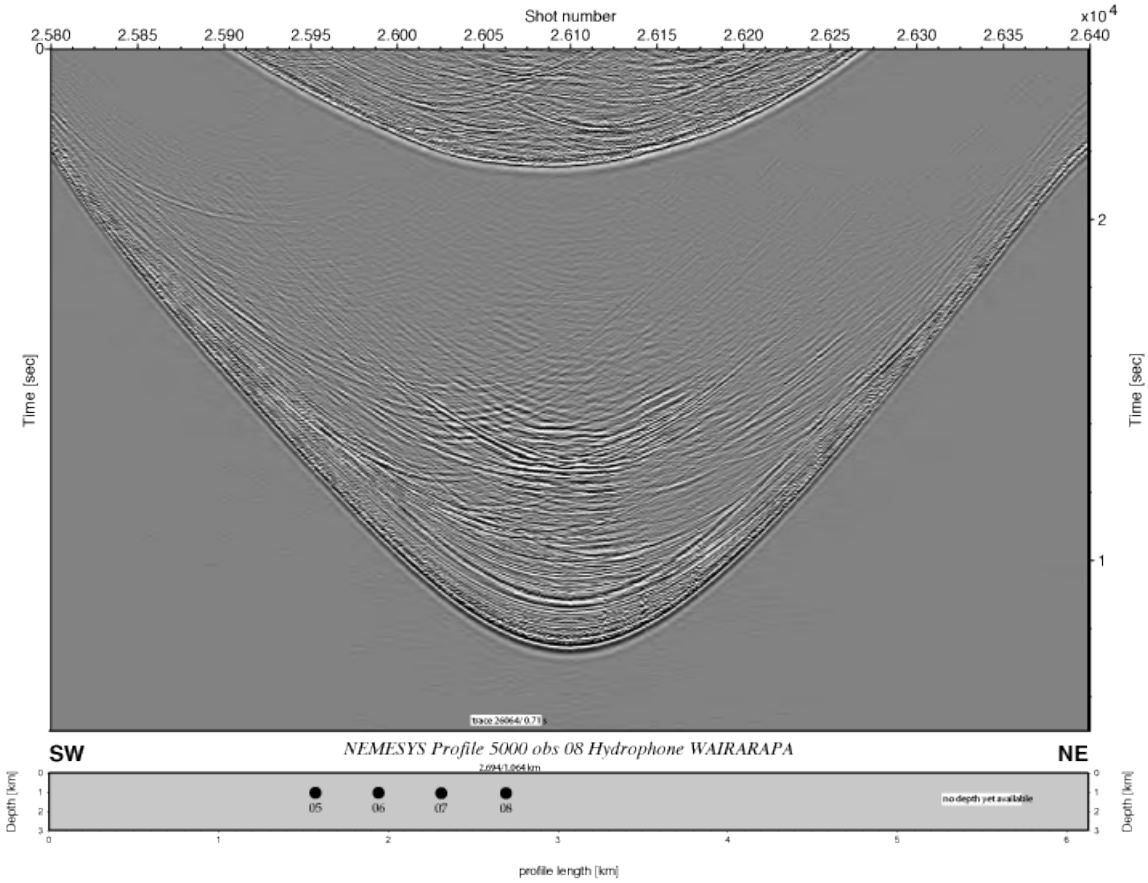

Figure 6.2.3.3.1 : Record section from obs 08 WAIRARAPA, Profile 5000.

6.3. Deep-towed sidescan sonar and streamer deployments

Ingo Klaucke and Ines Dumke

The deep-towed system consisting of the EdgeTech dual-frequency sidescan sonar with integrated Chirp sub bottom profiler (chapter 5.3) and the deep-towed seismic streamer (chapter 5.2.4) was deployed five times. The first deployment was dedicated to sidescan sonar mapping of the southwestern end of Omakere Ridge and the Rock Garden area (Fig. 6.3.1.1) while the other four deployments took place on Opouawe Bank and were designed to provide both sidescan sonar imagery and deep-towed seismic data (deployment 2) or just deep-towed seismic data (deployment 3 to 5).

Sidescan sonar data in the Omakere Ridge area were acquired from 00:55 UTC on March 17, 2011, to 06:03 UTC on March 18, 2011. In the northern part of the survey area, previous sidescan sonar surveys in 2007 (SO191) had identified 4 seep sites named Kea, Kaka, Kakapo and Bear's Paw, as well as a cold reef known as Moa. The objective of this survey was to revisit the already known sites as well as to map any new sites in the southern part of the ridge.

The survey comprised 5 parallel profiles of approximately 12 nm length and with a distance of 1300 m between adjacent profiles (Fig. 6.3.1.1), and a shorter profile in W-E direction crossing the locations of the known seep sites Kea, Kaka and Kakapo in the northern survey area. 75 kHz sonar data as well as 2-10 kHz sub bottom profiler data, both with a ping rate of 1 Hz, which resulted in a constant range of 750 m for the sidescan sonar system, were obtained on all 6 profiles. On profiles 1-5, the DTS-1 system was towed at an altitude of approximately 100 m above the seafloor. On profile 6, this altitude was reduced to approximately 20 m above the seafloor as the high resolution 410 kHz mode was operated in addition to the 75 kHz mode and the sub bottom profiler. However, the 410 kHz mode did not operate properly (no data was recorded) and consequently only 75 kHz and sub bottom profiler data were acquired on profile 6.

6.3.1 Omakere Ridge

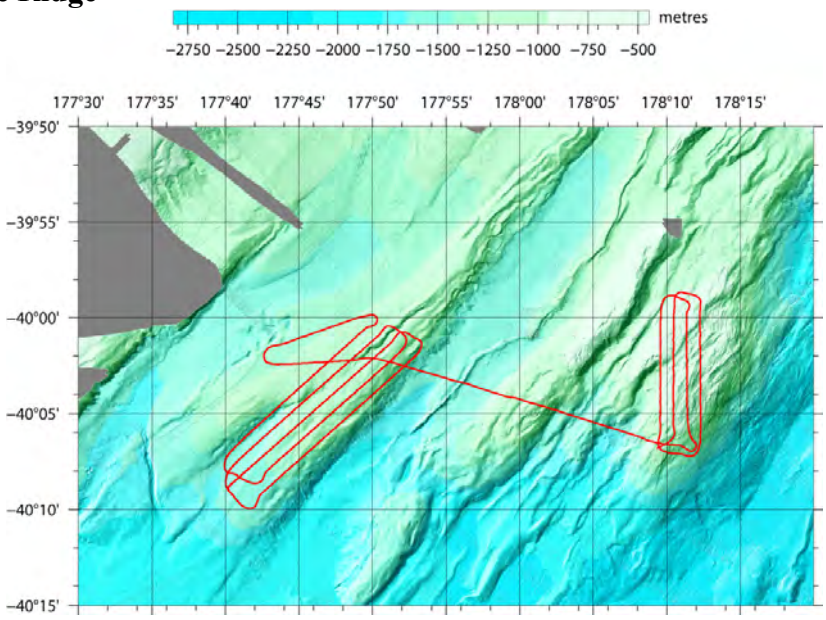

Fig. 6.3.1.1: Bathymetric map of the Omakere Ridge and Rock Garden working area showing the cruise track of the sidescan sonar fish during the deployment

The position of the towfish was calculated from the ship's position and the cable length using a layback method, as the Posidonia USBL system did not function properly. Processing of the sidescan sonar data consisted of an altitude correction, slant range correction, mosaicking and contrast enhancement and was done on-board using the software package Caraibes 3.2. The sub bottom profiler data were processed using in-house shell scripts based on Seismic Unix and GMT.

The three known seep sites in the northern survey area - Kea, Kaka and Kakapo – were clearly identified by high backscatter in the low-frequency (75 kHz) sonar data (Fig. 6.3.1.2). They appear to be associated with superficial faults oriented NW-SE that extend beyond the seep site but disappear after a few hundreds of metres. At the Kakapo site, a potential gas flare indicated by an acoustic anomaly in the water column of the raw sonar data was observed (Fig. 6.3.1.3).

Another flare was observed in the southern part of the survey area that had not been mapped previously. The flare is shown in Fig. 6.3.1.4. It occurred in the vicinity of a high-backscatter region indicating precipitation of authigenic carbonate and hence a new seep location. This site was named Toroa. Sub bottom profiler data acquired near the site show patches of higher amplitudes and acoustic turbidity in the upper 20 m below the seafloor (Fig. 6.3.1.5), thereby indicating the presence of free gas.

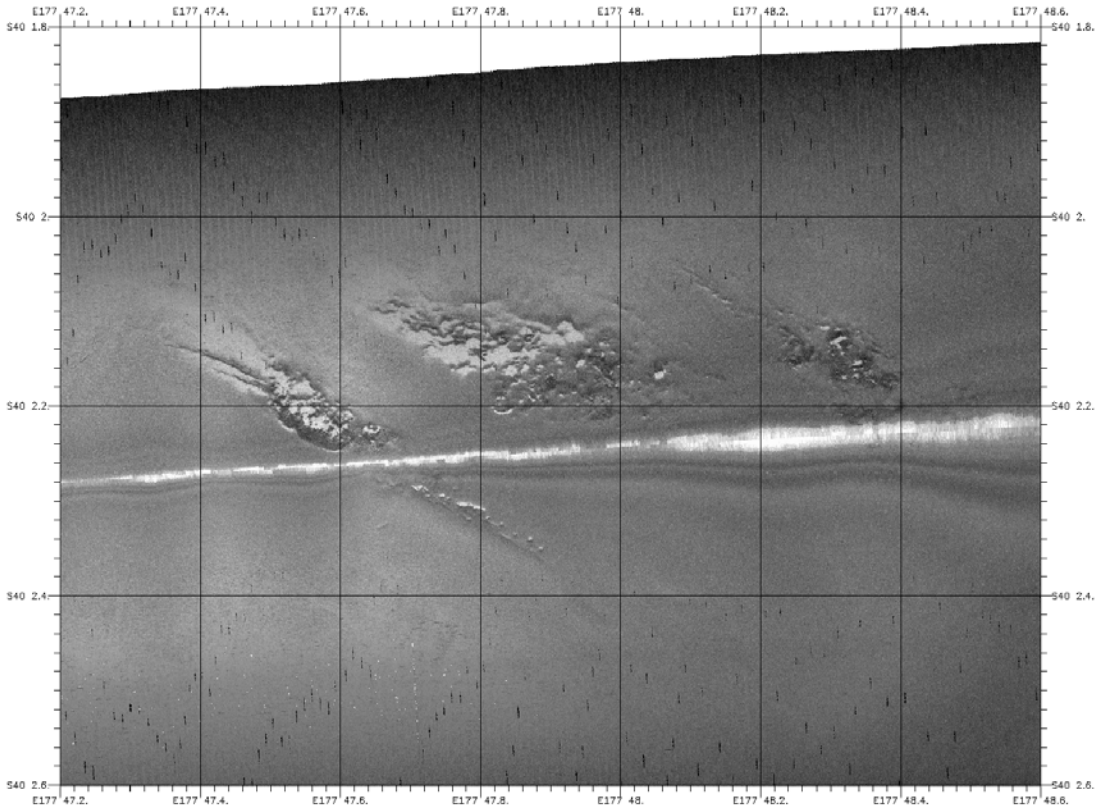

Fig. 6.3.1.2: 75 kHz sidescan sonar profiler crossing the Kea, Kaka and Kakapo seep sites. High backscatter intensity is dark.

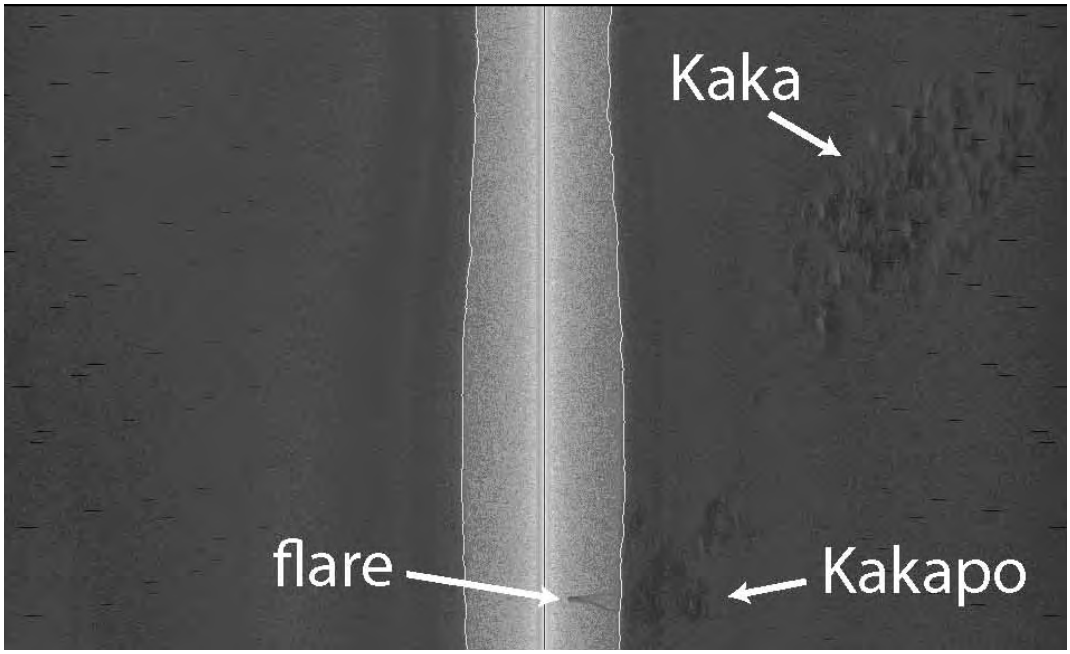

Fig. 6.3.1.3: Unprocessed 75 kHz sidescan sonar data showing gas flares in the water column at the Kakapo seep site. High backscatter intensity is dark.

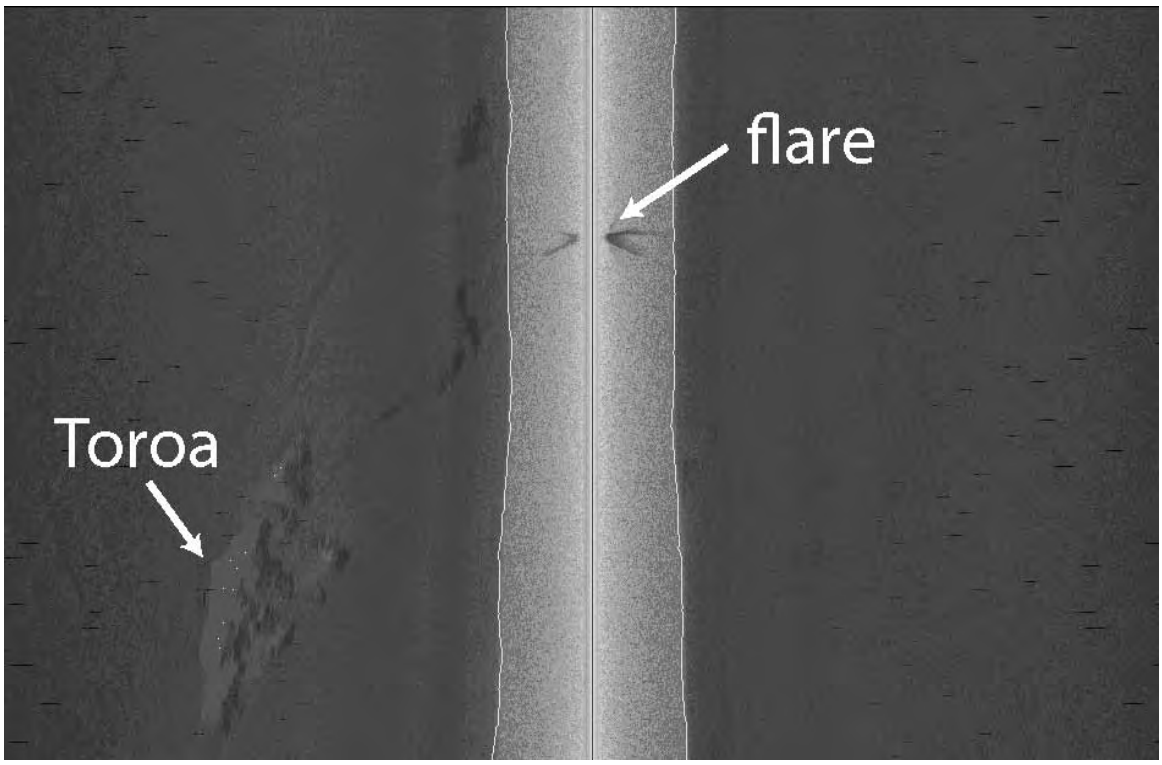

Fig. 6.3.1.4: Unprocessed 75 kHz sidescan sonar data showing gas flares in the water column at the newly discovered Toroa seep site. High backscatter intensity is dark.

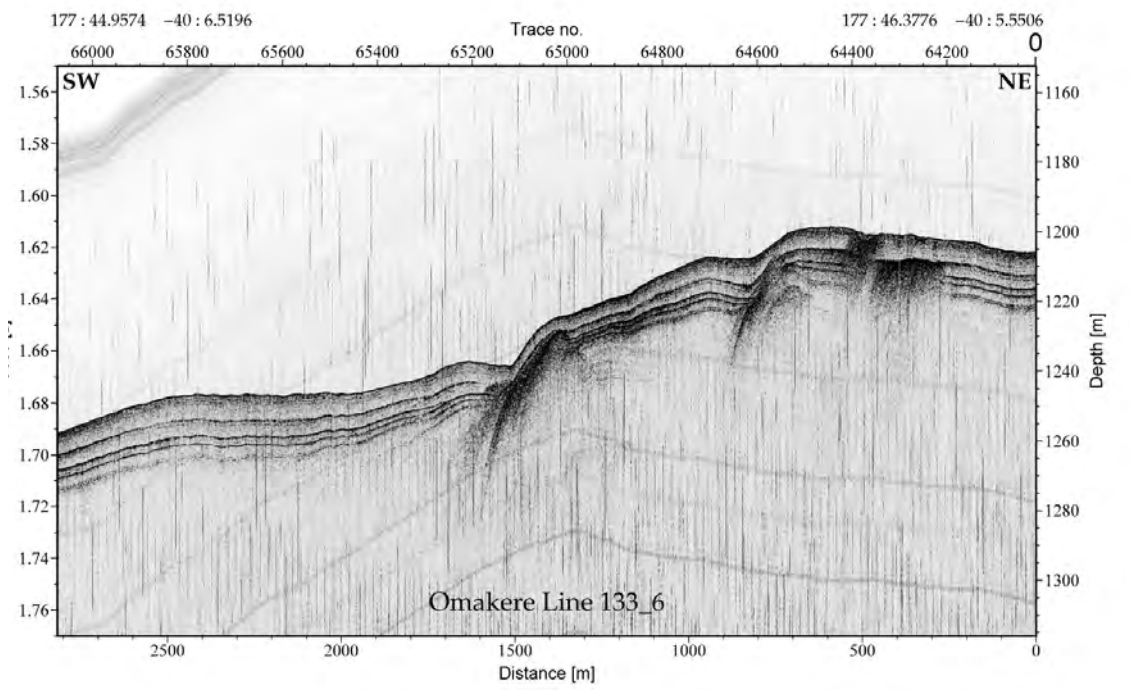

Fig. 6.3.1.5: Sediment echo sounder profile (2-10 kHz) marginally crossing the Toroa seep site. Profile locations correspond to figure 6.3.1.4.

Further to the East, part of another potential seep location which was named Matuku was observed from high backscatter at the outer edge of the easternmost profile (Fig. 6.3.1.6). This site was only partially mapped, but the patchiness of high backscatter intensities strongly suggests this feature to be a seep site.

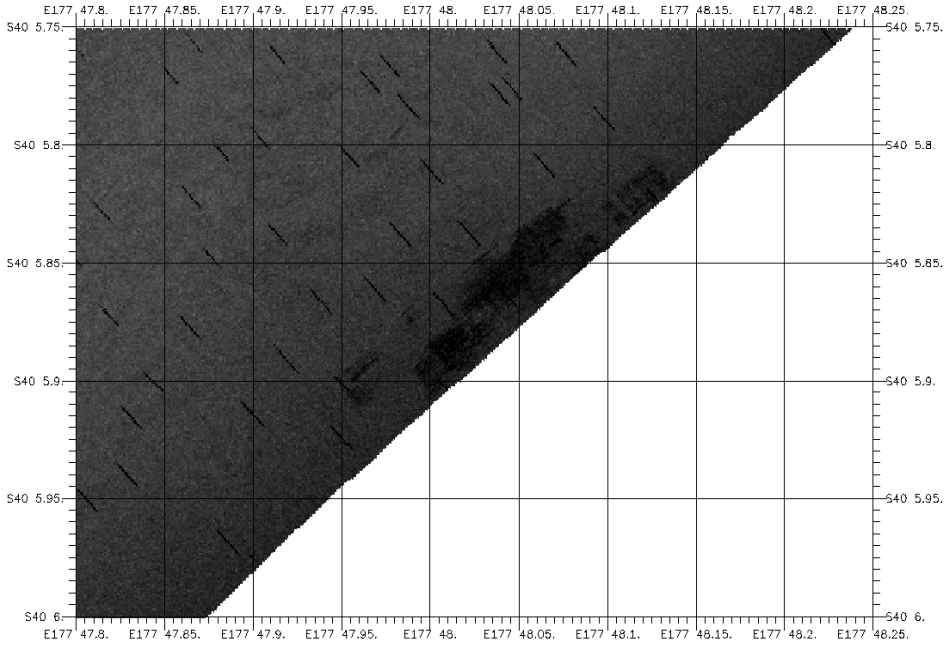

Fig. 6.3.1.6: 75 kHz sidescan sonar profiler showing the new seep site named Matuku at the outer edge of the profile. Also visible are acoustic disturbances generated by the Posidonia transponder, but Posidonia data were not registered. High backscatter intensity is dark.

The sites Moa and Bear's Paw, which were discovered in 2007 during SO191, were also clearly mapped and it was found that Moa appears to extend further to the south than shown by the previous records (Fig. 6.3.1.7).

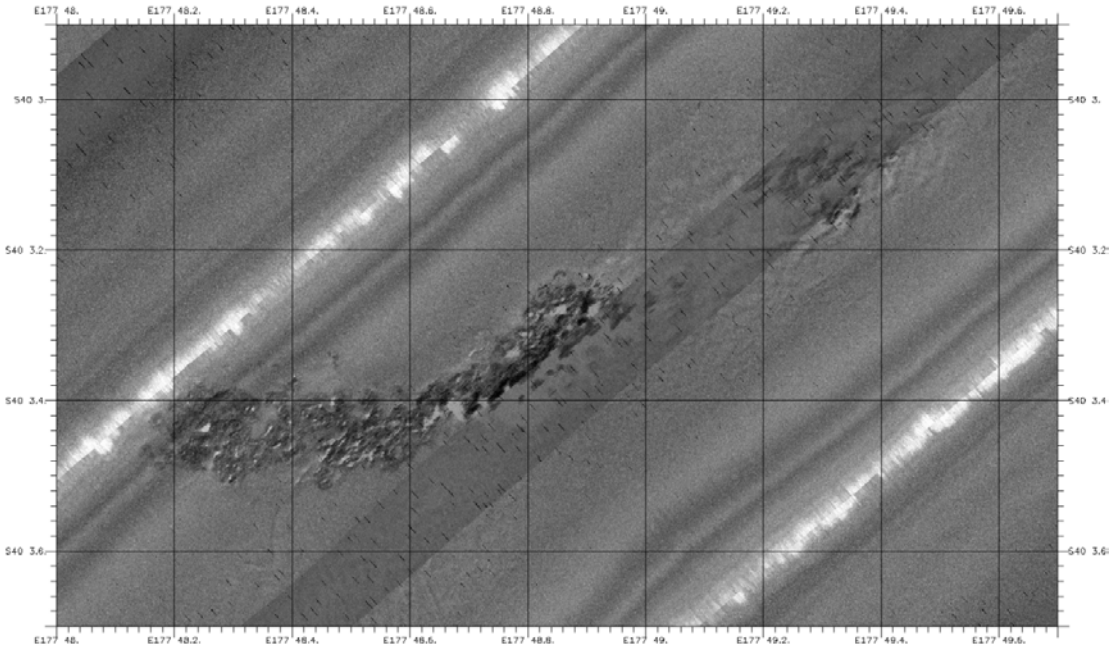

Fig. 6.3.1.7: Sidescan sonar mosaic (75 kHz) of the Moa and Bear's Paw seep sites. Note the difference in backscatter intensity between the Moa seep in the West and the adjacent Moa cold-water reef. High backscatter intensity is dark.

6.3.2 Rock Garden

Omakere Ridge and Rock Garden being only 15 miles apart I was decided to cover both areas during one deployment. Relief was fortunately not too strong so that the instrument was kept in operating range of the seafloor during transit between the two target areas. This transit crossed several small ridges running parallel to Omakere Ridge (Fig. 6.3.1.1). They generally showed high backscatter intensity due to the presence of sedimentary basement rocks being close to the seafloor but lacked evidence for fluid venting. The Rock Garden area was known to contain cold seeps from previous cruises. Sidescan sonar images of the Rock Garden area nicely show the structures of the sedimentary basement and the alignment of faults, but cold seeps are difficult to distinguish against the relatively high backscatter background (Fig. 6.3.2.1).

6.3.3 Wairarapa (Opouawe Bank)

The known seep sites at southern Opouawe Bank were the target of four deep-tow deployments. The first deployment on March 26, 2011 lasted from 03:27UTC until 20:15 UTC. It was planned to revisit the known seeps with 75 kHz sidescan sonar in order to detect potential seafloor changes within the past four years. At the same time deep-towed seismic data were to be collected. Unfortunately, the deep-towed seismic streamer did not work due to condensation water in several of the hydrophone nodes. Although the Posidonia transducer had been changed between this and the previous deployment, Posidonia data could only be recorded up to approximately 500 metres of range and towfish navigation consequently had to rely on cable length. The reason for this failure is still not known. The sidescan sonar images showed the presence of numerous gas flares in the water column. Detailed comparison of the

sidescan sonar mosaic obtained during this cruise and previous deployments in 2007 have to be carried later.

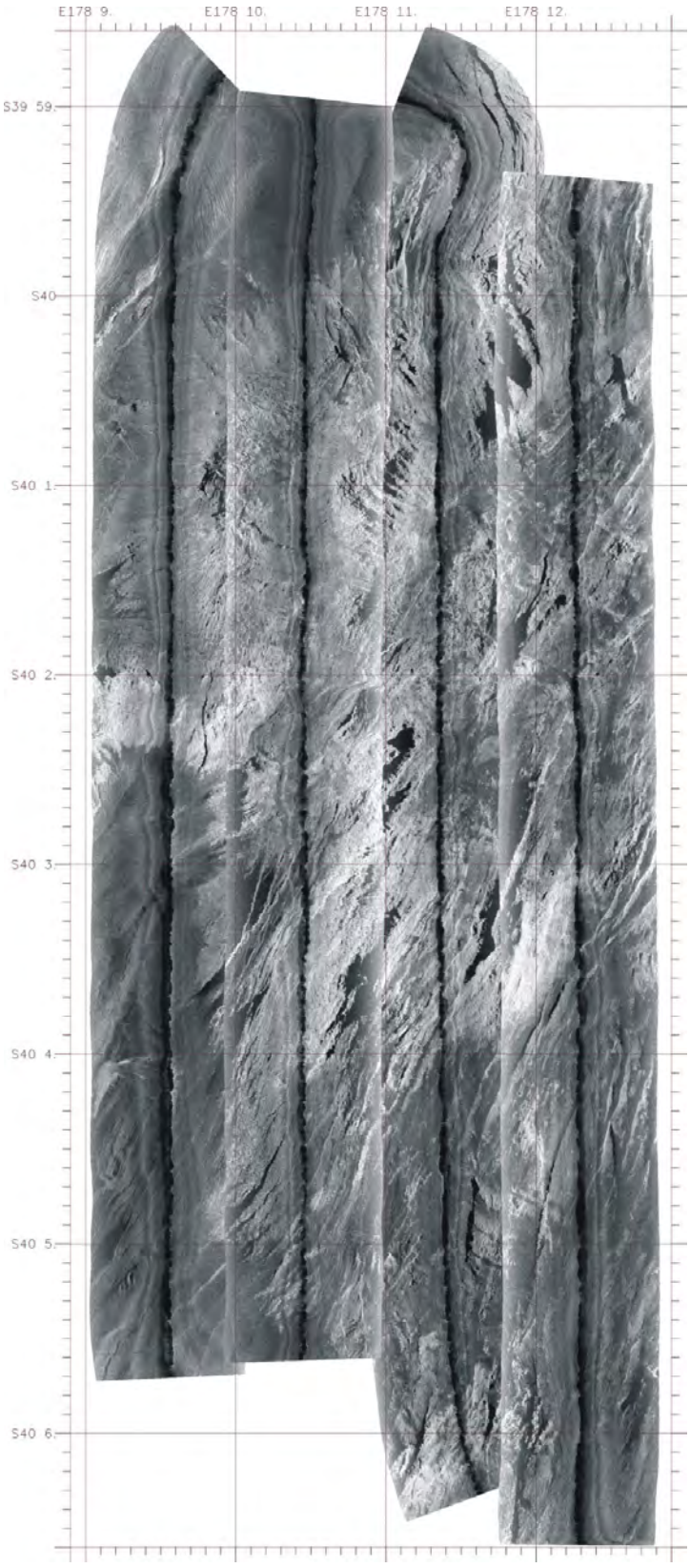

Fig. 6.3.2.1: Sidescan sonar mosaic of the Rock Garden working area showing the deformation structures within this area. High backscatter intensity is white.

A new attempt of recording deep-towed streamer data was made on April 2, 2011 at 00:20 using 31 nodes. This attempt again failed due to faulty connecting cables and water in two of the hydrophone nodes. The length of the streamer was subsequently reduced to 16

nodes and the deep-towed system redeployed on April 2, 2011 at 03:05 UTC until 07:56. This time, the streamer worked correctly for extended periods although halfway through the deployment only 7 nodes appeared to work properly. During the deployment, the system was lowered to roughly 800 metres water depth, i.e. 300 metres above the seafloor, and held constant at this water depth. The system appeared to be very sensitive to movements of the winch that produced noticeable noise in the data. After recovery of the system, all connections (especially those between node 7 and 8) were checked carefully, but no obvious problem could be detected. It was suspected that the problems during the profile were linked to the software and probably would have been overcome by a restart of the system. The system was re-deployed on April 2, 2011 22:40UTC until April 3, 2011 03:36 UTC for an additional profile running in the opposite direction. During this deployment all 16 streamer nodes worked properly for the entire deployment and the streamer was again kept in roughly 800 metres water depth. During both deployments a small, mobile transponder was attached to the sidescan sonar towfish, so that Posidonia data are available for these deployments. Figure 6.3.3.1 shows one channel of the streamer during the fourth deployment.

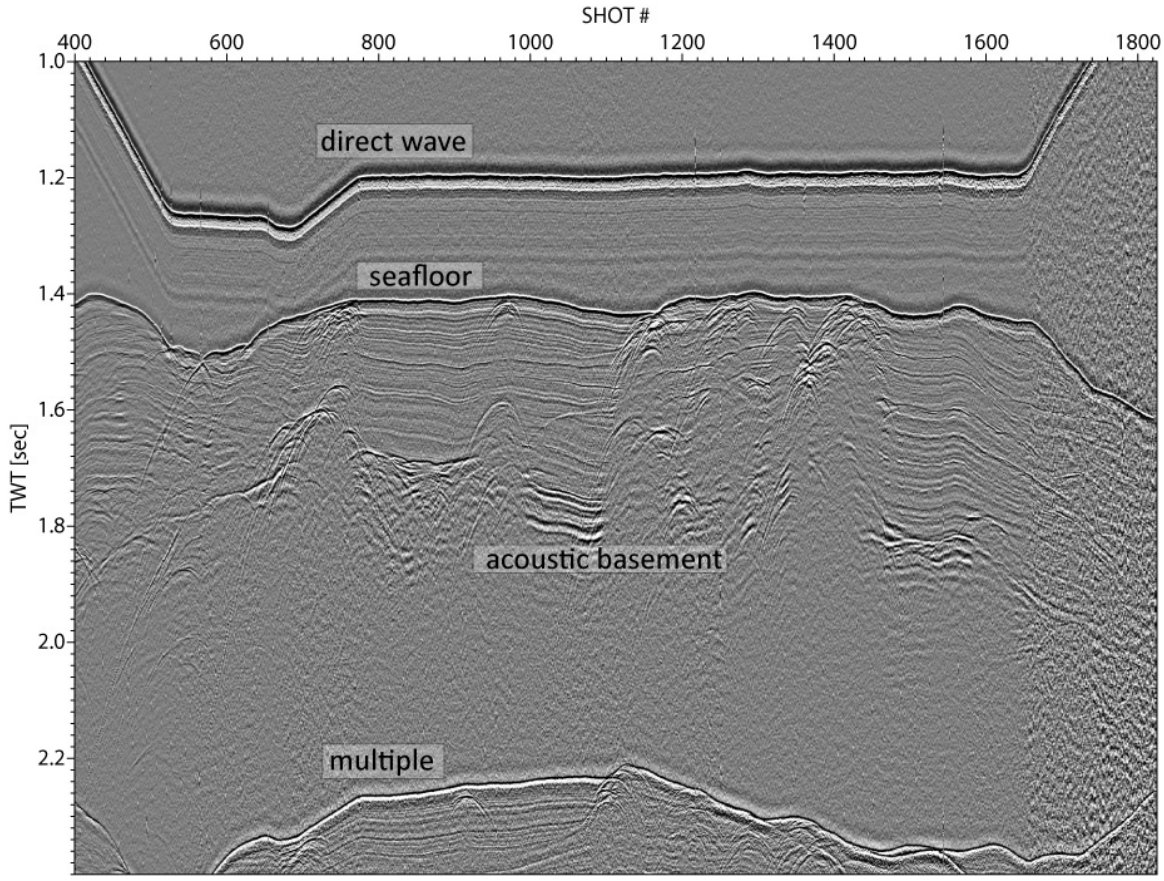

Fig. 6.3.3.1: Single channel display of deep-towed streamer data from the Opouawe Bank. The data have not been processed, only a moderate high-pass filter has been applied.

6.4. Marine CSEM

6.4.1 Marine CSEM-BGR at Opouawe Bank

Katrin Schwalenberg, Martin Engels, BGR Hannover

The two marine CSEM experiments were carried out on Opouawe Bank off the Wairarapa on the southern end of the Hikurangi Margin in water depth between 1000m and 1100m (see map). Several seep sites and vent structures were known from video observations and hydro-acoustic data during previous cruises on RV Tangaroa (TAN0616), and

particularly from voyage SO191 (project New Vents in 2007). During SO191 CSEM data were collected on Opouawe Bank along two profiles using on older, seafloor-towed electric dipole-dipole system. The locations of these profiles are shown in Fig. 6.4.1.1. Highly elevated resistivities suggesting gas hydrate concentrations of up to 25% at North Tower and South Tower seep sites, and moderately elevated resistivities at Takahe were observed along the profiles (Schwalenberg et al., 2010).

The aims of the CSEM experiments on SO214 were:

- Using the new BGR towed system to reveal lateral and vertical variations in the resistivity distribution along profiles
- Combining the results with the seismic data available, particularly with the high-resolution seismic data (P-Cable) and Parasound data collected during SO214-1
- Estimating the gas hydrate concentration along the profiles
- Deploying the IFM-GEOMAR CSEM experiment to collect a small scale (ca 1km x 1km) 3D data set over a known seep site for a detailed analysis.
- Analyze the 3D data set to derive the gas hydrate distribution below the seep site

HYDRA Deployments

During SO214-2 HYDRA was deployed two times over the seep sites on Opouawe Bank. One 8km long profile was successfully completed. The seafloor system got caught during the second deployment and only the pig could be recovered. Recovery of the system using video-guided equipment was almost successful, but had to be stopped due to the limited time schedule. After the cruise, NIWA vessel RV Kaharoa was chartered for two days by BGR and the receiver array and the data were successfully recovered.

Details of the deployments and preliminary results, followed by a brief description of the recovery attempts are following.

CSEM at Opouawe Bank

Opouawe Bank off the Wairarapa on the SE edge of the North Island was the focus working area on the second leg of SO214. Several seep sites were known from previous cruises, particularly from SO191 (project New Vents). In 2007 during SO191-1 two CSEM profiles across South Tower and Takahe, and intersecting South Tower and North Tower were completed using an older towed CSEM system, which is not in use anymore. The results from these experiments were highly anomalous resistivities below South Tower and North Tower suggesting concentrated gas hydrate below those seeps (Schwalenberg et al., 2010). During the first leg of SO214, seep structures and vents could be clearly identified in Parasound, deep-tow sidescan, and in the 3D seismic data sets collected with the P-Cable. OFOS observations from the second leg showed several plumes rising from the seep sites. The CSEM experiments were aiming at the resistivity structure below these seep sites, possibly identifying areas of elevated gas and gas hydrate accumulation. The locations of the CSEM profiles were chosen to cover most of the known and newly identified seep sites and seismic events. The location for the 3D CSEM survey concentrated on South Tower.

Figure 6.4.1.1 shows a map of southern Opouawe Bank with the outline of the seep sites picked from Parasound images (red circles), and the CSEM profiles completed in 2007 (grey dots). The profiles completed on SO214-2 are marked with black (CSEM-SO214-1) and green squares CSEM-SO214-2, 3). The OBEM receivers deployed for the 3D survey are marked blue. The box outlines the area of the 3D seismic survey.

Deployment 1: Sunday, April 10th 2011

HYDRA was deployed along profile CSEM-SO214-1 on April 10th, 2011. The deployment started at 9pm local time and the array was back on deck on April 11^{th,} 2011 at

3pm. Bottom time of the instrument was from 00:00am to 11:15am. The array was stopped on the seafloor at 26 sites along the 8km long NE-SW profile with an average site spacing of 300m providing sufficient overlap with the different transmitter-receiver-offsets. Useful data sets were also recorded while the array was moving forward on the seafloor. Details are listed in table CSEM-2.

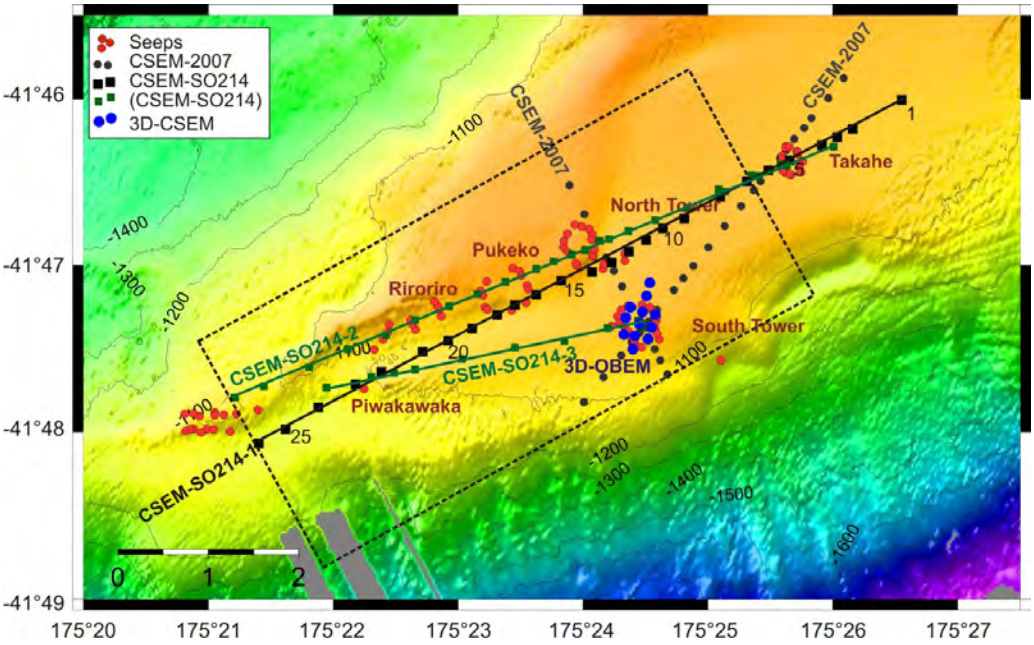

Figure 6.4.1.1: Map of Southern Opouawe Bank showing the outline of seep sites picked from Parasound data (red circles), two CSEM profiles from 2007 (CSEM-2007, grey circles), CSEM profiles from SO214 (CSEM-SO214-1, black squares, CSEM-SO214-2 3, green squares, instrument lost, data not recovered), the location of the OBEM receivers (blue circles), and the outline of the 3D seismic survey (dashed box).

Table 6.4.1.1: Deployment details, profile CSEM-SO214-1, 10.04.2011

Profile, Date	**CSEM-SO214-1, 10.04.2011**
Dipole Lengths	Length TX: 101.36m Length R1 10.03m Length R2 9.83m Length R3 15.05m Length R4 19.86m
Array Dimensions	Offset: TX – R1 159.39m Offset: TX – R2 262.21m Offset: TX – R3 405.07m Offset: TX – R4 753.38m
Source Signal	Square wave, 4.5A, 6s period, 100% duty cycle
Deployment Times and Ship Coordinates (times in UTC= Local Time -12h) Duration of experiment: 18 hrs. Time for Collecting Data: 10,25 hrs.	Start Deploy: 9:00am 175.4548 E -41.7615 S First Site 1: 01:00pm 175.4225 E -41.7745 S Last Site 26: 11:15pm 175.3367 E -41.8077 S End Deploy: 03:00am (11.04.11) 175.3089 E -41.773 S

PIG coordinates are listed in Appendix 9.4

Deployment 2: Thursday, April 14th 2011

The second deployment of HYDRA was carried out on April 14th, 2011. The plan was to tow the system along two, possibly along three profiles in one go without bringing the array back on board. Profile CSEM-214-2 was chosen after studying the 3D seismic block obtained from the P-Cable data, which was then available. It intersects with profile CSEM-SO214-1 at Takahe, but continues further to the North. The profile covers North Tower, Pukeko, and Rironiro seep sites. Profile CSEM-SO214-3 intersects with CSEM-SO214-1 at Piwakawaka and ends at South Tower where the seafloor get stuck and lost. Deployment details are listed in table CSEM-3.

Table 6.4.1.2: Deployment details, profile CSEM-SO214-2 and -3, 14.04.2011

Profile, Date	**CSEM-SO214-2, CSEM-SO214-3, 14.04.2011**
Dipole Lengths	Length TX: 101.36 m Length R1 10.03 m Length R2 9.83 m Length R3 14.73 m Length R4 19.86 m
Array Dimensions	Offset: TX – R1 159.39 m Offset: TX – R2 262.21 m Offset: TX – R3 404.80 m Offset: TX – R4 610.47 m
Source Signal	Square wave, 6 A, 6 s period, 100% duty cycle
Deployment Times and Ship Coordinates (time in UTC= Local Time -12 hrs.) Duration of experiment: 22 hrs. Time for Collecting Data: 11 hrs.	Start Deploy: 00:40am 175.4548 E -41.7615 S First Site P2: 04:23am 175.4225 E -41.7745 S Last Site P2: 11:32am 175.3367 E -41.8077 S First Site P3: 02:34pm 175.4225 E -41.7745 S Pig Stuck: 06:15pm 175.40874 -41.78915 Pig on deck: 11:50pm

PIG coordinates are listed in Appendix 9.4

Preliminary Results

Deployment 1: April 10th, 2011

Data were collected with all four receivers, and with the CTD Sensor. However, receiver 1 was running into saturation after site 6. Receiver 2 was out of range after site 24. Figure 6.4.1.2 shows 60 seconds long time series recording of the current signal, and the four receiver units. The seafloor array is stationary and the data have been averaged and decimated from the original sampling rate of 10kHz to a sampling rate of 1250Hz, which has the effect of a low pass filter. Considering the small source dipole moment of 4.5A x 100m, the data quality is extremely good. Even for the last receiver at an offset of 753m the receiver electronics is capable to measure electric field amplitudes smaller than micro Volts/m. As expected the replacement of the first data cable segment between control unit and receiver R1 with rope inhibited any noise propagation from the transmitter to the receivers.

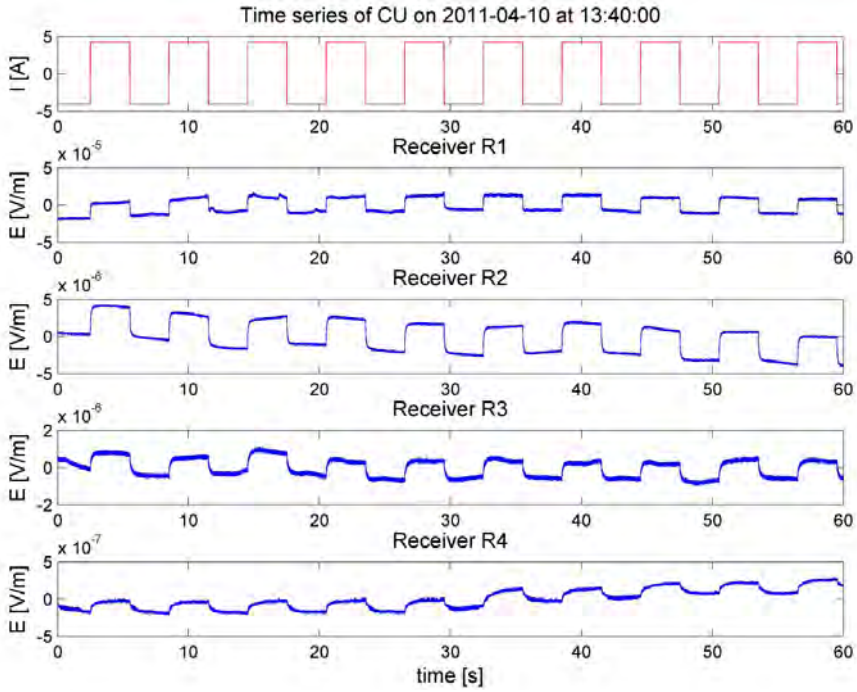

Figure 6.4.1.2: Data example: One minute long time series of the current signal recorded at the control unit and data from all four receiver units. The array was stationary. Data have been low-pass filtered. Offsets TX to R1: 159.39m, R2: 262.21m, R3: 405.07m, R4: 753.38m

In the next processing step the hundred best half-periods at each site and for each receiver were selected for stacking using an iterative scheme when the array was stationary. Figure 6.4.1.3 shows the stacked data sets recorded at receiver R3 for each site along the profile. Data sets recorded at sites 14,15,16,18, and 23 show a distinctively different shape than the remaining stacked data sets. Higher electric field amplitudes and earlier arrival times of the signal are caused by higher than normal resistivities at depth.

In the next step, stacked data sets from all sites along the profile were used to calculate a preliminary apparent resistivity profile for each receiver. 1D Marquardt-type inversion was applied where the only unknown was the resistivity of the underlying half space. The seawater resistivity was taken from the CTD measurements and fixed in the inversion. The resulting apparent resistivity profiles are shown in Figure CSEM-7.

Data recorded at receiver 1 were out of range from site 6 on and are not considered in Fig. 6.4.1.4. The inverted resistivity profiles are plotted over the site IDs and still have to be assigned to their real seafloor location. The profiles show several anomalies, particularly around sites 14-16 where the apparent resistivities are highly anomalous. Away from the seep sites, the inversion of the data revealed normal background resistivities between 1 and 2 Ohm-m at sites 1 to 12. First comparison of the resistivity anomalies with the seismically inferred seep site locations shows a good agreement with North Tower, Pukeko and Piwakawaka, and suggests the presence of highly concentrated gas hydrate accumulations and free gas below the seeps.

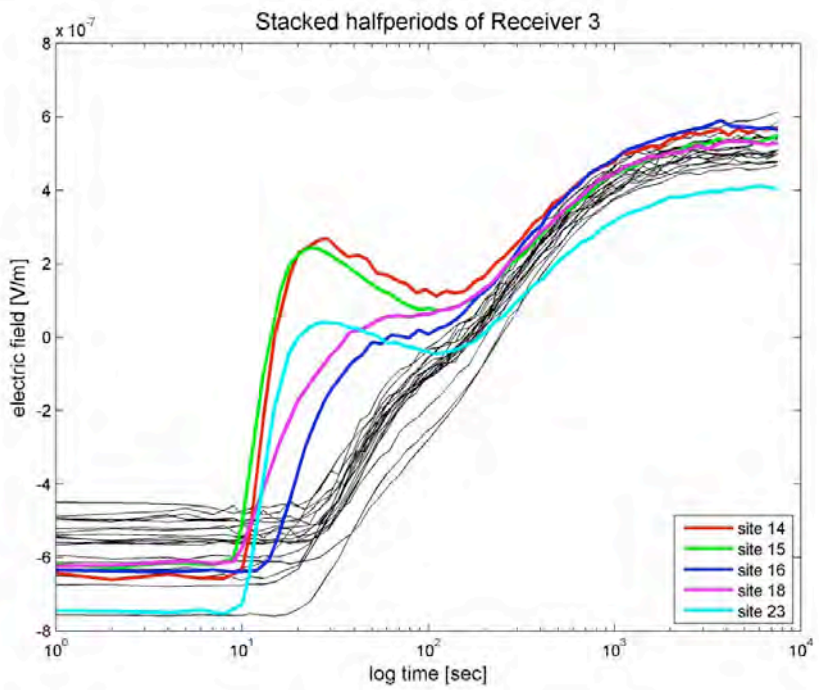

Figure 6.4.1.3: Stacked data sets recorded with receiver R3 at each site along the profile CSEM-SO214-1. Site 14-16, 18, and 23 show higher electric field amplitudes and earlier arrival times than the other data sets. This anomalous behaviour is significant for high resistivities below the sites.

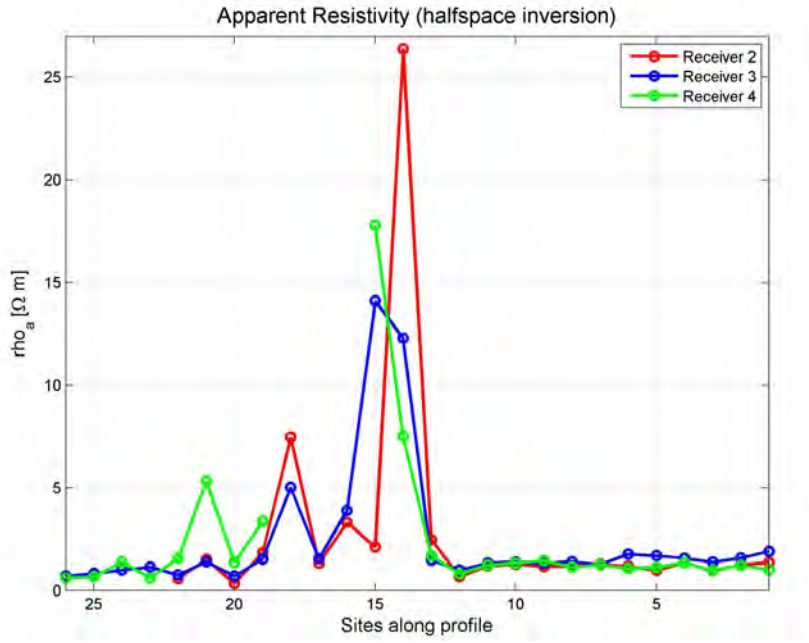

Figure 6.4.1.4: Apparent resistivity profiles derived from the stacked data at receivers 2, 3, 4 show highly anomalous resistivities over North Tower (sites 14-16), Pukeko (site 18) and Piwakawaka (site 21) seep sites. East of North Tower at sites 1 to 12, resistivities have normal background values between 1 and 2 Ohm-m.

CTD Measurements

Figure 6.4.1.5-6.4.1.7 show the conductivity profiles recorded with the CTD sensor (Sea & Sun, Model 60M), which was mounted inside the pig. The top panels of these figures show the profiles while the pig was lowered and lifted through the ocean layer. The bottom panels

show the profile while the pig was dragged on the seafloor in stop and go modus. The measurements are stable while the pig is stationary and noisy while the pig is moving, probably caused by suspended particles when the pig is moving on the seafloor. Bottom seawater conductivities vary between 32.2 and 33.5 mS/m along the three profiles. The values can be used as a-priori parameter for the inversion of the CSEM data.

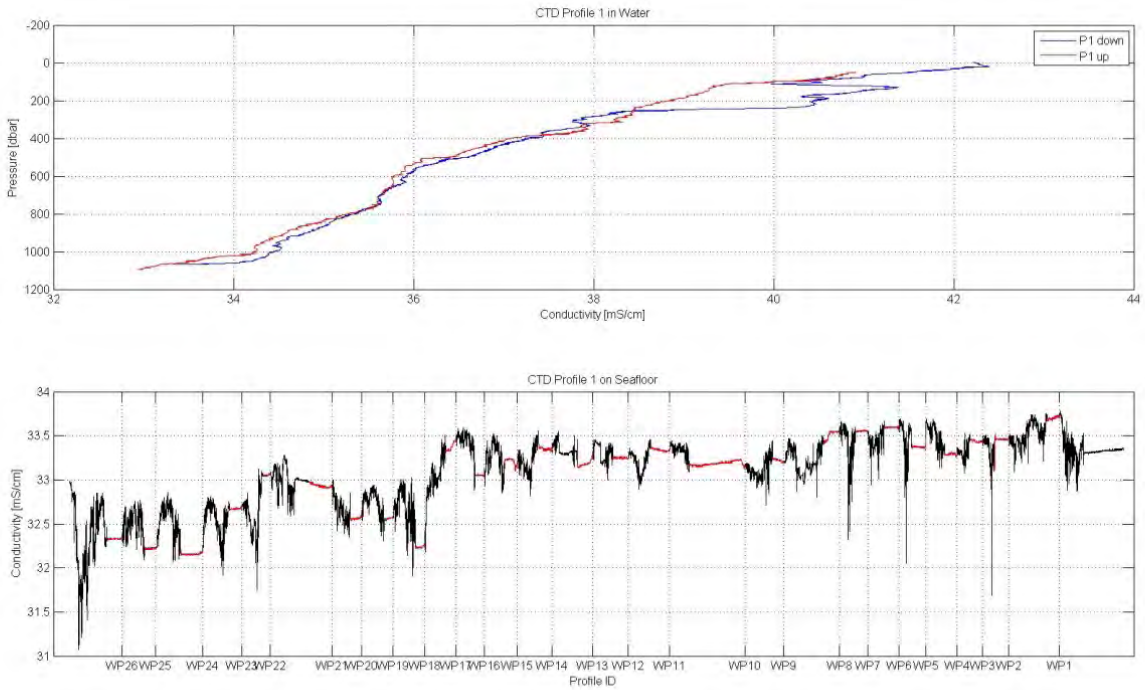

Figure 6.4.1.5: CTD profile along profile CSEM-SO214-1. Top panel shows the downward and upward conductivity profile through the ocean layer. The conductivity decreases from 42mS/m on the surface to values between 33 and 34mS/m on the seafloor. Bottom panel shows the conductivity profile on the seafloor. The conductivities are nearly constant while the pig (and the CTD sensor) was stationary and vary from 32.2 to 33.7mS/m. In between sites the conductivity data are noisy, probably due to suspended particles when the pig is moving.

Instrument Recovery Attempts during SO214

For the second deployment a R/V SONNE owned Posidonia transponder was attached to the pig to get full coordinates of the pig. The acoustic transponder system (deck unit with pinger and transponder in the pig), which we normally use only, provides the distance range between ship and pig. However, monitoring the Posidonia positions of the pig provided control where the array got lost on the seafloor. Figure 6.4.1.9- shows a blow-up of a sidescan sonar map of South Tower with the calculated positions of the pig when it got stuck and the four receivers. The array was stretched out over a length of 670m on the seafloor behind the pig. The video-guided grab and OFOS equipped with a hook were used for the recovery (Figure 6.4.1.8). Table CSEM-5 provides an overview of the recovery attempts. The cable could be easily seen on the camera-guided systems. The cable was picked up by the hook towed behind OFOS, but the array slipped off the hook about 270m above the seafloor. The last attempt was carried out with the TV grab. No video control was possible after the grab closed its claws. According to the tension the array was eventually picked up with the grab and slipped off again about 370m above the seafloor. Because the seafloor array has a total weight of only about 330kg in air, it is likely that the array is still caught on the seafloor around the first receiver.

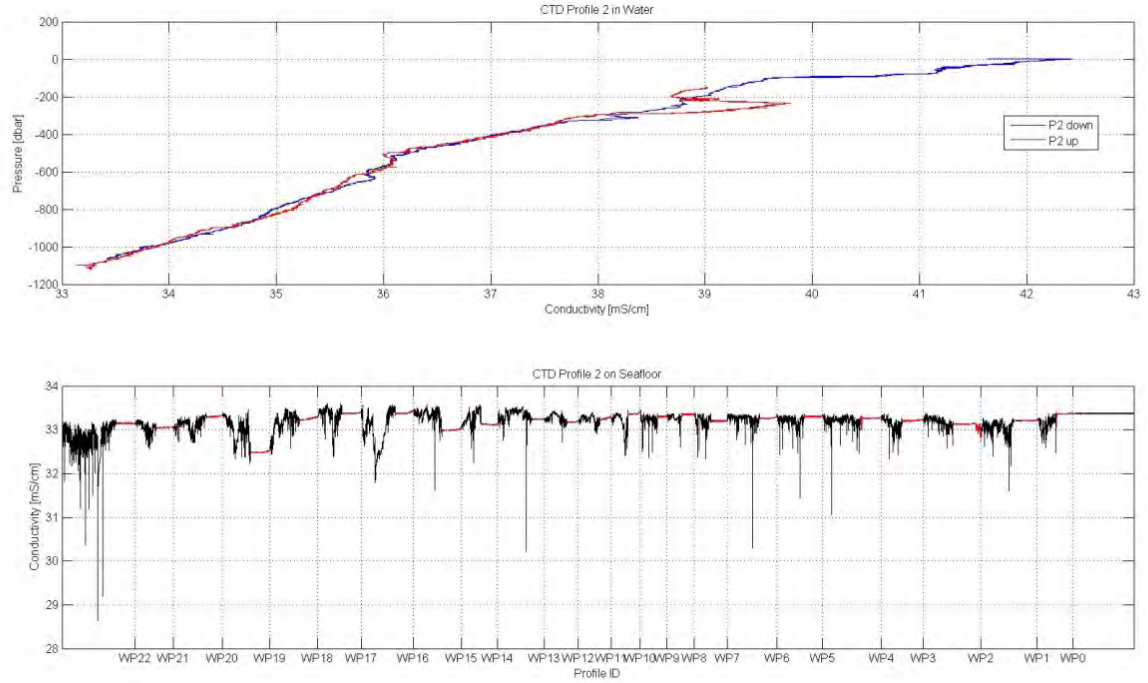

Figure 6.4.1.6: CTD profile along profile CSEM-SO214-2. Top panel: The conductivity decreases from 42mS/m on the surface to values around 33.2mS/m on the seafloor. Bottom panel: The conductivities vary from 32.5 to 33.5mS/m while the sensor is stationary.

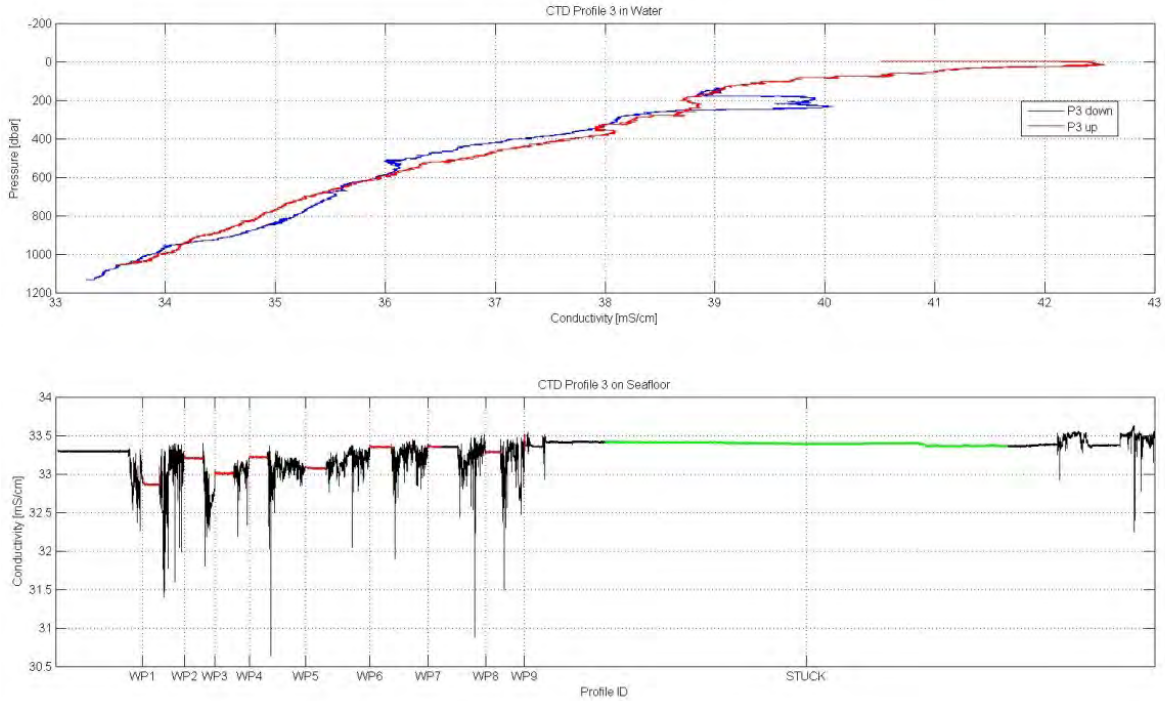

Figure 6.4.1.7: CTD profile along profile CSEM-So214-3. Top panel: The conductivity decreases from 42mS/m on the surface to values around 33.2mS/m on the seafloor. Bottom panel: The conductivities vary from 32.8 to 33.4mS/m while the sensor is stationary.

Figure 6.4.1.8: left: OFOS with recovery hook, top: TV Grab, bottom: Cable tension on TV Grab while pulling up. Increase and sudden release in tension suggests, the array slipped off the grab at 690m cable length (about 370m above seafloor).

Table 6.4.1.3: Estimated positions of lost seafloor array

Receiver	Coordinates
Pig	175:24.5245 -41:47.3489
R1	175:24.3786 -41:47.3628
R2	175:24.3056 -41:47.3732
R2	175:24.2072 -41:47.3879
R4	175:24.0635 -41:47.4079

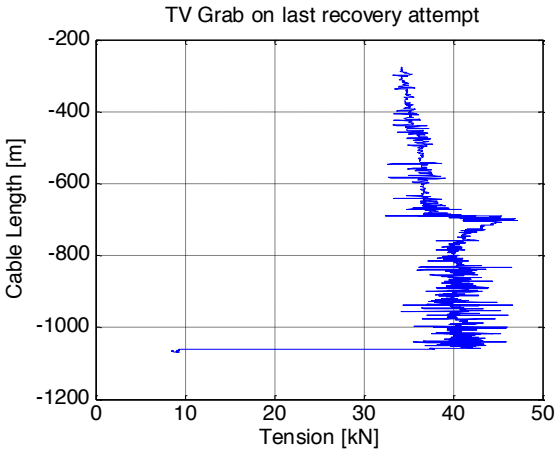

Table 6.4.1.4: Recovery Overview, Saturday, 16th April 2011

Time (UTC)	System	Action	Coordinates	Cable length/ water depth
20:16 (15.04)	TV Grab -1	Cable seen & grabbed (empty)	175:24.3423 -41:47.3771	
08:08:34	OFOS-Hook	Pick-up	175:24.2448 -41:47.3879	
08:33:40	OFOS-Hook	Slipped off	175:24.2677 -41:47.3469	784 m / 1055 m
10:26	TV Grab-2	Cable seen & grabbed	175:24.2604 -41:47.3680	
10:37	TV-Grab-3	Cable seen & grabbed	175:24.2530 -41:47.3670	
10:51:10	TV Grab-4	Pick-up	175:24.2743 -41:47.368	
11:14:09	TV Grab-4	Slipped off	175:24.3120 -41:47.3531	690 m / 1057 m

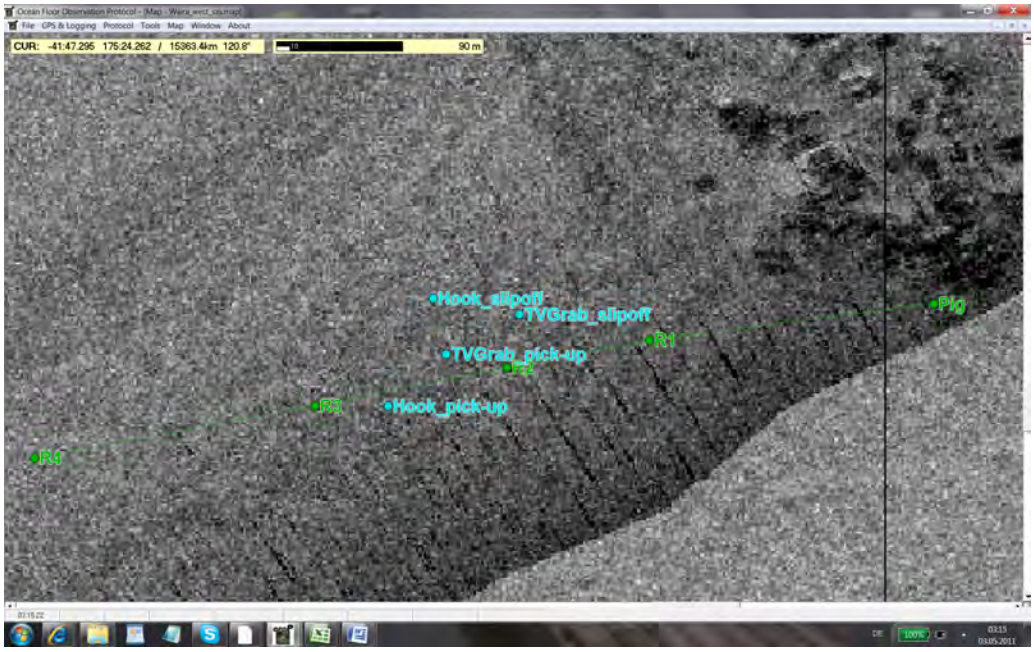

Figure 6.4.1.9: Screen print of side-scan sonar map of South Tower with estimated positions of the seafloor array. Also shown are positions where the array got picked up and dropped from the video-guided hook and grab.

Instrument Recovery with RV Kaharoa

After the cruise BGR chartered NIWA (New Zealand National Institute of Water and Atmospheric Research) vessel RV KAHARO to recover the lost CSEM receiver array. A time and weather window was found from May 9 -10th for the recovery. A set of three hooks with short stubby spikes connected with 1m long pieces of chain were connected to the 1600 m long wire on the trawl winch. The hooks were deployed over the starboard site of the ship, lowered to the seafloor and towed over the last known positions of the lost seafloor array. No video or acoustic equipment was available for the recovery. After each traverse, the wire was reeled in and the hooks were brought back on deck. The ship was turned around and the hooks were redeployed over the array in a different direction. The OFOP (Ocean Floor Observation Protocol) by J. Greinert was very useful to conduct the recovery procedure. After nine traverses the last receiver was finally picked up by the hooks and all four receivers were brought back safely on deck. As assumed the array was still stuck on the seafloor, but unexpectedly the rope was ripped off at the rear TX electrode. The transmitter dipole attached to the first 100m of rope both remained on the seafloor.

6.4.2 Marine CSEM- IFM-GEOMAR

Sebastian Hoelz

On April 10th, a total of 12 OBEM (ocean bottom electromagnetic) receivers were deployed (Fig. 6.4.2.1, black) over a promising seep site in the vicinity of South Tower. Nine stations were aimed at the centre of the structure on an array of approx. 400 x 400 m^2, three additional stations were placed to the NNE and SSW. Additionally, Fig. 6.4.2.1 shows the position of the CSEM-transmitter (cross) during the first (and only) measurement on April 13th, 2011.

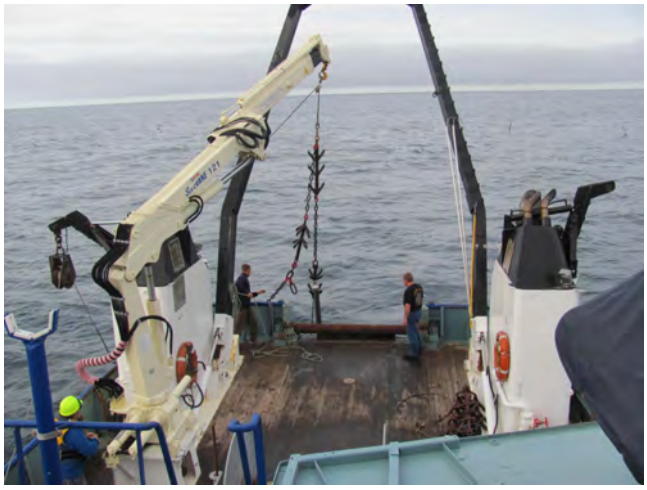

Figure 6.4.1.10: Instrument recovery on NIWA vessel RV Kaharoa. After nine attempts the last receiver was finally picked up by the hook. All four receiver units and the data were recovered.

A comparison of drop- and recovery-positions (Fig. 6.4.2.1, grey) shows that most stations were systematically shifted up to 500m towards the WNW. Therefore, the true positions of receives on the seafloor may only be estimated with large uncertainties from given drop- and recovery positions. This points out the necessity of ranging between transmitter and receivers.

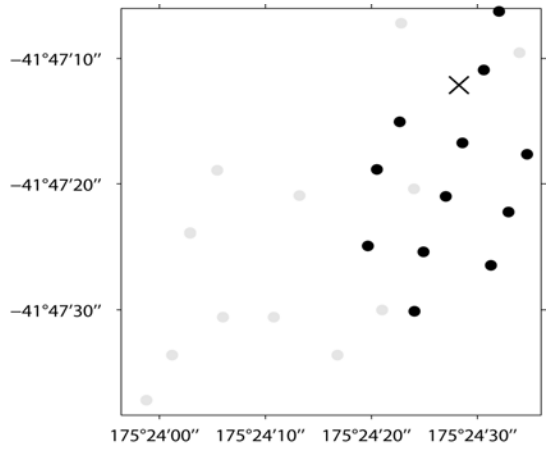

Fig.6.4.2.1: Station map of OBEM receivers with drop positions (black) and recovery positions (grey). The CSEM-transmitter of the IFM-GEOMAR was deployed at a single location (cross).

During the first CSEM-profile of the BGR, which crossed North Tower, the IFM receivers were activated (April 10th, ~16:30 hrs. -21:30 hrs. UTC) to potentially record data during transmissions of the BGR transmitter. Distances between the receiver array and the BGR-profile were at minimum 700 m, thus, we only expected to see transients with very small amplitudes at the northernmost station(s).

A first deployment of the transmitter-system of the IFM-GEOMAR was started on the 12th of April (~3:00 hrs. UTC). It had to be cancelled shortly after lowering the transmitter frame into the water, when instabilities of the illumination were noticed on the video system. After recovery of the system on deck it was found that water had entered the pressure tube containing the transmitter electronics, causing short circuits and numerous subsequent failures of the electrical system. After an additional pressure test of the pressure tube (without electronics), a pinched O-ring in one of the SubConn-connectors was identified as cause for the water in-leakage. Refitting of the pressure tube and fixing of the main electric problems were finished within 24h. Some systems like the video could not be fully restored and remained unstable during operations.

On April 13th (~ 6:00 hrs.) the transmitter was finally lowered to the ocean floor. Because receiver stations had to be recovered in time before the set time release, there was just enough time left for a quick test of the transmitter system and one measurement. Ultimately, recovery of receivers was finished less than 3 hrs. before the set time release.

Fig. 6.4.2.2 depicts a measurement taken with the SBL ranging system. The interrogation pulse sent from the SBL system (s. Fig. 6.4.2.2, left) at a frequency of 11 kHz, is clearly visible as dominating pulse at ~0.1 s. From ~0.35 s onwards, the replies received from transducers mounted to the OBEM stations are visible at various frequencies. Exemplarily, a close-up of sonograms (not depicted) shows that the pulse from station OBEM01 (13.5 kHz) arrived at 0.3509 at transducer T_1 and at 0.3517 s at transducer T_4. Thus, not only the distance but also the direction of individual OBEM stations may be derived from the known geometry of the SBL system. However, it becomes increasingly difficult to pick phase differences at larger offsets / later times, because they are obscured by echoes and the arrival of signals from closer stations.

On the seafloor, the CSEM transmitter was tested for output currents between 10A and 50A for both polarizations. Internal measurements of the current function showed that the transmitting unit was fully functional. Without video surveillance it was not possible to check, whether or not the electrode arms did indeed unfold fully.

A first check of data recorded at the OBEM-receivers revealed massive problems with several loggers: corrupted time-stamps and scrambled files currently prevent the evaluation of data. After return of the devices to Germany, a first analysis with the manufacturer of loggers has shown that problems with the internal clock prevented correct recording of data. This problem is currently investigated further and it remains unclear, how much data can be recovered. However, at some stations, reasonable data was recorded. An example showing pre-stacked raw data recorded at station OBEM01 is shown in Fig. 6.4.2.3.

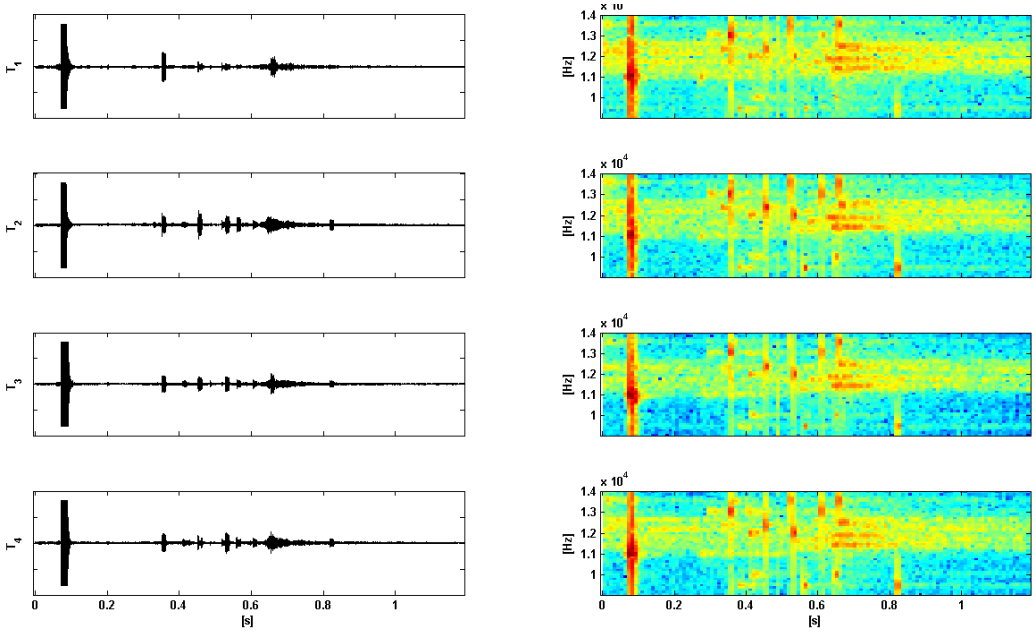

Fig. 6.4.2.2: Measurement with SBL system (April 13th, 4:41 hrs.). Each row shows the recording at on transducer head with the sonogram on the left and the according spectrogram on the right. The interrogation pulse sent from the transmitter frame (11 kHz) is visible at ~0.1s, answers from the transducer heads mounted to the OBEM-receivers are visible from ~0.35s onwards. Since transducers at receiver station were operated at different frequencies, an identification of individual stations is possible.

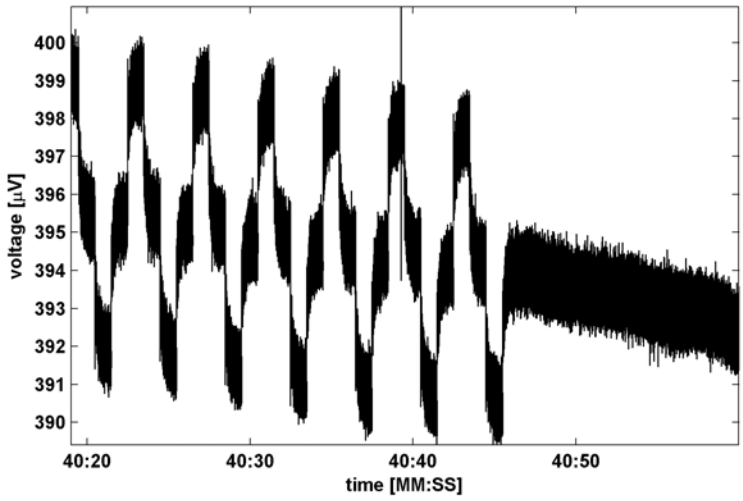

Fig. 6.4.2.3: Measured voltage (component V2) at receiver OBEM01 during transmission with CSEM transmitter.

6.5 CTD and CH4 measurements

Aneurin Henry-Edwards, Jens Greinert, Piet van Gaever, Peter Urban, Mario Veloso, Kamila Sztybor

During Leg 1 of SO214 we conducted 10 CTD casts to acquire sound velocity profiles and sample water at different depths close to selected seep sites. During Leg 2 we performed 13 CTD casts at Opouawe Bank to get an inventory of the methane concentration around the selected seep site Takahe.

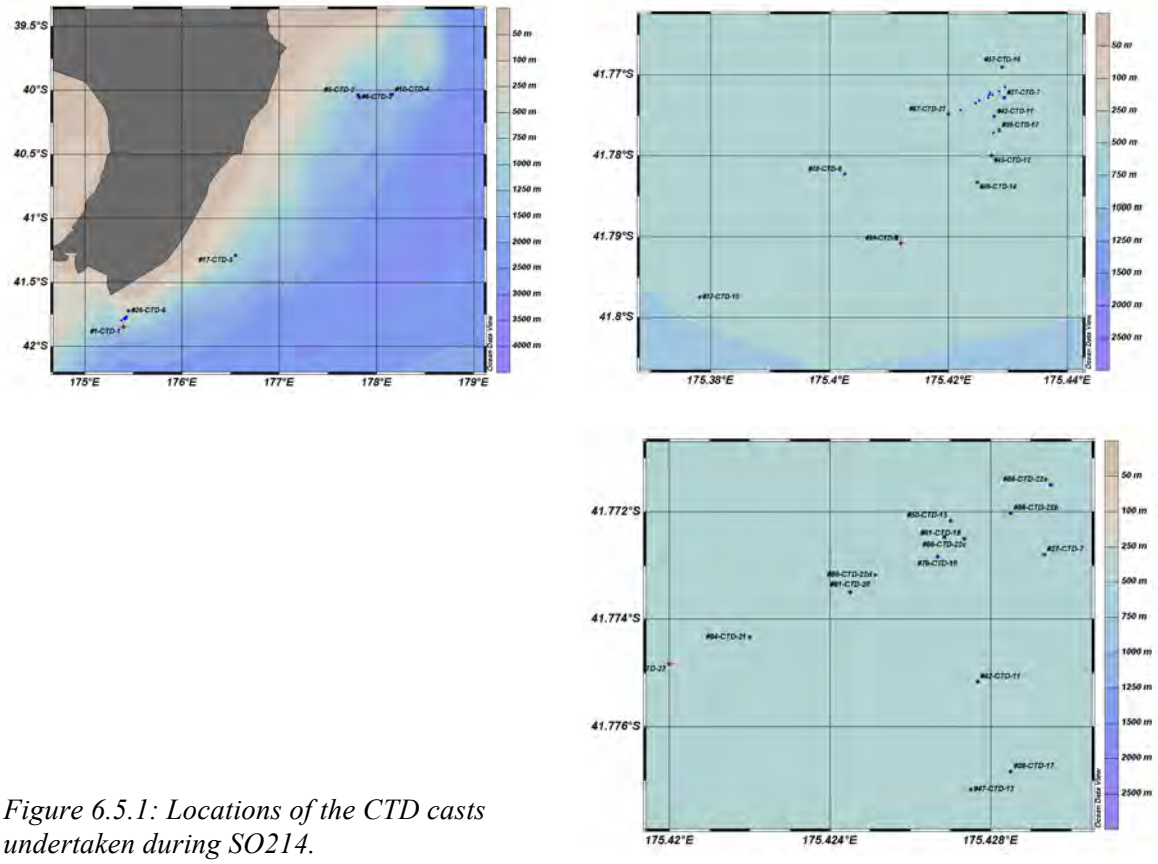

Figure 6.5.1: Locations of the CTD casts undertaken during SO214.

6.5.1 Opouawe Bank

During Leg 2 we performed 13 CTD casts at the Takahe seep site to create a north-south and an east-west transect across the site. One of these casts (CTD-22) was a towed CTD across the site from east to west with measurements taken in the 200m above the sea floor. During CTD cast 15, bottle 9 got a cable caught in the lid when it was closing but the calculated CH4 appears to follow the trend of the rest of the data and is included in the figures below. During CTD 12, a plug was accidentally left on the temperature and salinity gauge. CH4 calculations were made using salinity data taken from a neighbouring station. During casts 16-23 we attached an Optical Back Scatter (OBS) sensor to the CTD to evaluate the turbidity of the water.

OBS sensor data varied between 0 and 0.2 volts for all but one cast where values as high as 1 volt were observed on the downcast but not on the CTD up cast (Figure 6.5.2). As the CTD and ship had drifted somewhat during the deployment, we assume that this was a highly localized event but were not able to take any samples for analysis.

The buoyancy (Brunt–Väisälä) frequency N2 is shown in Figure 6.5.3 for three stations at the Takahe site one of which showed higher methane concentrations near the sea floor. All sites are weakly stratified below 200m with some instability in the upper layers. CTD cast 14 (taken a couple of days after some severe weather at the beginning of the cruise) shows a stratified upper 50m in comparison to cast 19, which was taken after a further week of calm weather. Both sites show some small local instabilities near the bottom of the water column. The third station (21) occurs a further 2 days later after a change in the salinity profile of the upper few hundred meters and is discussed further below.

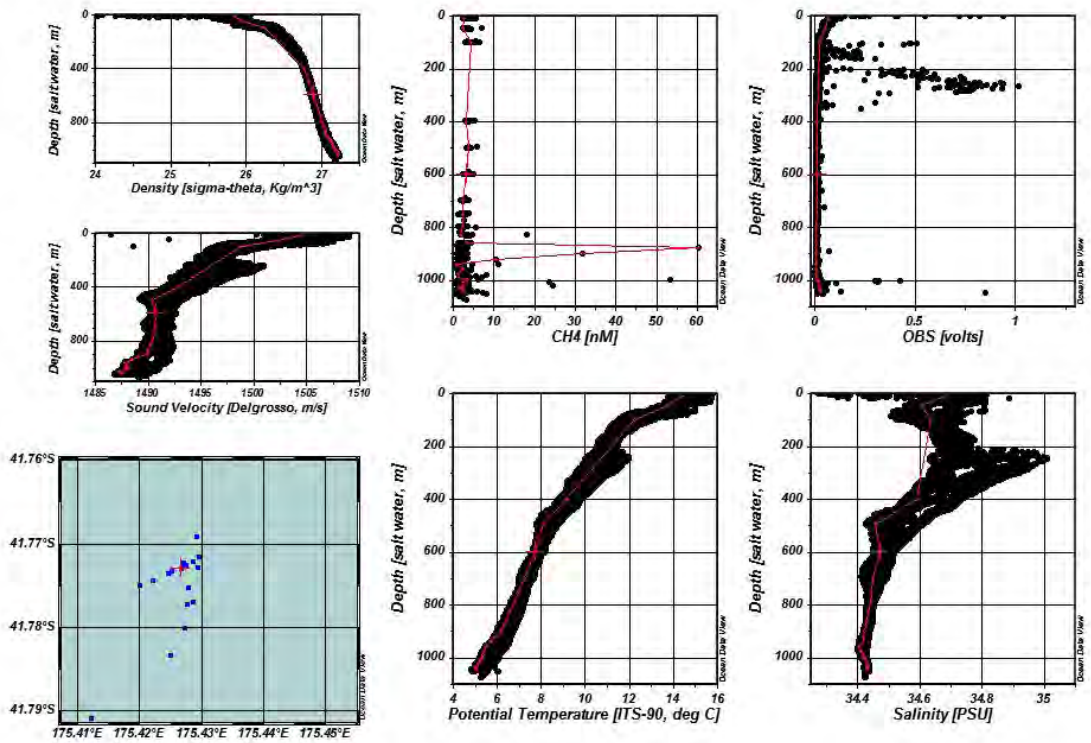

Figure 6.5.2: Stations and data from the Takahe site. Bottle measurements for station 19 are in red.

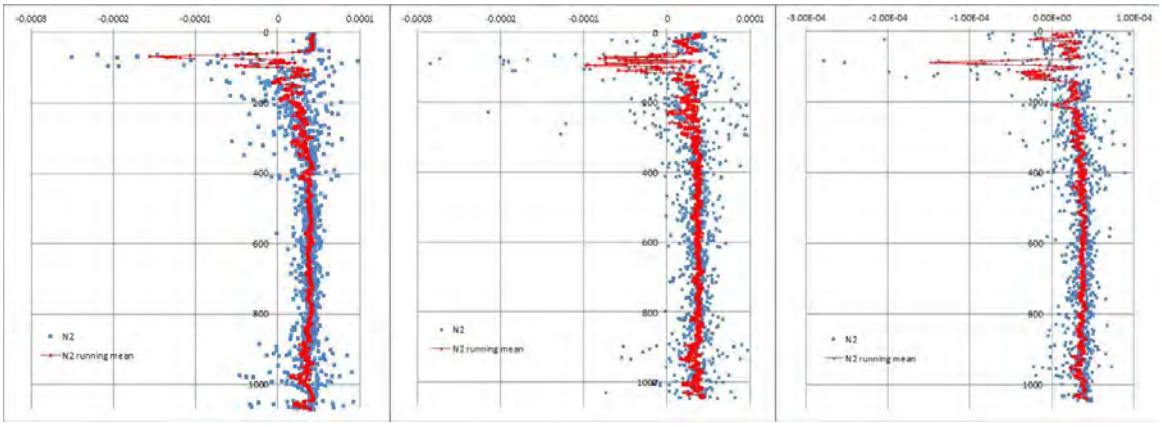

Figure 6.5.3: N2 calculated for stations 14, 19 and 21. Blue points show the N2 values calculated every meter. Red points show the running mean over 9 m. All stations are weakly stable below 200m with some instability in the upper layers (see Appendix for equation)

The physical properties were quite consistent up to the 13th of April when the upper 200 m showed a marked decrease in salinity and the depths 200 m – 400 m, showed a similar increase. We are still evaluating what could have caused this change but it may be linked to significant swell from a storm to the south of our research area around this time. Looking at N2 in Figure 6.5.3 it improves the stability of the water column below 200 m but decreases it in the upper 100 m as the salinity has a greater effect on the density gradient.

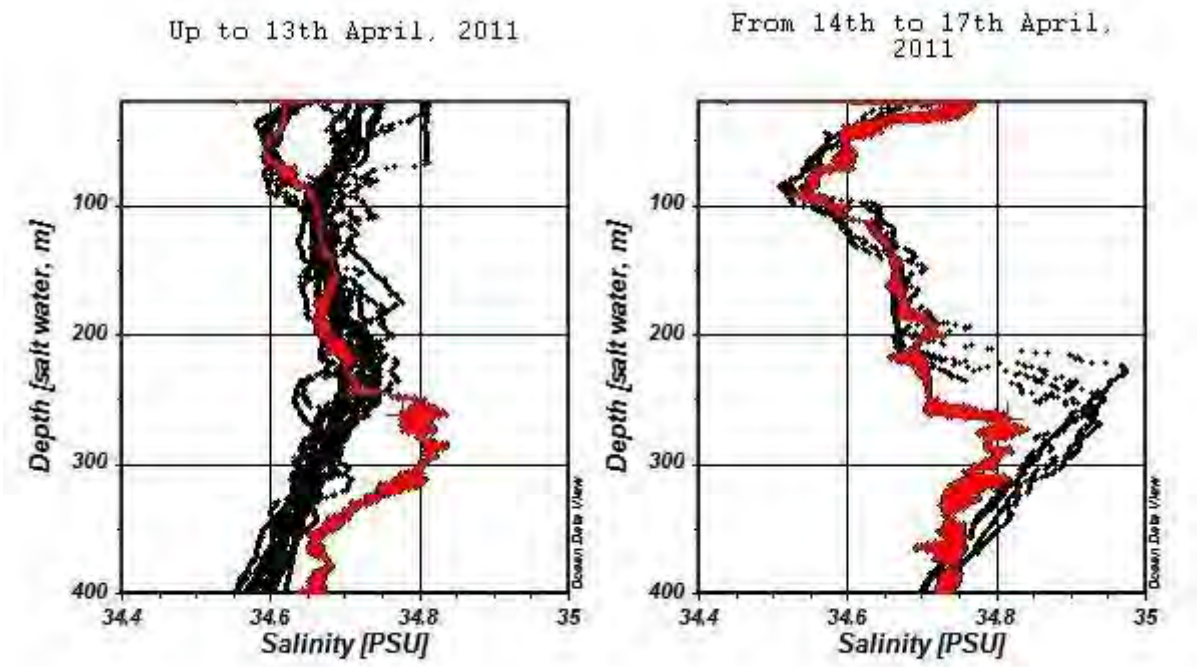

Figure 6.5.4: CTD salinity data in the upper 200m at the Takahe site before and after the 13th of April.

Rather surprising where the results from the two sections crossing the Takahe seep site. Despite a rather prominent flare seen in the Parasound data, the methane concentrations where very low for a seep site. We could not see any significant release from the area during the time of the second leg (Figure 6.5.5).

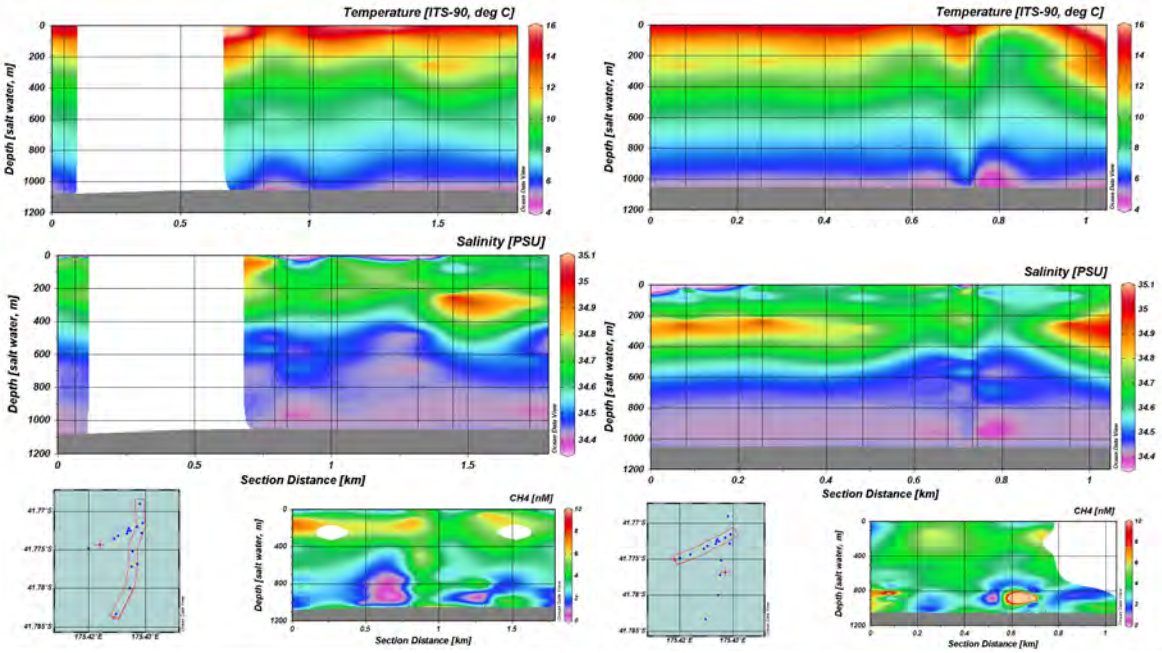

Figure 6.5.5: Sections in S-N direction (left) and W-E direction (right) over the Takahe seep site. The big gap in the salinity and temperature plot in the S-N section is caused by the not correct values of CTD 12.

In contrast to data from Takahe, higher methane concentrations have been measured at North and South Tower with up to 525 nM at South Tower (#36-CTD-9; Figure 6.5.6).

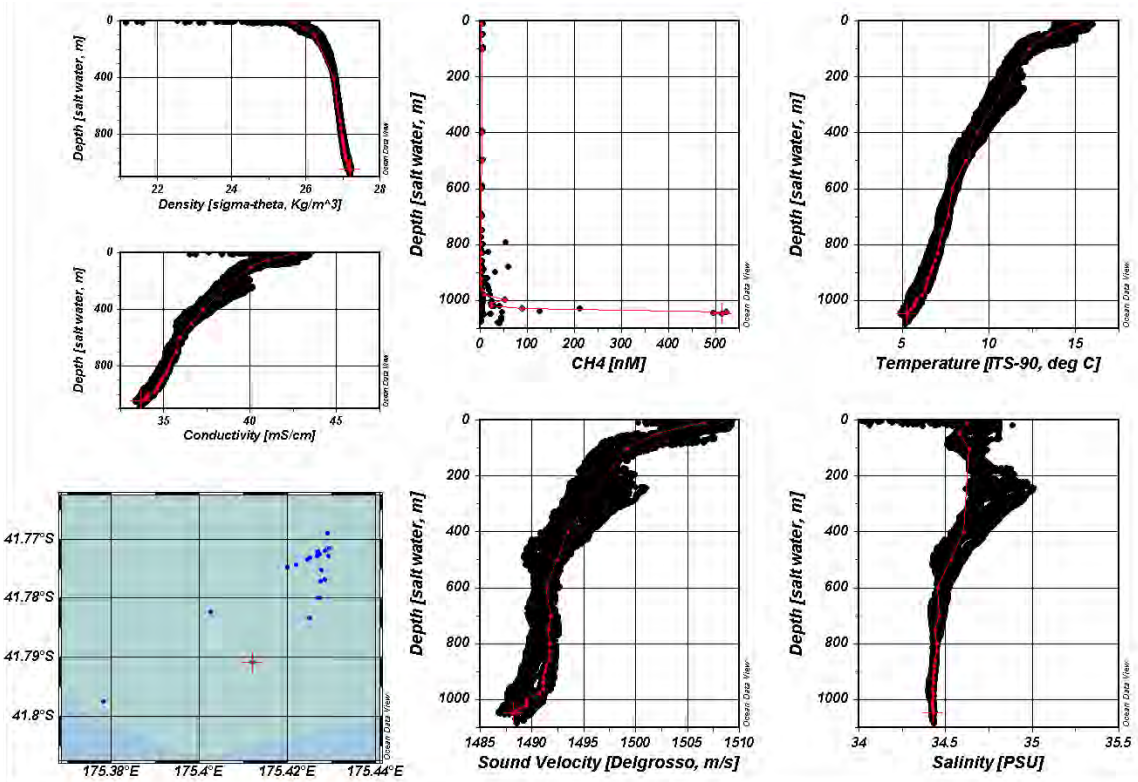

Figure 6.5.6: Data from Opouawe Bank showing the strongly enriched methane concentrations at North and South Tower (red line).

6.5.2 Omakere Ridge

Two CTD casts have been performed at Omakere Ridge during SO214, one at Bears' Paw (#6-CTD-3) and one at Kakapo (#5-CTD-2). All physical parameters are very similar to data from SO191. At Bears Paw very high methane concentrations of up to 625 nM where measured just above the bottom (Figure 6.5.7)

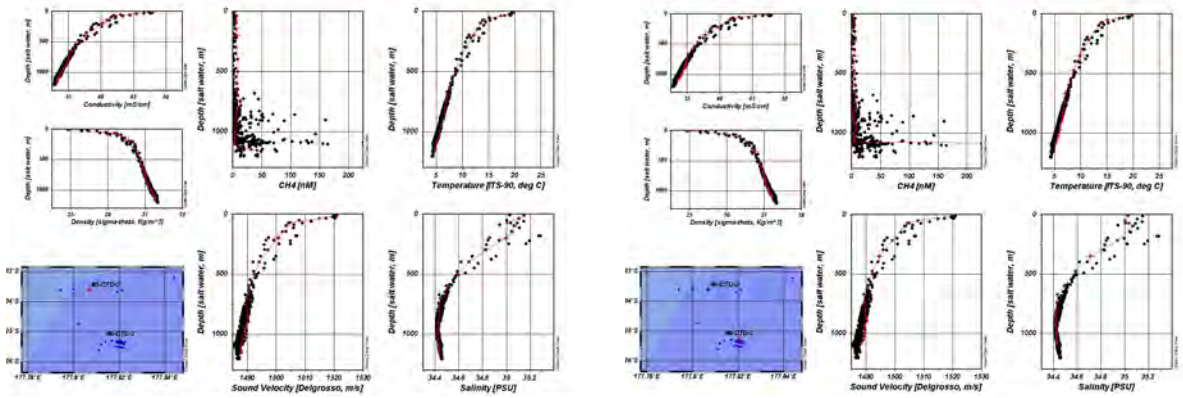

Data from #5-CTD-2 at Kakapo. *Data from #6-CTD-3 at Bears Paw.*

Figure 6.5.7: CTD and methane data from Omakere Ridge.

6.5.2 Rock Garden

We had only one CTD cast at the Faure Site during Leg 1. Physical properties fit very well with previous measurements from the Rock Garden area. The methane concentrations increase 30m above the seafloor to about 45 nM which in a relatively consistent high concentration layer of 35 m thickness.

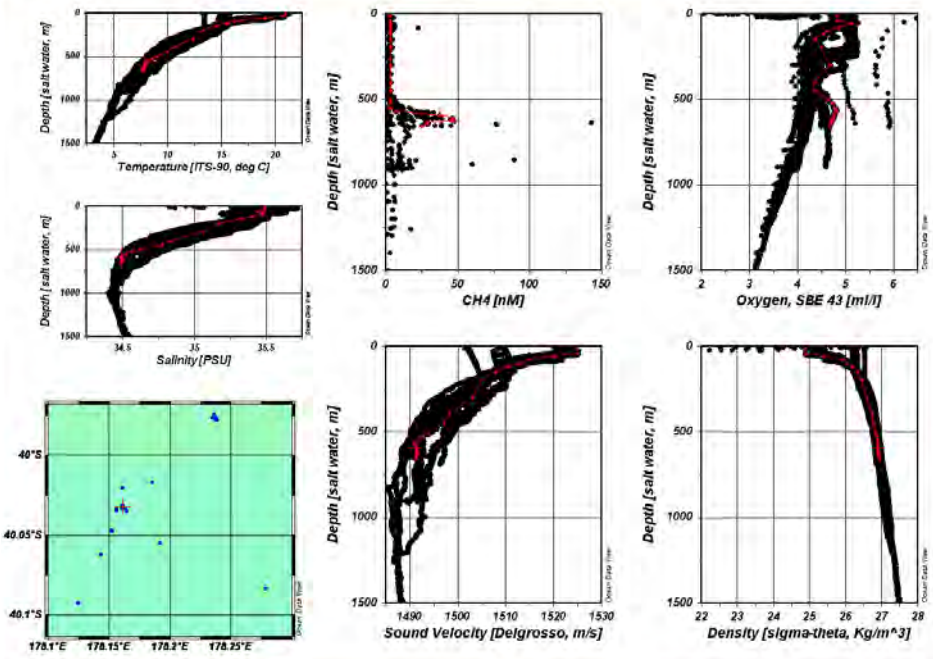

Figure 6.5.8: CTD and methane data from Rock Garden. In red the data from station #10-CTD-4 from SO214.

6.6 Ofos

David Bowden

6.6.1 Wairarapa

Six OFOS transects were completed across SSS targets on Opouawe Bank: one at North Tower; two at Takahe; one at Korora, and two at Piwakawaka (Table 6.6.1.1). A seventh short transect was recorded across sediments at the southeastern extremity of North Tower (OFOS-7) but this was primarily a camera test. OFOS was also deployed to search for a CSEM instrument lost on the seabed near South Tower (OFOS-8) but this covered a very small area of muddy sediments outside of the seep site and is not reported here. Characteristic seep-associated substrates and fauna were observed at all of the putative sites studied except for Korora, which consisted of high-relief (>1 m high), smoothly rounded rock outcrops with no chemosynthetic fauna.

Initial comparisons between towed camera observations from previous voyages (TAN0616, SO191-2) indicated inaccuracies in the geo-referencing of the SSS images from SO214-1. Because direct observation of seabed features using a USBL tracked camera system is a reliable means for geo-referencing, the main SSS image for the Opouawe Bank seep sites was re-referenced such that observations of hard substrates in video transects from the earlier voyages matched the distribution of strong backscatter in the SSS image. Re-referencing was based on North Tower, as this is the site with the greatest camera coverage, and all subsequent OFOS transects at sites covered by this SSS image (i.e. North Tower, Takahe, and Piwakawaka) corresponded closely with areas of high backscatter.

Station	OFOS	Site	Distance (m)	Duration (hh:mm:ss)	Still images	Video quality	Comments
41	OFOS-1	North Tower	2 500	01:11:27	135	SD	No strobe lighting HD out of focus
64	OFOS-2	Takahe	739	00:47:00	209	HD	5 video files
65	OFOS-3	Takahe	1 080	01:13:50	299	HD	9 video files
69	OFOS-4	Korora	1 046	00:49:36	211	HD	10 video files
70	OFOS-5	Piwakawaka	1 124	00:39:09	163	SD	HD out of focus
71	OFOS-6	Piwakawaka	748	00:30:16	125	SD	HD out of focus
73	OFOS-7	North Tower	357	00:14:33	59	HD	Dirt on video lens

Table 6.6.1.1. OFOS towed camera transects: seabed distance covered, duration of recorded seabed video, number of still photographs, video quality (SD, standard definition in .vob format; HD, high definition 1080 50i digital in .MTS format [MTS = MPEG transport stream]), and comments

#41-OFOS-1

Location: North Tower seep site, Opouawe Bank

Tow direction: North to South

North Tower is associated with a strong and persistent water column flare and shows as two regions of moderate to high backscatter in the sss image: a larger, eastern region with high backscatter, and a less well-defined region of moderate backscatter to the west (Figure 6.6.1.2). The two regions combined cover an area of ca. 52,000 m^2, of which the main, eastern, area constitutes ca. 28,500 m^2. OFOS-1 crossed the eastern side of the main part of

North Tower (Figure 6.6.1.2). Substrates within the high backscatter region consisted of large authigenic carbonate blocks and continuous chemoherm reef structure interspersed by fine muddy sediments which were often rich in sulphides, as indicated by black colouring. Carbonates were associated with populations of the large siboglinid tubeworm *Lamellibrachia* sp., whereas sulphidic sediment areas were associated with shells and live individuals of the vesicomyid clam, *Calyptogena* sp. and bacterial mats (Figure 6.6.1.3). Most observations of clams were of dead shells on the sediment surface, but smaller numbers of live clams could be seen partially buried in the sulphidic patches. The white, seep-associated demosponge, *Pseudosuberites* sp., was locally abundant on carbonate rocks.

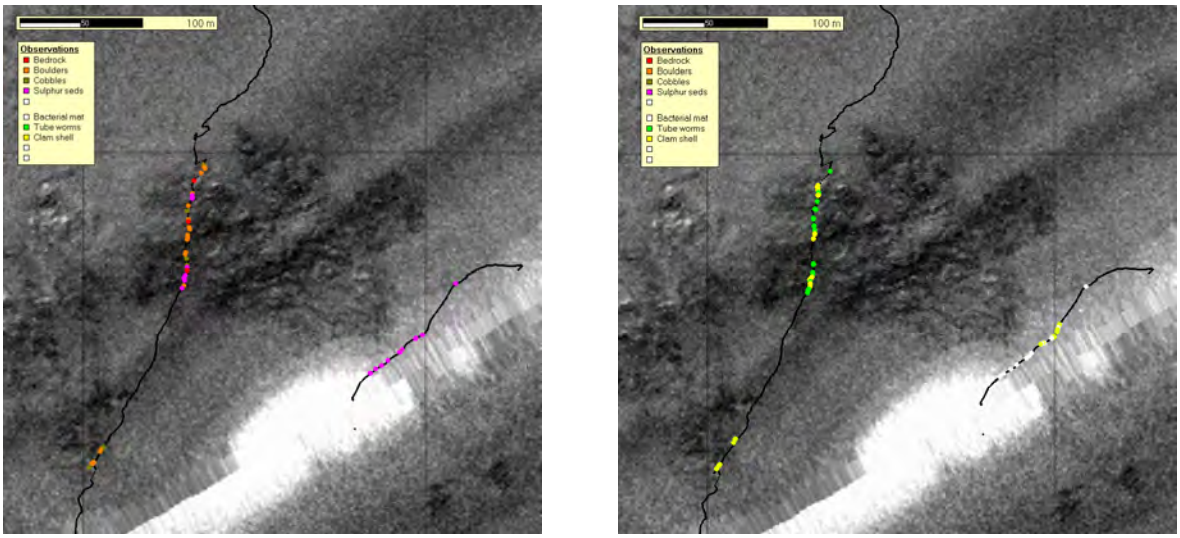

Figure 6.6.1.2. North Tower seep, showing the tracks of OFOS-1 (left) and OFOS-7 (right) against sidescan sonar image. Top: seep-related substrates, with 'Bedrock', 'Boulders', and 'Cobbles' denoting different size ranges of authigenic carbonate blocks. Substrate in all other sections of the tracks is muddy sediment. Bottom: occurrence of seep-associated megafauna.

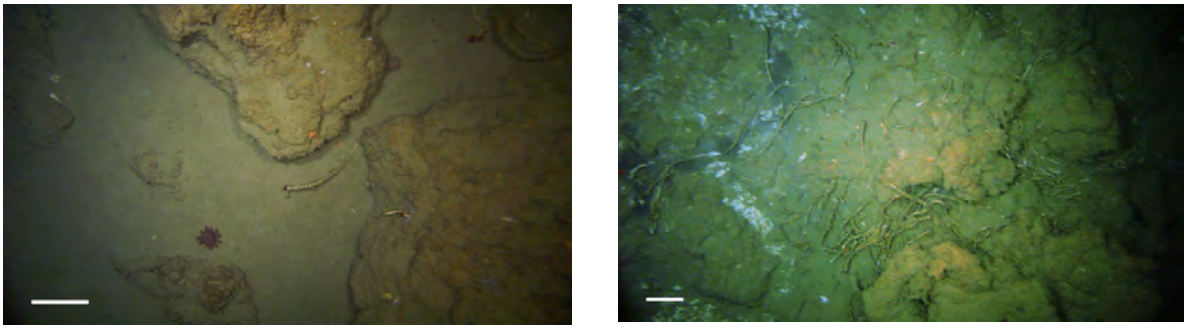

Figure 6.6.1.3. OFOS-1, North Tower seep. Top: authigenic carbonate boulders and muddy sediment substrata with Lamellibrachia sp. siboglinid tube worms and a zooanthid-pagurid association (star-shaped organism at centre left). Bottom: authigenic carbonate chemoherm (labelled as „bedrock" in video analyses) with sulphidic sediments (dark areas at upper left), Lamellibrachia sp. tube worms, and shells of Calyptogena sp. clams. Scale bars show 20 cm.

#64-OFOS-2 and **#65-OFOS-3**
Location: Takahe seep site, Opouawe Bank
Tow direction: South to North

Takahe seep is associated with a water column flare and shows in the SSS image as an area of backscatter only weakly differentiated from surrounding sediments (Figure 6.6.1.4). The region of elevated backscatter covers a seabed area of ca. 130,000 m^2, with stronger backscatter in the northern sector. OFOS-2 and OFOS-3 were run from South to North across the northern part of the area of stronger backscatter. The only seabed signs of seepage visible

in the transects were areas of weakly-defined sulphidic sediments which were associated with well-developed bacterial mats (Figure 6.6.1.5), and a few *Calyptogena* sp. Clam shells at the outer edges of the seep area (Figure 6.6.1.6). Sulphidic sediment patches showed the characteristic ‚raindrop' pattern indicative of the presence of ampharetid polychaetes, but these were much less pronounced than has been recorded at other sites during previous voyages (Sommer et al. 2007)

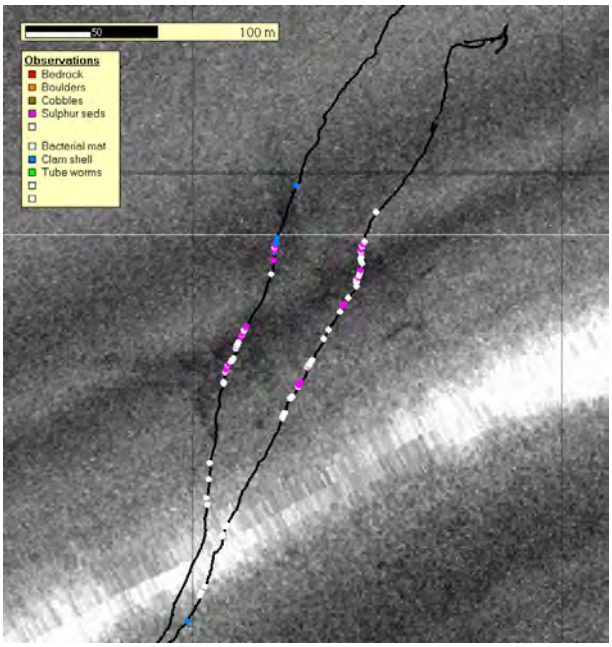

Figure 6.6.1.4: Takahe seep, showing the tracks of OFOS-2 (left) and OFOS-3 (right). Seep-related observations are colour-coded: sulphidic sediments; bacterial mats, and clam shells (see legend). Background substrata were muddy sediments throughout, and no carbonates were observed. All seep-associated observations are shown, including fauna.

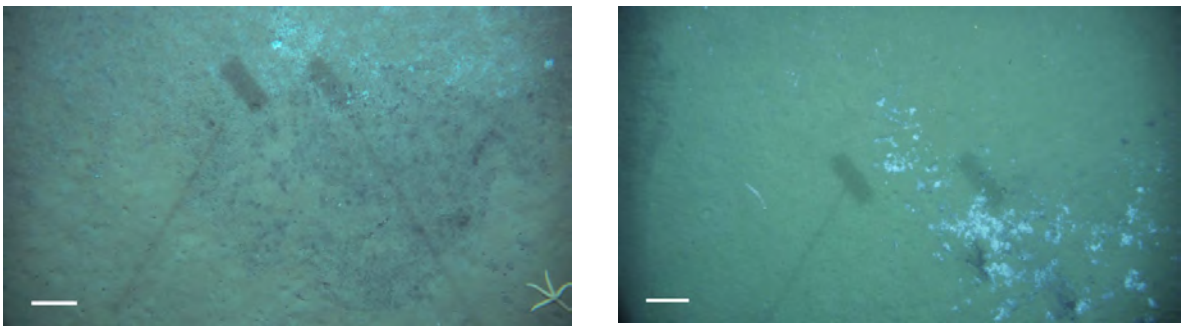

Figure 6.6.1.5: Takahe seep, OFOS-2 and OFOS-3. Sulphidic sediments (dark areas) and bacterial patches (light areas) on muddy substrata. Scale bars show 20 cm.

#69-OFOS-4
Location: Korora
Tow direction: South to North

Korora shows as an area of very strong backscatter and acoustic shadow in the sss image (Figure 6.6.1.6), indicating high relief rock outcrops, but is not associated with a water-column flare. A single transect, OFOS-4, running SW to NE across the sss target showed steep, rounded, rock formations which had none of the characteristics of authigenic carbonates seen at active seeps sites elsewhere on the Hikurangi Margin. Rocks were covered in a layer of fine sediments, and there were noticeably greater quantities of suspended material in the water column than at the other sites (Figure 6.6.1.6). Benthic fauna were sparse

on the southern side of the rock outcrop, but to the north, the regular echinoid *Gracilechinus multidentatus* was recorded at densities of up to ca. 8 inds m^{-2}.

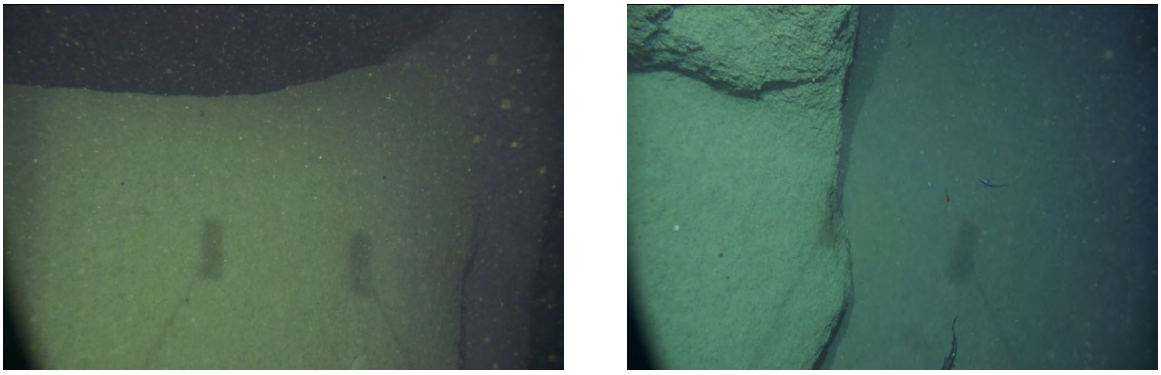

Figure 6.6.1.6: Korora, OFOS-4; high-relief rock formations. Note the high concentrations of suspended particulate matter.

#70-OFOS-5
Location: Piwakawaka
Tow direction: East to West

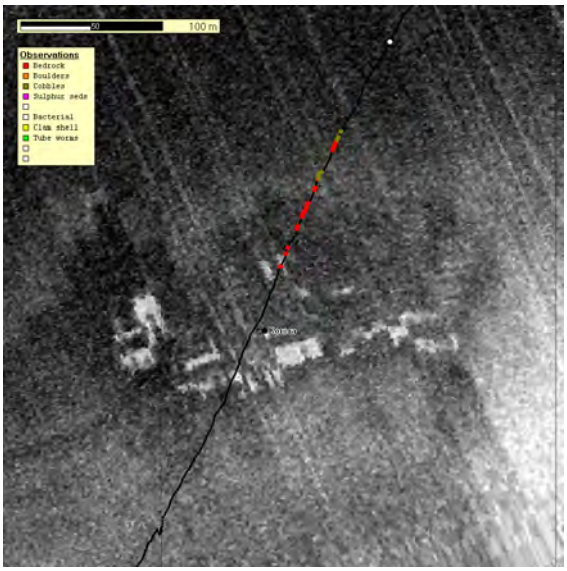

Figure 6.6.1.7: Korora site, OFOS-5. No seep-related substrates or fauna were observed at this site. Note, the geo-referencing of either the sidescan sonar image or the OFOS track is evidently incorrect because the high-relief substrate indicated by strong backscatter in the sonar image should coincide with the observations of bedrock outcrops from the OFOS video.

#71-OFOS-6
Location: Piwakawaka
Tow direction: North to South

Piwakawaka seep is associated with a strong, persistent, water column flare and shows in the sss image as a region of stronger backscatter covering a seabed area of ca. 23,000 m^2. The two transects across the site, OFOS-5 and OFOS-6 (Figure 8), revealed well-developed authigenic carbonate chemoherm interspersed by carbonate blocks embedded in muddy, sulphidic, sediments. The site was similar in physical and biological character to North Tower. Substrates within the high backscatter region consisted of large authigenic carbonate blocks and continuous chemoherm reef areas interspersed by fine muddy sediments with many well-defined dark sulphidic patches. Close inspection of these patches in the high-resolution still images indicated that they are likely to have dense populations of ampharetid polychaetes. Carbonate block and chemoherm areas were associated with *Lamellibrachia* sp. tubeworms, and sulphidic sediment areas were associated with *Calyptogena* sp. clams (Figure

8 and Figure 9). Most observations of clams were of dead shells on the sediment surface, but smaller numbers of live clams could be seen partially buried in the sulphidic patches.

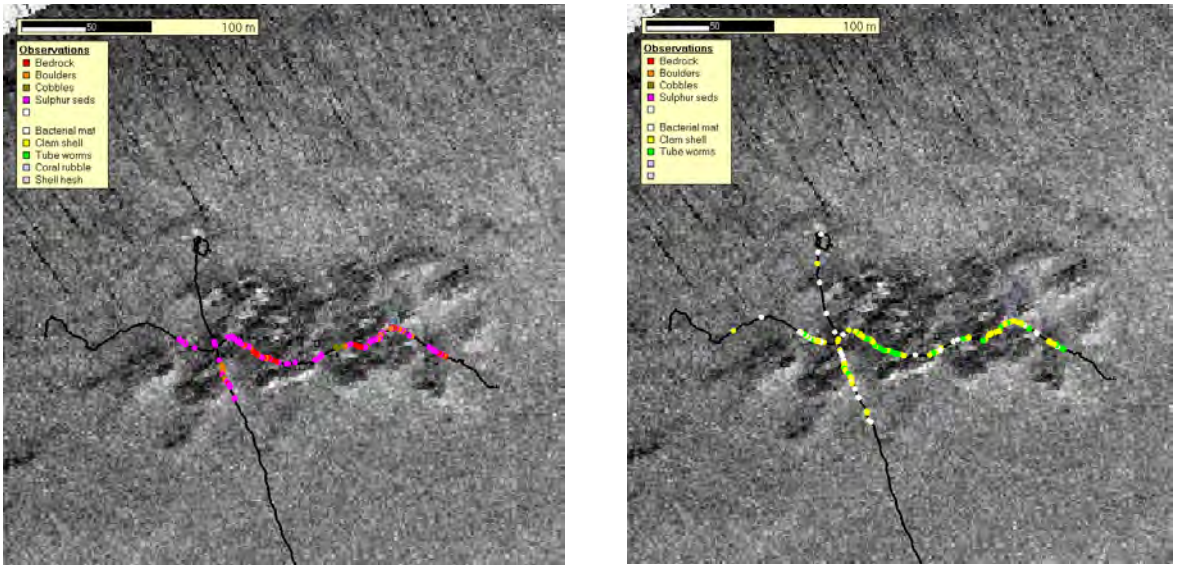

Figure 6.6.1.8: Piwakawaka, OFOS-5 (E-W) and OFOS-6 (N-S). Top; seep-associated substrates (see text for interpretation), Bottom; seep-associated megafauna.

#73-OFOS-7
Location: North Tower
Tow direction: north-east to south-west

This transect was run across sediments at the south-eastern edge of North Tower, primarily as a camera test. Sediments were mostly of uniform, non-seep, mud with numerous burrows, but several patches of dark sulphidic sediment were recorded in the latter half of the transect.

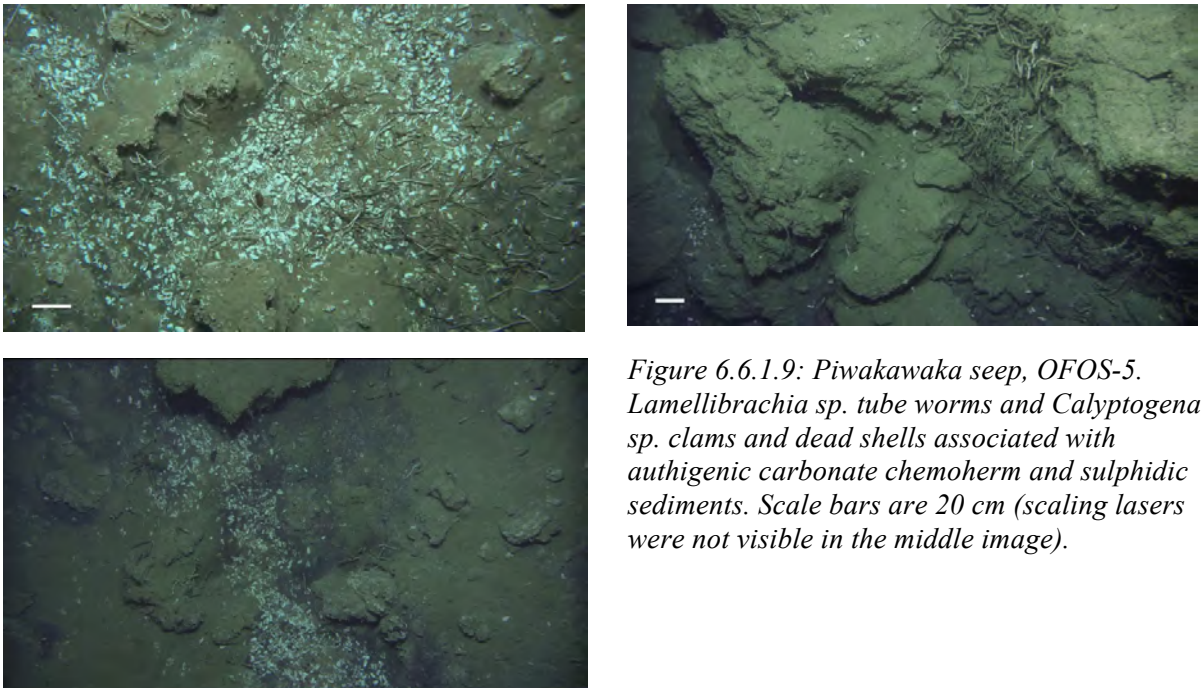

Figure 6.6.1.9: Piwakawaka seep, OFOS-5. Lamellibrachia sp. tube worms and Calyptogena sp. clams and dead shells associated with authigenic carbonate chemoherm and sulphidic sediments. Scale bars are 20 cm (scaling lasers were not visible in the middle image).

#89-OFOS-8 and #90-OFOS-9
Location: west of South Tower
Tow direction: variable

These OFOS deployments were attempts to recover CSEM gear lost on the seabed in the vicinity of South Tower. The seabed area coved by both was small and no seep-associated substrates or fauna were seen.

#94-OFOS-10
Location: Moa
Tow direction: north-east to south-west

OFOS-10 crossed the south-western extremity of Moa, to the west of transects completed across the main high relief of the feature during SO191. The SSS backscatter at this part of Moa has characteristics similar to those at Bear's Paw at the north-eastern extremity of Moa. Background sediments were of well-oxygenated muddy sediments with burrows and other bioturbation marks. Authigenic carbonates were observed throughout the transit of the high backscatter section of the transect, and chemoherm areas with abundant seep-associated megafauna and elevations of ca. 1-2 m were present throughout. *Lamellibrachia* sp. Tube worms and *Calyptogena* sp. Clams and shells were seen wherever carbonate rocks and sulphidic sediments occurred, but the site was remarkable for the presence of very high population densities of a species of spherical hexactinellid sponge. This species was recorded during TAN0616 from the LM9 seep site, but in lower numbers, and has not been noted at any of the other main seep sites on the Hikurangi Margin.

[The USBL position was unreliable during OFOS-10; the deployment map figure will follow once the navigation file has been re-constructed]

6.7 Biology

Andrew R. Thurber

Direct biological sampling was undertaken to identify NZ's seep biodiversity and to quantify the functional link between the metazoan (multicellular) and microbial fauna within seep sediments. A total of 7 video-guided multicore deployments were made, 5 recovering samples with a newly-adapted video guidance system provided by NIOZ. The multiple corer used was an Ocean Instruments model leant by NIWA Wellington, which use a 9.8cm internal diameter liners. Three of the samples were of microbial mats at Takahe seep area with one in located in the sulfidic sediment patches (ampharetid beds) at Bear's Paw. Each of the successful deployments was used for a variety of chemical and biological analysis as detailed below (Table 6.7.1).

Macrofaunal community analysis – One core from each successful deployment was preserved for quantitative description of the macrofaunal community. Macrofauna is defined by those species, which are retained on a 0.3 mm mesh. After vertically sectioning in 0-1, 1-2, 2-3, 3-5, 5-10, and 10-20 cm fractions, cores were preserved in 10% buffered formaldehyde. These cores will have the macrofauna identified to the species level, enumerated, and biomassed upon return to Florida International University. Species, which are new to science, will be returned to New Zealand for description and storage at the NIWA Benthic Invertebrate Collections. In addition to these preserved cores, 37 putative species identified while at sea had their photos taken (Figure 6.7.1) and vouchers collected in both formalin (for morphological analysis) and ethanol (molecular analysis) allowing complete species descriptions of those novel fauna discovered.

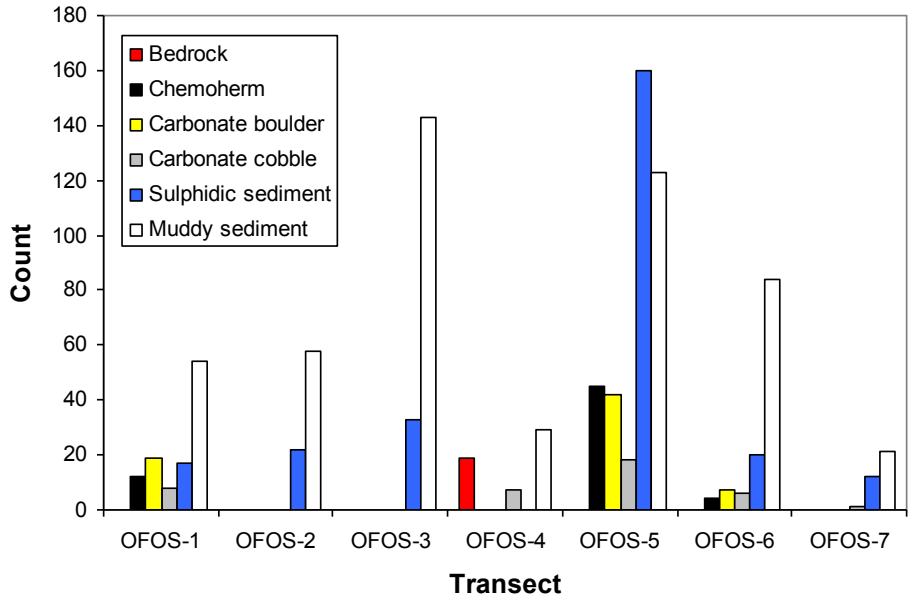

Figure 6.6.1.10. OFOS: summary of real-time substrate observations from seabed video. Values are counts of individual observations summed from the time of the first seep-related observation (i.e. either the substrates shown here, or fauna shown in Fig. 11) to the last such observation, and thus indicate the relative composition of substrates between transects. Interpretations are as follows: Bedrock, apparently non-carbonate rock fills the entire image frame; Chemoherm; authigenic carbonate rock fills the entire image frame; Carbonate boulder, carbonate blocks >ca. 25 cm embedded in soft sediments; Carbonate cobble, carbonate blocks >ca. 25 cm embedded in soft sediments; Sulphidic sediment, black muddy sediment; Muddy sediment, background muddy sediments.

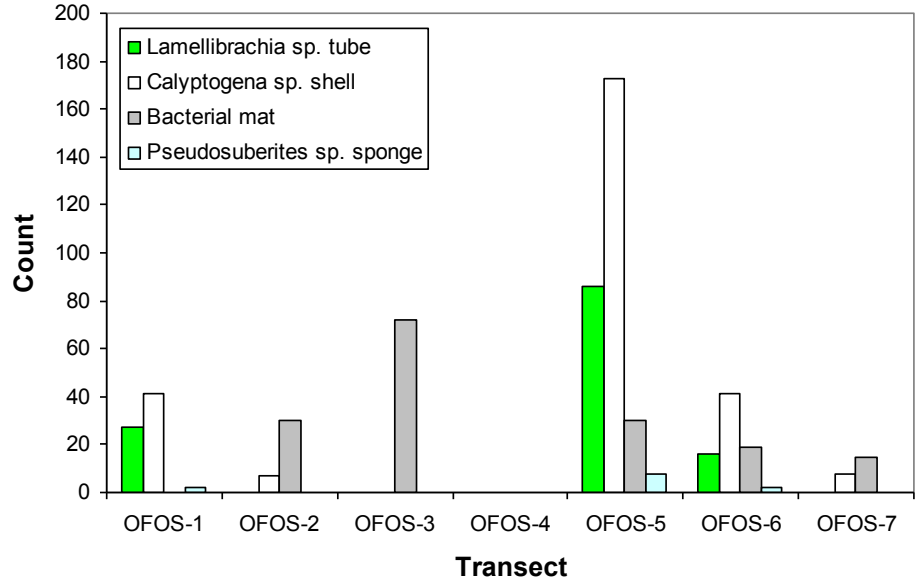

Figure 6.6.1.11: OFOS: summary of real-time observations of conspicuous seep-associated benthic megafauna from seabed video. Values are counts of individual observations summed from the time of the first seep-related observation (see Figure 10 above). Counts are indicative only of relative abundances in each transect. Accurate population densities can only be derived from post-voyage analysis of the recorded HD video and still images.

Stat	MUC	Location	Habitat	Latitude	Longitude	Fate
43	1	Takahe	Microbial Mat	41° 46.314' S	175° 25.735'E	Macro, Sed, Trophic, Enrich, Taxon
44	2	Takahe	Control	41° 46.329' S	175° 25.739'E	Enrich, Su, Foram
66	3	Takahe	Microbial Mat	41° 46.314' S	175° 25.682'E	Macro, Sed, Trophic, Enrich, Taxon, Foram, Su
67	4	Takahe	Microbial Mat	41° 46.307' S	175° 25.682'E	Macro, Sed, Trophic, Enrich, Taxon, Foram, Su
72	6	Wairarapa N. Tower	No sample	41° 46.925' S	175° 24.152'E	No suitable habitat was found.
95	7	Bear's Paw	Amphareti d bed	40° 3.218' S	177° 49.144'E	Macro, Sed, Trophic, Taxon, Foram, Su

Table 6.7.1 Multicore stations and numbers during Sonne cruise SO214 and the fate of the samples collected. Macro = Sediment preserved for community analysis (abundance, biomass, community composition); Trophic = Sample for fatty acid and isotopic analysis; Sed = Fatty acid analysis of microbial community; Meio = meiofaunal community analysis; Foram = Foraminiferal analysis; Enrich = food web analysis using ^{13}C bicarbonate and ^{15}N Ammonium enrichments; Su = Anoxic sulphide analysis; Taxon= voucher specimen collection for taxonomic work. Core 5 is discussed in the Foraminiferal section of this report.

Sediment Analysis – To characterize the available food sources for the macrofaunal community, a core was vertically sliced at 1cm intervals and frozen at -80°C. These sediment sections will be used to extract the lipids present within the sediment which is a means to identify the microbial community and can later be coupled to molecular identification of the bacteria and Archaea present within the sediment. Through these analyses we will also be able to identify the dominant microbial processes within the sediment and how their vertical range overlaps with the vertical distribution of the fauna.

Macrofaunal Trophic Analysis - Trophic linkages (i.e. the diet of consumers) can be a driving factor in ecosystem function. Methane seeps provide an area where the active producers are also those species, which consume methane, thus the trophic connection between animals, which consume these species, may impact the biogeochemical cycling within the sediment. To identify these trophic linkages a variety of diet analyses will be undertaken of the fauna present. Fauna from cores were sorted live at sea, identified to putative species and either preserved for stable isotopic analysis or FA analysis. Stable isotopic analysis or the relative ration of carbon 12 to carbon 13 is a powerful way to identify the relative role of methane in the diet of a species. This is possible due to extreme selectivity of the enzymes responsible for methanogenesis by Archaea. As most of the methane present within the New Zealand margin is the result of archaeal methanogenesis, this provides an easy way to identify if a species is eating methanotrophic microbial biomass (either aerobic or anaerobic). Both of these methanotrophic microbial metabolisms form the sediment filter and understanding those forces, which act upon those, is a key question of this work as it has direct relevance to the magnitude of methane emission from the sediment. Individuals of every species present with the cores had a portion (approximately 0.2 mg) of tissue removed and put in pre-weighed tin boats for later analysis on an Isotope-ratio mass spectrometer. By combining the biomass of the samples as measured during the macrofaunal community analysis and an isotopic mixing model, an estimate of the amount of methane used on a per m^{-2} basis can be estimated. A total of 193 samples were taken during this cruise for isotopic analysis belonging to 36 species from these seep habitats.

Fatty acid (FA) analysis is a complimentary method to stable isotopic analysis as it has both get greater resolution of food sources and can identify the relative importance of aerobic vs. anaerobic processes. Fatty acids are key components of bacterial and eukaryotic membranes yet most species can only synthesize a subset of the FAs, which they need for growth and reproduction, the remaining FAs they must get from their diet. As many of the microbial populations, which occur in seep sediments, have diagnostic FAs, through analysing the FA composition of consumers, one can gain a robust measure of a species diet. In this study, abundant species were preserved (through freezing at -80^{o}C) after allowing the species to evacuate their guts in seawater. In all instances representatives of each species were also taken for isotopic analysis thus the two techniques can be combined for a thorough identification of the trophic linkages within seep sediments. Of the 193 isotopic samples collected, 93 were coupled FA and isotopic collections.

Food Web Elucidation through Pulse-Chase Experiments – Stable-isotopic enrichment experiments were conducted to identify which species were consuming active bacteria and which were consuming active chemosynthetic bacteria to corroborate natural biomarker approaches. Sub cores were taken from three of the deployments and injected with $Na_2{}^{13}CO_3$ and $(^{15}NH_4)_2(SO_3)$ starting at the sediment surface and extending 10 cm into the sediment at 2cm intervals. In general active prokaryotes take up ammonium thus the role of active microbes in a food web can be identified by looking for enriched nitrogen in consumers within incubations. These cores were incubated at 4 ^{o}C for 48 and 60 hours. Cores were then sacrificed and half taken for microbial community analysis and the other half sorted live to look at incorporation of the stable isotopic label into the food web. A control core was run to mimic applying oxygenated seawater (n=1) or just the $Na_2{}^{13}CO_3$ (n=1) to control for the likely use of ammonium as an energy source by bacteria within the sediment. To identify the distribution and use of solutes from the overlying water column (i.e. as a proxy for bioirrigation), two subcores were taken and their top water replaced by isotopically labelled seawater or (as a control) non-labelled seawater. After 36 hours incubation, these cores were vertically sectioned and frozen. By comparing the isotopic composition of the bacteria and Archaea within these two cores we can identify the magnitude and importance of bioirrigation within this habitat for microbial processes. These cores were frozen.

6.7.1 Wairarapa

A total of 1,040 animals were identified and sorted into putative species at the Takahe methane seep area. Adding to our knowledge of a "classic" seep habitat, microbial mats, three samples were taken for community analysis (Figure 6.7.1). Although MC 1 resulted in a clear microbial mat, MC 3 and 4 were similar habitats yet covered in a fresh deposition of phytodetritus. Independent of this deposition the macrofaunal community was similar among the cores, largely dominated by spionids polychaetes and abundant cumaceans. Although cumaceans have been long found to be an abundant component of NZ's seep habitats, the ampharetids which are normally more abundant were not as common (e.g. a ratio of 140 cumaceans: 10 ampharetids in MC 1). Thus the microbial mat community is distinct from the ampharetid bed community discovered in 2007 during the Sonne 191 yet only in the distribution of fauna rather than the species: there was a 100% overlap in species present in 2007 in the ampharetid beds and those present in the microbial mats sampled during this expedition. In addition a variety of amphipods were present in many of the habitats, which, like the ampharetid beds, appears to be a unique feature of the New Zealand seeps. Unique among the drops was MC-4, which contained an abundance of orbiniid polychaetes, which were almost as abundant as the ampharetids.

The "control core" which was taken in the vicinity of the seeps but had little in the way sulphide present and was composed of a much more even and diverse community, although with reduced abundance. As no quantitative core was collected from this sampling only the live sorted samples are available to identify the community patterns. Yet the species overlap was very small compared to the seep habitat with only a single species of amphinomid, one amphipod and a total of 5 cumaceans present in the two cores, which had been used, for enrichment experiments. No species made up more than 5 individuals in either of the subcores taken (these are not quantitative). Many of the species collected will add to the museum collections of New Zealand.

6.7.2 Omakere Ridge

A single multiple corer deployment at the Bear's Paw region of Omakere ridge resulted in the only sampling of the ampharetid bed community (Figure 6.7.1). Within the live core 188 specimens were found belonging to 12 species, including the second species of ampharetid, which had heretofore not been found during this cruise. The rough abundance calculation for this core is cf. 25,000 individuals per m2, putting it at the low end for density of ampharetid beds, yet the fauna was very diagnostic of those habitats. As these data are preliminary, based only on the semi-quantitative live sort, the actual abundance (and biomass) will be resolved with processing of the quantitative cores upon careful processing. This core will provide an excellent comparison when studying the relative importance of aerobic methanotrophy vs. anaerobic methanotrophy in ampharetid beds (Bear's paw) vs. microbial mats (Takahe).

6.8 Geochemistry of the Takahe site (Wairarapa)

A. Dale, L. Haffert, E. Hütten

Study site

Pore water geochemical investigations mainly focused on the Takahe site, where gravity core positions were chosen based on Parasound images acquired during SO214 Leg 1. These images showed a clearly defined seismic blanking zone of ca. 230 m in diameter that is likely generated by trapped gas. The acoustic blanking was shallowest (several mbsf) towards the north (Figure 6.8.1C). Another strong, slightly deeper (ca. 15 mbsf) seismic reflector within the same blanking zone was present towards the south of the Takahe seep site (Figure 6.8.1). Most gravity cores were positioned along a transect of Takahe in order to evaluate the spatial extend of the gassy sediments. In the northern part of the area, three further gravity cores were taken, roughly aligned on an east-west transect (Figure 6.8.1A).

Initial on-board geochemical and biological analysis of the sediments strongly indicated the presence of upward flow of methane-rich fluids at Takahe, although further chemical analysis of the samples at the onshore laboratory (IFM-GEOMAR) will be required to corroborate this hypothesis. An additional sediment sampling by MUC was carried at a different site further north (Bear's Paw), which also displayed signs of methane seepage (data not shown).

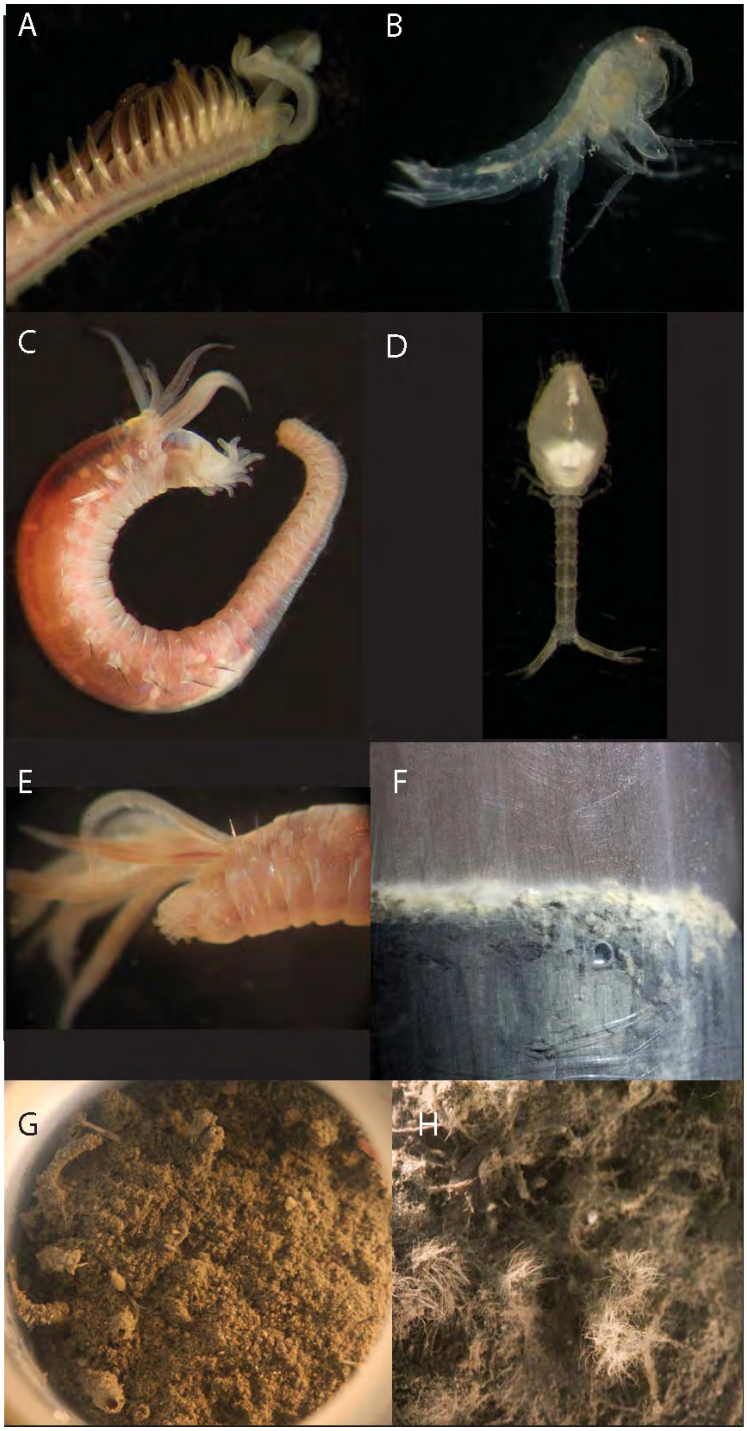

Figure 6.7.1 Summary images of the biology of the Multiple corer deployments: A - The species of spionids polychaete which was abundant in the microbial mat cores collected off of Takahe; B – Amphipods were and abundant component of the fauna present within all MUC samples, including this particular species of Gammerid; C - At the Takahe microbial mats, only this species of ampharetid polychaete was present and not in the same density which is found in the ampharetid bed habitats; D – Cumacean's are sometimes the numerically dominant component of the NZ seep fauna; E - This second species of ampharetid polychaete was only found at the Bear's Paw methane seep habitat and was not present in the microbial mat samples; F – A thick mat of phytodetritus was present on the microbial mats at Takahe for MC 3 and 4; G – a view of the ampharetid bed habitat collected during MUC 7, a layer of phytodetritus was also present on these cores; H – A close up of the microbial mat collected during MUC 1.

Core characteristics

Sediment recovery at the Takahe sites was generally between 2 m and 4.5 m and massive carbonates were absent (with the exception of a carbonate concreted burrow in 91GC13). The cores at all sites are dominated by olive clay-rich sediments occasionally intersected by thin (<1 cm) sandy layers and black smears. Gas hydrate layers, sometimes several cm thick, were discovered in GC 2, 8, 10 and 13 at depth below 125 cm bsf (Figure 6.8.2). Intervals of softer and wetter sediments were indicative of dissociated gas hydrates. Degassing of the sediment upon recovery was a common phenomenon resulting in typical features when the gravity cores were opened, such as cracked sediments, gas exit holes and displacement of sediment within the core.

Pore water profiles

Ammonium and silicate:

On board analytical results agree well with data acquired during SO191 investigating the same area (*Bialas et al., 2007*). Ammonium concentrations at the Takahe seep sites were anomalously low (not exceeding 100 µmol/L) compared to the reference sites (up to 400 µmol/L) (Figure 6.8.3). Down core profiles of ammonium were very variable with local minima and maxima. Interference by sulphide in some cores and a lack of sufficient pore water for ammonium analysis in many instances hindered a more complete description of its behaviour at Takahe. At the reference site, however, ammonium concentrations showed the expected down-core increase characteristic of organic matter mineralization.

Silicate concentrations generally increased with depth in the sediment, although many sites showed a subsurface minimum (~50 cmbsf), which was not observed during, cruise SO191. In some cases (GC10, GC11, GC12) the silicate profiles showed comparatively little variations with depth.

Methane concentration and origin:

Methane concentrations and higher order hydrocarbons (e.g. ethane, propane) were determined on-board from heated (~30 min, 50 °C) 3 mL sediment in a 17.5 ml headspace of air (see chapter 5.5.1 & 6.7). The highest methane concentrations (up to 50 mmol/L, GC8) were found towards the northern margin of the Takahe seep sites, where the surface of the blanking zone approached the seafloor (Figure 6.8.1). A second, slightly lower peak in methane concentrations was found towards the southern margin of the seep site (up to 10 mmol/L, GC13). Immediately beyond the blanking zone, methane concentrations dropped to concentrations below 0.1 mmol/L, which clearly demonstrates the contained localized nature of this seep site.

Based on the ratio methane (C1) to higher order hydrocarbons (C2 and C3) a first estimate of the origin of methane can be made, which will be verified later when carbon isotopic data is available. Towards the centre of the seep sites, the maximum C1/(C2+C3) ratio varied between 2000 and 50000 indicating a dominantly biogenic origin for the bulk of methane present (Figure 6.8.1B and 6.8.4). Towards the margins the ratio dropped below 100, which could be interpreted as an increase in thermogenic methane. However, analytical errors introduced towards the lower end of the methane concentration range could also be responsible for the shift in the ratio.

Sulphide and total alkalinity:

Outside the margins of the seep site (GC5 and GC11), the alkalinity profiles showed a gentle increase with depth, not exceeding 10 mmol/L, while sulphide concentrations were at or close to detection limit (Figure 6.8.5 and 6.8.1B). As is typical for seep sites (GC8, 4, 9 and 13), alkalinity and sulphide increased sharply down core, reaching a maximum around 150 cmbsf. Detailed pore water analysis at the onshore laboratory is expected to show that

sulphate and methane are co-consumed at this depth due to the anaerobic oxidation of methane (AOM, $CH_4 + SO_4^{2-} \rightarrow HS^- + HCO_3^- + H_2O$). Despite the few data available from on-board methane analysis, a decrease of methane at the depth of sulphide and alkalinity maxima can be observed in the profiles (Figure 6.8.5 and 6.8.6).

As for methane, maximum sulphide and alkalinity concentrations also showed a bimodal distribution with maxima towards the margin of the seep site (Figure 6.8.1B). It should be noted that, unlike for methane, the highest peak for sulphide and alkalinity was towards the southern margin with concentrations of up to 15 mmol/L and 40 mmol/L, respectively.

The fact that the highest concentrations of sulphide and methane occurred towards the margins rather than the centre of the seep site suggests that during the course of the seep site evolution, processes such as gas hydrate formation has possibly reduced the sedimentary porosity to such an extent that alternative escape paths for methane were favoured.

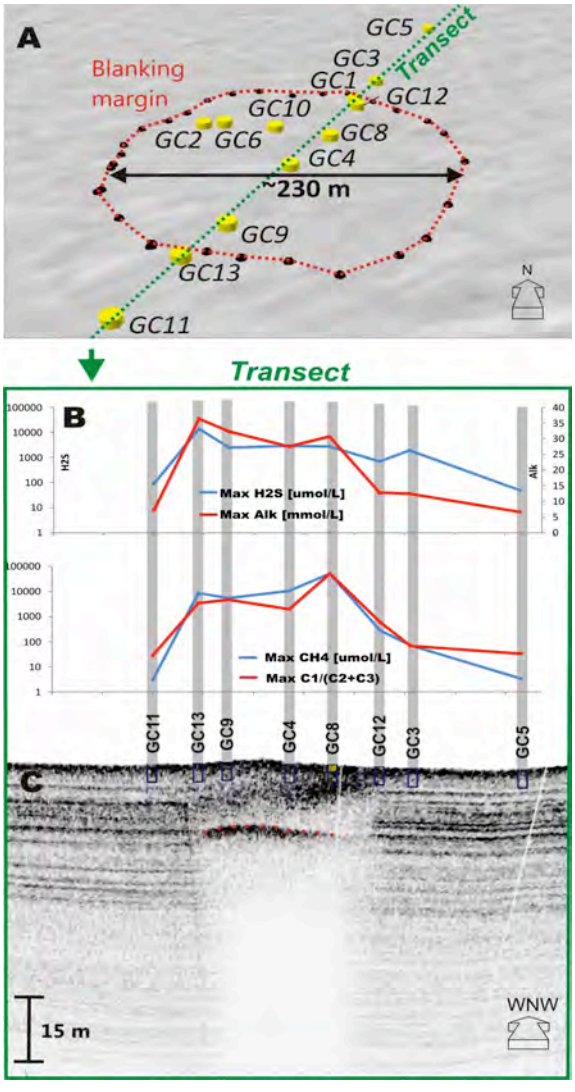

Figure 6.8.1 ***A****: Locations of the gravity cores taken at the Takahe seep site plotted on a topographic map. The extent of seismic blanking observed in Parasound data is outlined (dotted red line).* ***B****: Maximum values of CH_4 (µmol/L), H_2S (µM) TA (mmol/L) and the C1/(C2+C3) ratio versus distance along the transect.* ***C****: Seismic image acquired from Parasound data along the transect showing gravity core locations, the blanking zone and the top of the gas layer (red dots).*

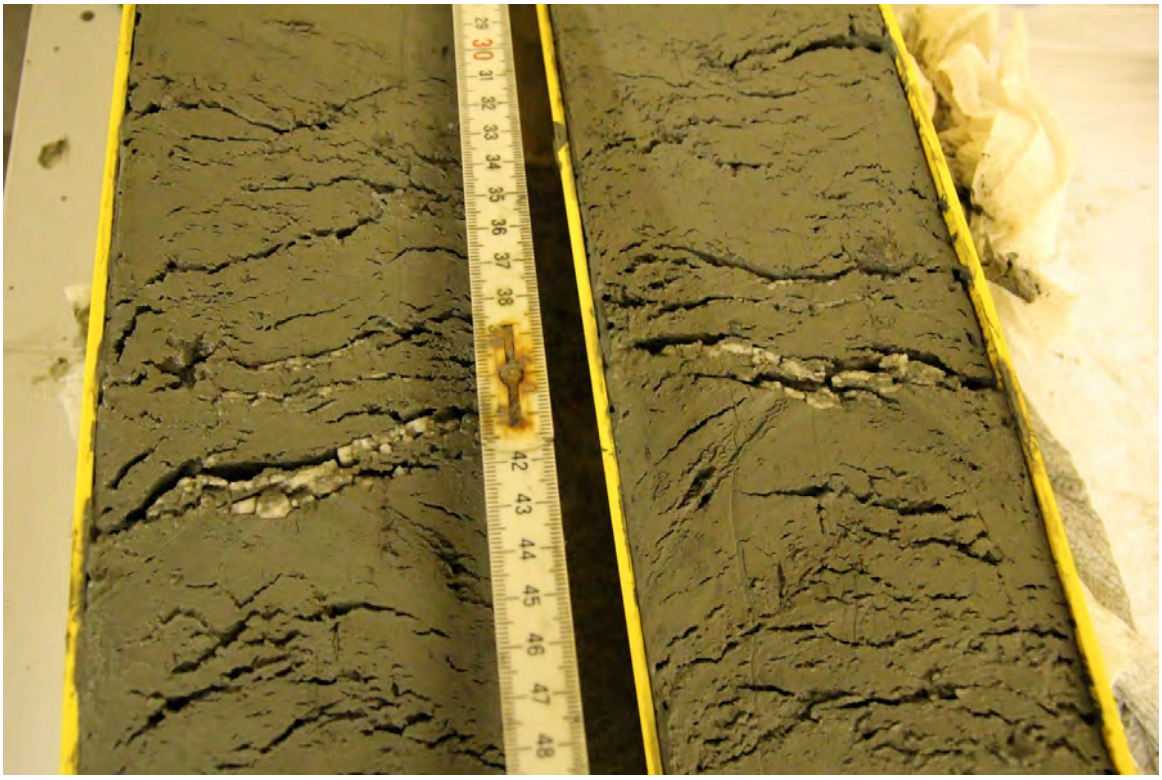

Figure 6.8.2: Photograph of the typical occurrence of gas hydrates at the Takahe sites (scale bar)

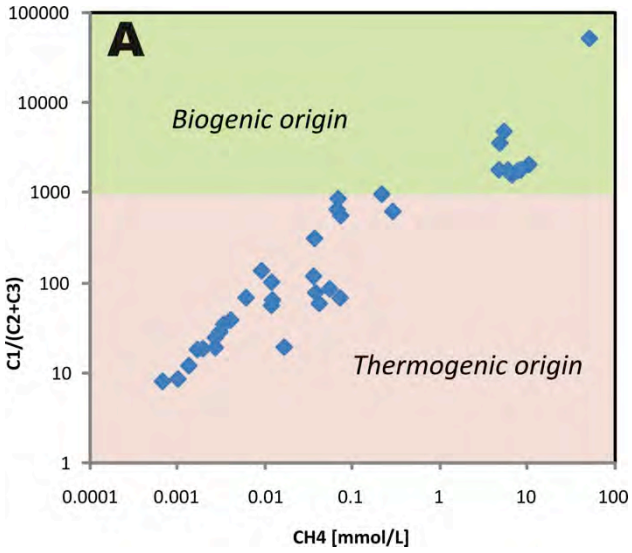

Figure 6.8.4: The ratio methane (C1) to higher order hydrocarbons (C2 and C3) versus methane concentrations in pore water (mmol/L).

6.9 Gravity cores

Henk de Haas and Henko de Stigter

A total of 13 gravity cores were taken during cruise SO-214 leg 2. The distribution of core locations was chosen to provide a profile from background sedimentation into the alternated seep site area of Takahe (Table 6.9.1, Fig. 6.9.2).

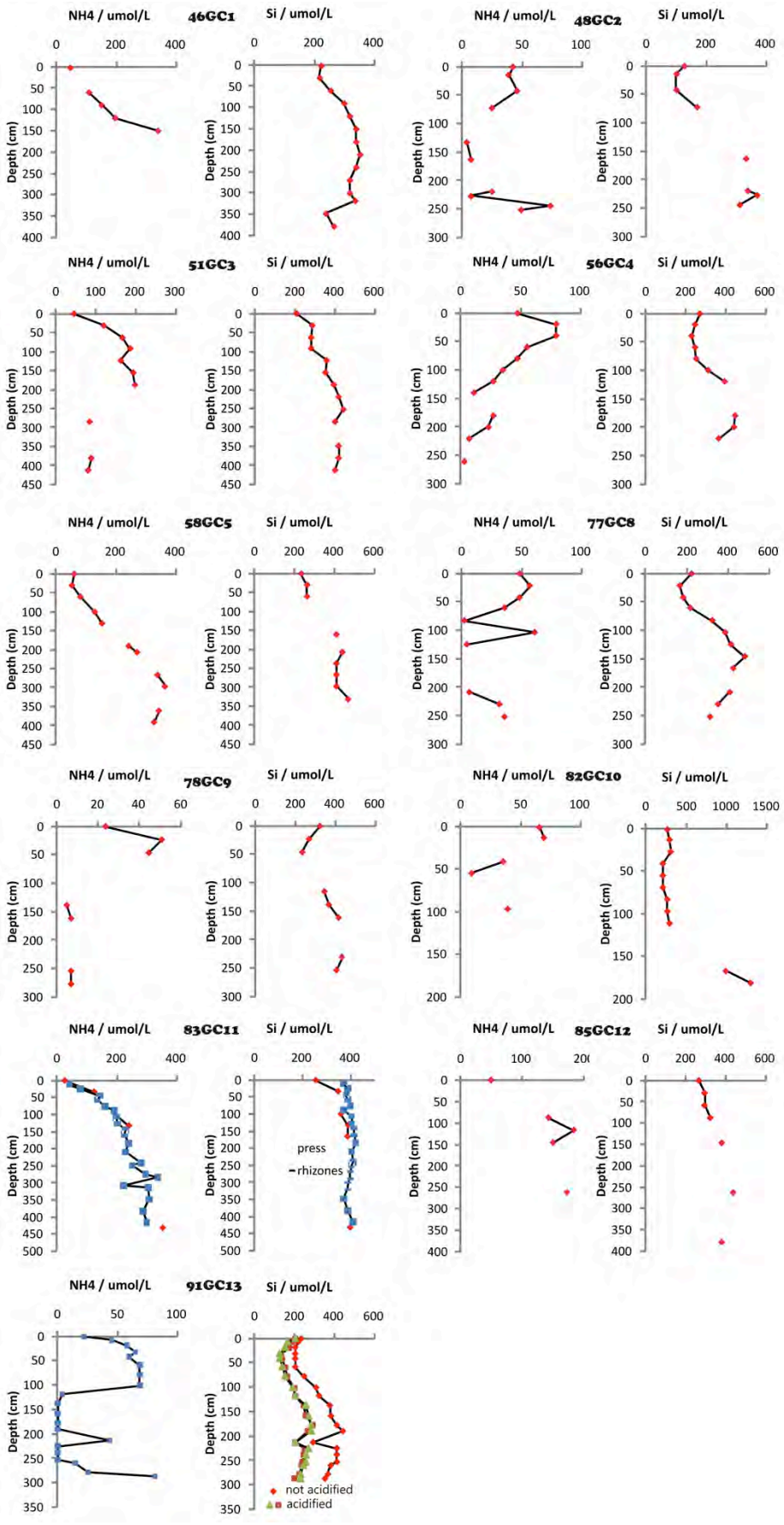

Figure 6.8.3: Ammonium and silicate pore water profiles of all SO214 gravity cores. (units µmol/L)

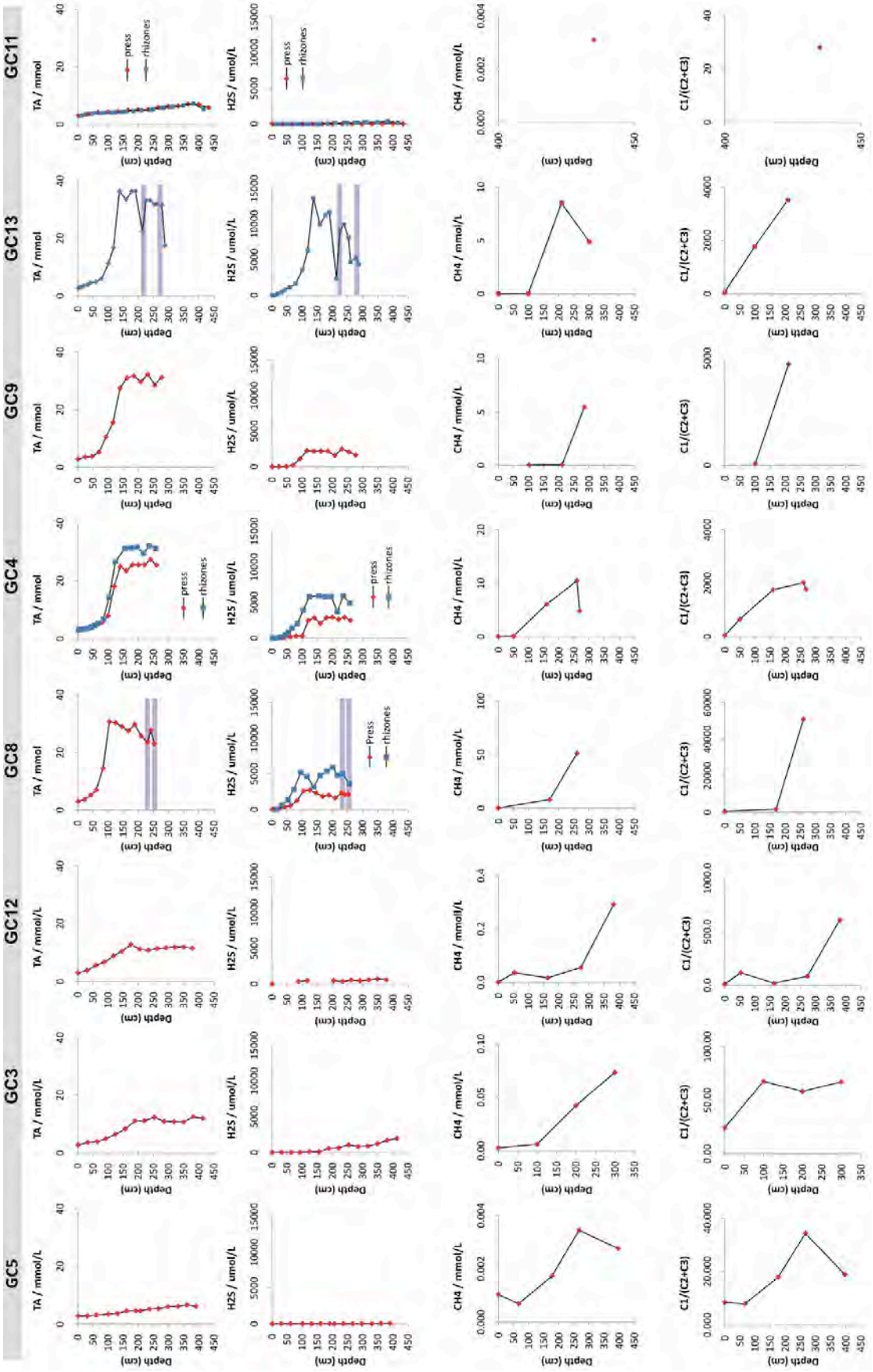

Figure 6.8.5: TA, H_2S, CH_4 and the C1/(C2+C3) ratio along the Takahe seep site transect. Gas hydrate layers are indicated by the blue bands. (units mmol/L)

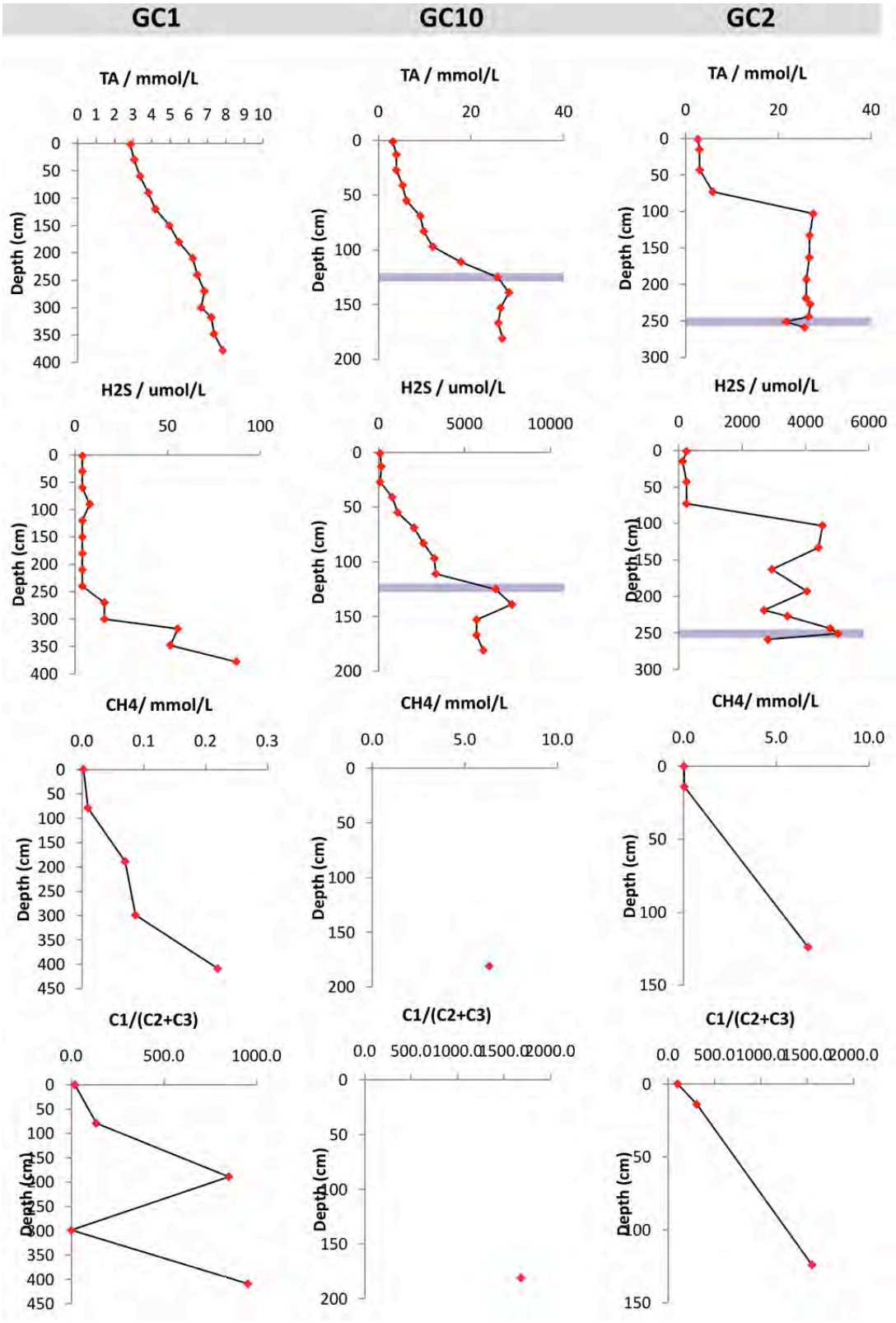

Figure 6.8.6: Alkalinity, H_2S, CH_4 and C1/(C2+C3) ratio pore water profiles for the cores that lie in the northern part of the Takahe seep site on an approximate east-west profiles (see Figure 6.8.1 for core positions). Observed massive gas hydrate layers are indicated by a blue shaded band. (units mmol/L)

Core GC1 was taken at the edge of the active seepage zone in the Takahe area. Determined from mud present on the outside of the barrel it was concluded that the corer penetrated at least 4.45 m into the seabed sediments. The core has a length of 4.14 m. It entirely consists of olive grey bioturbated (near the top vaguely mottled) silty clay. This core has been sampled for on board analysis of its gas content and pore water analysis at 30 cm intervals.

Table 6.9.1: Location of gravity cores taken during SO214

Station	Time Date (UTC)	Lat / Lon (ddd:mm.mmm)	Area	Remarks
GC-1	11:23:16 9-4-2011	-41:46.3040 175:25.7040	Takahe, center	
GC-2	14:53:11 9-4-2011	-41:46.3380 175:25.6290	Takahe, center	Gas Hydrate
GC-3	20:30:39 9-4-2011	-41:46.2770 175:25.7170	North just outside Takahe	
GC-4	09:44:39 11-4-2011	-41:46.3809 175:25.6724	Takahe, center	
GC-5	12:42:39 11-4-2011	-41:46.1840 175:25.7570	North of Takahe	
GC-6	16:09:35 11-4-2011	-41:46.3363 175:25.6389	Takahe, center	Foil, failed
GC-7	19:53:51 11-4-2011	-41:47.5682 175:25.0902	Unconformity at southern slope of Opouawe Bank	Unconformity, very hard
GC-8	18:51:18 13-4-2011	-41:46.3473 175:25.6908		Gas hydrate
GC-9	21:10:53 13-4-2011	-41:46.4323 175:25.6498	Southern part of Takahe	
GC-10	05:43:34 15-4-2011	-41:46.3410 175:25.6640	Takahe, center	Foil, gas hydrate
GC-11	07:39:31 15-4-2011	-41:46.4910 175:25.6180	South of Takahe	
GC-12	11:08:31 15-4-2011	-41:46.3120 175:25.7050	Takahe center	Repetition of GC-1
GC-13	14:10:39 16-4-2011	-41:46.4540 175:25.6350	Southern edge of Takahe	Gas hydrate

Core GC2 was taken in the active seepage zone in the Takahe area. Although the corer penetrated at least 3.85 m into the seabed, it has a length of only 2.95 m, including some small voids (in total about 36 cm). While the corer was hoisted on deck an intense bubbling of gas (like boiling water) and very strong H_2S smell was observed coming from the top end of the bomb, where the one-way valve is located. Between core sections 1 and 2 (2.32 m core depth) a 50 cm long void was present at the moment of cutting the core in sections on deck. This void is not included in the total core length reported here. The sediments consist of greyish olive, grey and blackish olive silty clay. Many (partly open) burrows are present. Open cracks, small (cm sized) voids and gas vesicles are present throughout the core. A strong H_2S smell was observed while opening the core. At 2.72 m core depth a cm-sized lump of gas hydrate was found. This core was sampled for gas and pore water analysis at irregular intervals.

Core GC3 was taken in the same area as the previous two cores, but this time well outside the active zone of seepage. This to allow for comparison of the type of sediments and biogeochemical processes in- and outside the zone of active seepage and to see to what extend seepage zones influence the surrounding seabed where no massive seepage (flares on acoustic profiles) can be observed. Core GC3 penetrated 4.63 m into the seabed and has a length of 4.145 m. It consists of greyish olive to olive grey silty clay. Mottling and bioturbation are observed throughout the core. The core gave of a slight smell of H_2S during opening. This core was subsampled every 30 cm for gas and pore water analysis.

Gravity core GC4 penetrated 3.33 m into the seabed in the Takahe area, resulting in a core length of 2.69 m. When hoisted on deck a small number of gas bubbles, leaking from the top of the bomb were seen. The core gave of a faint H_2S smell. The core consists of olive grey and olive black bioturbated silty clay. Thin (2-5 mm thick) silt layers are present, irregularly distributed, throughout this core. A vesicular structure, probably related to gas expansion, is

present at about half the core depth. Samples for gas and pore water analysis were taken at irregular intervals.

Gravity core GC5 was taken on the core transect in the Takahe area, away from the active seep site. It penetrated 448 into the seabed and has a length of 3.905 m. The sediments recovered within this core consist of bioturbated greyish olive silty clays alternating with 3-5 mm thick silt layers. This core lacks an H_2S smell. Samples for gas and pore water analysis were taken at intervals of approximately 30 cm.

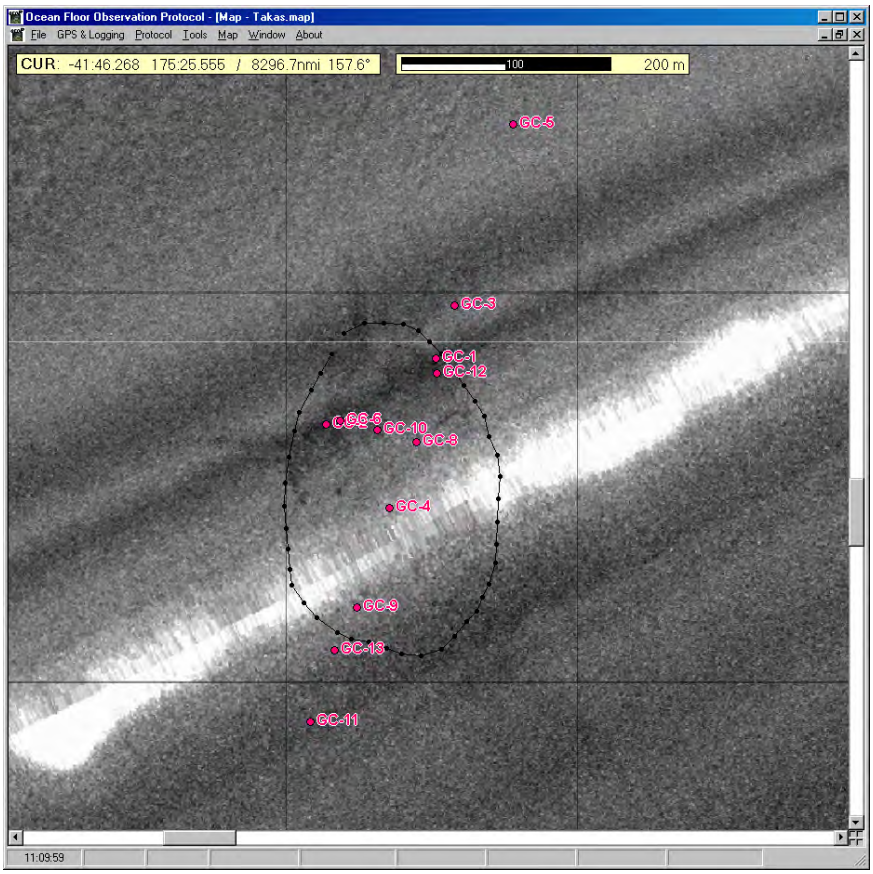

Figure 6.9.2: Locations of the GC stations at the Takahe site.

Gravity core GC6 was taken in the centre of the seepage zone in the Takahe area with the aim to collect as much gas hydrate as possible. For this purpose a plastic sleeve was inserted into the liner. Upon retrieval the sleeve would immediately be pulled out of the liner and the gas hydrates would be available for collection without any time delays caused by core cutting and splicing. In order to be able to insert the sleeve, the valve at the top of the liner had to be removed. It was presumed that the silty clays would be sticky enough to adhere to the sleeve. In addition to this the core catcher was expected to be strong enough to stop the expected retrieved sediment column (< 3 m in GC2). Unfortunately this was not the case. The sediment column appeared to be too heavy for the core catcher and the corer did not contain any sediment when it was hoisted on deck.

Core GC7 was taken away from the Takahe transect. The aim of this core was to sample sediments that are present below an unconformity that was recognised throughout a 3D Parasound survey recorded during leg 1 of this cruise. Hopefully the recovered sediments will help in further interpretation of the acoustic lines. The exact penetration of core GC7 could not be determined, but it was probably very low. The recovery is only about 60 cm, including the sediments in the nose of the core. The sediments found in the nose consist of grey clay

containing brown angular (sandstone) pebbles with a diameter up to 7 cm. On top of this, soft greyish clay is present. The exact length could not be determined because the soft clay had slumped in the corer while it was lying horizontally on deck.

Core GC8, also taken on the Takahe transect, penetrated 3.13 m into the seabed. The recovery of this core is 2.74 m. A continuous stream of large gas bubbles was observed coming from the nose of the core when it was hoisted up but still several meters below the water surface. A piece of gas hydrate was present in nose section of this core. The sediments consist of largely olive grey silty clays showing some mottling and bioturbation. Discontinuous silty layers are scattered throughout the core. Two gas hydrate layers were found in the lower part of this core. In addition vesicular structures and voids up to 6 cm wide as well as the clear H_2S smell are supporting evidence for the presence of free gas and/or gas hydrate. Samples for pore water and gas analysis were taken at irregular intervals.

Core GC9 also forms parts of the Takahe transect. It penetrated at least 2.98 into the seabed and had a recovery of 2.975 m. It consists of olive greyish to olive black silty clay. The sediments show evidence of bioturbation, contain a pervasive micro crack/vesicular structure and have a persistent H_2S smell. The sediments are overall fairly dry, but the presence of moist intervals and some voids resulting from gas expansion suggest the presence of gas hydrate in the seabed. From this core samples were taken at 20-30 cm intervals for the analysis of pore water and gas.

Core GC10 was taken in the centre of the Takahe gas seep area. The corer penetrated 2.09 m into the seabed and had a recovery of 1.85 m. This core was taken with the aim to recover as much gas hydrate as possible. In order to achieve this, a plastic sleeve was inserted into the liner, which was removed as soon as the corer was on deck. In this manner no time is lost with cutting the core into sections during which gas hydrates can disintegrate. So the same procedure was followed as with core 6, but this time the liner was slightly modified allowing the combined use of sleeve and the top valve. This time the sleeve-coring was successful. On deck the sleeve containing the core was cut lengthwise to collect any possible gas hydrates. The disadvantage of this method is that the core is disturbed and not suitable for any later detailed sedimentological or other analysis requiring undisturbed sediments. The sediments in this core consist of bioturbated olive grey to olive black silty clays. The middle section of the core contains thin silty layers. At 1.10-1.30 m core depth calcareous concretions with a diameter of about 1 cm are present that formed around 3-5 mm diameter burrows. The lower 45 cm of the core consists of silty clay showing a clear micro crack structure, possibly resulting from gas expansion. This section revealed a clear H_2S smell. A piece of gas hydrate with a diameter of about 5 cm was found in the lower part of the core. Some smaller pieces of gas hydrate were found in the nose of the corer. This core was sampled for gas and pore water analysis at irregular intervals.

Core GC11 was taken along the southern end of the Takahe transect. Mud traces on the outside of the barrel indicated that the corer penetrated at least 4.28 m into the sea floor, but this must have been more, since the recovery was 4.34 m. The corer was likely stopped by something hard (carbonate crust?) in the subsurface, since the core catcher and nose were empty and the nails attaching the nose to the barrel were damaged. The core consists of greyish olive silty clays intercalated with 2-5 mm thick silty layers. Mud-filled burrows are abundant throughout the core. In the top of the core a large Fe-oxide stained burrow is present. Subsamples for gas and pore water analysis were taken at about 30 cm intervals.

Gravity core GC12 was taken at the same location as core GC1 to check the unexpected results of the on board geochemical analysis. The core penetrated 4.29 m in to the sediments and had a recovery of 3.84 m. The core is made up of greyish olive to olive grey bioturbated

silty clay. Some thin (<3 mm) silty layers are present at various depths within the sedimentary column. Samples for gas and pore water analysis were taken at roughly 30 cm intervals.

Core GC13 was taken near the edge of the gas seep zone in the Takahe area. It penetrated 3.13 m into the seabed and had a recovery of 3.03 m. When the corer was hoisted near the water surface a strong bubbling coming out of the top of the bomb as well as a strong H_2S smell was observed. Between core sections 1 and 2 (2.08 m core depth) 12 cm gas expansion was present. This is not included in the core length. The sediments within this core consist of olive grey to greyish olive silty clays. The upper half of the core shows clear burrows. At about 115 cm core depth one of these burrows shows a carbonate rim, comparable to those present in core GC10. In the lower half of the core these get more and more obliterated by gas expansion structures (micro cracks in the sediment). The lower part also has a strong H_2S smell. At about 2.20, 2.45 and 2.70 m core depth 0.5-1 cm thick gas hydrate layers are present. In addition the nose and core catcher contained 3 lumps of centimetre-sized gas hydrate. Subsamples were taken for further analysis of the gas contents and composition of the pore water.

Copies of the on board core description forms are shown in Appendix 9.2

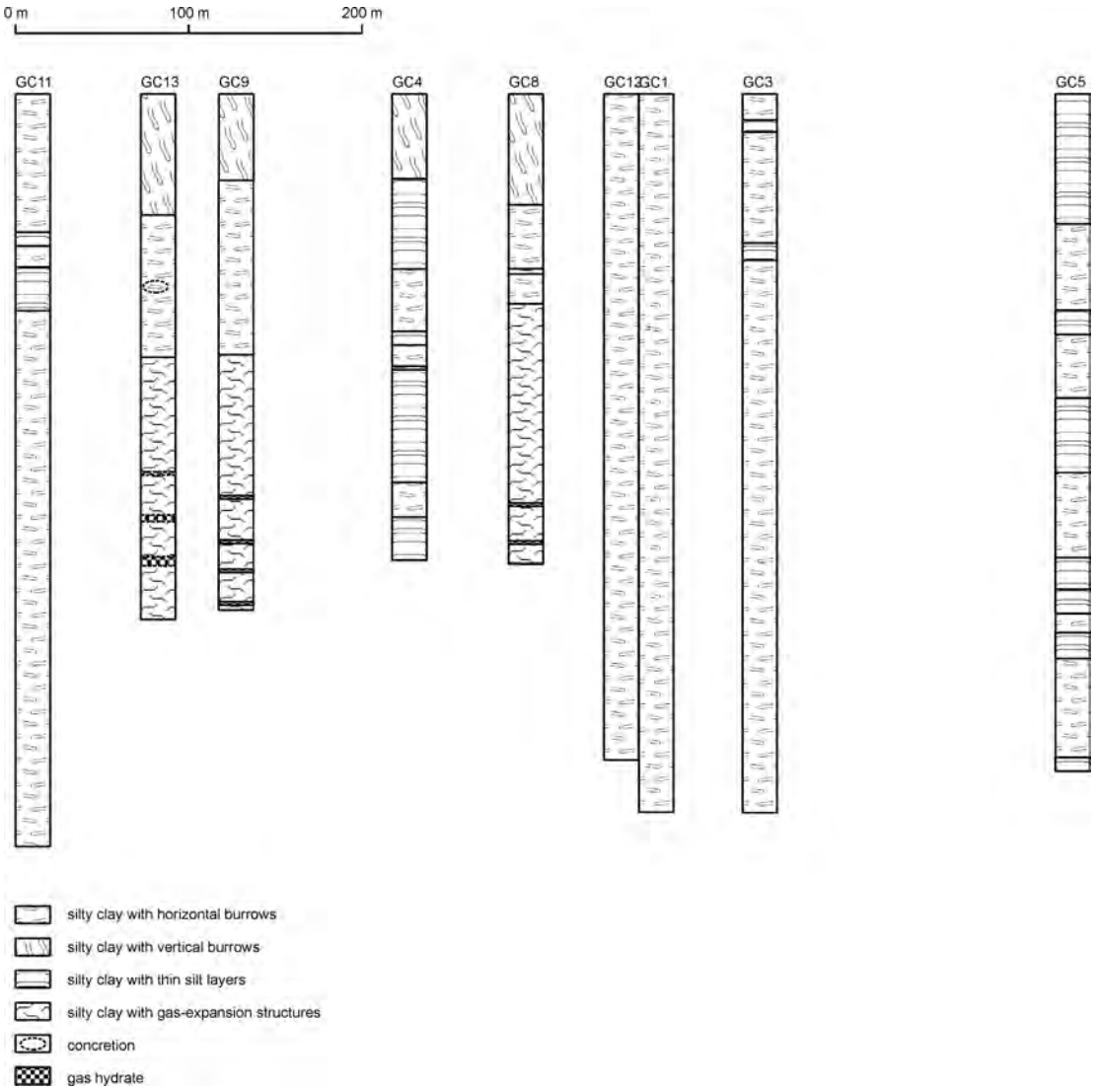

Figure 6.9.3: Overview of the gravity cores taken across seep Takahe

6.10 Results of sediment temperature measurements

Jens Greinert

A total of 12 gravity corer deployments gave temperature measurement results from the Takahe site at Opouawe Bank. Core positions and descriptions can be taken from section 6.9 and the station list. The list below gives the station names and depth of each THP sensor in the sediment during the measurement. The data are stored as simple ASCII files and can be request for joined research.

Table 6.10.1: Depth of THP sensor in the sediment during deployment (cm). Negative values are above the seafloor.

Station	27002 (bottom)	24005	24004	24001	24002 (top)
GC-1	386	336	285	185	84.5
GC-2	326	276	225.5	125.5	24.5
GC-3	404	354	303.5	203.5	102.5
GC-4	274	224	173.5	73.5	-27.5
GC-5	389	339	288.5	188.5	87.5
GC-6	250	200	149.5	49.5	-51.5
GC-7 (fell over)	-	-	-	-	-
GC-8	254	204	153.5	53.5	47.5
GC-9	239	189	138.5	38.5	-62.5
GC-10	2.11	-	110.5	10.5	-90.5
GC-11	376	-	275.5	175.5	74.5
GC-12	370	320	269.5	169.5	68.5
GC-13	254	204	153.5	53.5	-47.5

The different data set are shown in Figure 1. A summary of all temperature profiles is presented in Figure 2. During GC-10 and GC-11 THP sensor 24005 has been forgotten to be switched on (both cores were taken back-to-back and dates were not read out in between the two deployments).

Figure 6.10.1: Temperature as measured during the 15 minute long time the THP sensors where in the sediment. The steep rise in temperature at the beginning is caused by the friction when the sensors penetrate into the seafloor.

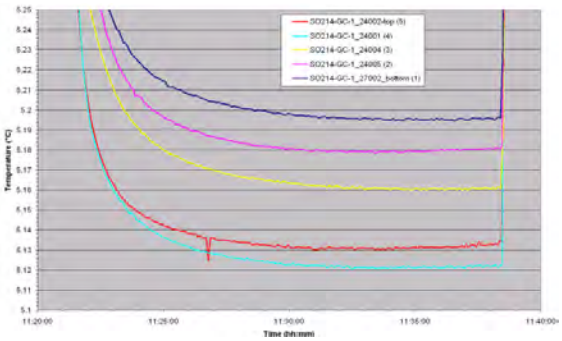

GC-1

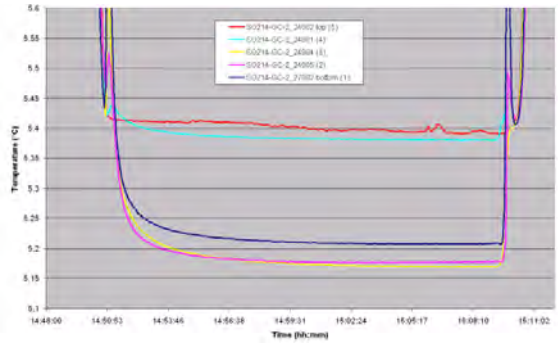

GC-2

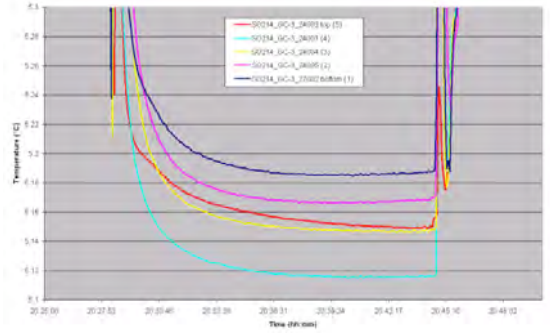

GC-3

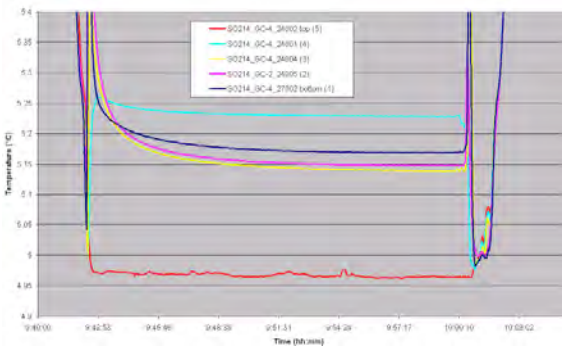

GC-4

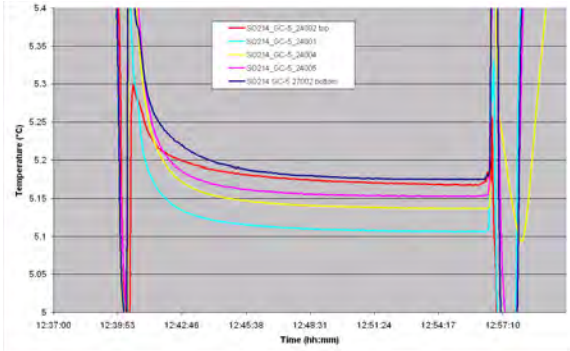

GC-5

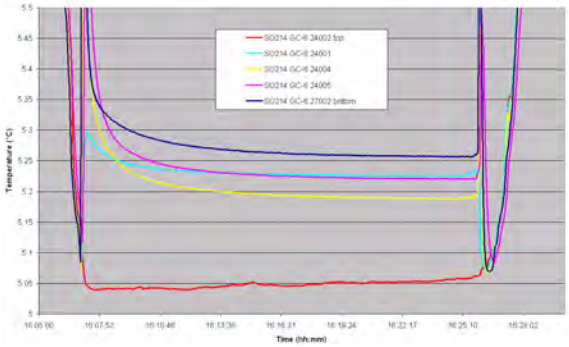

GC-6

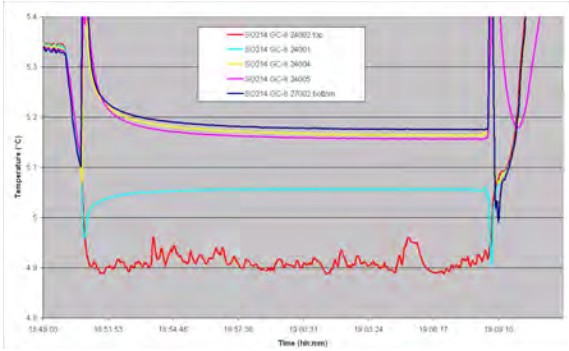

GC-8

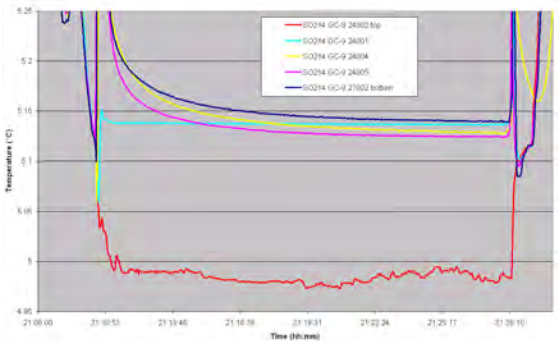

GC-9

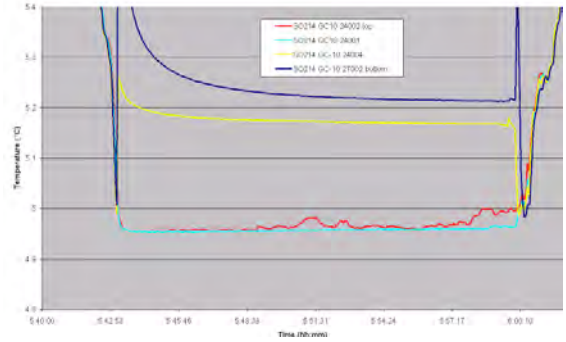

GC-10

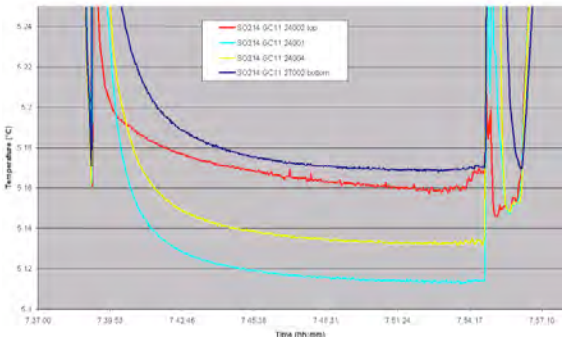

GC-11

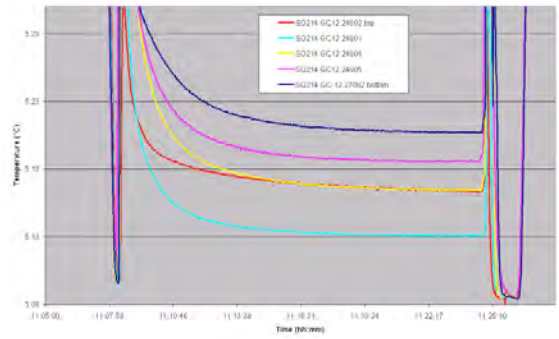

GC-12

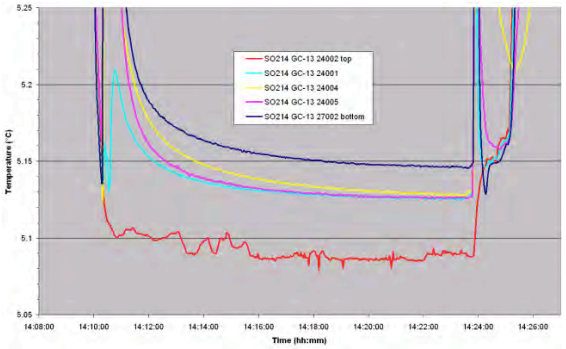

GC-13

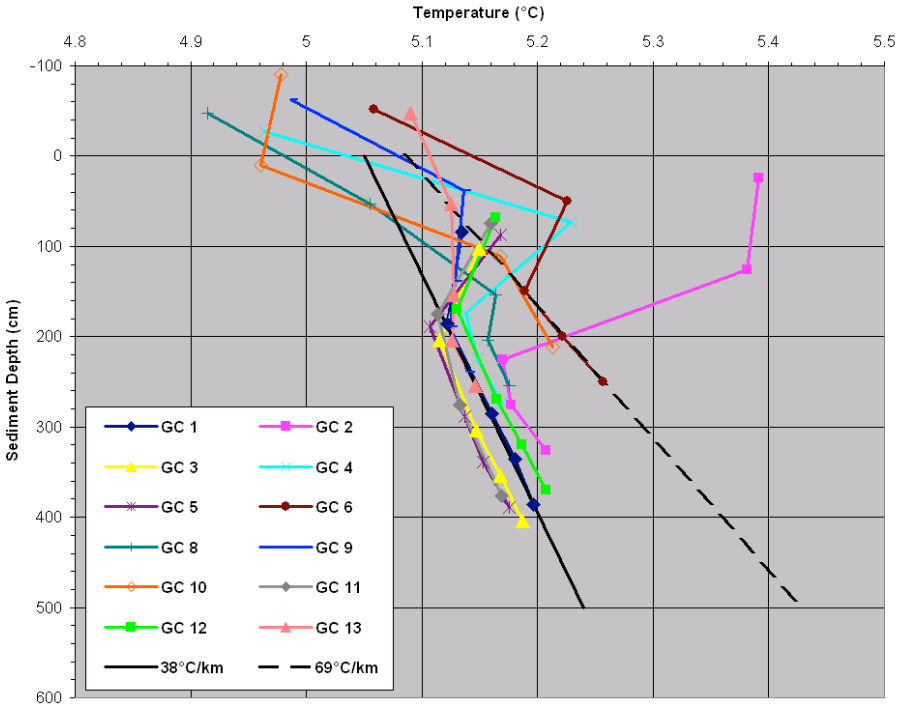

Figure 6.10.2: Preliminary results from the temperature sensor measurements show a normal thermal gradient of about 38°C/km in most of the cores independently of the position relative to the acoustic chimney of the Takahe site and the occurrence of gas hydrates. Only gas hydrate core GC-6 shows a significant higher gradient of 69°C/km.

7. Acknowledgments

The cruise SO214 NEMESYS Leg 1 and 2 was financed by the German Federal Ministry for Education and Research (Bundesministerium für Bildung und Forschung, BMBF) under project No. 03G0214. We are grateful to the continuous support of marine sciences with an outstanding platform such as R/V SONNE.

We acknowledge the financial support of the 3D seismic acquisition by GNS.

The authors wish to express their gratitude to all the colleagues who have supported the work before, during and after the cruise. Much of the work done during the cruise was only made possible by the scientists', technicians' and the crews' experience.

Particular thanks are directed to Captain Oliver Meyer and to the entire crew of R/V SONNE for their excellent support throughout the cruise.

Martina Ikert provided extensive help with the compilation of all contributions into the final volume.

All meta data of the cruise are available through the IFM-GEOMAR Data Management Portal (https://portal.ifm-geomar.de/web/guest/home)

8. References

Baco, A. R., A. A. Rowden, L. A. Levin, C. R. Smith, and D. A. Bowden (2010), Initial characterization of cold seep faunal communities on the New Zealand Hikurangi margin, *Marine Geology*, *272*(1-4), 251-259.

Bialas, J., and E. R. Flüh (1999), A new Ocean Bottom Seismometer (with a new type of data logger), *Sea Technology*, *40*(4), 41-46.

Bialas, J., M. Hardieck, G. L. Netzeband, and A. Krabbenhöft (2007a), Pseudo 3-D analysis of seismic data at seep locations in the Wairarapa area offshore new Zealand, in *AGU Fall Meeting*, edited, American Geophysical Union, San Francisco.

Bialas, J., J. Greinert, P. Linke, and O. Pfannkuche (2007b), FS Sonne Fahrtbericht / Cruise Report SO 191 - New Vents "Puaretanga Hou" 11.01. - 23.03.2007*Rep. 9*, 190 pp pp, IFM-GEOMAR, Kiel.

Campbell, K. A., D. A. Francis, M. Collins, M. R. Gregory, C. S. Nelson, J. Greinert, and P. Aharon (2008), Hydrocarbon seep-carbonates of a Miocene forearc (East Coast Basin), North Island, New Zealand, *Sediment Geol*, *204*(3-4), 83-105.

Campbell, K. A., et al. (2010), Geological imprint of methane seepage on the seabed and biota of the convergent Hikurangi Margin, New Zealand: Box core and grab carbonate results, *Marine Geology*, *272*(1-4), 285-306.

Collot, J. Y., et al. (1996), From oblique subduction to intra-continental transpression: Structures of the southern Kermadec-Hikurangi margin from multibeam athymetry, side-scan sonar and seismic reflection, *Marine Geophysical Researches*, *18*, 357-381.

Crutchley, G. J., A. R. Gorman, I. A. Pecher, S. Toulmin, and S. A. Henrys Geological controls on focused fluid flow through the gas hydrate stability zone on the southern Hikurangi Margin of New Zealand, evidenced from multi-channel seismic data, *Marine and Petroleum Geology*, *In Press, Corrected Proof*.

Davy, B., and R. Wood (1994), Gravity and magnetic modelling of the Hikurangi Plateau, *Marine Geology*, *118*(1-2), 139-151.

Faure, K., J. Greinert, J. S. v. Deimling, D. F. McGinnis, R. Kipfer, and P. Linke (2010), Methane seepage along the Hikurangi Margin of New Zealand: Geochemical and physical data from the water column, sea surface and atmosphere, *Marine Geology*, *272*, 170-188.

Faure, K., J. Greinert, I. Pecher, I. Graham, G. Massoth, C. De Ronde, I. Wright, E. Baker, and E. Olson (2006), Methane seepage and its relation to slumping and gas hydrate at the Hikurangi margin, New Zealand, *New Zeal J Geol Geop*, *49*, 503-516.

Flüh, E., and J. Bialas (1996), A digital, high data capacity ocean bottom recorder for marine seismic investigations, *Underwater System Designs*, *18*(3), 18-20.

Giggenbach, W. F., M. K. Stewart, Y. Sano, R. L. Goguel, and G. L. Lyon (1993), Isotopic and chemical composition of the waters and gases from the East Coast accretionary prism, New Zealand, paper presented at Proceedings of the Final Research Coordination Meeting on the Application of Isotope and Geochemical Techniques to Geothermal Exploration in the Middle East, Asia, the Pacific and Africa.

Grasshoff, K., M. Ehrhardt, and K. Kremmling (1997), *Methods of seawater analysis*, 419 pp., Wiley-VCH, Weinheim.

Greinert, J., J. Bialas, K. Lewis, and E. Suess (2010), Methane seeps at the Hikurangi Margin, New Zealand, *Marine Geology*, *272*(1-4), 1-3.

Greinert, J., K. B. Lewis, J. Bialas, I. A. Pecher, A. Rowden, D. A. Bowden, M. D. Batist, and P. Linke (2010), Methane seepage along the Hikurangi Margin, New Zealand: Overview of studies in 2006 and 2007 and new evidence from visual, bathymetric and hydroacoustic investigations, *Marine Geology*, *272*, 6-25.

Grevemeyer, I., N. Kaul, and J. L. Diaz-Naveas (2006), Geothermal evidence for fluid flow through the gas hydrate stability field off Central Chile - transient flow related to large subduction zone earthquakes ?, *Geophysical Journal International*, *166*(1), 461-468.

Henrys, S., S. Ellis, and C. Uruski (2003), Conductive heat flow variations from bottom-simulating reflectors on the Hikurangi margin, New Zealand, *Geophys. Res. Lett.*, *30*(2).

Huetten, E., and J. Greinert (2008), Software controlled guidance, recording and post-processing of seafloor observationsnext term by previous termROV and other towednext term devices: the previous termsoftwarenext term package OFOP, paper presented at EGU, Vienna.

Ivanenkov, V. N., and Y. I. Lyakhin (1978), Determination of total alkalinity in seawater, in *Methodes of hydrochemical investigations in the ocean*, edited by O. K. Bordovsky and V. N. Ivanenkov, pp. 110-114, Nauka Publ. House, Moscow.

Lewis, K., and B. Marshall (1996), Seep faunas and other indicators of methane-rich dewatering on New Zealand convergent margins, *New Zeal J Geol Geop*, *39*, 181-200.

Liu, X. L., and P. B. Flemings (2007), Dynamic multiphase flow model of hydrate formation in marine sediments, *J Geophys Res-Sol Ea*, *112*(B3), -.

Marquardt, M., C. Hensen, E. Piñero, K. Wallmann, and M. Haeckel (2010), A transfer function for the prediction of gas hydrate inventories in marine sediments, *Biogeosciences*, *7*(9), 2925-2941.

Netzeband, G. L., A. Krabbenhöft, M. Zillmer, C. Petersen, C. Papenberg, and J. Bialas (2010), The structures beneath submarine methane seeps: Seismic evidence from Opouawe Bank, Hikurangi Margin, New Zealand, *Marine Geology*, *272*, 59-70.

Pecher, I., W. Wood, R. Funnell, S. Toulmin, L. Hamdan, R. Coffin, S. Henrys, and N. Kukowski (2010), Discrepancies in thermal gradients from BSR depth and seafloor thermometry on the Hikurangi Margin, New Zealand - possible implications for gas hydrate formation and subduction-zone processes, in *AGU Fall Meeting*, edited, EOS Transactions, San Francisco.

Pecher , I. A., R. Coffin, and S. Henrys (2007), Tangaroa TAN0607 Cruise Report: gas hydrate exploration on the East Coast, North Island, New Zealand*Rep.*, 119 pp, GNS, Wellington.

Pecher, I. A., et al. (2010), Focussed fluid flow on the Hikurangi Margin, New Zealand -- Evidence from possible local upwarping of the base of gas hydrate stability, *Marine Geology*, *272*(1-4), 99-113.

Schmale, O., S. E. Beaubien, G. Rehder, J. Greinert, and S. Lombardi (2010), Gas seepage in the Dnepr paleo-delta area (NW-Black Sea) and its regional impact on the water column methane cycle, *J Marine Syst*, *80*(1-2), 90-100.

Schwalenberg, K., M. Haeckel, J. Poort, and M. Jegen (2010a), Evaluation of gas hydrate deposits in an active seep area using marine controlled source electromagnetics: Results from Opouawe Bank, Hikurangi Margin, New Zealand, *Marine Geology*, *272*(1-4), 79-88.

Schwalenberg, K., W. Wood, I. Pecher, L. Hamdan, S. Henrys, M. Jegen, and R. Coffin (2010b), Preliminary interpretation of electromagnetic, heat flow, seismic, and geochemical data for gas hydrate distribution across the Porangahau Ridge, New Zealand, *Marine Geology*, *272*, 89-98.

Thurber, A. R., K. Krˆger, C. Neira, H. Wiklund, and L. A. Levin (2010), Stable isotope signatures and methane use by New Zealand cold seep benthos, *Marine Geology*, *272*(1-4), 260-269.

Wiesenburg, D. A., and N. L. Guinasso (1979), Equilibrium solubilities of methane, carbon monoxide, and hydrogen in water and sea water, *Journal of Chemical & Engineering Data*, *24*(4), 356-360.

Wood, W. T., I. Pecher, S. Henrys, and R. Coffin (2008), The transient nature of heat and fluid flux on the Porangahau Ridge, New Zealand, in *Eos Trans. AGU, Fall Meeting Suppl.*, edited.

9. Appendices

9.1. List of Pore water Sampling Sites and Collected Sub-samples.

Station	Working area	Longitude	Latitude	Water Depth / m	Pore water extraction method		NH_4^+	H_4SiO_4	H_2S	TA	ICP-AES	IC	Porosity & CNS	^{18}O	^{35}S	CH_4	Length / cm	No. of samples
					Press	Rhizones												
44 MUC 2	Opouawe	175 °E 25.697	41 °S 46.309	1053		X			X	X	X	X			X		41	13
46 GC 1	Opouawe	175 °E 25.703	41 °S 46.302	1050	X		X	X	X	X	X	X	X	X		X	410	15
48 GC 2	Opouawe	175 °E 25.629	41 °S 46.338	1050	X		X	X	X	X	X	X	X	X		X	280	13
51 GC 3	Opouawe	175 °E25.717	41 °S 46.277	1051	X		X	X	X	X	X	X	X	X		X	415	14
56 GC 4	Opouawe	175 °E 25.612	41 °S 46.399	1049	X	X	X	X	X	X	X	X	X	X	X	X	269	29
58 GC 5	Opouawe	175 °E 25.763	41 °S 46.186	1051	X		X	X	X	X	X	X	X	X		X	296	14
66 MUC 3	Opouawe	175 °E 25.660	41 °S 46.338	1052		X			X	X	X	X	X		X		25	11
77 GC 8	Opouawe	175 °E 25.688	41 °S 46.350	1049	X	X	X	X	X	X	X	X	X	X	X	X	260	27
78 GC 9	Opouawe	175 °E 25.651	41 °S 46.450	1049	X		X	X	X	X	X	X	X	X		X	285	13
82 GC 10	Opouawe	175 °E 25.667	41 °S 46.339	1049	X		X	X	X	X	X	X	X	X		X	182	14
83 GC 11	Opouawe	175 °E 25.615	41 °S 46.489	1049	X	X	X	X	X	X	X	X	X	X	X	X	435	35
85 GC 12	Opouawe	175 °E 25.709	41 °S 46.315	1051	X		X	X	X	X	X	X	X	X		X	383	14
91 GC 13	Opouawe	175 °E 25.625	41 °S 46.454	1050		X	X	X	X	X	X	X	X	X	X	X	302	33
95 MUC 7	Bear's Paw	177 °E 49.159	40 °S 03.192	1103		X	X	X	X	X	X	X	X				15	9

9.2 On board description of GCs

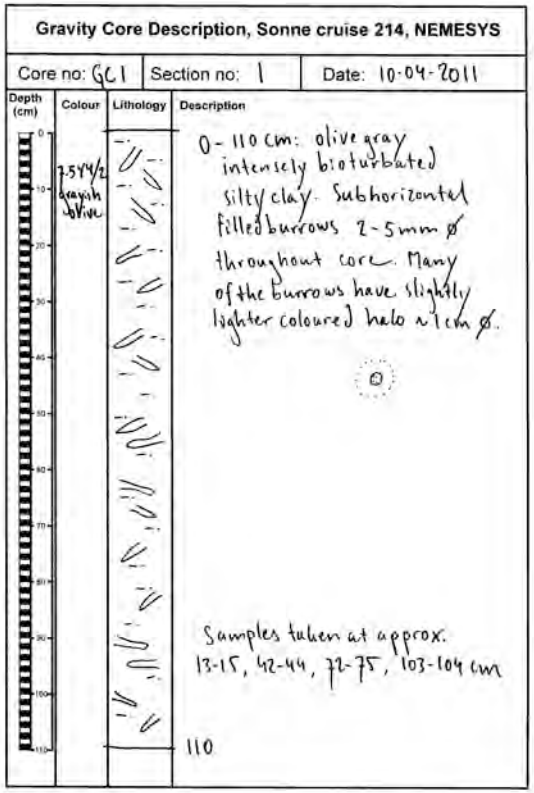
Gravity Core Description, Sonne cruise 214, NEMESYS

Core no: GC1 | Section no: 1 | Date: 10-04-2011

Depth (cm) | Colour | Lithology | Description

Colour: 7.5Y4/2 grayish olive

0-110 cm: olive gray intensely bioturbated silty clay. Subhorizontal filled burrows 2-5mm ø throughout core. Many of the burrows have slightly lighter coloured halo ~1cm ø.

Samples taken at approx. 13-15, 42-44, 72-75, 103-104 cm

110

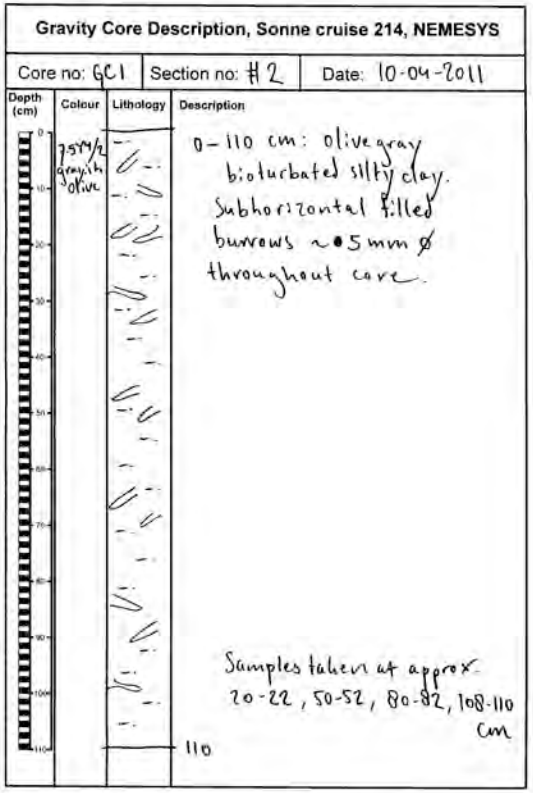
Gravity Core Description, Sonne cruise 214, NEMESYS

Core no: GC1 | Section no: #2 | Date: 10-04-2011

Depth (cm) | Colour | Lithology | Description

Colour: 7.5Y4/2 grayish olive

0-110 cm: olive gray bioturbated silty clay. Subhorizontal filled burrows ~5mm ø throughout core.

Samples taken at approx. 20-22, 50-52, 80-82, 108-110 cm

110

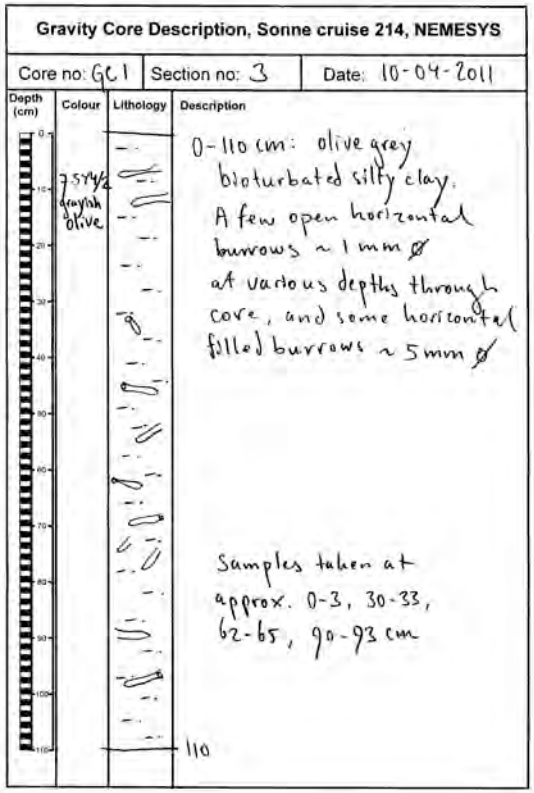
Gravity Core Description, Sonne cruise 214, NEMESYS

Core no: GC1 | Section no: 3 | Date: 10-04-2011

Depth (cm) | Colour | Lithology | Description

Colour: 7.5Y4/2 grayish olive

0-110 cm: olive grey bioturbated silty clay. A few open horizontal burrows ~1mm ø at various depths through core, and some horizontal filled burrows ~5mm ø

Samples taken at approx. 0-3, 30-33, 62-65, 90-93 cm

110

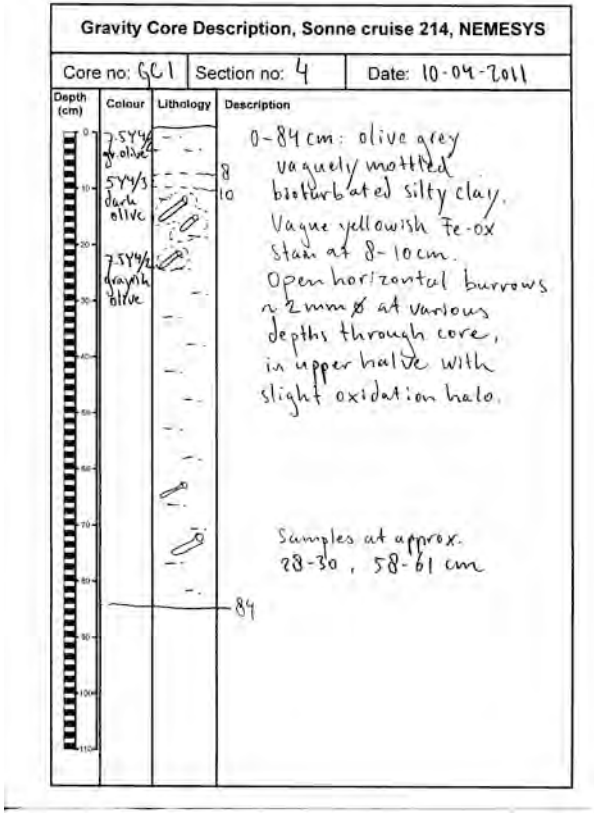
Gravity Core Description, Sonne cruise 214, NEMESYS
Core no: GC1
Section no: 4
Date: 10-04-2011
Depth (cm)
Colour
Lithology
Description
0-84 cm: olive grey vaguely mottled bioturbated silty clay. Vague yellowish Fe-ox stain at 8-10 cm. Open horizontal burrows ~2 mm Ø at various depths through core, in upper half with slight oxidation halo.
7.5Y4/2 grayish olive
5Y4/3 dark olive
7.5Y4/2 grayish olive
8
10
84
Samples at approx. 28-30, 58-61 cm

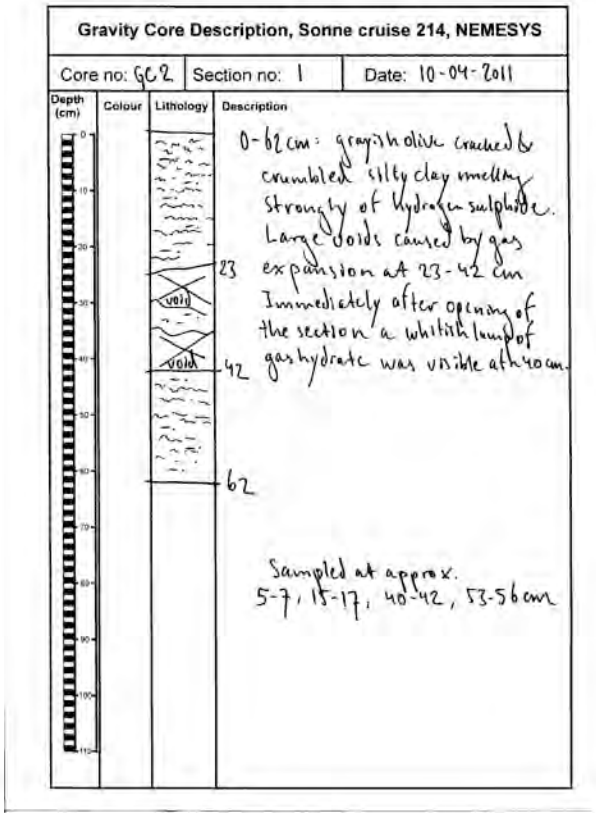
Gravity Core Description, Sonne cruise 214, NEMESYS
Core no: GC2
Section no: 1
Date: 10-04-2011
Depth (cm)
Colour
Lithology
Description
0-62 cm: grayish olive cracked & crumbled silty clay smelling strongly of hydrogen sulphide. Large voids caused by gas expansion at 23-42 cm. Immediately after opening of the section a whitish lump of gas hydrate was visible at 40 cm.
VOID
VOID
23
42
62
Sampled at approx. 5-7, 15-17, 40-42, 53-56 cm

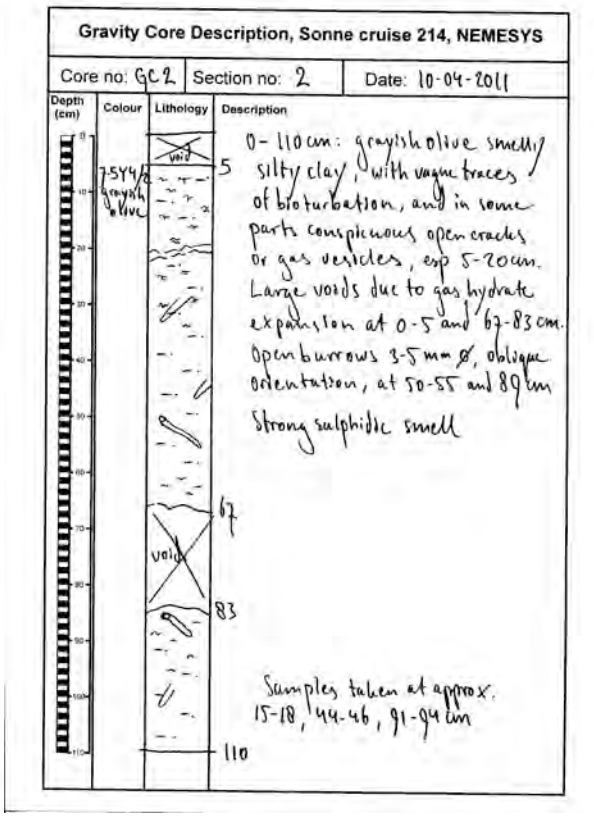
Gravity Core Description, Sonne cruise 214, NEMESYS
Core no: GC2
Section no: 2
Date: 10-04-2011
Depth (cm)
Colour
Lithology
Description
0-110 cm: grayish olive smelly silty clay, with vague traces of bioturbation, and in some parts conspicuous open cracks or gas vesicles, esp 5-20 cm. Large voids due to gas hydrate expansion at 0-5 and 67-83 cm. Open burrows 3-5 mm Ø, oblique orientation, at 50-55 and 89 cm. Strong sulphidic smell
VOID
VOID
7.5Y4/2 grayish olive
5
67
83
110
Samples taken at approx. 15-18, 44-46, 91-94 cm

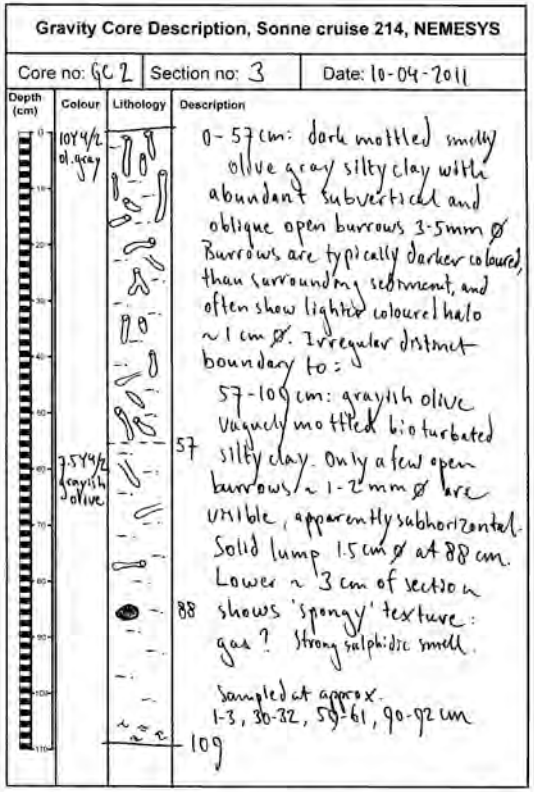
Gravity Core Description, Sonne cruise 214, NEMESYS
Core no: GC 2
Section no: 3
Date: 10-04-2011
Depth (cm)
Colour
Lithology
Description
10YR 4/2 dl. gray
7.5Y 4/2 grayish olive
0-57 cm: dark mottled smelly olive gray silty clay with abundant subvertical and oblique open burrows 3-5mm ø. Burrows are typically darker coloured than surrounding sediment, and often show lighter coloured halo ~1 cm ø. Irregular distinct boundary to:
57-109 cm: grayish olive vaguely mottled bioturbated silty clay. Only a few open burrows, ~1-2 mm ø are visible, apparently subhorizontal. Solid lump 1.5 cm ø at 88 cm. Lower ~3 cm of section shows 'spongy' texture: gas? Strong sulphidic smell.
Sampled at approx. 1-3, 30-32, 59-61, 90-92 cm
57
88
109

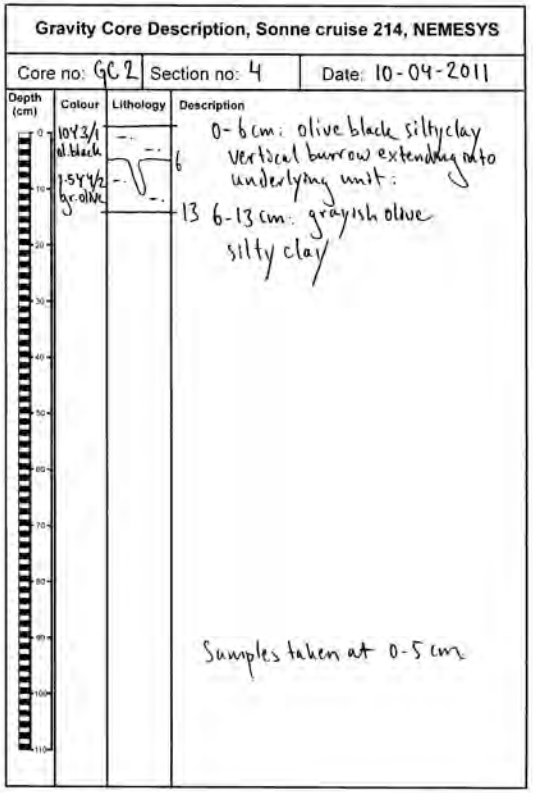
Gravity Core Description, Sonne cruise 214, NEMESYS
Core no: GC 2
Section no: 4
Date: 10-04-2011
Depth (cm)
Colour
Lithology
Description
10YR 3/1 vl. black
7.5Y 4/2 gr. olive
0-6 cm: olive black silty clay vertical burrow extending down to underlying unit:
6-13 cm: grayish olive silty clay
6
13
Samples taken at 0-5 cm

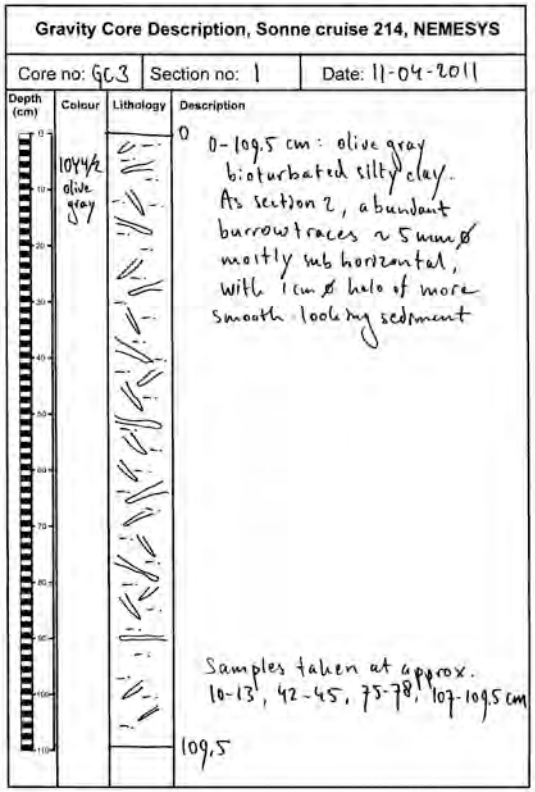
Gravity Core Description, Sonne cruise 214, NEMESYS
Core no: GC 3
Section no: 1
Date: 11-04-2011
Depth (cm)
Colour
Lithology
Description
10YR 4/2 olive gray
0
0-109.5 cm: olive gray bioturbated silty clay. As section 2, abundant burrow traces ~5 mm ø mostly sub horizontal, with 1 cm ø halo of more smooth looking sediment
Samples taken at approx. 10-13, 42-45, 75-78, 107-109.5 cm
109.5

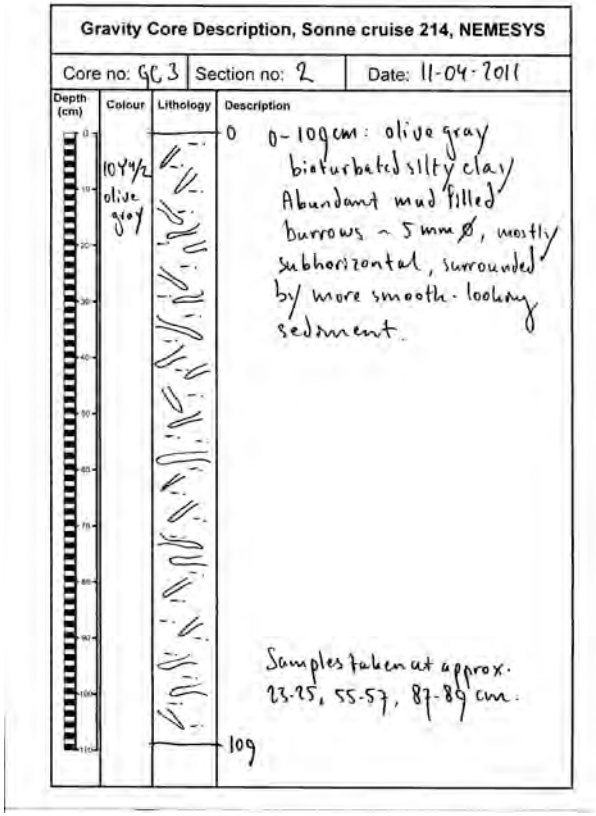
Gravity Core Description, Sonne cruise 214, NEMESYS
Core no: GC3 Section no: 2 Date: 11-04-2011
Depth (cm)
Colour
Lithology
Description
10Y4/2 olive gray
0 0-109 cm: olive gray bioturbated silty clay/ Abundant mud filled burrows ~ 5 mm Ø, mostly subhorizontal, surrounded by more smooth-looking sediment.
Samples taken at approx. 23-25, 55-57, 87-89 cm.
109

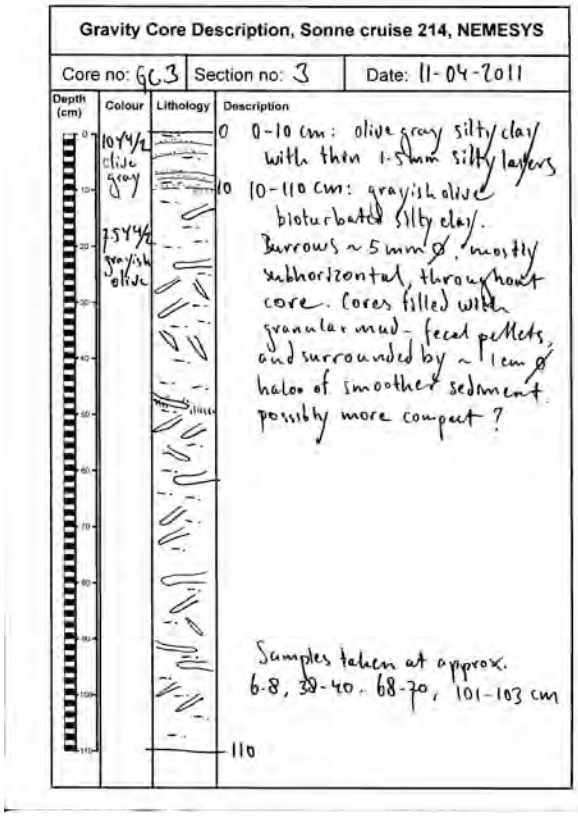
Gravity Core Description, Sonne cruise 214, NEMESYS
Core no: GC3 Section no: 3 Date: 11-04-2011
Depth (cm)
Colour
Lithology
Description
10Y4/2 olive gray
2.5Y4/2 grayish olive
0 0-10 cm: olive gray silty clay with thin 1-5mm silty layers
10 10-110 cm: grayish olive bioturbated silty clay. Burrows ~ 5 mm Ø, mostly subhorizontal, throughout core. Cores filled with granular mud - fecal pellets, and surrounded by ~ 1 cm Ø halos of smoother sediment possibly more compact?
Samples taken at approx. 6-8, 39-40, 68-70, 101-103 cm
110

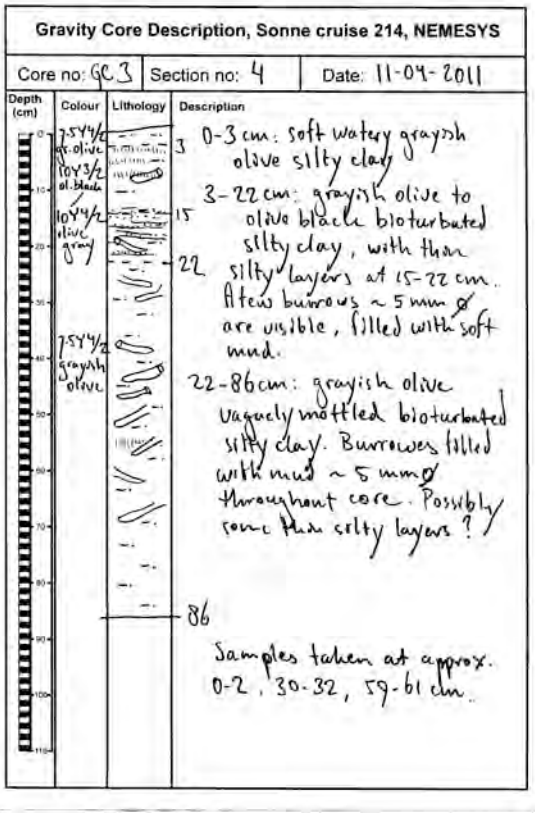
Gravity Core Description, Sonne cruise 214, NEMESYS
Core no: GC3 Section no: 4 Date: 11-04-2011
Depth (cm)
Colour
Lithology
Description
2.5Y4/2 dk. olive
10Y3/2 ol. black
10Y4/2 olive gray
2.5Y4/2 grayish olive
3 0-3 cm: soft watery grayish olive silty clay
3-22 cm: grayish olive to olive black bioturbated silty clay, with thin silty layers at 15-22 cm. Few burrows ~ 5 mm Ø are visible, filled with soft mud.
15
22
22-86 cm: grayish olive vaguely mottled bioturbated silty clay. Burrowes filled with mud ~ 5 mm Ø throughout core. Possibly some thin silty layers?
86
Samples taken at approx. 0-2, 30-32, 59-61 cm.

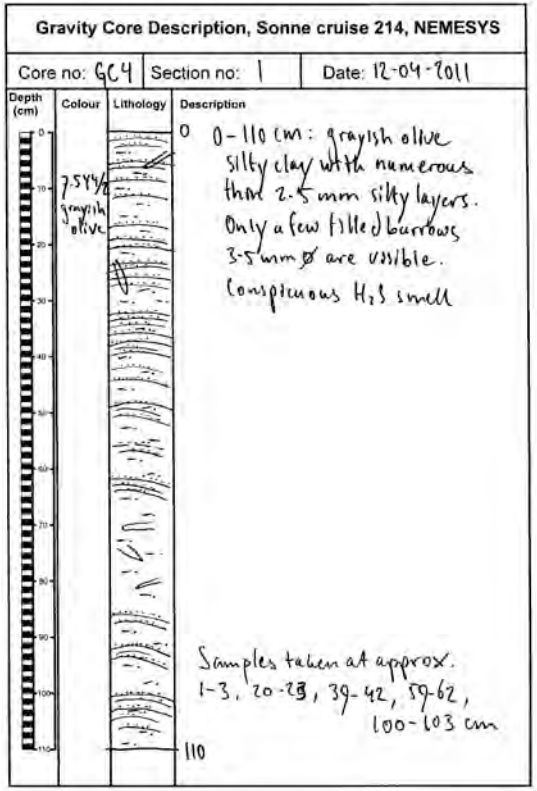
Gravity Core Description, Sonne cruise 214, NEMESYS
Core no: GC4
Section no: 1
Date: 12-04-2011
Depth (cm)
Colour
Lithology
Description
0
0-110 cm: grayish olive silty clay with numerous thin 2-5 mm silty layers. Only a few filled burrows 3-5 mm Ø are visible. Conspicuous H2S smell
7.5Y4/2 grayish olive
Samples taken at approx. 1-3, 20-23, 39-42, 59-62, 100-103 cm
110

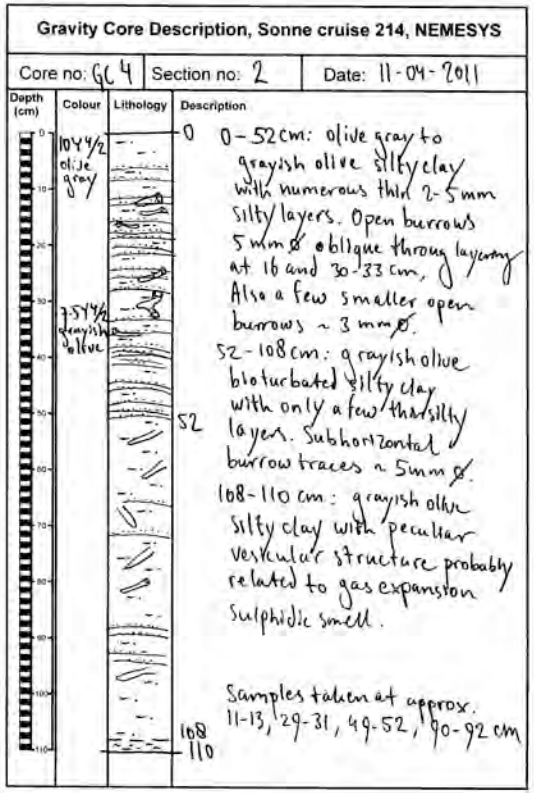
Gravity Core Description, Sonne cruise 214, NEMESYS
Core no: GC4
Section no: 2
Date: 11-04-2011
Depth (cm)
Colour
Lithology
Description
0
0-52 cm: olive gray to grayish olive silty clay with numerous thin 2-5 mm silty layers. Open burrows 5 mm Ø oblique through layering at 16 and 30-33 cm. Also a few smaller open burrows ~ 3 mm Ø.
10Y4/2 olive gray
7.5Y4/2 grayish olive
52
52-108 cm: grayish olive bioturbated silty clay with only a few thin silty layers. Subhorizontal burrow traces ~ 5 mm Ø.
108-110 cm: grayish olive silty clay with peculiar vesicular structure probably related to gas expansion. Sulphidic smell.
Samples taken at approx. 11-13, 29-31, 49-52, 90-92 cm
108
110

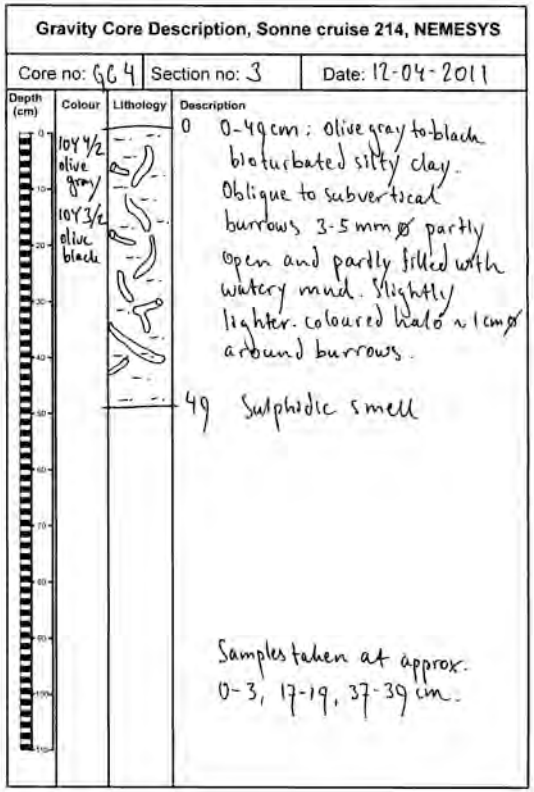
Gravity Core Description, Sonne cruise 214, NEMESYS
Core no: GC4
Section no: 3
Date: 12-04-2011
Depth (cm)
Colour
Lithology
Description
0
0-49 cm: olive gray to black bioturbated silty clay. Oblique to subvertical burrows 3-5 mm Ø partly open and partly filled with watery mud. Slightly lighter coloured halo ~ 1 cm Ø around burrows.
10Y4/2 olive gray
10Y3/2 olive black
49
Sulphidic smell
Samples taken at approx. 0-3, 17-19, 37-39 cm.

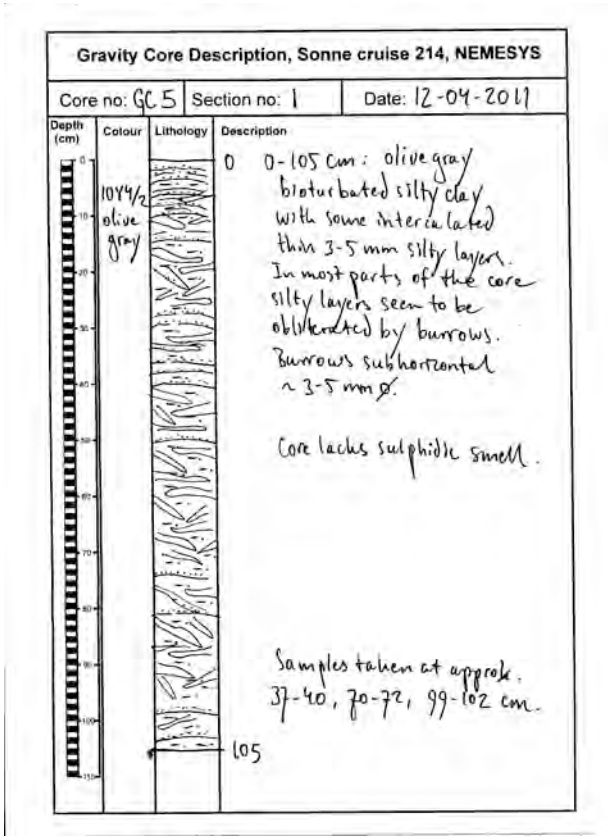
Gravity Core Description, Sonne cruise 214, NEMESYS
Core no: GC 5
Section no: 1
Date: 12-04-2011
Depth (cm)
Colour
Lithology
Description
0
10Y4/2 olive gray
105
0-105 cm: olive gray bioturbated silty clay with some intercalated thin 3-5 mm silty layers. In most parts of the core silty layers seem to be obliterated by burrows. Burrows subhorizontal ~3-5 mm Ø.
Core lacks sulphidic smell.
Samples taken at approx. 37-40, 70-72, 99-102 cm.

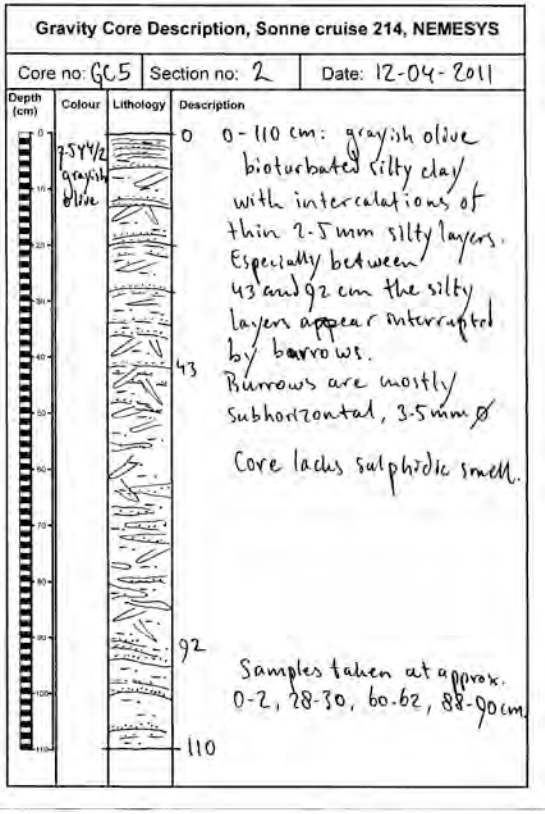
Gravity Core Description, Sonne cruise 214, NEMESYS
Core no: GC5
Section no: 2
Date: 12-04-2011
Depth (cm)
Colour
Lithology
Description
0
7.5Y4/2 grayish olive
43
92
110
0-110 cm: grayish olive bioturbated silty clay with intercalations of thin 2-5 mm silty layers. Especially between 43 and 92 cm the silty layers appear interrupted by burrows.
Burrows are mostly subhorizontal, 3-5 mm Ø
Core lacks sulphidic smell.
Samples taken at approx. 0-2, 28-30, 60-62, 88-90 cm

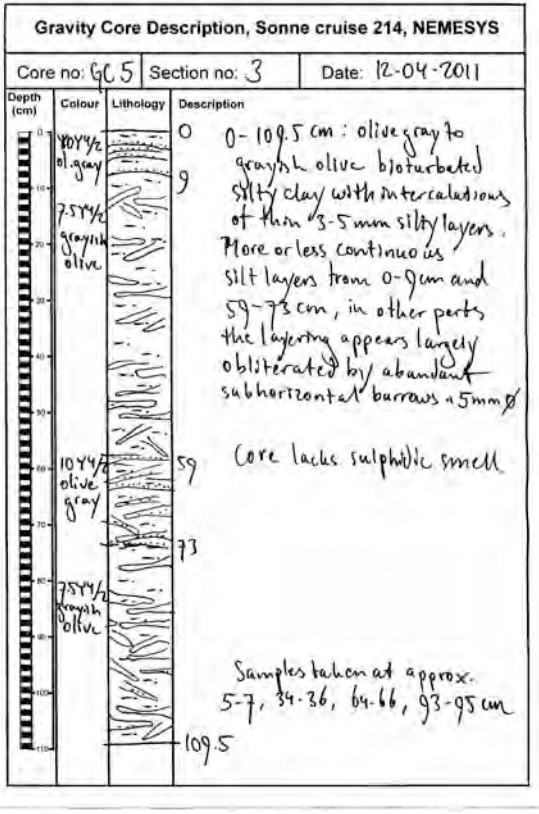
Gravity Core Description, Sonne cruise 214, NEMESYS
Core no: GC 5
Section no: 3
Date: 12-04-2011
Depth (cm)
Colour
Lithology
Description
0
10Y4/2 ol. gray
9
7.5Y4/2 grayish olive
59
10Y4/2 olive gray
73
7.5Y4/2 grayish olive
109.5
0-109.5 cm: olive gray to grayish olive bioturbated silty clay with intercalations of thin 3-5 mm silty layers. More or less continuous silt layers from 0-9 cm and 59-73 cm, in other parts the layering appears largely obliterated by abundant subhorizontal burrows ~5 mm Ø
Core lacks sulphidic smell
Samples taken at approx. 5-7, 34-36, 64-66, 93-95 cm

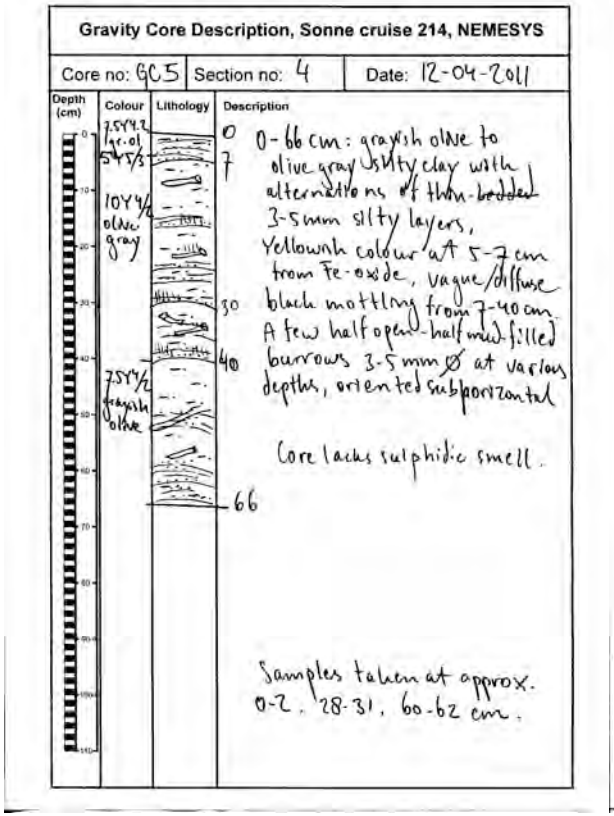
Gravity Core Description, Sonne cruise 214, NEMESYS
Core no: GC5
Section no: 4
Date: 12-04-2011
Depth (cm)
Colour
Lithology
Description
7.5Y4/2 grayish olive
10Y4/2 olive gray
7.5Y4/2 grayish olive
0
7
30
40
66
0-66 cm: grayish olive to olive gray silty clay with alternations of thin-bedded 3-5 mm silty layers, Yellowish colour at 5-7 cm from Fe-oxide, vague/diffuse black mottling from 7-40 cm. A few half open-half mud-filled burrows 3-5 mm Ø at various depths, oriented subhorizontal
Core lacks sulphidic smell.
Samples taken at approx. 0-2, 28-31, 60-62 cm.

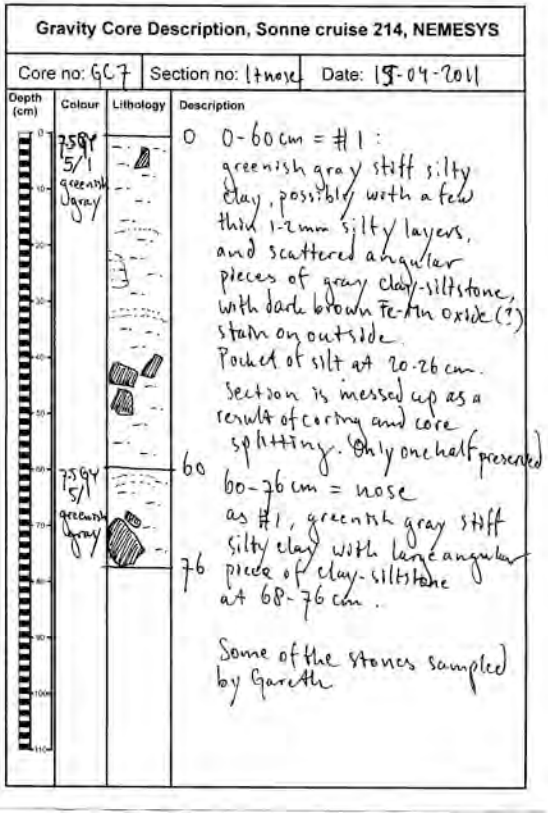
Gravity Core Description, Sonne cruise 214, NEMESYS
Core no: GC7
Section no: 1+nose
Date: 15-04-2011
Depth (cm)
Colour
Lithology
Description
7.5GY 5/1 greenish gray
7.5GY 5/1 greenish gray
0
60
76
0-60 cm = #1: greenish gray stiff silty clay, possibly with a few thin 1-2 mm silty layers, and scattered angular pieces of gray clay-siltstone, with dark brown Fe-Mn oxide (?) stain on outside. Pocket of silt at 20-26 cm. Section is messed up as a result of coring and core splitting. Only one half preserved
60-76 cm = nose as #1, greenish gray stiff silty clay with large angular piece of clay-siltstone at 68-76 cm.
Some of the stones sampled by Gareth

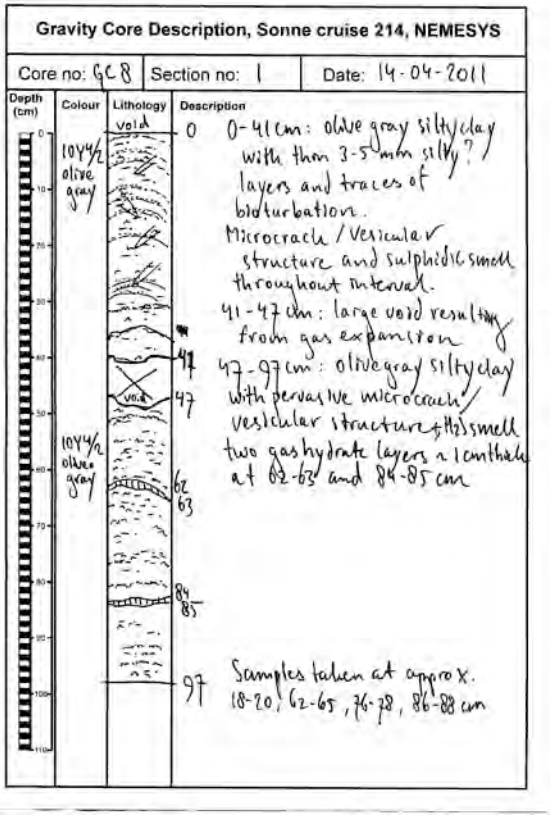
Gravity Core Description, Sonne cruise 214, NEMESYS
Core no: GC8
Section no: 1
Date: 14-04-2011
Depth (cm)
Colour
Lithology
Description
void
10Y4/2 olive gray
10Y4/2 olive gray
void
0
41
47
62
63
84
85
97
0-41 cm: olive gray silty clay with thin 3-5 mm silty? layers and traces of bioturbation. Microcrack / vesicular structure and sulphidic smell throughout interval.
41-47 cm: large void resulting from gas expansion
47-97 cm: olive gray silty clay with pervasive microcrack/vesicular structure & H2S smell two gas hydrate layers a 1 cm thick at 62-63 and 84-85 cm
Samples taken at approx. 18-20, 62-65, 76-78, 86-88 cm

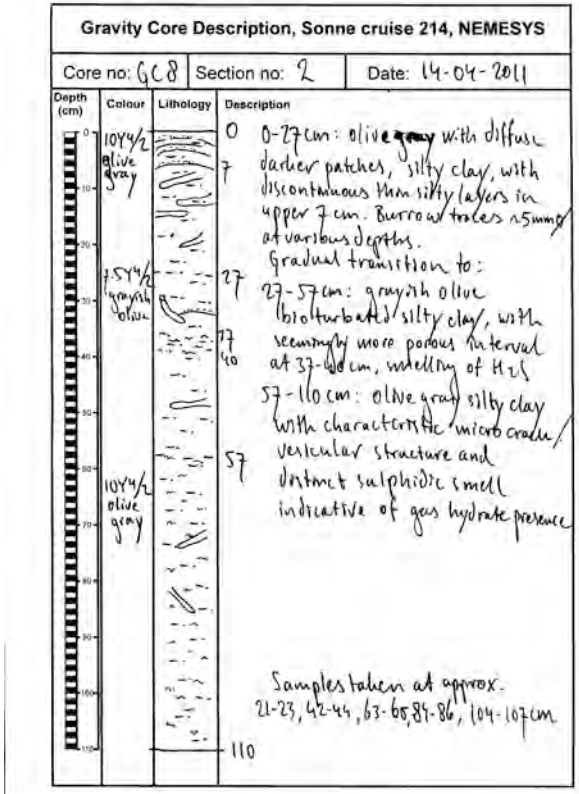
Gravity Core Description, Sonne cruise 214, NEMESYS
Core no: GC 8
Section no: 2
Date: 14-04-2011
Depth (cm)
Colour
Lithology
Description
10Y4/2 olive gray
7.5Y4/2 grayish olive
10Y4/2 olive gray
0
7
27
77
40
57
110
0-27 cm: olive gray with diffuse darker patches, silty clay, with discontinuous thin silty layers in upper 7 cm. Burrow traces ≤5mm Ø at various depths.
Gradual transition to:
27-57 cm: grayish olive bioturbated silty clay, with seemingly more porous interval at 37-40 cm, smelling of H2S
57-110 cm: olive gray silty clay with characteristic microbrecciated vesicular structure and distinct sulphidic smell indicative of gas hydrate presence
Samples taken at approx.
21-23, 42-44, 63-65, 84-86, 104-107 cm

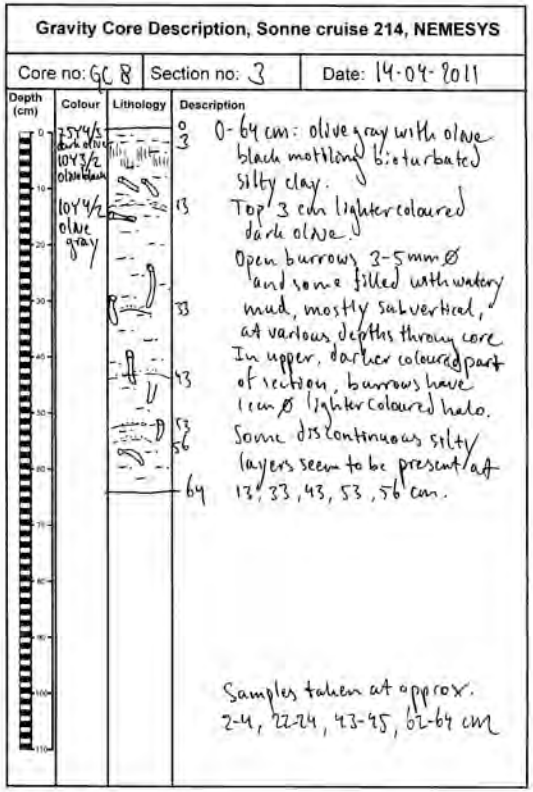
Gravity Core Description, Sonne cruise 214, NEMESYS
Core no: GC 8
Section no: 3
Date: 14-04-2011
Depth (cm)
Colour
Lithology
Description
10Y4/2 olive gray
0
3
13
33
43
53
56
64
0-64 cm: olive gray with olive black mottling, bioturbated silty clay.
Top 3 cm lighter coloured dark olive.
Open burrows 3-5 mm Ø and some filled with watery mud, mostly subvertical, at various depths throughout core.
In upper, darker coloured part of section, burrows have 1 cm Ø lighter coloured halo.
Some discontinuous silty layers seem to be present at 13, 33, 43, 53, 56 cm.
Samples taken at approx.
2-4, 22-24, 43-45, 62-64 cm

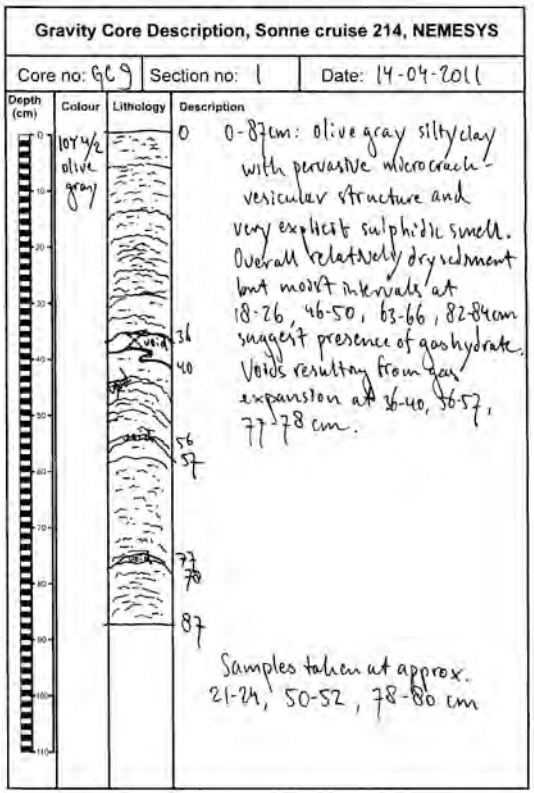
Gravity Core Description, Sonne cruise 214, NEMESYS
Core no: GC 9
Section no: 1
Date: 14-04-2011
Depth (cm)
Colour
Lithology
Description
10Y4/2 olive gray
0
36
40
56
57
77
78
87
0-87 cm: olive gray silty clay with pervasive microcrack-vesicular structure and very explicit sulphidic smell. Overall relatively dry sediment but moist intervals at 18-26, 46-50, 63-66, 82-84 cm suggest presence of gas hydrate. Voids resulting from gas expansion at 36-40, 56-57, 77-78 cm.
Samples taken at approx.
21-24, 50-52, 78-80 cm

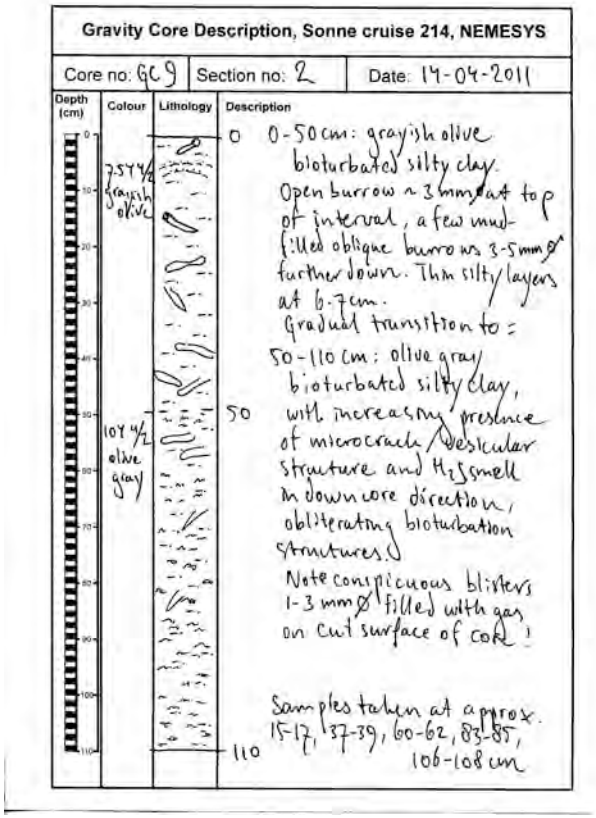
Gravity Core Description, Sonne cruise 214, NEMESYS
Core no: GC 9
Section no: 2
Date: 14-04-2011
Depth (cm)
Colour
Lithology
Description
0
0-50 cm: grayish olive bioturbated silty clay. Open burrow ~ 3 mm Ø at top of interval, a few mud-filled oblique burrows 3-5 mm Ø further down. Thin silty layers at 6-7 cm. Gradual transition to:
50
50-110 cm: olive gray bioturbated silty clay, with increasing presence of microcrack/vesicular structure and H2S smell in down core direction, obliterating bioturbation structures. Note conspicuous blisters 1-3 mm Ø filled with gas on cut surface of core!
Samples taken at approx. 15-17, 37-39, 60-62, 83-85, 106-108 cm
110
7.5Y 4/2 grayish olive
10Y 4/2 olive gray

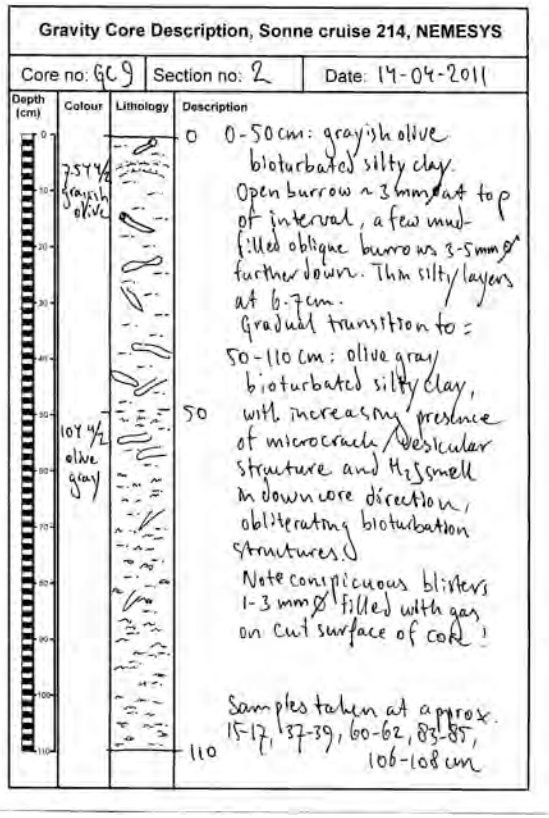
Gravity Core Description, Sonne cruise 214, NEMESYS
Core no: GC 9
Section no: 2
Date: 14-04-2011
Depth (cm)
Colour
Lithology
Description
0
0-50 cm: grayish olive bioturbated silty clay. Open burrow ~ 3 mm Ø at top of interval, a few mud-filled oblique burrows 3-5 mm Ø further down. Thin silty layers at 6-7 cm. Gradual transition to:
50
50-110 cm: olive gray bioturbated silty clay, with increasing presence of microcrack/vesicular structure and H2S smell in down core direction, obliterating bioturbation structures. Note conspicuous blisters 1-3 mm Ø filled with gas on cut surface of core!
Samples taken at approx. 15-17, 37-39, 60-62, 83-85, 106-108 cm
110
7.5Y 4/2 grayish olive
10Y 4/2 olive gray

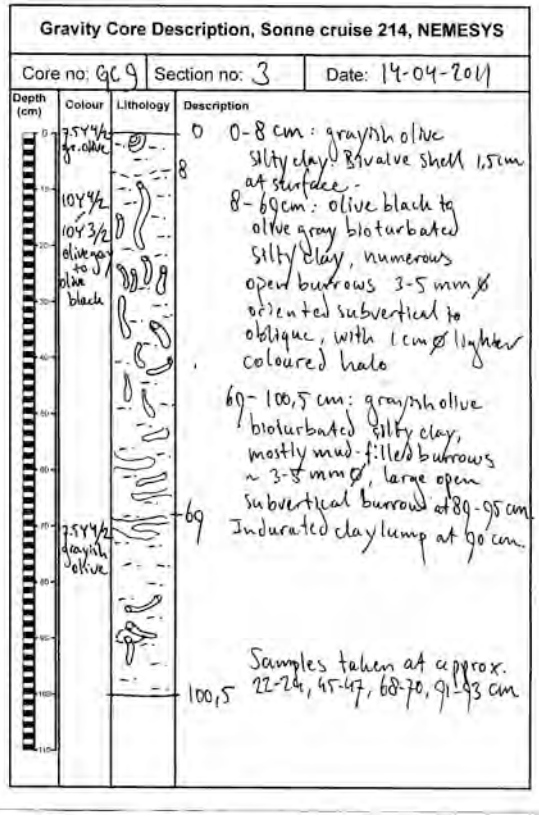
Gravity Core Description, Sonne cruise 214, NEMESYS
Core no: GC 9
Section no: 3
Date: 14-04-2011
Depth (cm)
Colour
Lithology
Description
0
0-8 cm: grayish olive silty clay. Bivalve shell 1,5 cm at surface.
8
8-69 cm: olive black to olive gray bioturbated silty clay, numerous open burrows 3-5 mm Ø oriented subvertical to oblique, with 1 cm Ø lighter coloured halo
69
69-100,5 cm: grayish olive bioturbated silty clay, mostly mud-filled burrows ~ 3-5 mm Ø, large open subvertical burrow at 89-95 cm. Indurated clay lump at 90 cm.
Samples taken at approx. 22-24, 45-47, 68-70, 91-93 cm
100,5
7.5Y 4/2 gr. olive
10Y 4/2
10Y 3/2 olive gray to olive black
7.5Y 4/2 grayish olive

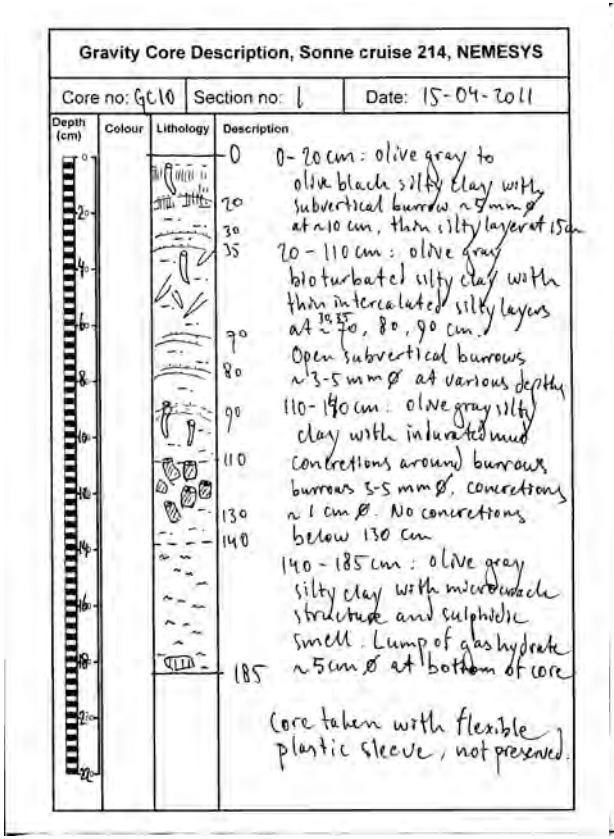

Gravity Core Description, Sonne cruise 214, NEMESYS

Core no: GC10 | Section no: 1 | Date: 15-04-2011

Depth (cm) | Colour | Lithology | Description

0 – 0-20 cm: olive gray to olive black silty clay with subvertical burrow ~5 mm Ø at ~10 cm, thin silty layer at 15 cm

20

30

35 – 20-110 cm: olive gray bioturbated silty clay with thin intercalated silty layers at ~70, 80, 90 cm. Open subvertical burrows ~3-5 mm Ø at various depths

70

80

90 – 110-140 cm: olive gray silty clay with indurated mud concretions around burrows, burrows 3-5 mm Ø, concretions ~1 cm Ø. No concretions below 130 cm

110

130

140 – 140-185 cm: olive gray silty clay with microburrow structure and sulphidic smell. Lump of gashydrate ~5 cm Ø at bottom of core

185

Core taken with flexible plastic sleeve, not preserved.

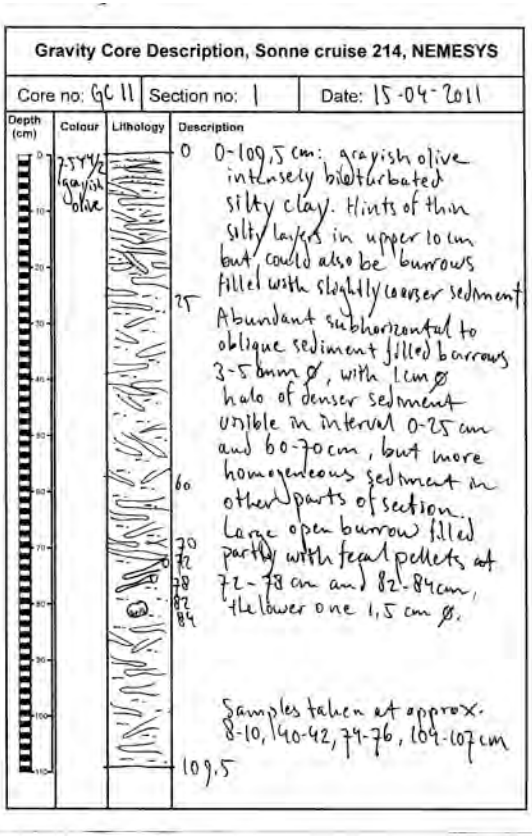

Gravity Core Description, Sonne cruise 214, NEMESYS

Core no: GC11 | Section no: 1 | Date: 15-04-2011

Depth (cm) | Colour | Lithology | Description

7.5Y4/2 grayish olive

0 – 0-109,5 cm: grayish olive intensely bioturbated silty clay. Hints of thin silty layers in upper 10 cm but could also be burrows filled with slightly coarser sediment

25 – Abundant subhorizontal to oblique sediment filled burrows 3-5 mm Ø, with 1 cm Ø halo of denser sediment visible in interval 0-25 cm and 60-70 cm, but more homogeneous sediment in other parts of section. Large open burrow filled partly with fecal pellets at 72-78 cm and 82-84 cm, the lower one 1,5 cm Ø.

60

70

72

78

82

84

Samples taken at approx. 8-10, 140-142, 74-76, 104-107 cm

109,5

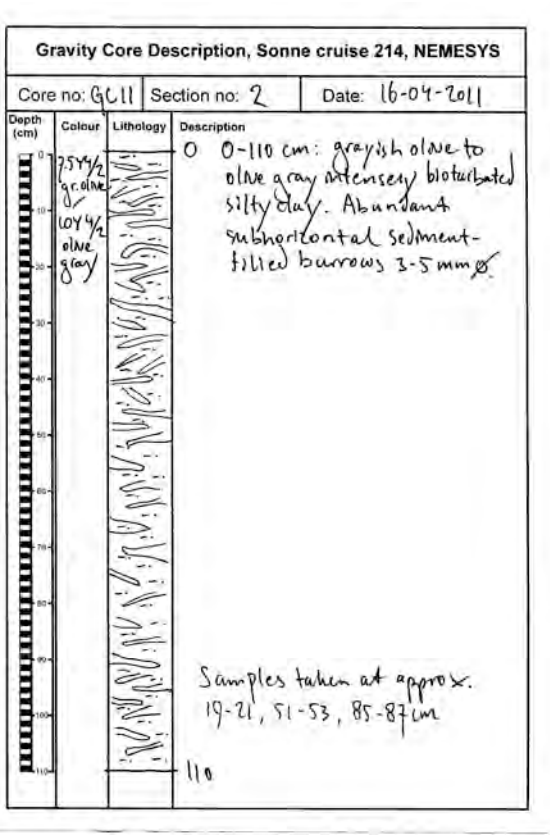

Gravity Core Description, Sonne cruise 214, NEMESYS

Core no: GC11 | Section no: 2 | Date: 16-04-2011

Depth (cm) | Colour | Lithology | Description

7.5Y4/2 gr. olive

10Y4/2 olive gray

0 – 0-110 cm: grayish olive to olive gray intensely bioturbated silty clay. Abundant subhorizontal sediment-filled burrows 3-5 mm Ø.

Samples taken at approx. 19-21, 51-53, 85-87 cm

110

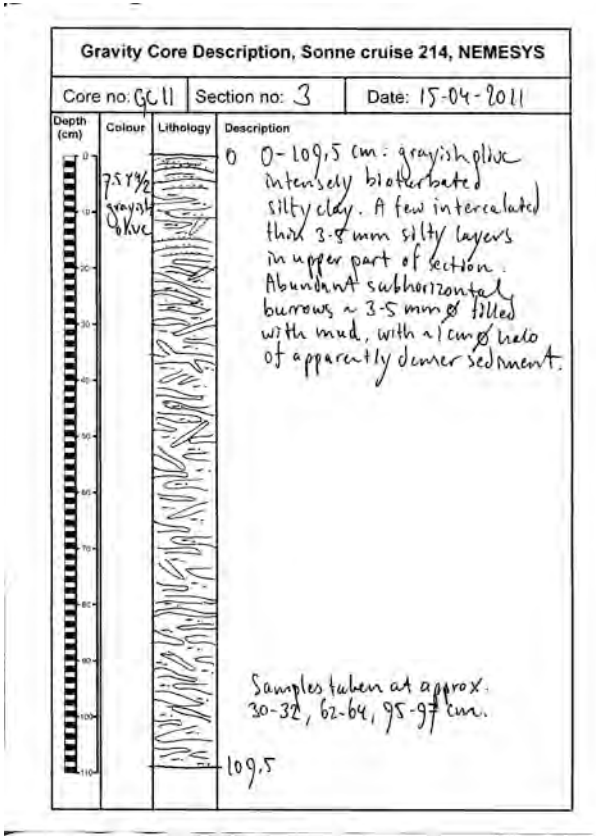
Gravity Core Description, Sonne cruise 214, NEMESYS
Core no: GC 11
Section no: 3
Date: 15-04-2011
Depth (cm)
Colour
Lithology
Description
0 0-109,5 cm: grayish olive intensely bioturbated silty clay. A few intercalated thin 3-8 mm silty layers in upper part of section. Abundant subhorizontal burrows ~ 3-5 mm Ø filled with mud, with ~1 cm Ø halo of apparently denser sediment.
7.5Y 3/2 grayish olive
Samples taken at approx. 30-32, 62-64, 95-97 cm.
109,5

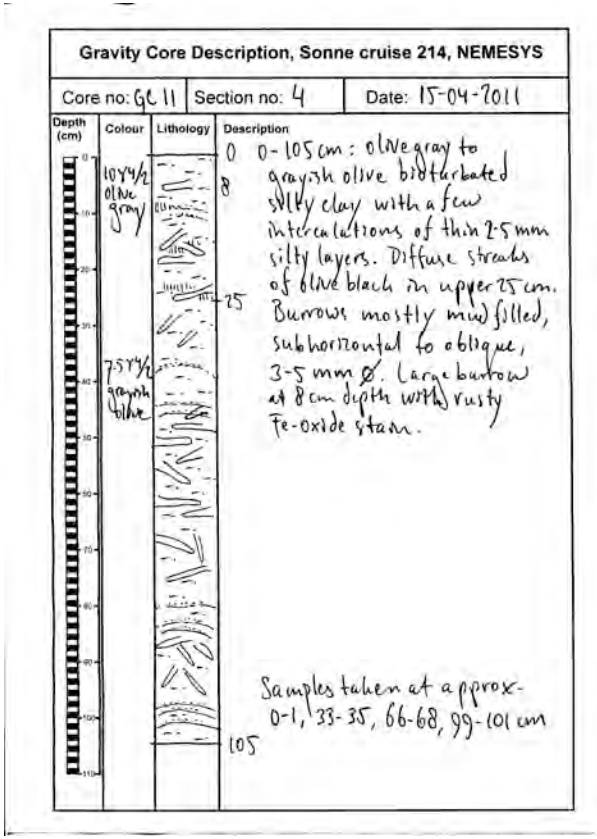
Gravity Core Description, Sonne cruise 214, NEMESYS
Core no: GC 11
Section no: 4
Date: 15-04-2011
Depth (cm)
Colour
Lithology
Description
0 0-105 cm: olive gray to grayish olive bioturbated silty clay with a few intercalations of thin 2-5 mm silty layers. Diffuse streaks of olive black in upper 25 cm. Burrows mostly mud filled, subhorizontal to oblique, 3-5 mm Ø. Large burrow at 8 cm depth with rusty Fe-oxide stain.
10Y 4/2 olive gray
7.5Y 3/2 grayish olive
8
25
Samples taken at approx. 0-1, 33-35, 66-68, 99-101 cm
105

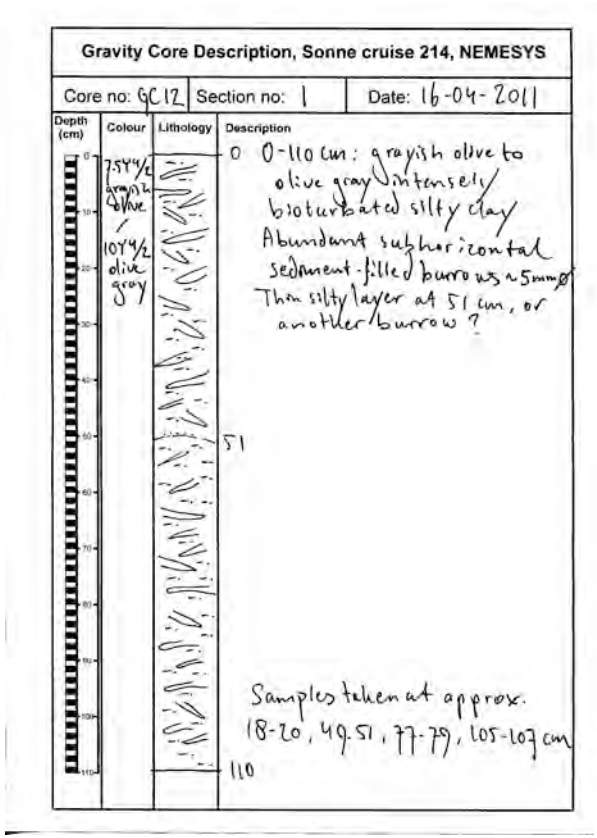
Gravity Core Description, Sonne cruise 214, NEMESYS
Core no: GC 12
Section no: 1
Date: 16-04-2011
Depth (cm)
Colour
Lithology
Description
0 0-110 cm: grayish olive to olive gray intensely bioturbated silty clay. Abundant subhorizontal sediment-filled burrows ~5 mm Ø. Thin silty layer at 51 cm, or another burrow?
7.5Y 3/2 grayish olive
10Y 4/2 olive gray
51
Samples taken at approx. 18-20, 49-51, 77-79, 105-107 cm
110

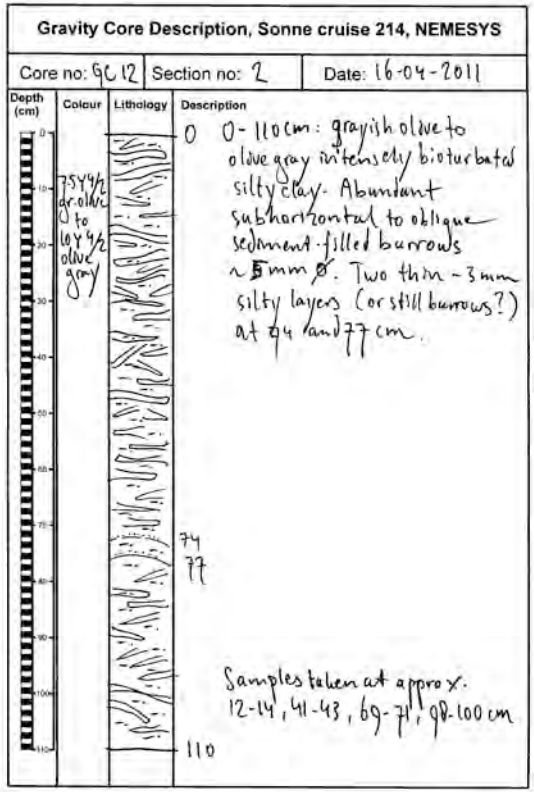
Gravity Core Description, Sonne cruise 214, NEMESYS
Core no: GC 12
Section no: 2
Date: 16-04-2011
Depth (cm)
Colour
Lithology
Description
0
0-110 cm: grayish olive to olive gray intensely bioturbated silty clay. Abundant subhorizontal to oblique sediment-filled burrows ~5 mm Ø. Two thin ~3 mm silty layers (or still burrows?) at 74 and 77 cm.
7.5Y 4/2 gr. olive to 10Y 4/2 olive gray
74
77
Samples taken at approx. 12-14, 41-43, 69-71, 98-100 cm
110

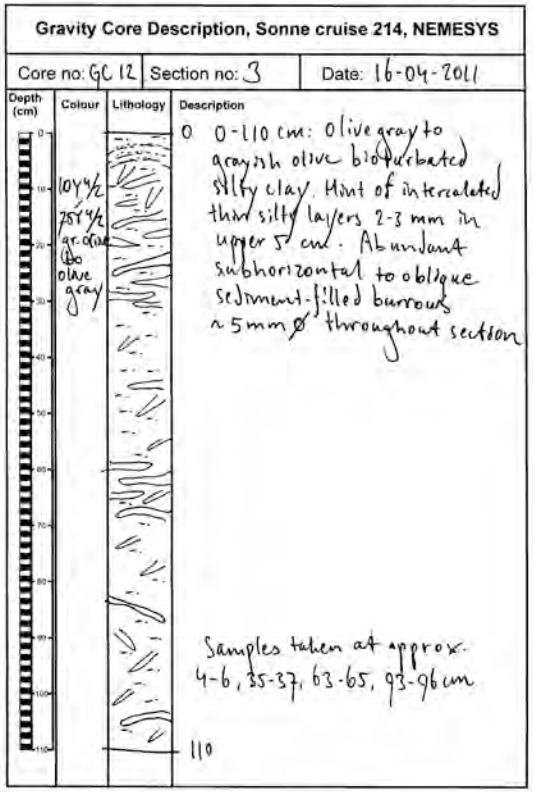
Gravity Core Description, Sonne cruise 214, NEMESYS
Core no: GC 12
Section no: 3
Date: 16-04-2011
Depth (cm)
Colour
Lithology
Description
0
0-110 cm: olive gray to grayish olive bioturbated silty clay. Hint of intercalated thin silty layers 2-3 mm in upper 5 cm. Abundant subhorizontal to oblique sediment-filled burrows ~5 mm Ø throughout section
10Y 4/2
7.5Y 4/2 gr. olive to olive gray
Samples taken at approx. 4-6, 35-37, 63-65, 93-96 cm
110

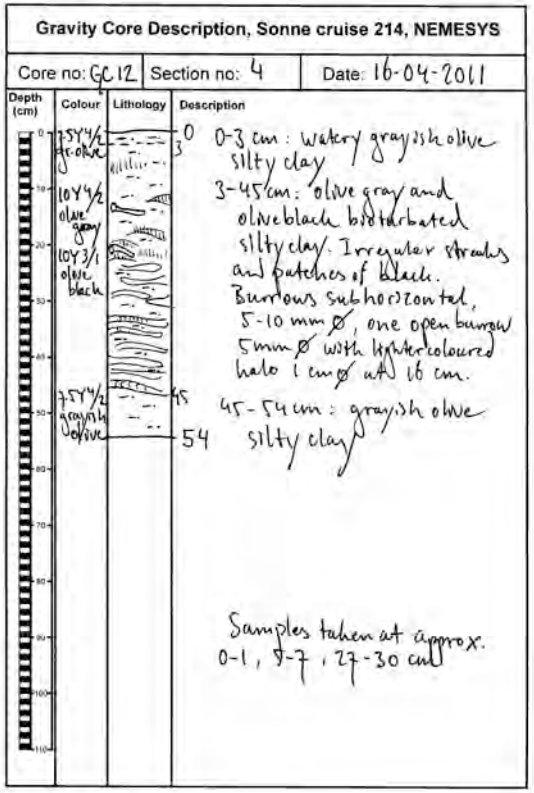
Gravity Core Description, Sonne cruise 214, NEMESYS
Core no: GC 12
Section no: 4
Date: 16-04-2011
Depth (cm)
Colour
Lithology
Description
0
0-3 cm: watery grayish olive silty clay
3-45 cm: olive gray and olive black bioturbated silty clay. Irregular streaks and patches of black. Burrows subhorizontal, 5-10 mm Ø, one open burrow 5 mm Ø with lighter coloured halo 1 cm Ø at 16 cm.
7.5Y 4/2 gr. olive
10Y 4/2 olive gray
10Y 3/1 olive black
3
45
45-54 cm: grayish olive silty clay
54
Samples taken at approx. 0-1, 5-7, 27-30 cm

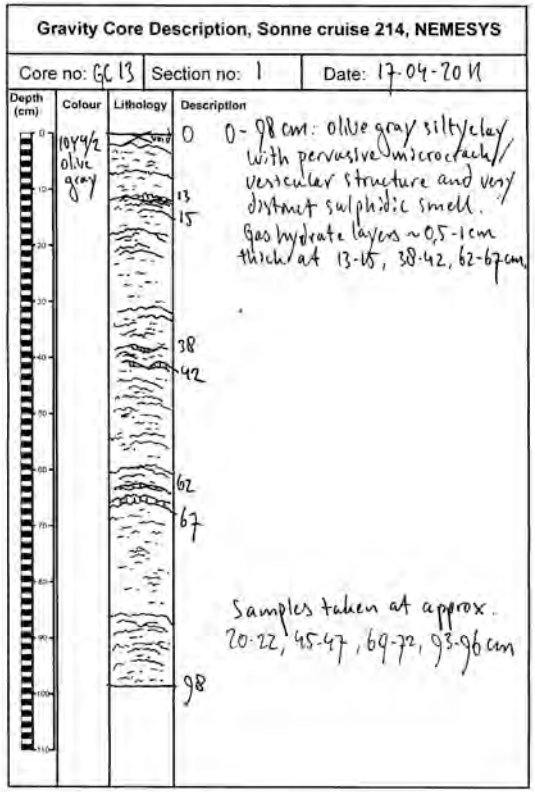

Gravity Core Description, Sonne cruise 214, NEMESYS

Core no: GC 13 | Section no: 1 | Date: 17-04-2011

Depth (cm)	Colour	Lithology	Description
0	10Y4/2 olive gray		0-98 cm: olive gray silty clay with pervasive microcracks/ vesicular structure and very distinct sulphidic smell. Gas hydrate layers ~0,5-1 cm thick at 13-15, 38-42, 62-67 cm.
13			
15			
38			
42			
62			
67			
98			Samples taken at approx. 20-22, 45-47, 69-72, 93-96 cm

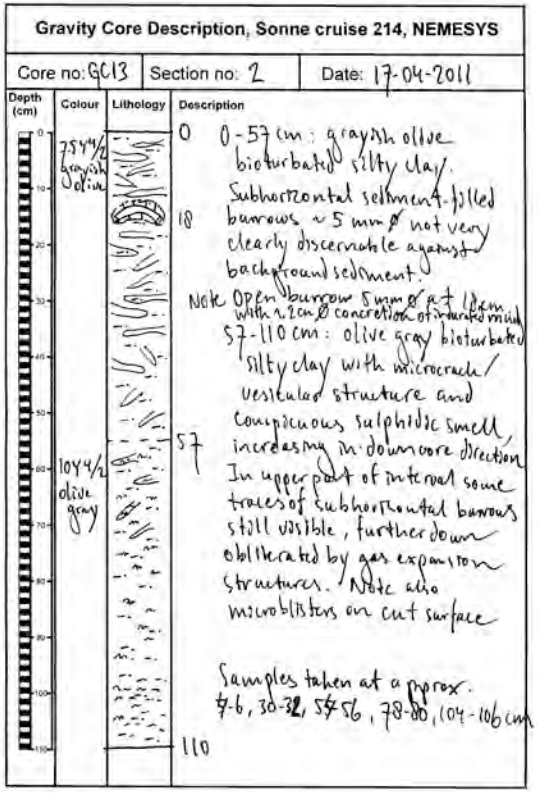

Gravity Core Description, Sonne cruise 214, NEMESYS

Core no: GC13 | Section no: 2 | Date: 17-04-2011

Depth (cm)	Colour	Lithology	Description
0	7.5Y4/2 grayish olive		0-57 cm: grayish olive bioturbated silty clay. Subhorizontal sediment-filled burrows ~5 mm Ø not very clearly discernable against background sediment.
18			Note: Open burrow 5 mm Ø at 18 cm with a 2 cm Ø concretion of surrounding mud
57	10Y4/2 olive gray		57-110 cm: olive gray bioturbated silty clay with microcrack/ vesiculated structure and conspicuous sulphidic smell, increasing in downcore direction. In upper part of interval some traces of subhorizontal burrows still visible, further down obliterated by gas expansion structures. Note also microblisters on cut surface
110			Samples taken at approx. 4-6, 30-32, 54-56, 78-80, 104-106 cm

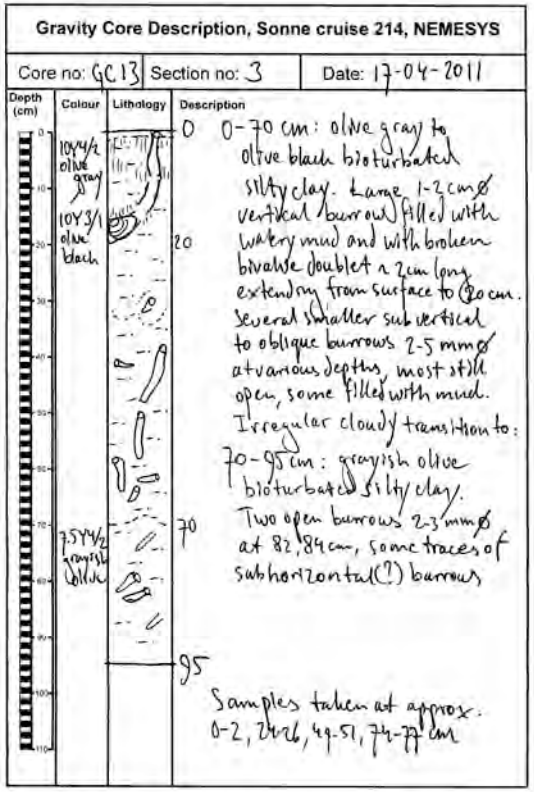

Gravity Core Description, Sonne cruise 214, NEMESYS

Core no: GC13 | Section no: 3 | Date: 17-04-2011

Depth (cm)	Colour	Lithology	Description
0	10Y4/2 olive gray		0-70 cm: olive gray to olive black bioturbated silty clay. Large 1-2 cm Ø vertical burrow filled with watery mud and with broken bivalve doublet ~2 cm long extending from surface to 20 cm. Several smaller subvertical to oblique burrows 2-5 mm Ø at various depths, most still open, some filled with mud. Irregular cloudy transition to:
20	10Y3/1 olive black		70-95 cm: grayish olive bioturbated silty clay. Two open burrows 2-3 mm Ø at 82, 84 cm, some traces of subhorizontal(?) burrows
70	7.5Y4/2 grayish olive		
95			Samples taken at approx. 0-2, 24-26, 49-51, 74-77 cm

9.3. OBS Station lists

9.3.1 P1 Omakere

SO214-PROFILE1 OMAKERE

STATION	FLOATATION	LATITUDE (S)	LONGITUDE (E)	DEPTH (m)	DEPLOY. DATE	RELEASECODE	INSTRUMENT	CH.	CYLINDER	RECORDER
OBS_01	35	40°3,513'	177°49,618'	1093	12.03.11	131351	HTI 59 + Owen 1001-120	C	72	MLS 050817
OBS_02 + Methan	804	40°3,349'	177°49,435'	1095	12.03.11	533770	HTI 117 + Owen 87	B	96	MLS 081001
OBS_03 + Methan	59	40°3,104'	177°49,259'	1088	12.03.11	646426	HTI 30 + Owen 33	C	77	MLS 991260
OBS_04	50	40°3,035'	177°49,086'	1100	12.03.11	133664	HTI 51 + Owen ?	C	87	MLS 991251
OBS_05	18	40°2,864'	177°48,912'	1131	12.03.11	442144	HTI 29 + Owen 1001-114	D	K 10	MLS 010408
OBS_06	39	40°2,461'	177°48,257'	1164	12.03.11	133770	OAS 46 + Owen 1001-113	C	44	MLS 9912
OBS_07	57	40°2,274'	177°48,080'	1157	12.03.11	131245	HTI 38 + Owen 0509075	D	39	MBS 020501
OBS_08 +Sercel	809	40°2,117'	177°47,898'	1157	12.03.11	534071	HTI 46 + Owen 90	D	809	MBS 980902
OBS_09	54	40°1,953'	177°47,712'	1174	12.03.11	134071	HTI ? + Owen 1001-118	A	66	MBS 980904
OBS_10	41	40°1,789'	177°47,535'	1194	12.03.11	143175	HTI 90 + Owen 1001-121	A	K 19	MLS 991258

9.3.2 P2 Porangahau

SO214-PROFILE2 PORANGAHAU

STATION	FLOATATION	LATITUDE (S)	LONGITUDE (E)	DEPTH (m)	DEPLOY. DATE	RELEASECODE	INSTRUMENT	CH.	CYLINDER	RECORDER
OBS_01 + Methan	41	40°48.421'	177°24.854'	1954	20.03.11	143175	HTI 90 + Owen 1001-121 + Methan T25/T28	D	96	MBS 980902
OBS_02 + Methan	50	40°48.945'	177°24.655'	1947	20.03.11	133664	HTI 51 + Owen ? + Methan T25/T29	C	39	MLS 991260
OBS_03 + Methan	59	40°49.174'	177°25.565'	2018	20.03.11	646426	HTI 30 + Owen 33 + Methan T25/T27	D	66	MLS 081001
OBS_04	804	40°48.662'	177°25.774'	2014	20.03.11	533770	HTI 117 + Owen 87	B	77	MBS 980901/980904
OBS_10	54	40°48.673'	177°23.701'	1961	24.03.11	134071	HTI ? + Owen 1001-118	D	K 49	MLS 991252
OBS_11	57	40°48.819'	177°24.179'	1956	24.03.11	131245	HTI 38 + Owen 0509075	A	72?	MLS 991234
OBS_12	18	40°48.975'	177°24.901'	1947	24.03.11	442144	HTI 29 + Owen 1001-114	A	72?	MLS 040304
OBS_13	809	40°49.089'	177°25.242'	1992	24.03.11	534071	HTI 46 + Owen 90	C	K 10	MLS 991246
OBS_14	39	40°49.263'	177°26.063'	2051	24.03.11	133770	OAS 46 + Owen 1001-113	C	87	MLS 991256

9.3.3 P3 Wairarapa

Station	Latitude (S)	Longitude (E)	Depth (m)	Deploy.Date	Recov. Date	Release Code	Recorder	Floatation	Hydrophone	Geophone (4,5Hz)	Remarks
OBS 01	41° 46.943'	175° 22.734'	1045	28.03.2011	02.04.2011	534071	MLS 991234	809	46	90	
OBS 02	41° 46.774'	175° 23.282'	1023	28.03.2011	02.04.2011	442144	MBS 980901	18	29	1001-114	
OBS 03	41° 46.619'	175° 23.714'	1025	28.03.2011	02.04.2011	131351	MLS 040304	35	59	1001-120	
OBS 04	41° 46.857'	175° 24.200'	1054	28.03.2011	02.04.2011	134071	MLS 040803	54	?	1001-118	
OBS 05	41° 46.979'	175° 23.958'	1034	28.03.2011	05.04.2011	533770	MLS 991246	804	117	87	Time release
OBS 06	41° 47.065'	175° 23.715'	1044	28.03.2011	02.04.2011	133664	MLS 980902	50	51	?	
OBS 07	41° 47.150'	175° 23.473'	1051	28.03.2011	02.04.2011	133770	MLS 991256	?	?	?	T29 Methane
OBS 08	41° 47.247'	175° 23.231'	1064	28.03.2011	02.04.2011	131245	MBS 020501	57	38	55	
OBS 09	41° 47.337'	175° 22.992'	1071	28.03.2011	02.04.2011	533664	MLS 010403	808	73	103311	
OBS 10	41° 47.423'	175° 22.762'	1085	28.03.2011	02.04.2011	143175	MLS 010402	41	90	?	
OBS 11	41° 47.699'	175° 23.264'	1099	28.03.2011	02.04.2011	534224	MLS 991240	811	83	103312	
OBS 12	41° 47.495'	175° 23.778'	1079	28.03.2011	02.04.2011	533622	MLS 081201	812	87	?	
OBS 13	41° 47.336'	175° 24.205'	1070	28.03.2011	02.04.2011	534165	MLS 010406	806	75	88	

9.4 CSEM Deployment Details

Pig Coordinates **Profile CSEM-SO214-1**

Times on Sites (UTC)			
13:01:10 - 13:08:59	Pig1	175:26.5523	-41:46.0072
13:34:25 - 13:42:48	Pig2	175:26.1597	-41:46.1797
13:51:15 - 13:52:30, 13:52:54 -13:57:24	Pig3	175:26.0367	-41:46.2287
14:08:00 - 14:08:59, 14:09:15 - 14:09:55	Pig4	175:25.9137	-41:46.2797
14:10:10 - 14:11:10, 14:11:30 - 14:12:05			
14:12:20 - 14:13:59, 14:14:37 - 14:15:50			
14:28:25 - 14:32:35, 14:32:55 - 14:36:15	Pig5	175:25.6547	-41:46.3679
14:36:28 - 14:36:59			
14:46:00 - 14:48:05, 14:48:17 - 14:52:22	Pig6	175:25.4819	-41:46.4287
14:52:45 - 14:54:48			
15:06:00 - 15:13:30	Pig7	175:25.3144	-41:46.4973
15:24:15 - 15:33:59	Pig8	175:25.0998	-41:46.5855
16:00:10 - 16:07:25	Pig9	175:24.8093	-41:46.7188
16:25:25 - 16:56:59	Pig10	175:24.6392	-41:46.7756
17:14:12 - 17:25:59	Pig11	175:24.5058	-41:46.8481
17:41:00 - 17:50:40	Pig12	175:24.3670	-41:46.9167
18:05:10 - 18:13:52	Pig13	175:24.2283	-41:46.9814
18:30:30 - 18:38:59	Pig14	175:24.0739	-41:47.0382
18:53:00 - 18:59:59	Pig15	175:23.8253	-41:47.0892
19:14:12 - 19:19:50	Pig16	175:23.6238	-41:47.1754
19:32:40 - 19:38:59	Pig17	175:23.4537	-41:47.2361
19:53:10 - 19:58:45	Pig18	175:23.3124	-41:47.2969
20:13:20 - 20:18:45	Pig19	175:23.1135	-41:47.3792
20:34:00 - 20:40:50	Pig20	175:22.9198	-41:47.4478
20:53:00 - 21:07:30	Pig21	175:22.7157	-41:47.5183
21:32:40 - 21:37:10	Pig22	175:22.3859	-41:47.6359
21:51:20 - 21:52:30	Pig23	175:22.1792	-41:47.7143
22:16:45 - 22:30:40	Pig24	175:21.8782	-41:47.8514
22:47:00 - 22:53:40	Pig25	175:21.6191	-41:47.9827
23:09:00 - 23:13:59	Pig26	175:21.4045	-41:48.0670

Pig Coordinates **Profile CSEM-SO214-2**

Times on Sites (UTC)	Calibration		
03:01:18 – 03:05:10	P2_00		
03:51:24 – 03:53:58	P2_01	-41:46.2877	175:26.0078
04:18:00 – 04:25:52	P2_02	-41:46.4007	175:25.6331
04:45:00 – 04:58:20	P2_03	-41:46.4591	175:25.3508
05:12:35 – 05:22:40	P2_04	-41:46.5429	175:25.0880
05:32:52 – 05:41:42	P2_05	-41:46.6531	175:24.8313
06:01:00 – 06:09:32	P2_06	-41:46.7269	175:24.5795
06:22:50 – 06:31:01	P2_07	-41:46.7925	175:24.3619
06:46:35 – 06:53:22	P2_08	-41:46.8415	175:24.2066
07:02:30 – 07:08:10	P2_09	-41:46.8537	175:24.1330
07:15:35 – 07:19:51	P2_10	-41:46.9088	175:24.0186

07:28:08 – 07:34:16	P2_11	-41:46.9353	175:23.9097
07:42:15 – 07:47:27	P2_12	-41:46.9761	175:23.7653
07:58:00 – 08:03:09	P2_13	-41:47.0210	175:23.6237
08:14:20 – 08:20:08	P2_14	-41:47.0985	175:23.3785
08:36:35 – 08:43:40	P2_15	-41:47.1719	175:23.1524
08:54:00 – 09:03:10	P2_16	-41:47.2440	175:22.9263
09:16:50 – 09:25:30	P2_17	-41:47.3254	175:22.6549
09:42:00 – 09:50:52	P2_18	-41:47.4183	175:22.4234
10:02:45 – 10:11:31	P2_19	-41:47.5018	175:22.1163
10:25:40 – 10:34:45	P2_20	-41:47.6105	175:21.8071
10:48:24 – 10:56:04	P2_21	-41:47.7239	175:21.4452
11:11:45 – 11:19:59	P2_22	-41:47.7924	175:21.2117
11:30:10 – 11:39:20			

Pig Coordinates **Profile CSEM-SO214-3**

Times on Sites (UTC)			
14:49:10 – 14:57:23	P3_01	-41:47.7312	175:21.9449
15:09:40 – 15:18:52	P3_02	-41:47.6659	175:22.3037
15:24:53 – 15:33:59	P3_03	-41:47.6441	175:22.4879
15:41:53 – 15:50:35	P3_04	-41:47.6223	175:22.6560
16:09:40 – 16:19:48	P3_05	-41:47.5618	175:23.0310
16:41:40 – 16:52:14	P3_06	-41:47.4916	175:23.4544
17:10:25 – 17:16:40	P3_07	-41:47.4529	175:23.8520
17:38:45 – 17:46:03	P3_08	-41:47.3754	175:24.1947
17:57:55 – 17:58:57	P3_09	-41:47.3286	175:24.4403

9.5 CTD Locations

Table 6.5.1: Location of CTD casts undertaken during SO214

Station	Date	Time	Longitude	Latitude	Depth [m]	Remarks
#1-CTD-1	3/11/2011	5:47	175:23.8920	-41:50.8200	2120	SVP station S-Opouawe
#5-CTD-2	3/16/2011	8:00	177:48.4080	-40:02.1600	1164	Omakere Ridge
#6-CTD-3	3/16/2011	10:11	177:49.2300	-40:03.1800	1096	Omakere Ridge
#10-CTD-4	3/19/2011	2:44	178:09.6900	-40:01.9200	670	Faure Site
#17-CTD-5	3/23/2011	10:45	176:33.0180	-41:17.4600	720	Uruti Ridge
#26-CTD-6	3/27/2011	22:22	175:27.1620	-41:43.4400	815	Tui
#27-CTD-7	3/28/2011	0:19	175:25.7580	-41:46.3800	1055	Takahe
#28-CTD-8	3/28/2011	2:58	175:24.1500	-41:46.9200	1059	Takahe
#36-CTD-9	4/3/2011	5:35	175:24.7200	-41:47.4600	1055	Takahe
#37-CTD-10	4/3/2011	7:52	175:22.6920	-41:47.8800	1090	Takahe
#42-CTD-11	4/9/2011	1:29	175:25.6620	-41:46.5000	1055	Takahe
#45-CTD-12	4/9/2011	9:00	175:25.6320	-41:46.8000	1058	Takahe
#47-CTD-13	4/9/2011	12:31	175:25.6500	-41:46.6200	1052	Takahe
#49-CTD-14	4/9/2011	16:17	175:25.4880	-41:46.9800	1082	Takahe
#50-CTD-15	4/9/2011	18:23	175:25.6200	-41:46.3200	1054	Takahe
#57-CTD-16	4/11/2011	10:49	175:25.7400	-41:46.1400	1056	Takahe
#59-CTD-17	4/11/2011	13:43	175:25.7100	-41:46.6200	1054	Takahe
#61-CTD-18	4/11/2011	17:04	175:25.6380	-41:46.3200	1053	Takahe
#76-CTD-19	4/13/2011	16:13	175:25.6020	-41:46.3800	1054	Takahe
#81-CTD-20	4/15/2011	3:10	175:25.4700	-41:46.3800	1053	Takahe
#84-CTD-21	4/15/2011	8:42	175:25.3200	-41:46.4400	1052	Takahe
#86-CTD-22a	4/15/2011	12:22	175:25.7700	-41:46.2600	1059	Takahe
#86-CTD-22b	4/15/2011	12:22	175:25.7100	-41:46.3200	1059	Takahe
#86-CTD-22c	4/15/2011	12:22	175:25.6080	-41:46.3200	1059	Takahe
#86-CTD-22d	4/15/2011	12:22	175:25.5060	-41:46.3800	1059	Takahe
#87-CTD-23	4/15/2011	16:37	175:25.2000	-41:46.5000	1051	Takahe

Equation used for calculating the N^2 (Brunt–Väisälä) frequency:

ρ=sigma-theta + 1000 [kg/m^3]

Sv = sound velocity [m/s]

Depth [m]

$_{(1)}$ = upper layer

$_{(2)}$ = lower layer

g = 9.81 [m/s^2]

$$N^2 = \frac{-g}{\rho} \times \left(\frac{\partial \sigma_\theta}{\partial z} - \frac{g\rho}{Sv^2} \right)$$

Or

N^2 = -g / (sigma-theta$_{(2)}$+1000) * [(sigma-theta$_{(2)}$ - sigma-theta$_{(1)}$)/(depth$_{(2)}$ - depth$_{(1)}$) - (g * (sigma-theta$_{(2)}$+1000)) / sv^2]

IFM-GEOMAR
Leibniz-Institut für Meereswissenschaften
an der Universität Kiel

IFM-GEOMAR Reports

No.	Title
1	RV Sonne Fahrtbericht / Cruise Report SO 176 & 179 MERAMEX I & II (Merapi Amphibious Experiment) 18.05.-01.06.04 & 16.09.-07.10.04. Ed. by Heidrun Kopp & Ernst R. Flueh, 2004, 206 pp. In English
2	RV Sonne Fahrtbericht / Cruise Report SO 181 TIPTEQ (from The Incoming Plate to mega Thrust EarthQuakes) 06.12.2004.-26.02.2005. Ed. by Ernst R. Flueh & Ingo Grevemeyer, 2005, 533 pp. In English
3	RV Poseidon Fahrtbericht / Cruise Report POS 316 Carbonate Mounds and Aphotic Corals in the NE-Atlantic 03.08.–17.08.2004. Ed. by Olaf Pfannkuche & Christine Utecht, 2005, 64 pp. In English
4	RV Sonne Fahrtbericht / Cruise Report SO 177 - (Sino-German Cooperative Project, South China Sea: Distribution, Formation and Effect of Methane & Gas Hydrate on the Environment) 02.06.-20.07.2004. Ed. by Erwin Suess, Yongyang Huang, Nengyou Wu, Xiqiu Han & Xin Su, 2005, 154 pp. In English and Chinese
5	RV Sonne Fahrtbericht / Cruise Report SO 186 – GITEWS (German Indonesian Tsunami Early Warning System 28.10.-13.1.2005 & 15.11.-28.11.2005 & 07.01.-20.01.2006. Ed. by Ernst R. Flueh, Tilo Schoene & Wilhelm Weinrebe, 2006, 169 pp. In English
6	RV Sonne Fahrtbericht / Cruise Report SO 186 -3 – SeaCause II, 26.02.-16.03.2006. Ed. by Heidrun Kopp & Ernst R. Flueh, 2006, 174 pp. In English
7	RV Meteor, Fahrtbericht / Cruise Report M67/1 CHILE-MARGIN-SURVEY 20.02.-13.03.2006. Ed. by Wilhelm Weinrebe und Silke Schenk, 2006, 112 pp. In English
8	RV Sonne Fahrtbericht / Cruise Report SO 190 - SINDBAD (Seismic and Geoacoustic Investigations Along The Sunda-Banda Arc Transition) 10.11.2006 - 24.12.2006. Ed. by Heidrun Kopp & Ernst R. Flueh, 2006, 193 pp. In English
9	RV Sonne Fahrtbericht / Cruise Report SO 191 - New Vents "Puaretanga Hou" 11.01. - 23.03.2007. Ed. by Jörg Bialas, Jens Greinert, Peter Linke, Olaf Pfannkuche, 2007, 190 pp. In English
10	FS ALKOR Fahrtbericht / Cruise Report AL 275 - Geobiological investigations and sampling of aphotic coral reef ecosystems in the NE-Skagerrak, 24.03. - 30.03.2006, Eds.: Andres Rüggeberg & Armin Form, 39 pp. In English

IFM-GEOMAR
Leibniz-Institut für Meereswissenschaften
an der Universität Kiel

No.	Title
11	FS Sonne / Fahrtbericht / Cruise Report SO 192-1: MANGO: Marine Geoscientific Investigations on the Input and Output of the Kermadec Subduction Zone, 24.03. - 22.04.2007, Ernst Flüh & Heidrun Kopp, 127 pp. In English
12	FS Maria S. Merian / Fahrtbericht / Cruise Report MSM 04-2: Seismic Wide-Angle Profiles, Fort-de-France – Fort-de-France, 03.01. - 19.01.2007, Ed.: Ernst Flüh, 45 pp. In English
13	FS Sonne / Fahrtbericht / Cruise Report SO 193: MANIHIKI Temporal, Spatial, and Tectonic Evolution of Oceanic Plateaus, Suva/Fiji – Apia/Samoa 19.05. - 30.06.2007, Eds.: Reinhard Werner and Folkmar Hauff, 201 pp. In English
14	FS Sonne / Fahrtbericht / Cruise Report SO195: TOTAL TOnga Thrust earthquake Asperity at Louisville Ridge, Suva/Fiji – Suva/Fiji 07.01. - 16.02.2008, Eds.: Ingo Grevemeyer & Ernst R. Flüh, 106 pp. In English
15	RV Poseidon Fahrtbericht / Cruise Report P362-2: West Nile Delta Mud Volcanoes**,** Piräus – Heraklion 09.02. - 25.02.2008, Ed.: Thomas Feseker, 63 pp. In English
16	RV Poseidon Fahrtbericht / Cruise Report P347: Mauritanian Upwelling and Mixing Process Study (MUMP), Las-Palmas - Las Palmas, 18.01. - 05.02.2007, Ed.: Marcus Dengler et al., 34 pp. In English
17	FS Maria S. Merian Fahrtbericht / Cruise Report MSM 04-1: Meridional Overturning Variability Experiment (MOVE 2006), Fort de France – Fort de France, 02.12. – 21.12.2006, Ed.: Thomas J. Müller, 41 pp. In English
18	FS Poseidon Fahrtbericht /Cruise Report P348: SOPRAN: Mauritanian Upwelling Study 2007**,** Las Palmas - Las Palmas**,** 08.02. - 26.02.2007, Ed.: Hermann W. Bange, 42 pp. In English
19	R/V L'ATALANTE Fahrtbericht / Cruise Report IFM-GEOMAR-4: Circulation and Oxygen Distribution in the Tropical Atlantic, Mindelo/Cape Verde - Mindelo/Cape Verde, 23.02. - 15. 03.2008, Ed.: Peter Brandt, 65 pp. In English
20	RRS JAMES COOK Fahrtbericht / Cruise Report JC23-A & B: CHILE-MARGIN-SURVEY, OFEG Barter Cruise with SFB 574, 03.03.-25.03. 2008 Valparaiso – Valparaiso, 26.03.-18.04.2008 Valparaiso - Valparaiso, Eds.: Ernst Flüh & Jörg Bialas, 242 pp. In English
21	FS Poseidon Fahrtbericht / Cruise Report P340 – TYMAS "Tyrrhenische Massivsulfide"**,** Messina – Messina**,** 06.07.-17.07.2006, Eds.: Sven Petersen and Thomas Monecke, 77 pp. In English

IFM-GEOMAR
Leibniz-Institut für Meereswissenschaften
an der Universität Kiel

No.	Title
22	RV Atalante Fahrtbericht / Cruise Report HYDROMAR V (replacement of cruise MSM06/2), Toulon, France - Recife, Brazil, 04.12.2007 - 02.01.2008, Ed.: Sven Petersen, 103 pp. In English
23	RV Atalante Fahrtbericht / Cruise Report MARSUED IV (replacement of MSM06/3), Recife, Brazil - Dakar, Senegal, 07.01. - 31.01.2008, Ed.: Colin Devey, 126 pp. In English
24	RV Poseidon Fahrtbericht / Cruise Report P376 ABYSS Test, Las Palmas - Las Palmas, 10.11. - 03.12.2008, Eds.: Colin Devey and Sven Petersen, 36 pp, In English
25	RV SONNE Fahrtbericht / Cruise Report SO 199 CHRISP Christmas Island Seamount Province and the Investigator Ridge: Age and Causes of Intraplate Volcanism and Geodynamic Evolution of the south-eastern Indian Ocean, Merak/Indonesia – Singapore, 02.08.2008 - 22.09.2008, Eds.: Reinhard Werner, Folkmar Hauff and Kaj Hoernle, 210 pp. In English
26	RV POSEIDON Fahrtbericht / Cruise Report P350: Internal wave and mixing processes studied by contemporaneous hydrographic, current, and seismic measurements, Funchal – Lissabon, 26.04.-10.05.2007 Ed.: Gerd Krahmann, 32 pp. In English
27	RV PELAGIA Fahrtbericht / Cruise Report Cruise 64PE298: West Nile Delta Project Cruise - WND-3, Heraklion - Port Said, 07.11.-25.11.2008, Eds.: Jörg Bialas & Warner Brueckmann, 64 pp. In English
28	FS POSEIDON Fahrtbericht / Cruise Report P379/1: Vulkanismus im Karibik-Kanaren-Korridor (ViKKi), Las Palmas – Mindelo, 25.01.-12.02.2009, Ed.: Svend Duggen, 74 pp. In English
29	FS POSEIDON Fahrtbericht / Cruise Report P379/2: Mid-Atlantic-Researcher Ridge Volcanism (MARRVi), Mindelo- Fort-de-France, 15.02.-08.03.2009, Ed.: Svend Duggen, 80 pp. In English
30	FS METEOR Fahrtbericht / Cruise Report M73/2: Shallow drilling of hydrothermal sites in the Tyrrhenian Sea (PALINDRILL), Genoa – Heraklion, 14.08.2007 – 30.08.2007, Eds.: Sven Petersen & Thomas Monecke, 235 pp. In English
31	FS POSEIDON Fahrtbericht / Cruise Report P388: West Nile Delta Project - WND-4, Valetta – Valetta, 13.07. - 04.08.2009, Eds.: Jörg Bialas & Warner Brückmann, 65 pp. In English
32	FS SONNE Fahrtbericht / Cruise Report SO201-1b: KALMAR (Kurile-Kamchatka and ALeutian MARginal Sea-Island Arc Systems): Geodynamic and Climate Interaction in Space and Time, Yokohama, Japan - Tomakomai, Japan, 10.06. - 06.07.2009, Eds.: Reinhard Werner & Folkmar Hauff, 105 pp. In English
33	FS SONNE Fahrtbericht / Cruise Report SO203: WOODLARK Magma genesis, tectonics and hydrothermalism in the Woodlark Basin, Townsville, Australia - Auckland, New Zealand 27.10. - 06.12.2009, Ed.: Colin Devey, 177 pp. In English

IFM-GEOMAR
Leibniz-Institut für Meereswissenschaften
an der Universität Kiel

No.	Title
34	FS MARIA S. MERIAN Fahrtbericht / Cruise Report MSM 03-2: HYDROMAR IV: The 3rd dimension of the Logatchev hydrothermal field, Fort-de-France - Fort-de-France, 08.11. - 30.11.2006, Ed.: Sven Petersen, 98 pp. In English
35	FS SONNE Fahrtbericht / Cruise Report SO201-2 **KALMAR: K**urile-Kamchatka and **AL**eutian **MAR**ginal Sea-Island Arc Systems: Geodynamic and Climate Interaction in Space and Time Busan/Korea – Tomakomai/Japan, 30.08. - 08.10.2009, Eds.: Wolf-Christian Dullo, Boris Baranov, and Christel van den Bogaard, 233 pp. In English
36	RV CELTIC EXPLORER Fahrtbericht / Cruise Report CE0913: Fluid and gas seepage in the North Sea, Bremerhaven – Bremerhaven, 26.07. - 14.08.2009, Eds.: Peter Linke, Mark Schmidt, CE0913 cruise participants, 90 pp. In English
37	FS SONNE Fahrtbericht / Cruise Report: TransBrom SONNE, Tomakomai, Japan - Townsville, Australia, 09.10. - 24.10.2009, Eds.: Birgit Quack & Kirstin Krüger, 84 pp. In English
38	FS POSEIDON Fahrtbericht / Cruise Report POS403, Ponta Delgada (Azores) - Ponta Delgada (Azores), 14.08. - 30.08.2010, Eds.: Torsten Kanzow, Andreas Thurnherr, Klas Lackschewitz, Marcel Rothenbeck, Uwe Koy, Christopher Zappa, Jan Sticklus, Nico Augustin, 66 pp. In English
39	FS SONNE Fahrtbericht/Cruise Report SO208 Leg 1 & 2 Propagation of Galápagos Plume Material in the Equatorial East Pacific (PLUMEFLUX), Caldera/Costa Rica – Guayaquil/Ecuador 15.07. - 29.08.2010, Eds.: Reinhard Werner, Folkmar Hauff and Kaj Hoernle, 230 pp, In English
40	Expedition Report "Glider fleet", Mindelo (São Vincente), Republic of Cape Verde, 05. – 19.03.2010, Ed.: Torsten Kanzow, 26 pp, In English
41	FS SONNE Fahrtbericht / Cruise Report SO206, Caldera, Costa Rica – Caldera, Costa Rica, 30.05. – 19.06.2010, Ed.: Christian Hensen, 95 pp, In English
42	FS SONNE Fahrtbericht / Cruise Report SO212, Talcahuano, Chile – Valparaiso, Chile, 22.12. – 26.12.2010, Ed.: Ernst Flüh, 47 pp, in English
43	RV Chakratong Tongyai Fahrtbericht / Cruise Report MASS-III, Morphodynamics and Slope Stability of the Andaman Sea Shelf Break (Thailand), Phuket - Phuket (Thailand), 11.01. - 24.01.2011, Ed.: Sebastian Krastel, 42 pp, in English.
44	FS SONNE Fahrtbericht / Cruise Report SO-210, Identification and investigation of fluid flux, mass wasting and sediments in the forearc of the central Chilean subduction zone (ChiFlux), Valparaiso – Valparaiso, 23.09. – 01.11.2010, Ed.: Peter Linke, 112 pp, in English.
45	RV Poseidon POS389 & POS393 & RV Maria S. MerianMSM15/5, TOPO-MED - Topographic, structural and seismotectonic consequences of plate re-organization in the Gulf of Cadiz and Alboran Sea – POS 389: Valletta, Malta – Malaga, Spain, 06.–17.08.2009, POS393: Malaga, Spain – Faro, Portugal, 14.–24.01.2010, MSM15/5: Valletta, Malta - Rostock, Germany, 17.–29.07.2010, I. Grevemeyer, xx pp.

IFM-GEOMAR
Leibniz-Institut für Meereswissenschaften
an der Universität Kiel

No.	Title
46	FS POSEIDON Fahrtbericht / Cruise Report, P408 - The Jeddah Transect, Jeddah - Jeddah, Saudi Arabia, 13.01.–02.03.2011, M. Schmidt, C. Devey, A. Eisenhauer and cruise participants, 80 pp.
47	FS SONNE Fahrtbericht / Cruise Report, SO-214 NEMESYS, Wellington – Wellington, 09.03. - 05.04.2011, Wellington - Auckland 06. - 22.04.2011, Ed.: J. Bialas, 174 pp.

Das Leibniz-Institut für Meereswissenschaften ist ein Institut der Wissenschaftsgemeinschaft Gottfried Wilhelm Leibniz (WGL)

The Leibniz-Institute of Marine Sciences is a member of the Leibniz Association (Wissenschaftsgemeinschaft Gottfried Wilhelm Leibniz).

Leibniz-Institut für Meereswissenschaften / Leibniz-Institute of Marine Sciences
IFM-GEOMAR
Dienstgebäude Westufer / West Shore Building
Düsternbrooker Weg 20
D-24105 Kiel
Germany

Leibniz-Institut für Meereswissenschaften / Leibniz-Institute of Marine Sciences
IFM-GEOMAR
Dienstgebäude Ostufer / East Shore Building
Wischhofstr. 1-3
D-24148 Kiel
Germany

Tel.: ++49 431 600-0
Fax: ++49 431 600-2805
www.ifm-geomar.de